

PDF hosted at the Radboud Repository of the Radboud University Nijmegen

The following full text is a publisher's version.

For additional information about this publication click this link.

<http://hdl.handle.net/2066/131645>

Please be advised that this information was generated on 2017-12-05 and may be subject to change.

Small RNA-based antiviral defense in insects

Walter Bronkhorst

Cover Illustration: Two virus-infected *Drosophila melanogaster* (w^{1118}) that face each other. A fruit fly infected with IIV-6 wildtype virus (left) and a fruit fly infected with IIV-6 mutant (green fluorescent protein, GFP) virus (right).

Cover design: Walter Bronkhorst

Cover lay-out: Promotie In Zicht, Arnhem

Printed by Ipskamp Drukkers, Enschede

© 2014 by Walter Bronkhorst

All rights reserved. No parts of this publication may be reproduced or transmitted in any form or by any means without prior written permission of the author and the publisher holding the copyright of the published articles.

The research described in this thesis was performed at the Department of Medical Microbiology, Radboud University Medical Center, Radboud Institute for Molecular Life Sciences, Nijmegen, The Netherlands.

Small RNA-based antiviral defense in insects

Proefschrift

ter verkrijging van de graad van doctor
aan de Radboud Universiteit Nijmegen
op gezag van de rector magnificus prof. dr. Th.L.M. Engelen,
volgens besluit van het college van decanen
in het openbaar te verdedigen op vrijdag 21 november 2014
om 10.30 uur precies

door

Alfred Willem (Walter) Bronkhorst

geboren op 8 februari 1985
te Apeldoorn

Promotor:

Prof. dr. J.M.D. Galama

Copromotor:

Dr. R.P. van Rij

Manuscriptcommissie:

Prof. dr. G.J.M. Pruijn

Dr. W.J.A.J. Hendriks

Prof. dr. J. van der Oost (Wageningen UR)

Table of contents

Chapter 1	General introduction	7
Chapter 2	Convergent evolution of Argonaute-2 Slicer antagonism in two distinct insect RNA viruses	37
Chapter 3	The DNA virus Invertebrate iridescent virus 6 is a target of the <i>Drosophila</i> RNAi machinery	71
Chapter 4	Small RNAs tackle large viruses: RNA interference-based antiviral defense against DNA viruses in insects	107
Chapter 5	A dsRNA-binding protein of a complex invertebrate DNA virus suppresses the <i>Drosophila</i> RNAi response	125
Chapter 6	Arbovirus-derived piRNAs exhibit a ping-pong signature in mosquito cells	153
Chapter 7	General discussion	169
Chapter 8	Summary	194
	Samenvatting	197
Dankwoord		201
Curriculum Vitae		206
List of publications		207

Chapter 1

General introduction

Adapted from:

Alfred W. Bronkhorst and Ronald P. van Rij

The long and short of antiviral defense: Small RNA-based immunity
in insects

Current Opinion in Virology 2014, 7C:19-28

All living organisms encounter a wide variety of microbial pathogens throughout their lifetime. A potent immune response is required to control or eliminate the pathogen and to ensure survival of the infected host. Mosquitoes and other blood-feeding insects transmit important human and animal viruses (arthropod-borne viruses, arboviruses), some of which are associated with debilitating disease and worldwide epidemics. With the increasing global threat of arboviruses, it is essential to understand the virus-vector interactions that determine virus transmission. Insights into the mechanisms of antiviral immunity will help us to understand arbovirus transmission cycles and to define novel strategies to restrict transmission and spread of pathogenic viruses.

Over the last years it has become apparent that RNA interference (RNAi) is an important antiviral defense mechanism in insects, including the major vector mosquitoes and the model insect *Drosophila melanogaster* (fruit fly). The importance of the antiviral RNAi pathway is underscored by the observation that viruses have evolved sophisticated mechanisms to counteract this small RNA-based immune response. More recently, it was proposed that another small RNA silencing mechanism, the piRNA pathway, also processes viral RNAs in *Drosophila* and mosquitoes. Here, we review recent insights into the mechanism of antiviral RNAi, viral small RNA profiles, and viral counter-defense mechanisms in insects.

RNA silencing pathways

MicroRNAs (miRNAs), small interfering RNAs (siRNAs) and Piwi-interacting RNAs (piRNAs) are the three major classes of small regulatory RNAs that control different cellular processes in animals. These small RNA-mediated gene silencing pathways can generally be distinguished by the mechanism of small RNA biogenesis, the specific protein member of the Argonaute family to which the small RNA associates, as well as the mode of target recognition and silencing that is mediated by the protein-RNA effector complex.

The RNAi pathway in insects

In RNAi, small interfering RNAs (siRNA) guide the Argonaute-2 (AGO2) protein onto target RNAs to induce their degradation. The central trigger of the RNAi pathway is double-stranded (ds) RNA. Endogenous dsRNA substrates, such as those derived from transposons, overlapping transcripts or long structured RNA loci, are processed by the RNase III enzyme Dicer-2 (Dcr-2) into 21-nt siRNA duplexes with 5' monophosphates and 2-nt 3' hydroxyl overhangs (1, 2). The dsRNA-binding proteins (dsRBP) Loquacious

PD isoform (Loqs-PD) and R2D2 are Dcr-2 co-factors that are required for efficient siRNA biogenesis and loading onto AGO2 within the RNA induced silencing complex (RISC) (3). Arsenic resistance protein 2 (Ars2) is a Dcr-2 interacting protein that contributes to the efficiency of dsRNA processing (4).

The generated siRNAs are subsequently bound by the RISC loading complex (RLC), a heterodimer composed of Dcr-2 and its dsRBP partner R2D2 (5-9). The RLC senses the thermodynamic stability and intrinsic structure of the siRNA duplex and defines which of the two strands will be retained in RISC (5, 10-12). R2D2 binds the most stable 5' end of the duplex and thereby selects the passenger strand, while the opposite strand that is bound by Dcr-2 at its 5' end will become the guide strand (5-9, 12).

Loading of the siRNA duplex into Argonaute-2 (AGO2) protein, the catalytic component of RISC, requires the HSP70/HSP90 chaperone machinery. During this ATP-dependent process, AGO2 most likely undergoes a conformational change to facilitate efficient siRNA-loading (13-15). Correct loading of siRNA duplexes into AGO2 might occur in specialized cytoplasmic granules, called D2 bodies, as proposed for the sorting of endo-siRNAs (16).

Once loaded into RISC, one strand of the siRNA duplex (passenger strand) is eliminated from RISC (3). This process requires the endonuclease activity of AGO2 to cleave the passenger strand as well as the endonuclease complex C3PO (Component 3 Promoter of RISC), a multimeric complex of Translin and Trax (17, 18). The guide strand is retained in RISC and is 2'-O-methylated at its 3' terminal nucleotide by the RNA methyltransferase DmHen1, resulting in a mature, active RISC that is competent in inducing sequence-specific target cleavage by AGO2 (slicing) (19, 20).

The miRNA pathway in insects

MicroRNAs (miRNAs) are another class of small regulatory RNAs that mediate post-transcriptional gene silencing. The miRNA pathway is involved in host gene silencing to fine-tune gene expression during biological processes, such as developmental timing and cell proliferation (21). Canonical miRNA biogenesis initiates with RNA polymerase II-dependent production of noncoding RNAs, which contains one or more imperfect stem-loop structures (Figure 1) (22). The nuclear Microprocessor complex, composed of the RNase III enzyme Droscha and the dsRBP Pasha (DiGeorge syndrome critical region 8, DGCR8 in humans), processes these long primary miRNA (pri-miRNAs) transcripts into 60-70 nt sized precursor miRNAs (pre-miRNAs). The Droscha-dependent production of pre-miRNAs creates a stem-loop with a 2-nt 3' overhang, determining one end of the mature miRNA (23-28). Pre-miRNAs hairpins are subsequently transported to the cytoplasm in an Exportin-5-dependent manner (29). Within the cytoplasm, Dicer-1 and the adaptor protein Loquacious (Loqs)-PB recognize and cleave the pre-miRNA

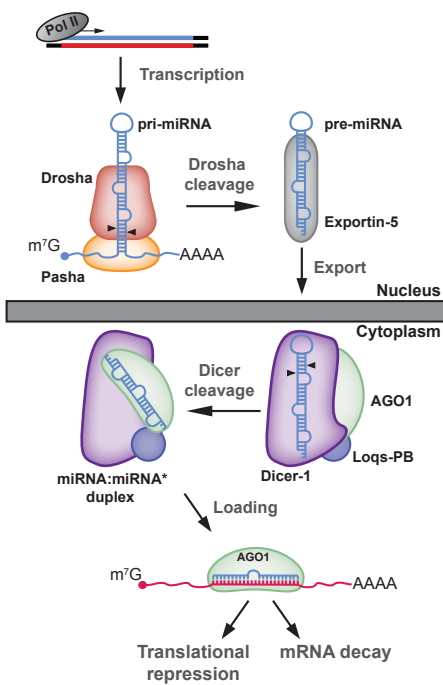


Figure 1. The miRNA pathway in insects. The RNA Polymerase II (Pol II)-transcribed primary miRNA (pri-miRNA) is processed by Drosha into a precursor miRNA (pre-miRNA). The pre-miRNA is subsequently transported to the cytoplasm in an Exportin-5-dependent manner. In the cytoplasm, the pre-miRNA is further processed by Dicer-1, yielding a mature microRNA (miRNA) duplex. Finally, the mature miRNA is loaded into Argonaute-1 (AGO1) to mediate target recognition which results in translational repression or mRNA decay.

into a 22-nt mature miRNA:miRNA* duplex. This second cleavage step leaves 5' monophosphates and 2-nt 3' hydroxyl overhangs, which are characteristic RNase III signatures (30-32). In analogy to duplex siRNA loading, the loading of imperfect miRNA duplexes depends on thermodynamic stability in which the least stable 5' end remains incorporated in the AGO1-containing RISC to guide target recognition (10, 11). The 5' nucleotide identity and internal structure of the small miRNA duplex serve as additional features for AGO1 sorting. Notably, the intrinsic structure of the central region of siRNA or miRNA duplexes appears to be a major determinant for proper Argonaute sorting, with imperfect miRNA duplexes being preferentially loaded into AGO1, and perfect complementary siRNA duplexes being loaded into AGO2 (12, 33-37). In contrast to the slicing-mediated siRNA passenger strand elimination, the miRNA* is discarded from RISC by cleavage-independent unwinding activities (37). Following duplex unwinding, the mature miRNA guides RISC to its target site through partial complementarity between mRNA targets (usually in the 3' untranslated

region of protein coding mRNAs) and the miRNA seed region (nucleotide 2 to 8 of the mature miRNA). In addition, the 3' region of a miRNA (supplementary region, nucleotide 13-16) sometimes enhances pairing to its target (21). Target recognition results in inhibition of protein synthesis through translational repression, mRNA deadenylation and decay (38).

Next to canonical miRNA biogenesis from pri-miRNA precursor transcripts, alternative pathways can also generate mature miRNAs. For example, intronic pre-mRNA splicing products can adopt pre-miRNA structures, thus bypassing the Drosha cleavage step,

and these short hairpin introns (called mirtrons) feed into the canonical biogenesis pathway (39, 40). Alternatively, mature miRNA biogenesis might occur in a Dicer-1-independent, but in a Drosha- and AGO2-dependent manner (41-43).

Although the miRNA and siRNA biogenesis pathways are functionally separated in *Drosophila*, recent studies revealed that the miRNA* strand is preferentially sorted to AGO2 and becomes 2'-O-methylated at its 3' end (33-35). Importantly, AGO2-associated small RNAs that contain central bulges can induce translational repression of the target mRNA (44), suggesting that the miRNA* is not merely a byproduct of miRNA biogenesis. Together, these studies indicate that cross-talk between the miRNA and siRNA machineries occurs.

The piRNA pathway in insects

The PIWI-interacting RNA (piRNA) pathway is a small RNA-based gene regulatory mechanism in which 23-30 nt single-stranded (ss) RNAs associate with proteins of the PIWI family (45-49). In *Drosophila* germ cells, the PIWI proteins Piwi, Aubergine (Aub), and Argonaute 3 (AGO3) inhibit the mobilization of transposable elements (50, 51). Two mechanisms for piRNA biogenesis have been characterized: primary piRNA biogenesis and a complex feed-forward amplification loop, termed the ping-pong amplification cycle (Figure 2). In contrast to the dsRNA-induced miRNA and siRNA pathways, the piRNA pathway is initiated by single-stranded precursor RNAs that are processed in a Dicer-independent manner (47). Primary precursor piRNAs are derived from long genomic regions that are composed of transposon remnants, called piRNA clusters (46, 52). In *Drosophila*, primary piRNAs that associate with Piwi or Aub are antisense to transposon transcripts and are enriched for a uridine at their 5' terminus (1U). It is not clear whether this strong nucleotide bias results from piRNA biogenesis of primary antisense transcripts, which was suggested to be mediated by the endoribonuclease Zucchini, or whether Piwi and Aub selectively incorporate 1U piRNAs (52-57). Following 5' end formation and incorporation of these piRNA intermediates into PIWI proteins, the mature 3' end is generated by an unknown 3'-5' exonuclease named Trimmer (58). As a final step in primary piRNA biogenesis, the mature Piwi-loaded piRNA is methylated at its 3' end by the methyltransferase DmHen1, which protects the piRNA from degradation (20, 58). Mature primary piRNAs guide Aub, but not Piwi, to complementary, sense RNA targets (mRNAs of active transposons) to induce the ping-pong amplification cycle. Aub subsequently cleaves the target at the tenth nucleotide from the 5' end of the mature primary piRNA. Notably, Aub-mediated slicing not only inactivates the transposon, but also defines the 5' end of newly generated secondary piRNAs that consequently harbor a typical bias for adenine at position 10 (10A). Secondary, sense piRNAs are incorporated in AGO3 to subsequently find and

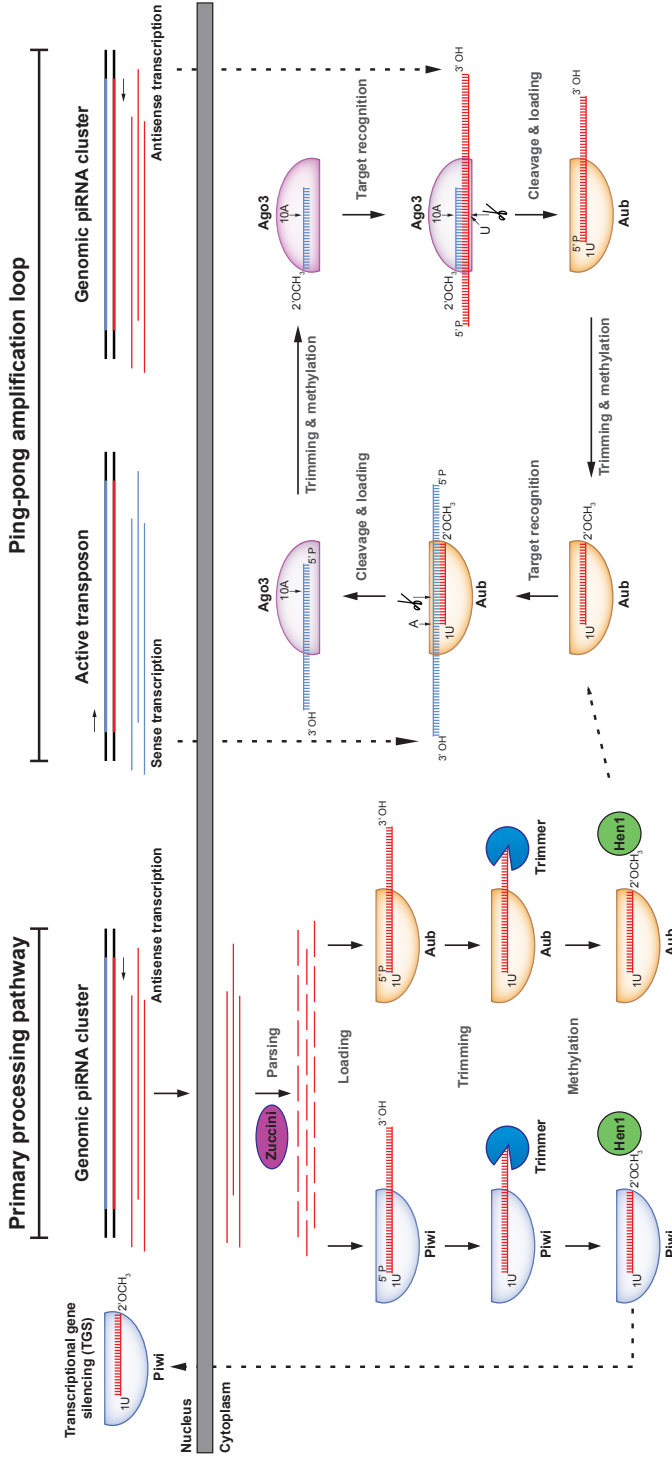


Figure 2. The piRNA pathway in *Drosophila*. In the primary processing pathway, single-stranded precursor RNAs, derived from genomic piRNA clusters, are processed into piRNA intermediates. Cytoplasmic primary piRNAs that contain a uridine at their 5' end (1U) associate with Piwi or Aubergine (Aub) and are subsequently truncated at their 3' end by the exonuclease Trimmer, followed by 3' end methylation by the methyltransferase DmHen1. Piwi-associated primary piRNAs that are translocated to the nucleus mediate transcriptional gene silencing (TGS). Aub-associated mature piRNAs recognize a complementary sense target RNA to induce the ping-pong amplification loop. Following recognition, the sense target RNA is cleaved by Aub, yielding a secondary piRNA with a specific 10A-bias. The secondary piRNA is incorporated into Argonaute-3 (AGO3), trimmed and methylated at its 3' end. The mature secondary piRNA subsequently recognizes a complementary antisense target RNA, leading to the production of new 1U piRNAs that continue the amplification loop to mediate post-transcriptional gene silencing of transposons in the cytoplasm.

cleave new complementary antisense targets, leading to the production of more 1U piRNAs that continue the amplification process. The secondary pathway in *Drosophila* requires cytoplasmic AGO3 and Aub slicing activities, and as a consequence of this amplification process, AGO3- and Aub-associated piRNAs show a characteristic 10-nt overlap at their 5' ends (59). It is currently unknown how the 3' ends of secondary piRNAs are processed to generate mature secondary piRNAs.

In contrast to germ cells where Piwi, Aub and AGO3 are all co-expressed, only Piwi is present in somatic follicle cells that surround the ovary. Consequently, only the primary piRNA pathway is active in somatic cells (60-62). In germ cells and in somatic cells, Piwi localizes to the nucleus upon piRNA loading and this re-localization of Piwi is required for transposon silencing (57). Interestingly, recent studies revealed that transcriptional gene silencing by nuclear Piwi does not require Slicer activity (61, 63), but instead relies on Piwi-induced epigenetic changes and subsequent heterochromatin formation (64-69). Taken together, the primary piRNA pathway silences transposons at the transcriptional level in the nucleus (through Piwi) and induces the secondary piRNA biogenesis pathway, which mediates post-transcriptional gene silencing in the cytoplasm (through AGO3 and Aub).

The antiviral RNAi pathway in insects

DsRNA is not detectable in uninfected, healthy cells, but accumulates upon virus infection (70). Viral dsRNA may thus feed into the RNAi machinery to restrict virus replication (Figure 3). Genetic studies underscore the essential role of the RNAi response in controlling virus infection. *Drosophila* mutants for core components of the RNAi pathway (*Dcr-2*, *R2D2*, or *AGO2*) are highly sensitive to RNA virus infection, which correlates with an increase in viral RNA accumulation (71-74). Similarly, in arbovirus-infected mosquitoes, higher viral loads are observed upon knockdown or inactivation of RNAi pathway components (75-79). Recent studies demonstrated that DNA viruses are also targets of the antiviral RNAi response in insects (80-84).

Dcr-2 processes viral dsRNA into 21-nt viral small interfering RNAs (vsiRNAs). Interestingly however, Dcr-2 does not require its cofactors Loqs-PD and R2D2 for production of vsiRNAs during RNA virus infection (85, 86), but R2D2 is required for their loading into RISC (71, 72, 74, 85, 86). The Dcr-2 associated protein Ars2 seems to contribute to antiviral defense, but its direct role in vsiRNA biogenesis remains elusive (4).

Viral dsRNA is an essential intermediate in replication of ssRNA viruses and it has been suggested that Dcr-2-mediated cleavage of such intermediates is sufficient to explain the

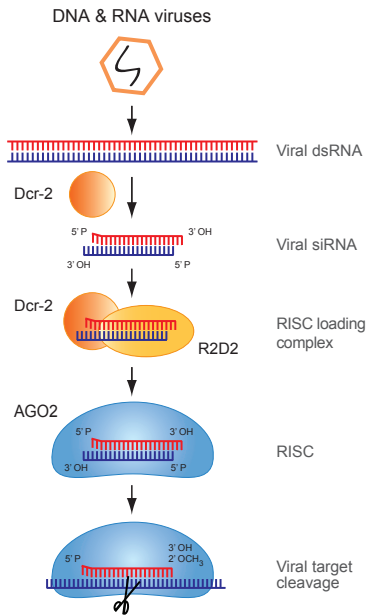


Figure 3. The antiviral RNAi pathway in insects. Dicer-2 (Dcr-2) detects viral double-stranded RNA, produced by RNA and DNA viruses, and generates viral small interfering RNAs (vsiRNAs). Dcr-2 and R2D2 are required for vsiRNA incorporation in Argonaute-2 (AGO2), within the RNA-induced silencing complex (RISC). The strand that remains incorporated in RISC guides the recognition and cleavage of target viral RNA to restrict virus replication.

antiviral activity of RNAi. Several lines of evidence suggest that viruses are also restricted by RISC-mediated cleavage of viral ssRNAs. *R2D2* and *AGO2* mutant flies are more sensitive to virus infection (71, 72, 74, 85, 86), which implies a role for vsiRNA-loaded RISC in antiviral defense. Indeed, viral siRNAs are resistant to beta-elimination treatment (which shortens RNA containing non-modified 2'- and 3' hydroxyl groups at the 3' terminus), suggesting that at least some vsiRNAs are AGO2-associated and 2'-O-methylated at their 3' end (33, 87). More recently, it was demonstrated that Slicer-incompetent *AGO2* mutants are highly susceptible to infection with the negative strand (-) RNA virus Vesicular stomatitis virus (85). Another line of support comes from the observation that two unrelated insect RNA viruses (Cricket paralysis virus and Nora virus) have evolved antagonists that inhibit Slicer activity of pre-assembled RISC (88, 89). Together these studies indicate that antiviral defense depends on dicing and slicing of viral RNAs.

Substrates for viral siRNA biogenesis

A hallmark of an antiviral RNAi response is the Dcr-2-dependent production of vsiRNAs. Putative Dcr-2 substrates include viral replication intermediates of ssRNA viruses, viral genomes of dsRNA viruses, structured RNA elements in viral ssRNA genomes or viral transcripts, and dsRNA that is formed by hybridization of overlapping transcripts of DNA viruses. Several recent studies used deep sequencing to analyze small RNAs in virus-infected samples. The detection of vsiRNA provides direct support for Dicer-mediated processing of viral dsRNA. Moreover, vsiRNA sequences can be mapped to

the viral genome and this information can be used to deduce the viral substrates that are processed by Dcr-2.

Small RNA profiles from (+) RNA viruses

During replication of positive-strand (+) RNA viruses, the viral (+) RNA strand serves as a template for negative strand (-) RNA synthesis. The (-) RNA strand in turn serves as a template for the production of (+) viral RNA progeny (90). Viral RNA replication is in general asymmetric: the viral (+) RNA strand greatly outnumbers the viral (-) RNA strand. Nevertheless, upon infection of insect hosts with different (+) RNA viruses, vsRNAs of positive and negative polarity were recovered in roughly equal numbers. This observation, together with the finding that vsRNAs map along the entire length of the viral genome (Table 1), indicates that viral dsRNA replication intermediates are a major substrate for Dcr-2 during (+) RNA virus infection.

Nevertheless, in some (+) RNA virus infections, Dcr-2 may process additional substrates. In Flock House virus (FHV) infection of *Drosophila*, for example, vsRNAs mainly derive from the (+) RNA strand across the two segments of the viral RNA genome (86). This suggests that intramolecular base pairing within viral ssRNA genomes form dsRNA substrates for Dicer. FHV encodes the RNAi antagonist B2 that binds dsRNA (Table 2, discussed below) and markedly affects vsRNA profiles (91-93). Infection with a B2 deficient mutant FHV (FHV Δ B2) resulted in the production of vsRNAs that mapped in similar numbers to the (+) and (-) strands at the 5' terminal region of RNA segment 1 (86, 87). Similar to wildtype FHV infection, vsRNAs also mainly derive from the viral (+) RNA strand in infections with the (+) RNA virus *Drosophila* C virus (DCV) (83, 94). Like FHV, DCV encodes a dsRNA binding RNAi suppressor protein (1A) that is thought to shield the replication intermediates from Dicer (72). These results might suggest that the 1A and B2 proteins shield replication intermediates for Dicer-mediated cleavage and that under these conditions other viral RNA substrates are processed into vsRNAs. Remarkably however, infection of *Aedes aegypti* mosquitoes with recombinant Sindbis virus (which is thought not to encode an RNAi suppressor) engineered to encode the FHV B2 protein resulted in strongly reduced vsRNA levels, without a concomitant shift towards (+) viral small RNAs (78). These data suggest that viral RNAi suppressor proteins might affect vsRNA profiles, but that this might be virus and host species dependent.

Small RNA profiles from (-) RNA viruses

Analogous to (+) RNA viruses, the viral genomic RNA strand is template for the production of complementary RNA strands during (-) RNA virus replication. Due to asymmetric replication, the genomic strand of (-) RNA viruses is more abundant than

the antigenome (+) RNA during infections (95, 96). Genome replication of (-) RNA viruses occurs in ribonucleoprotein complexes, which requires the initial assembly of the viral RNA with the viral nucleocapsid protein (N) (95, 97). The formation of the RNA-N protein complex might explain why dsRNA is not readily detectable in (-) RNA virus infection (70).

An additional RNA species in (-) RNA virus infections is the viral messenger RNA, which may be expressed at different relative levels during infection. For example, a gradient of mRNA transcripts ($N > P > M > G > L$) is produced by the viral RNA polymerase of the non-segmented Vesicular stomatitis virus, which is the net result from the sequential mode of transcription based on gene order (95).

Small RNA profiling in (-) RNA virus infections, demonstrated that vsiRNAs are generally equally distributed over genomic and antigenomic RNA strands and that they are produced from the full-length genome (71, 83, 85, 98-100). These observations suggest that replication intermediates are the predominant Dcr-2 substrate in (-) RNA virus infection of adult flies and of *Drosophila* or mosquito cells (Table 1). For Vesicular stomatitis virus, it was suggested that viral genome-transcript hybrids provide a putative dsRNA template that can be recognized by Dcr-2 (85). An additional Dcr-2 substrate was suggested for the tri-segmented (L, M and S) Rift Valley fever virus. Here, Dcr-2-dependent vsiRNAs were unevenly distributed across the S segment and were most likely derived from an intergenic hairpin (83).

Small RNA profiles from dsRNA viruses

Genome replication of most dsRNA viruses occurs within the viral capsid that encapsulates the viral dsRNA (101). Some dsRNA viruses, such as members of the *Birnaviridae* family, protect their genome by forming ribonucleoprotein complexes (102, 103). Nevertheless, several studies indicate that viral dsRNA genomes are accessible for Dcr-2. For example, small RNA deep sequencing of persistently infected *Drosophila* cell lines revealed roughly equal numbers of (+) and (-) vsiRNAs for three different dsRNA viruses (*Drosophila* totivirus, *Drosophila* X virus, *Drosophila* birnavirus), indicating that the viral dsRNA genome is cleaved by Dcr-2 (94, 104). Similarly, vsiRNAs of both polarities were recovered in equal proportions from *Aedes* mosquito-derived cell lines infected with Bluetongue virus, with vsiRNAs evenly distributed across the viral genome (100).

Small RNA profiles from DNA virus infections

In contrast to RNA viruses, DNA viruses do not replicate via a dsRNA replication intermediate. Nevertheless, we and others showed that the RNAi machinery contributes to control of DNA virus infection in insects (80-82) and therefore other dsRNA sources

must be processed by Dcr-2 (Table 1). Indeed, overlapping bidirectional transcripts base pair to form dsRNA substrates for Dcr-2-dependent vsiRNA biogenesis in *Drosophila* (80, 81, 84). A number of recent publications have now analyzed vsiRNA profiles in DNA virus infections in different invertebrate model systems and these studies further underscore that convergent transcripts are a major source of vsiRNA production, but that other substrates, such as structured RNA elements (83), can also contribute to the vsiRNA profile (84).

Virus-derived piRNAs

Recent small RNA profiling studies have implicated the piRNA pathway in antiviral defense in mosquitoes. The potential of the piRNA pathway to process viral RNAs was first suggested by the detection of piRNA-sized viral RNAs in persistently infected *Drosophila* ovarian sheet cells (104, 105). Several studies that detected arboviral small RNAs of positive polarity within the piRNA size-range suggested that the piRNA pathway also processes viral RNAs in mosquitoes (98, 106, 107).

More recently, small 25-30 nt RNAs with clear features of ping-pong-dependent piRNAs were recovered from *Aedes* mosquitoes or mosquito-derived cells infected with (+) RNA arboviruses from the *Togaviridae* family (Sindbis virus, Semliki Forest virus and Chikungunya virus) and (-) RNA arboviruses from the *Bunyaviridae* family (La Crosse virus, Schmallenberg virus and Rift Valley fever virus). Virus-derived piRNAs (vpiRNAs) of positive polarity showed a non-uniform distribution across the viral genome and presented an 10A bias, whereas vpiRNAs of negative polarity were enriched for 1U (99, 100, 108-110). Together, these results indicate that *de novo* vpiRNAs are produced in a ping-pong-dependent manner upon RNA virus infection of major vector mosquitoes (Table 1). In *Aedes* mosquitoes, the PIWI gene family greatly expanded and expression of at least some of the eight PIWI family members does not seem to be restricted to germ line tissues (108, 109, 111), raising the possibility that the piRNA pathway has functionally diversified in mosquitoes.

The intriguing identification of viral piRNAs in mosquitoes raises important questions about their biogenesis and functions. Interestingly, knockdown of *Piwi4* in *Aedes aegypti* cells resulted in increased Semliki Forest virus viral loads, suggesting a role of the piRNA pathway in restricting virus replication (110). Similarly, knockdown of *AGO3* in *Anopheles* mosquitoes lead to increased O'nyong-nyong virus titers (75), although production of vpiRNAs has yet to be demonstrated in this mosquito species.

Table 1. Small RNA profiles from naturally and experimentally infected insects

Virus	Virus family	Genome segments (number)	Virus (abbr.)	Infected host	Experimental system	Proposed Dicer substrates	Reference
(+) RNA virus	<i>Togaviridae</i>	1	Sindbis virus	<i>D. melanogaster</i> ; <i>Ae. aegypti</i> ; <i>Ae. albopictus</i>	Cell; <i>in vivo</i>	dsRNA replication intermediates; structured ssRNA	(78, 85, 98, 109)
			O' nyong-nyong virus	<i>An. gambiae</i>	In vivo	dsRNA replication intermediates; structured ssRNA	(125)
			Semliki Forest virus	<i>Ae. albopictus</i> ; <i>Ae. aegypti</i>	Cell	dsRNA replication intermediates	(110, 126)
			Chikungunya virus	<i>Ae. aegypti</i> ; <i>Ae. albopictus</i>	Cell; <i>in vivo</i>	dsRNA replication intermediates	(108)
	<i>Dicistroviridae</i>	1	Drosophila C virus (DCV)	<i>D. melanogaster</i>	Cell	dsRNA replication intermediates; structured ssRNA	(83, 94, 104)
	<i>Flaviviridae</i>	1	Dengue virus	<i>Ae. aegypti</i> ; <i>Ae. albopictus</i>	Cell; <i>in vivo</i>	dsRNA replication intermediates	(106, 107)
			West Nile virus	<i>D. melanogaster</i> ; <i>Ae. albopictus</i> ; <i>C. quinquefasciatus</i>	Cell; <i>in vivo</i>	dsRNA replication intermediates; structured ssRNA	(98, 127)
			Cell fusing agent virus	<i>Ae. aegypti</i> ; <i>Ae. albopictus</i>	Cell	dsRNA replication intermediates	(106)
	<i>Nodaviridae</i>	2	Flock House virus (FHV)	<i>D. melanogaster</i>	Cell; <i>in vivo</i>	dsRNA replication intermediates; defective RNAs; structured ssRNA	(2, 86, 87, 94, 104, 128)
			American Nodavirus	<i>D. melanogaster</i>	Cell	dsRNA replication intermediates; defective RNAs	(94, 104)
	<i>Terraviridae</i>	1	Drosophila A Virus ^a	<i>D. melanogaster</i>	Cell	dsRNA replication intermediates	(104)
	Unassigned	1	Nora virus	<i>D. melanogaster</i>	Cell; <i>in vivo</i>	dsRNA replication intermediates	(89, 104)

(-) RNA	<i>Bunyaviridae</i>	3	Rift Valley fever virus	<i>D. melanogaster</i> ; <i>Ae. aegypti</i> ; <i>Ae. albopictus</i>	Cell	dsRNA replication intermediates; intergenic RNA hairpin	(83, 99)
			La Crosse virus	<i>D. melanogaster</i> ; <i>Ae. albopictus</i>	Cell	dsRNA replication intermediates; structured ssRNA	(98)
			Schmallenberg virus	<i>Ae. aegypti</i> ; <i>Culicoides sonorensis</i>	Cell	dsRNA replication intermediates	(100)
	<i>Rhabdoviridae</i>	1	Vesicular stomatitis virus	<i>D. melanogaster</i>	Cell; <i>in vivo</i>	dsRNA replication intermediates; viral genome-transcript hybrids	(71, 83, 85)
dsRNA	<i>Reoviridae</i>	10	Bluetongue virus	<i>Ae. aegypti</i> ; <i>Culicoides sonorensis</i>	Cell	genomic dsRNA	(100)
	<i>Birnaviridae</i>	2	Culex Y Virus ^b	<i>C. tarsalis</i> ; <i>An. Sinensis</i>	Cell; <i>in vivo</i>	genomic dsRNA	(129) Unp. obs.
		2	Drosophila X virus	<i>D. melanogaster</i>	Cell	genomic dsRNA	(94, 104)
		2	Drosophila birnavirus	<i>D. melanogaster</i>	Cell	genomic dsRNA	(104)
	<i>Totiviridae</i>	1	Drosophila totivirus	<i>D. melanogaster</i>	Cell	genomic dsRNA	(104)
ssDNA	<i>Parvoviridae</i>	1	Culex tritaeniorhynchus virus	<i>C. pipiens molestus</i>	In vivo	structured ssRNA; inverted repeats at non-coding genomic termini	(130)
dsDNA	<i>Iridoviridae</i>	1	Invertebrate Iridescent virus type 6	<i>D. melanogaster</i>	Cell; <i>in vivo</i>	convergent overlapping transcripts	(80, 81, 84)
	<i>Poxviridae</i>	1	Vaccinia virus	<i>D. melanogaster</i>	Cell	convergent overlapping transcripts; tandem repeats at genomic termini; structured ssRNA	(83)

Unp. obs., our unpublished observations

^a Referred to as Drosophila tettravirus in this study; but high sequence identity to Drosophila A virus (DAV) suggest that it is a strain of DAV (131).

^b Referred to as Mosquito X virus by Huang et al (129). High sequence identity between Culex Y virus (132) and Mosquito X virus suggests that they are variants of a single virus species within the *Entomobirnavirus* genus.

Viral suppression of RNAi

Viruses have evolved suppressors of RNAi (VSRs) to antagonize the RNAi-based antiviral immune response. These VSRs may target different critical steps of the antiviral RNAi pathway (Table 2). It is not surprising that many VSRs sequester dsRNA or siRNAs, as these molecules are the initiators and sequence specificity determinants of RNAi. For example, the natural fly pathogen DCV encodes the 1A protein that binds long dsRNA and protects it from Dcr-2 processing. It was thus proposed that 1A protects replication intermediates from Dcr-2-mediated processing (72), although more recently it was reported that DCV 1A may also interfere with RISC loading (88). Members of the *Alphanodavirus* genus (*Nodaviridae* family), including FHV, Nodamura virus (NoV) and Wuhan nodavirus (WhNV), encode the B2 protein that suppresses RNAi via a multimode mechanism. B2 binds long dsRNA and siRNAs, thereby inhibiting Dcr-2 processing and RISC loading, respectively (93, 112-114). Additionally, the FHV and WhNV B2 proteins directly associate with Dcr-2, which likely contributes to their RNAi suppressive activity (115, 116). Despite the similar mechanism of action, only limited amino acid identity exists between the B2 proteins of these viruses (23.5% identity between WhNV and FHV; 26.4% identity between NoV and FHV). Nevertheless, the structures of NoV and FHV are strikingly similar (117), suggesting that they derive from a common ancestral sequence.

An alternative mechanism to interfere with the initiation of the antiviral RNAi response is used by *Heliothis virescens* ascovirus-3e. This virus encodes an RNase III enzyme (orf 27) that degrades dsRNA (118). Thus, the orf27 protein may compete with Dcr-2 for dsRNA substrates or degrade siRNA duplexes to prevent their incorporation into AGO2 in a manner analogous to the RNase III protein of the plant virus sweet potato chlorotic stunt virus (119). Viruses may also target the effector phase of the antiviral RNAi response. For example, Nora virus VP1 and Cricket paralysis virus 1A interact with AGO2 and thereby inhibit RISC-mediated slicing of target RNAs (88, 89).

The transmission of arboviruses relies on mosquito vectors that support a productive virus infection. Despite a functional RNAi-response, arboviruses establish a persistent, non-pathogenic infection in mosquitoes. Although Nodamura virus, a putative arbovirus, was known to encode an RNAi suppressor (Table 2), it was for a long time believed that most arboviruses do not encode a VSR, as this would lead to pathology and killing of the vector thus preventing efficient virus transmission. Indeed, the introduction of a VSR (FHV B2) in recombinant Sindbis virus induced pathogenicity and led to mortality of infected mosquitoes (78, 79).

Recently, it was suggested that the Dengue virus NS4B protein suppresses RNAi by inhibiting Dicer processing independent of dsRNA-binding (120). Alternatively,

flaviviruses may use non-coding ssRNA molecules to counteract RNAi in mammals and insects. West Nile virus and Dengue virus, for example, produce large amounts of subgenomic flavivirus (sf) RNA that contains extensive secondary structures. It was proposed that sfRNAs compete with other dsRNA substrates, such as essential viral replication intermediates, for Dicer-mediated cleavage to inhibit an antiviral RNAi response (121).

Strong genetic evidence supports the importance of B2 protein in FHV infection. Indeed, in the absence of a suppressor protein (Δ B2), abundant vsRNAs are produced and, as a consequence, no potent FHV infection was established in wildtype embryos and adult flies. Importantly, the replication defect of FHV Δ B2 was rescued by genetic inactivation of RNAi genes (74, 86, 87, 122). However, such genetic evidence is lacking for VSRs of most other viruses, in some cases due to the lack of a reverse genetics system to engineer these viruses. For some VSRs, proof-of-concept for a role in suppressing RNAi was provided by rescuing replication of the FHV Δ B2 replicon or by analyzing virus replication of a recombinant Alphavirus engineered to express the VSR of interest (Table 2). Nevertheless, future studies are needed to provide insights into the role of the identified VSRs in viral pathogenesis and transmission.

Many insect viruses encode suppressors of RNAi; yet in other viruses, including some well-characterized arboviruses, attempts to identify RNAi suppressive activities have not been successful (unpublished observations). Although this might mean that those viruses do not encode RNAi suppressors, an alternative explanation might be that RNAi reporter assays that are frequently used to detect RNAi suppressive activity fail to identify *bona fide* VSRs. This could be due to technical limitations of the assay, the use of non-host systems, or the inability of reporter assays to identify suppressors that work in *cis* (123). Also, RNAi reporter assays may not address all aspects of the antiviral RNAi response that are putative targets for viral interference. For example, systemic spread was proposed to be essential for efficient antiviral RNAi (124), but no reporter assays have been established that would identify suppressors of systemic antiviral RNAi responses.

Outline of this thesis

Research over the last several years revealed that RNAi is the major antiviral defense mechanism in insects and that viruses and their hosts co-evolve during their ongoing arms race. In this thesis we study the cellular small RNA-based antiviral responses in insects as well as viral counter-defense mechanisms. In **chapter 2** we analyzed the interaction between Nora virus and the RNAi machinery. By performing high-throughput sequencing of small RNAs, recovered from *Drosophila* laboratory strains

Table 2. Viral RNAi suppressors in insect viruses and arboviruses

Family	Virus (abbr.)	Host/Vector ^{ab}	Experimental insect host ^c	Suppressor	Mechanism
<i>Ascoviridae</i>	<i>Heliothis virescens</i> ascovirus-3e	<i>Heliothis virescens</i>	<i>Spodoptera frugiperda</i> ; <i>Heliothis virescens</i>	Orf 27 (RNase III)	Degradation of dsRNA
<i>Birnaviridae</i>	<i>Drosophila X</i> virus	<i>D. melanogaster</i>	<i>D. melanogaster</i>	VP3	Long dsRNA binding prevents Dicer-2 cleavage; siRNA binding
	<i>Culex Y</i> virus	<i>Culex pipiens</i>	<i>Culex tarsalis</i>	VP3	Long dsRNA binding prevents Dicer-2 cleavage; siRNA binding
<i>Dicistroviridae</i>	<i>Drosophila C</i> virus (DCV)	<i>D. melanogaster</i>	<i>D. melanogaster</i>	1A	Long dsRNA binding prevents Dicer-2 cleavage; interferes with RISC assembly
	Cricket paralysis virus	<i>Teleogryllus</i> sp.	<i>D. melanogaster</i>	1A	Inhibition of AGO2 endonuclease activity
<i>Flaviviridae</i>	Dengue virus	<i>Ae. aegypti</i> ; <i>Ae. albopictus</i>	<i>Spodoptera frugiperda</i>	NS4B	Inhibition of (human) Dicer processing activity
	West Nile virus	<i>Culex</i> spp.	<i>Ae. Albopictus</i> ; <i>D. melanogaster</i>	sRNA	Inhibition of (human) Dicer processing activity
	Dengue virus	<i>Ae. aegypti</i> ; <i>Ae. albopictus</i>	<i>Ae. albopictus</i>	sRNA	-
<i>Nodaviridae</i>	Flock House virus (FHV)	<i>Costelytra zealandica</i>	<i>D. melanogaster</i> ; <i>Spodoptera frugiperda</i> ; <i>Ae. aegypti</i> ; <i>Ae. albopictus</i>	B2	Long dsRNA binding prevents Dicer-2 cleavage; siRNA binding prevents RISC incorporation; Dicer-2 binding
	Nodamuravirus (NoV)	<i>Culex tritaeniorhynchus</i>	<i>D. melanogaster</i> ; <i>An. gambiae</i> ; <i>Ae. albopictus</i>	B2	Binding of long dsRNA and siRNA; inhibition of (human) Dicer processing activity
	Wuhan Nodavirus (WhNV)	<i>Pieris rapae</i>	<i>Pieris rapae</i> ; <i>D. melanogaster</i>	B2	Long dsRNA binding prevents Dicer-2 cleavage; siRNA binding prevents RISC incorporation; Dicer-2 binding
Unassigned	<i>Nora</i> virus	<i>D. melanogaster</i>	<i>D. melanogaster</i>	VP1	Inhibition of AGO2 endonuclease activity
	Dimm <i>Nora</i> -like virus	<i>D. immigrans</i>	<i>D. immigrans</i>	VP1	Inhibition of AGO2 endonuclease activity

Replication defect of VSR mutant virus ^d	Rescue of FHV Δ B2 replicon ^e	Increased replication of recombinant Alphavirus ^f	References
yes ^g	n.t.	n.t.	(118)
n.a.	yes	n.t.	(133) Unp. obs.
n.a.	yes	n.t.	Unp. obs.
n.a.	yes	yes	(72, 88, 134)
n.a.	yes	yes	(74, 88, 89)
n.t.	n.t.	n.t.	(120)
n.t.	n.t.	yes	(121)
n.t.	n.t.	n.t.	(121)
yes	yes	yes	(74, 78, 79, 87, 91-93, 108, 112, 115, 122, 134)
yes	yes	yes	(78, 86, 87, 108, 112, 114)
n.t.	n.t.	n.t.	(113, 116)
n.t.	yes	yes	(89) Unp. obs.
n.a.	n.t.	yes	Unp. obs.

Unp. obs, unpublished observations

^a The natural host range of most insect viruses is poorly defined. We report the species from which the virus was first isolated. For the arthropod-borne viruses from the *Flaviviridae*, we report the mosquito vector.

^b Common names: *Aedes aegypti*, yellow fever mosquito; *Aedes albopictus*, tiger mosquito; *Anopheles gambiae*, African malaria mosquito; *Culex tritaeniorhynchus*, *Culex tritaeniorhynchus*, -; *Culex tarsalis*, - (no common name); *Culex pipiens*, common house mosquito; *Drosophila melanogaster*, common fruit fly; *Drosophila immigrans*, -; *Heliothis virescens*, tobacco budworm; *Pieris rapae*, the small white (butterfly); *Spodoptera frugiperda*, Fall Army worm; *Teleogryllus oceanicus* and *Teleogryllus commodus*, Australian field crickets.

^c The experimental insect host that was used to show RNAi suppressive activity and/or study the mechanism of action.
^d Replication defect in VSR mutant virus/replicon and rescue of the defect by genetic inactivation of RNAi pathway components. n.t., not tested; n.a., infectious cDNA not available.

^e VSR-mediated rescue of replication defect of RNAi suppressor-defective FHV replicon (FHV Δ B2). n.t., not tested.

^f Increased replication and/or pathogenicity of VSR-expressing recombinant Alphavirus.

^g Less viral DNA upon vRNase III knockdown in HvAV-3e infection.

that were persistently infected with this (+) RNA virus, we showed that Nora virus-derived vsiRNAs could be detected in adult flies. Using a combination of functional and biochemical assays, we identified the VP1 protein of Nora virus as the viral suppressor that antagonizes the RNAi response by inhibiting the catalytic activity of AGO2. In **chapter 3** we investigated whether RNAi mediates antiviral defense against DNA viruses. We first show that RNAi mutant flies are more susceptible to infection with the dsDNA virus IIV-6. Subsequently, we identified Dcr-2-dependent vsiRNAs in IIV-6-infected flies. In addition, we demonstrate that sense and antisense transcripts are generated during IIV-6 replication, supporting a model in which base pairing between convergent overlapping transcripts generate the viral dsRNA substrate for vsiRNA production by Dcr-2. In **chapter 4** we further discuss our findings in relation to other publications that analyzed vsiRNA profiles in DNA virus infections. Together, these studies demonstrate that an antiviral RNAi response is mounted against distinct DNA viruses in different invertebrate hosts. However, it remained unknown whether DNA viruses antagonize this small RNA-based antiviral response. In **chapter 5** we therefore studied whether IIV-6 encodes an RNAi antagonist. We show that RNAi is suppressed in IIV-6-infected cells and we mapped RNAi suppressive activity to the viral protein 340R. Using biochemical assays we reveal that 340R suppresses RNA silencing through binding of RNA duplexes, thereby inhibiting Dcr-2 processing activity and blocking RISC loading. We propose that, in analogy to RNA viruses, DNA viruses antagonize the *Drosophila* antiviral RNAi response to establish a productive infection. In **chapter 6** we analyzed small RNA profiles of mosquito cells that were infected with different classes of RNA viruses, and report the *de novo* production of viral piRNAs. **Chapter 7** provides a general discussion of the results in this thesis, as well as directions for future research.

References

1. Okamura K & Lai EC (2008) Endogenous small interfering RNAs in animals. *Nat Rev Mol Cell Biol* 9:673-678.
2. Van Rij RP & Berezhikov E (2009) Small RNAs and the control of transposons and viruses in *Drosophila*. *Trends Microbiol* 17:139-178.
3. Ghildiyal M & Zamore PD (2009) Small silencing RNAs: an expanding universe. *Nat.Rev.Genet.* 10:94-108.
4. Sabin LR, Zhou R, Gruber JJ, Lukinova N, Bambina S, Berman A, Lau CK, Thompson CB, & Cherry S (2009) Ars2 regulates both miRNA- and siRNA-dependent silencing and suppresses RNA virus infection in *Drosophila*. *Cell* 138:340-351.

5. Tomari Y, Matranga C, Haley B, Martinez N, & Zamore PD (2004) A protein sensor for siRNA asymmetry. *Science* 306:1377-1380.
6. Liu Q, Rand TA, Kalidas S, Du F, Kim HE, Smith DP, & Wang X (2003) R2D2, a bridge between the initiation and effector steps of the Drosophila RNAi pathway. *Science* 301:1921-1925.
7. Pham JW, Pellino JL, Lee YS, Carthew RW, & Sontheimer EJ (2004) A Dicer-2-dependent 80s complex cleaves targeted mRNAs during RNAi in Drosophila. *Cell* 117:83-94.
8. Pham JW & Sontheimer EJ (2005) Molecular requirements for RNA-induced silencing complex assembly in the Drosophila RNA interference pathway. *J Biol Chem* 280:39278-39283.
9. Liu X, Jiang F, Kalidas S, Smith D, & Liu Q (2006) Dicer-2 and R2D2 coordinately bind siRNA to promote assembly of the siRISC complexes. *RNA* 12:1514-1520.
10. Schwarz DS, Hutvagner G, Du T, Xu Z, Aronin N, & Zamore PD (2003) Asymmetry in the assembly of the RNAi enzyme complex. *Cell* 115:199-208.
11. Khvorova A, Reynolds A, & Jayasena SD (2003) Functional siRNAs and miRNAs exhibit strand bias. *Cell* 115:209-216.
12. Tomari Y, Du T, & Zamore PD (2007) Sorting of Drosophila small silencing RNAs. *Cell* 130:299-308.
13. Iwasaki S, Kobayashi M, Yoda M, Sakaguchi Y, Katsuma S, Suzuki T, & Tomari Y (2010) Hsc70/Hsp90 chaperone machinery mediates ATP-dependent RISC loading of small RNA duplexes. *Mol. Cell* 39:292-299.
14. Kawamata T & Tomari Y (2010) Making RISC. *Trends Biochem.Sci.* 35:368-376.
15. Miyoshi T, Takeuchi A, Siomi H, & Siomi MC (2010) A direct role for Hsp90 in pre-RISC formation in Drosophila. *Nat.Struct.Mol.Biol.* 17:1024-1026.
16. Nishida KM, Miyoshi K, Ogino A, Miyoshi T, Siomi H, & Siomi MC (2013) Roles of R2D2, a cytoplasmic D2 body component, in the endogenous siRNA pathway in Drosophila. *Mol Cell* 49:680-691.
17. Tian Y, Simanshu DK, Ascano M, Diaz-Avalos R, Park AY, Juranek SA, Rice WJ, Yin Q, Robinson CV, Tuschl T, *et al.* (2011) Multimeric assembly and biochemical characterization of the Trax-translin endonuclease complex. *Nat Struct Mol Biol* 18:658-664.
18. Liu Y, Ye X, Jiang F, Liang C, Chen D, Peng J, Kinch LN, Grishin NV, & Liu Q (2009) C3PO, an endoribonuclease that promotes RNAi by facilitating RISC activation. *Science* 325:750-753.
19. Horwich MD, Li C, Matranga C, Vagin V, Farley G, Wang P, & Zamore PD

- 1
- (2007) The *Drosophila* RNA methyltransferase, DmHen1, modifies germline piRNAs and single-stranded siRNAs in RISC. *Curr Biol* 17:1265-1272.
20. Saito K, Sakaguchi Y, Suzuki T, Siomi H, & Siomi MC (2007) Pimet, the *Drosophila* homolog of HEN1, mediates 2'-O-methylation of Piwi- interacting RNAs at their 3' ends. *Genes Dev* 21:1603-1608.
 21. Bartel DP (2009) MicroRNAs: target recognition and regulatory functions. *Cell* 136:215-233.
 22. Lee Y, Kim M, Han J, Yeom KH, Lee S, Baek SH, & Kim VN (2004) MicroRNA genes are transcribed by RNA polymerase II. *EMBO J* 23:4051-4060.
 23. Lee Y, Ahn C, Han J, Choi H, Kim J, Yim J, Lee J, Provost P, Radmark O, Kim S, *et al.* (2003) The nuclear RNase III Drosha initiates microRNA processing. *Nature* 425:415-419.
 24. Han J, Lee Y, Yeom KH, Kim YK, Jin H, & Kim VN (2004) The Drosha-DGCR8 complex in primary microRNA processing. *Genes Dev* 18:3016-3027.
 25. Han J, Lee Y, Yeom KH, Nam JW, Heo I, Rhee JK, Sohn SY, Cho Y, Zhang BT, & Kim VN (2006) Molecular basis for the recognition of primary microRNAs by the Drosha-DGCR8 complex. *Cell* 125:887-901.
 26. Denli AM, Tops BB, Plasterk RH, Ketting RF, & Hannon GJ (2004) Processing of primary microRNAs by the Microprocessor complex. *Nature* 432:231-235.
 27. Landthaler M, Yalcin A, & Tuschl T (2004) The human DiGeorge syndrome critical region gene 8 and Its D. melanogaster homolog are required for miRNA biogenesis. *Curr Biol* 14:2162-2167.
 28. Gregory RI, Yan KP, Amuthan G, Chendrimada T, Doratotaj B, Cooch N, & Shiekhattar R (2004) The Microprocessor complex mediates the genesis of microRNAs. *Nature* 432:235-240.
 29. Shibata S, Sasaki M, Miki T, Shimamoto A, Furuichi Y, Katahira J, & Yoneda Y (2006) Exportin-5 orthologues are functionally divergent among species. *Nucleic Acids Res* 34:4711-4721.
 30. Jiang F, Ye X, Liu X, Fincher L, McKearin D, & Liu Q (2005) Dicer-1 and R3D1-L catalyze microRNA maturation in *Drosophila*. *Genes Dev* 19:1674-1679.
 31. Forstemann K, Tomari Y, Du T, Vagin VV, Denli AM, Bratu DP, Klattenhoff C, Theurkauf WE, & Zamore PD (2005) Normal microRNA maturation and germ-line stem cell maintenance requires Loquacious, a double-stranded RNA-binding domain protein. *PLoS Biol* 3:e236.
 32. Saito K, Ishizuka A, Siomi H, & Siomi MC (2005) Processing of pre-microRNAs by the Dicer-1-Loquacious complex in *Drosophila* cells. *PLoS Biol* 3:e235.

33. Czech B, Zhou R, Erlich Y, Brennecke J, Binari R, Villalta C, Gordon A, Perrimon N, & Hannon GJ (2009) Hierarchical rules for Argonaute loading in *Drosophila*. *Mol. Cell* 36:445-456.
34. Okamura K, Liu N, & Lai EC (2009) Distinct mechanisms for microRNA strand selection by *Drosophila* Argonautes. *Mol. Cell* 36:431-444.
35. Ghildiyal M, Xu J, Seitz H, Weng Z, & Zamore PD (2010) Sorting of *Drosophila* small silencing RNAs partitions microRNA* strands into the RNA interference pathway. *RNA*. 16:43-56.
36. Forstemann K, Horwich MD, Wee L, Tomari Y, & Zamore PD (2007) *Drosophila* microRNAs are sorted into functionally distinct argonaute complexes after production by *dicer-1*. *Cell* 130:287-297.
37. Kawamata T, Seitz H, & Tomari Y (2009) Structural determinants of miRNAs for RISC loading and slicer-independent unwinding. *Nat Struct Mol Biol* 16:953-960.
38. Filipowicz W, Bhattacharyya SN, & Sonenberg N (2008) Mechanisms of post-transcriptional regulation by microRNAs: are the answers in sight? *Nat Rev Genet* 9:102-114.
39. Ruby JG, Jan CH, & Bartel DP (2007) Intronic microRNA precursors that bypass Drosha processing. *Nature* 448:83-86.
40. Okamura K, Hagen JW, Duan H, Tyler DM, & Lai EC (2007) The mirtron pathway generates microRNA-class regulatory RNAs in *Drosophila*. *Cell* 130:89-100.
41. Cheloufi S, Dos Santos CO, Chong MM, & Hannon GJ (2010) A *dicer*-independent miRNA biogenesis pathway that requires Ago catalysis. *Nature* 465:584-589.
42. Cifuentes D, Xue H, Taylor DW, Patnode H, Mishima Y, Cheloufi S, Ma E, Mane S, Hannon GJ, Lawson ND, *et al.* (2010) A novel miRNA processing pathway independent of *Dicer* requires Argonaute2 catalytic activity. *Science* 328:1694-1698.
43. Yang JS, Maurin T, Robine N, Rasmussen KD, Jeffrey KL, Chandwani R, Papapetrou EP, Sadelain M, O'Carroll D, & Lai EC (2010) Conserved vertebrate mir-451 provides a platform for *Dicer*-independent, Ago2-mediated microRNA biogenesis. *Proc Natl Acad Sci U S A* 107:15163-15168.
44. Iwasaki S, Kawamata T, & Tomari Y (2009) *Drosophila* argonaute1 and argonaute2 employ distinct mechanisms for translational repression. *Mol. Cell* 34:58-67.
45. Kim VN, Han J, & Siomi MC (2009) Biogenesis of small RNAs in animals. *Nat Rev Mol Cell Biol* 10:126-139.

46. Brennecke J, Aravin AA, Stark A, Dus M, Kellis M, Sachidanandam R, & Hannon GJ (2007) Discrete small RNA-generating loci as master regulators of transposon activity in *Drosophila*. *Cell* 128:1089-1103.
47. Vagin VV, Sigova A, Li C, Seitz H, Gvozdev V, & Zamore PD (2006) A distinct small RNA pathway silences selfish genetic elements in the germline. *Science* 313:320-324.
48. Saito K, Nishida KM, Mori T, Kawamura Y, Miyoshi K, Nagami T, Siomi H, & Siomi MC (2006) Specific association of Piwi with rasiRNAs derived from retrotransposon and heterochromatic regions in the *Drosophila* genome. *Genes Dev* 20:2214-2222.
49. Gunawardane LS, Saito K, Nishida KM, Miyoshi K, Kawamura Y, Nagami T, Siomi H, & Siomi MC (2007) A slicer-mediated mechanism for repeat-associated siRNA 5' end formation in *Drosophila*. *Science* 315:1587-1590.
50. Siomi MC, Sato K, Pezic D, & Aravin AA (2011) PIWI-interacting small RNAs: the vanguard of genome defence. *Nat.Rev.Mol.Cell Biol.* 12:246-258.
51. Luteijn MJ & Ketting RF (2013) PIWI-interacting RNAs: from generation to transgenerational epigenetics. *Nat Rev Genet* 14:523-534.
52. Malone CD, Brennecke J, Dus M, Stark A, McCombie WR, Sachidanandam R, & Hannon GJ (2009) Specialized piRNA pathways act in germline and somatic tissues of the *Drosophila* ovary. *Cell* 137:522-535.
53. Voigt F, Reuter M, Kasarhuo A, Schulz EC, Pillai RS, & Barabas O (2012) Crystal structure of the primary piRNA biogenesis factor Zucchini reveals similarity to the bacterial PLD endonuclease Nuc. *RNA* 18:2128-2134.
54. Nishimasu H, Ishizu H, Saito K, Fukuhara S, Kamatani MK, Bonnefond L, Matsumoto N, Nishizawa T, Nakanaga K, Aoki J, *et al.* (2012) Structure and function of Zucchini endoribonuclease in piRNA biogenesis. *Nature* 491:284-287.
55. Ipsaro JJ, Haase AD, Knott SR, Joshua-Tor L, & Hannon GJ (2012) The structural biochemistry of Zucchini implicates it as a nuclease in piRNA biogenesis. *Nature* 491:279-283.
56. Pane A, Wehr K, & Schupbach T (2007) zucchini and squash encode two putative nucleases required for rasiRNA production in the *Drosophila* germline. *Dev Cell* 12:851-862.
57. Li C, Vagin VV, Lee S, Xu J, Ma S, Xi H, Seitz H, Horwich MD, Syrzycka M, Honda BM, *et al.* (2009) Collapse of germline piRNAs in the absence of Argonaute3 reveals somatic piRNAs in flies. *Cell* 137:509-521.
58. Kawaoka S, Izumi N, Katsuma S, & Tomari Y (2011) 3' End Formation of PIWI-Interacting RNAs In Vitro. *Mol.Cell* 43:1015-1022.

59. Aravin AA, Hannon GJ, & Brennecke J (2007) The Piwi-piRNA pathway provides an adaptive defense in the transposon arms race. *Science* 318:761-764.
60. Saito K, Inagaki S, Mituyama T, Kawamura Y, Ono Y, Sakota E, Kotani H, Asai K, Siomi H, & Siomi MC (2009) A regulatory circuit for piwi by the large Maf gene traffic jam in *Drosophila*. *Nature* 461:1296-1299.
61. Saito K, Ishizu H, Komai M, Kotani H, Kawamura Y, Nishida KM, Siomi H, & Siomi MC (2010) Roles for the Yb body components Armitage and Yb in primary piRNA biogenesis in *Drosophila*. *Genes Dev* 24:2493-2498.
62. Olivieri D, Sykora MM, Sachidanandam R, Mechtler K, & Brennecke J (2010) An in vivo RNAi assay identifies major genetic and cellular requirements for primary piRNA biogenesis in *Drosophila*. *EMBO J* 29:3301-3317.
63. Klenov MS, Sokolova OA, Yakushev EY, Stolyarenko AD, Mikhaleva EA, Lavrov SA, & Gvozdev VA (2011) Separation of stem cell maintenance and transposon silencing functions of Piwi protein. *Proc Natl Acad Sci U S A* 108:18760-18765.
64. Darricarrere N, Liu N, Watanabe T, & Lin H (2013) Function of Piwi, a nuclear Piwi/Argonaute protein, is independent of its slicer activity. *Proc Natl Acad Sci U S A* 110:1297-1302.
65. Huang XA, Yin H, Sweeney S, Raha D, Snyder M, & Lin H (2013) A major epigenetic programming mechanism guided by piRNAs. *Dev Cell* 24:502-516.
66. Rozhkov NV, Hammell M, & Hannon GJ (2013) Multiple roles for Piwi in silencing *Drosophila* transposons. *Genes Dev* 27:400-412.
67. Sienski G, Donertas D, & Brennecke J (2012) Transcriptional silencing of transposons by Piwi and maelstrom and its impact on chromatin state and gene expression. *Cell* 151:964-980.
68. Le Thomas A, Rogers AK, Webster A, Marinov GK, Liao SE, Perkins EM, Hur JK, Aravin AA, & Toth KF (2013) Piwi induces piRNA-guided transcriptional silencing and establishment of a repressive chromatin state. *Genes Dev* 27:390-399.
69. Wang SH & Elgin SC (2011) *Drosophila* Piwi functions downstream of piRNA production mediating a chromatin-based transposon silencing mechanism in female germ line. *Proc Natl Acad Sci U S A* 108:21164-21169.
70. Weber F, Wagner V, Rasmussen SB, Hartmann R, & Paludan SR (2006) Double-stranded RNA is produced by positive-strand RNA viruses and DNA viruses but not in detectable amounts by negative-strand RNA viruses. *J Virol* 80:5059-5064.
71. Mueller S, Gausson V, Vodovar N, Deddouche S, Troxler L, Perot J, Pfeffer S, Hoffmann JA, Saleh MC, & Imler JL (2010) RNAi-mediated immunity

- provides strong protection against the negative-strand RNA vesicular stomatitis virus in *Drosophila*. *Proc.Natl.Acad.Sci.U.S.A* 107:19390-19395.
72. Van Rij RP, Saleh MC, Berry B, Foo C, Houk A, Antoniewski C, & Andino R (2006) The RNA silencing endonuclease Argonaute 2 mediates specific antiviral immunity in *Drosophila melanogaster*. *Genes Dev* 20:2985-2995.
 73. Galiana-Arnoux D, Dostert C, Schneemann A, Hoffmann JA, & Imler JL (2006) Essential function in vivo for Dicer-2 in host defense against RNA viruses in *drosophila*. *Nat Immunol* 7:590-597.
 74. Wang XH, Aliyari R, Li WX, Li HW, Kim K, Carthew R, Atkinson P, & Ding SW (2006) RNA interference directs innate immunity against viruses in adult *Drosophila*. *Science* 312:452-454.
 75. Keene KM, Foy BD, Sanchez-Vargas I, Beaty BJ, Blair CD, & Olson KE (2004) From the Cover: RNA interference acts as a natural antiviral response to O'nyong-nyong virus (Alphavirus; Togaviridae) infection of *Anopheles gambiae*. *Proc Natl Acad Sci U S A* 101:17240-17245.
 76. Campbell CL, Keene KM, Brackney DE, Olson KE, Blair CD, Wilusz J, & Foy BD (2008) *Aedes aegypti* uses RNA interference in defense against Sindbis virus infection. *BMC Microbiol* 8:47.
 77. Sanchez-Vargas I, Scott JC, Poole-Smith BK, Franz AW, Barbosa-Solomieu V, Wilusz J, Olson KE, & Blair CD (2009) Dengue virus type 2 infections of *Aedes aegypti* are modulated by the mosquito's RNA interference pathway. *PLoS Pathog* 5:e1000299.
 78. Myles KM, Wiley MR, Morazzani EM, & Adelman ZN (2008) Alphavirus-derived small RNAs modulate pathogenesis in disease vector mosquitoes. *Proc. Natl.Acad.Sci.U.S.A* 105:19938-19943.
 79. Cirimotich CM, Scott JC, Phillips AT, Geiss BJ, & Olson KE (2009) Suppression of RNA interference increases alphavirus replication and virus-associated mortality in *Aedes aegypti* mosquitoes. *BMC Microbiol* 9:49.
 80. Bronkhorst AW, van Cleef KW, Vodovar N, Ince IA, Blanc H, Vlaskovic JM, Saleh MC, & van Rij RP (2012) The DNA virus Invertebrate iridescent virus 6 is a target of the *Drosophila* RNAi machinery. *Proc Natl Acad Sci U S A* 109:E3604-3613.
 81. Kemp C, Mueller S, Goto A, Barbier V, Paro S, Bonnay F, Dostert C, Troxler L, Hetru C, Meignin C, *et al.* (2013) Broad RNA interference-mediated antiviral immunity and virus-specific inducible responses in *Drosophila*. *J Immunol* 190:650-658.
 82. Jayachandran B, Hussain M, & Asgari S (2012) RNA interference as a cellular defense mechanism against the DNA virus baculovirus. *J Virol* 86:13729-

- 13734.
83. Sabin LR, Zheng Q, Thekkat P, Yang J, Hannon GJ, Gregory BD, Tudor M, & Cherry S (2013) Dicer-2 processes diverse viral RNA species. *PLoS One* 8:e55458.
 84. Bronkhorst AW, Miesen P, & van Rij RP (2013) Small RNAs tackle large viruses: RNA interference-based antiviral defense against DNA viruses in insects. *Fly*, 7, 216-223.
 85. Marques JT, Wang JP, Wang X, de Oliveira KP, Gao C, Aguiar ER, Jafari N, & Carthew RW (2013) Functional specialization of the small interfering RNA pathway in response to virus infection. *PLoS Pathog* 9:e1003579.
 86. Han YH, Luo YJ, Wu Q, Jovel J, Wang XH, Aliyari R, Han C, Li WX, & Ding SW (2011) RNA-based immunity terminates viral infection in adult *Drosophila* in the absence of viral suppression of RNA interference: characterization of viral small interfering RNA populations in wild-type and mutant flies. *J Virol* 85:13153-13163.
 87. Aliyari R, Wu Q, Li HW, Wang XH, Li F, Green LD, Han CS, Li WX, & Ding SW (2008) Mechanism of induction and suppression of antiviral immunity directed by virus-derived small RNAs in *Drosophila*. *Cell Host Microbe* 4:387-397.
 88. Nayak A, Berry B, Tassetto M, Kunitomi M, Acevedo A, Deng C, Krutchinsky A, Gross J, Antoniewski C, & Andino R (2010) Cricket paralysis virus antagonizes Argonaute 2 to modulate antiviral defense in *Drosophila*. *Nat. Struct. Mol. Biol.* 17:547-554.
 89. van Mierlo JT, Bronkhorst AW, Overheul GJ, Sadanandan SA, Ekstrom JO, Heestermans M, Hultmark D, Antoniewski C, & van Rij RP (2012) Convergent evolution of argonaute-2 slicer antagonism in two distinct insect RNA viruses. *PLoS Pathog* 8:e1002872.
 90. Kopek BG, Perkins G, Miller DJ, Ellisman MH, & Ahlquist P (2007) Three-dimensional analysis of a viral RNA replication complex reveals a virus-induced mini-organelle. *PLoS Biol* 5:e220.
 91. Lingel A, Simon B, Izaurralde E, & Sattler M (2005) The structure of the flock house virus B2 protein, a viral suppressor of RNA interference, shows a novel mode of double-stranded RNA recognition. *EMBO Rep* 6:1149-1155.
 92. Chao JA, Lee JH, Chapados BR, Debler EW, Schneemann A, & Williamson JR (2005) Dual modes of RNA-silencing suppression by Flock House virus protein B2. *Nat Struct Mol Biol* 12:952-957.
 93. Lu R, Maduro M, Li F, Li HW, Broitman-Maduro G, Li WX, & Ding SW (2005) Animal virus replication and RNAi-mediated antiviral silencing in

- 1
- Caenorhabditis elegans *Nature* 436:1040-1043.
94. Vodovar N, Goic B, Blanc H, & Saleh MC (2011) In silico reconstruction of viral genomes from small RNAs improves virus-derived small interfering RNA profiling. *J Virol* 85:11016-11021.
 95. Banerjee AK (1987) Transcription and replication of rhabdoviruses. *Microbiological reviews* 51:66-87.
 96. Huszar T & Imler JL (2008) Drosophila viruses and the study of antiviral host-defense. *Adv Virus Res* 72:227-265.
 97. Conzelmann KK (1998) Nonsegmented negative-strand RNA viruses: genetics and manipulation of viral genomes. *Annu Rev Genet* 32:123-162.
 98. Brackney DE, Scott JC, Sagawa F, Woodward JE, Miller NA, Schilkey FD, Mudge J, Wilusz J, Olson KE, Blair CD, *et al.* (2010) C6/36 Aedes albopictus cells have a dysfunctional antiviral RNA interference response. *PLoS.Negl. Trop. Dis.* 4:e856.
 99. Leger P, Lara E, Jagla B, Sismeiro O, Mansuroglu Z, Coppee JY, Bonnefoy E, & Bouloy M (2013) Dicer-2- and piwi-mediated RNA interference in rift valley Fever virus-infected mosquito cells. *J Virol* 87:1631-1648.
 100. Schnettler E, Ratniner M, Watson M, Shaw AE, McFarlane M, Varela M, Elliott RM, Palmarini M, & Kohl A (2013) RNA interference targets arbovirus replication in Culicoides cells. *J Virol* 87:2441-2454.
 101. Ahlquist P (2006) Parallels among positive-strand RNA viruses, reverse-transcribing viruses and double-stranded RNA viruses. *Nat.Rev.Microbiol.* 4:371-382.
 102. Hjalmarsson A, Carlemalm E, & Everitt E (1999) Infectious pancreatic necrosis virus: identification of a VP3-containing ribonucleoprotein core structure and evidence for O-linked glycosylation of the capsid protein VP2. *J Virol* 73:3484-3490.
 103. Luque D, Saugar I, Rejas MT, Carrascosa JL, Rodriguez JF, & Caston JR (2009) Infectious Bursal disease virus: ribonucleoprotein complexes of a double-stranded RNA virus. *J Mol Biol* 386:891-901.
 104. Wu Q, Luo Y, Lu R, Lau N, Lai EC, Li WX, & Ding SW (2010) Virus discovery by deep sequencing and assembly of virus-derived small silencing RNAs. *Proc. Natl.Acad.Sci. U.S.A* 107:1606-1611.
 105. van Mierlo JT, van Cleef KWR, & Van Rij RP (2010) Small Silencing RNAs: Piecing Together a Viral Genome. *Cell Host & Microbe* 7:87-89.
 106. Scott JC, Brackney DE, Campbell CL, Bondu-Hawkins V, Hjelle B, Ebel GD, Olson KE, & Blair CD (2010) Comparison of dengue virus type 2-specific small RNAs from RNA interference-competent and -incompetent mosquito

- cells. *PLoS.Negl.Trop.Dis.* 4:e848.
107. Hess AM, Prasad AN, Pritsyn A, Ebel GD, Olson KE, Barbacioru C, Monighetti C, & Campbell CL (2011) Small RNA profiling of Dengue virus-mosquito interactions implicates the PIWI RNA pathway in anti-viral defense. *BMC. Microbiol.* 11:45.
 108. Morazzani EM, Wiley MR, Murreddu MG, Adelman ZN, & Myles KM (2012) Production of virus-derived ping-pong-dependent piRNA-like small RNAs in the mosquito soma. *PLoS Pathog* 8:e1002470.
 109. Vodovar N, Bronkhorst AW, van Cleef KW, Miesen P, Blanc H, van Rij RP, & Saleh MC (2012) Arbovirus-Derived piRNAs Exhibit a Ping-Pong Signature in Mosquito Cells. *PLoS One* 7:e30861.
 110. Schnettler E, Donald CL, Human S, Watson M, Siu RW, McFarlane M, Fazakerley JK, Kohl A, & Fragkoudis R (2013) Knockdown of piRNA pathway proteins results in enhanced Semliki Forest virus production in mosquito cells. *J Gen Virol* 94:1680-1689.
 111. Campbell CL, Black WC, Hess AM, & Foy BD (2008) Comparative genomics of small RNA regulatory pathway components in vector mosquitoes. *BMC. Genomics* 9:425.
 112. Li WX, Li H, Lu R, Li F, Dus M, Atkinson P, Brydon EW, Johnson KL, Garcia-Sastre A, Ball LA, *et al.* (2004) Interferon antagonist proteins of influenza and vaccinia viruses are suppressors of RNA silencing. *Proc Natl Acad Sci U S A* 101:1350-1355.
 113. Qi N, Cai D, Qiu Y, Xie J, Wang Z, Si J, Zhang J, Zhou X, & Hu Y (2011) RNA binding by a novel helical fold of b2 protein from wuhan nodavirus mediates the suppression of RNA interference and promotes b2 dimerization. *J Virol* 85:9543-9554.
 114. Sullivan C & Ganem D (2005) A virus encoded inhibitor that blocks RNA interference in mammalian cells. *J Virol* 79:7371-7379.
 115. Singh G, Popli S, Hari Y, Malhotra P, Mukherjee S, & Bhatnagar RK (2009) Suppression of RNA silencing by Flock house virus B2 protein is mediated through its interaction with the PAZ domain of Dicer. *FASEB J.* 23:1845-1857.
 116. Qi N, Zhang L, Qiu Y, Wang Z, Si J, Liu Y, Xiang X, Xie J, Qin CF, Zhou X, *et al.* (2012) Targeting of dicer-2 and RNA by a viral RNA silencing suppressor in *Drosophila* cells. *J Virol* 86:5763-5773.
 117. Korber S, Shaik Syed Ali P, & Chen JC (2009) Structure of the RNA-binding domain of Nodamura virus protein B2, a suppressor of RNA interference. *Biochemistry* 48:2307-2309.

118. Hussain M, Abraham AM, & Asgari S (2010) An Ascovirus-encoded RNase III autoregulates its expression and suppresses RNA interference-mediated gene silencing. *J Virol* 84:3624-3630.
119. Cuellar WJ, Kreuze JF, Rajamaki ML, Cruzado KR, Untiveros M, & Valkonen JP (2009) Elimination of antiviral defense by viral RNase III. *Proc Natl Acad Sci U S A* 106:10354-10358.
120. Kakumani PK, Ponia SS, S RK, Sood V, Chinnappan M, Banerjea AC, Medigeshi GR, Malhotra P, Mukherjee SK, & Bhatnagar RK (2013) Role of RNA interference (RNAi) in dengue virus replication and identification of NS4B as an RNAi suppressor. *J Virol* 87:8870-8883.
121. Schnettler E, Sterken MG, Leung JY, Metz SW, Geertsema C, Goldbach RW, Vlak JM, Kohl A, Khromykh AA, & Pijlman GP (2012) Noncoding flavivirus RNA displays RNA interference suppressor activity in insect and Mammalian cells. *J Virol* 86:13486-13500.
122. Li HW, Li WX, & Ding SW (2002) Induction and suppression of RNA silencing by an animal virus. *Science* 296:1319-1321.
123. Mari-Ordonez A, Marchais A, Etcheverry M, Martin A, Colot V, & Voinnet O (2013) Reconstructing de novo silencing of an active plant retrotransposon. *Nat Genet* 45:1029-1039.
124. Saleh MC, Tassetto M, Van Rij RP, Goic B, Gausson V, Berry B, Jacquier C, Antoniewski C, & Andino R (2009) Antiviral immunity in *Drosophila* requires systemic RNA interference spread. *Nature* 458:346-350.
125. Myles KM, Morazzani EM, & Adelman ZN (2009) Origins of alphavirus-derived small RNAs in mosquitoes. *RNA Biol* 6:387-391.
126. Siu RW, Fragkoudis R, Simmonds P, Donald CL, Chase-Topping ME, Barry G, Attarzadeh-Yazdi G, Rodriguez-Andres J, Nash AA, Merits A, *et al.* (2011) Antiviral RNA interference responses induced by Semliki Forest virus infection of mosquito cells: characterization, origin, and frequency-dependent functions of virus-derived small interfering RNAs. *J Virol* 85:2907-2917.
127. Brackney DE, Beane JE, & Ebel GD (2009) RNAi targeting of West Nile virus in mosquito midguts promotes virus diversification. *PLoS.Pathog.* 5:e1000502.
128. Flynt A, Liu N, Martin R, & Lai EC (2009) Dicing of viral replication intermediates during silencing of latent *Drosophila* viruses. *Proc.Natl.Acad. Sci.U.S.A* 106:5270-5275.
129. Huang Y, Mi Z, Zhuang L, Ma M, An X, Liu W, Cao W, & Tong Y (2013) Presence of entomobirnaviruses in Chinese mosquitoes in the absence of Dengue virus co-infection. *J Gen Virol* 94:663-667.
130. Ma M, Huang Y, Gong Z, Zhuang L, Li C, Yang H, Tong Y, Liu W, & Cao W

- (2011) Discovery of DNA viruses in wild-caught mosquitoes using small RNA high throughput sequencing. *PLoS One* 6:e24758.
131. Ambrose RL, Lander GC, Maaty WS, Bothner B, Johnson JE, & Johnson KN (2009) *Drosophila A* virus is an unusual RNA virus with a T=3 icosahedral core and permuted RNA-dependent RNA polymerase. *J Gen Virol* 90:2191-2200.
 132. Marklewitz M, Gloza-Rausch F, Kurth A, Kummerer BM, Drosten C, & Junglen S (2012) First isolation of an Entomobirnavirus from free-living insects. *J Gen Virol* 93:2431-2435.
 133. Valli A, Busnadiago I, Maliogka V, Ferrero D, Caston JR, Rodriguez JF, & Garcia JA (2012) The VP3 factor from viruses of Birnaviridae family suppresses RNA silencing by binding both long and small RNA duplexes. *PLoS One* 7:e45957.
 134. Berry B, Deddouche S, Kirschner D, Imler JL, & Antoniewski C (2009) Viral suppressors of RNA silencing hinder exogenous and endogenous small RNA pathways in *Drosophila*. *PLoS. One.* 4:e5866.

Chapter 2

Convergent evolution of Argonaute-2 Slicer antagonism in two distinct insect RNA viruses

Joël T. van Mierlo, Alfred W. Bronkhorst, Gijs J. Overheul, Sajna A. Sadanandan, Jens-Ola Ekström, Marco Heestermans, Dan Hultmark, Christophe Antoniewski and Ronald P. van Rij

PLoS Pathogens 2012, 8:e1002872

Abstract

RNA interference (RNAi) is a major antiviral pathway that shapes evolution of RNA viruses. We show here that Nora virus, a natural *Drosophila* pathogen, is both a target and suppressor of RNAi. We detected viral small RNAs with a signature of Dicer-2-dependent small interfering RNAs in Nora virus-infected *Drosophila*. Furthermore, we demonstrate that the Nora virus VP1 protein contains RNAi suppressive activity *in vitro* and *in vivo* that enhances pathogenicity of recombinant Sindbis virus in an RNAi-dependent manner. Nora virus VP1 and the viral suppressor of RNAi of Cricket paralysis virus (1A) antagonized Argonaute-2 (AGO2) Slicer activity of RNA induced silencing complexes preloaded with a methylated single-stranded guide strand. The convergent evolution of AGO2 suppression in two unrelated insect RNA viruses highlights the importance of AGO2 in antiviral defense.

Introduction

An efficient antiviral immune response is essential for the control or elimination of virus infection and for survival of the infected host. The immune system exerts a strong evolutionary pressure that shapes the genetic makeup of viral pathogens. Indeed, viruses evolved counter-defense mechanisms to evade, suppress or inactivate host immunity. Studying these mechanisms provides important insight in the critical steps of antiviral responses and may uncover novel components and regulators of immune pathways.

Plants, fungi, and invertebrate animals rely on the RNA interference (RNAi) pathway for antiviral defense (1, 2). The initial trigger of an antiviral RNAi response is the recognition and cleavage of viral double-stranded RNA (dsRNA) into viral small interfering RNAs (vsiRNAs), in insects by the ribonuclease Dicer-2 (Dcr-2). These vsiRNAs act as specificity determinants of the Argonaute-2 (AGO2) containing effector nuclease complex RISC (RNA induced silencing complex). RISC maturation involves a number of sequential steps: loading of the vsiRNA into AGO2, cleavage and elimination of the passenger RNA strand, and 2'-O-methylation of the 3'-terminal nucleotide of the retained guide strand. It is thought that vsiRNA-loaded RISC subsequently cleaves viral target RNA (Slicer activity). The hypersensitivity to viral infections of *AGO2* mutant flies and of *AGO2* knockdown mosquitoes provides genetic support for this hypothesis (3-7). Nevertheless, direct evidence supporting this model, for example by the detection of viral Slicer products, is lacking.

The evolution of viral suppressors of RNAi (VSRs) is a testament to the antiviral potential of the RNAi pathway in plants and insects. Given the central role of dsRNA and siRNAs as initiators and specificity determinants of the RNAi pathway, it is not surprising that many VSRs sequester dsRNA. For instance, the *Drosophila C virus* (DCV) 1A protein binds long dsRNA and shields it from processing by Dcr-2 (6). Flock House virus (FHV) B2 displays a dual RNA binding activity: it binds long dsRNA as well as siRNAs, thereby preventing their incorporation into RISC (8-10). Similarly, many plant VSRs display dsRNA binding activities, leading to the hypothesis that dsRNA or siRNA binding is a general mechanism for RNAi suppression (11, 12). Nevertheless, other mechanisms have been reported (1). The RNAi suppressive activity of the Cricket paralysis virus (CrPV) 1A protein, for example, relies on a direct interaction with AGO2 (13).

VSRs have been identified in dozens of plant viruses from all major virus families (1). In contrast, VSRs have thus far been identified in only three insect RNA viruses (FHV, CrPV, and DCV). These VSRs were characterized using genetic and biochemical approaches in the model organism *Drosophila melanogaster*. While these viruses indeed efficiently infect *Drosophila* laboratory stocks and cell lines, DCV is the only natural

Drosophila pathogen among these three viruses (14, 15). Although FHV and CrPV have a remarkable broad host range in the laboratory, they were originally isolated from non-*Drosophilid* host species: the New Zealand grass grub (*Costelytra zealandica*) and field crickets (*Teleogryllus oceanicus* and *T. commodus*), respectively (16-19).

Since viral counter-defense mechanisms co-evolve with the antiviral immune responses of the host species, it is essential to characterize a VSR within the correct evolutionary context. We therefore set out to identify an RNAi suppressor in Nora virus, a positive sense (+) RNA virus that persistently infects *Drosophila* laboratory stocks as well as *Drosophila* in the wild (20) (D.J. Obbard, personal communication). The genome organization and phylogeny suggest that Nora virus is the type member of a novel virus family within the order of *Picornavirales* (20). Here we show that Nora virus VP1, the protein product of open reading frame 1 (ORF1), suppresses RNAi in cell culture as well as in flies. In accordance, VP1 is an RNAi-dependent viral pathogenicity factor. In a series of biochemical assays, we show that both Nora virus VP1 as well as CrPV 1A inhibit Slicer activity of a pre-assembled RISC loaded with a methylated guide strand. The lack of amino acid sequence similarity between CrPV 1A and Nora virus VP1 suggests that their Slicer antagonistic activities resulted from convergent evolution, providing direct support for the critical role of AGO2 Slicer activity in antiviral defense.

Results

Nora virus is a target of RNAi *in vivo*

Nora virus is an enteric (+) RNA virus that successfully establishes a persistent infection in flies (20). The mechanism by which this virus establishes persistent infections is unknown. To determine whether Nora virus is a target for Dcr-2, we analyzed the presence of Nora virus small RNAs in the *w¹¹¹⁸* *Drosophila* strain that is widely used as a recipient strain for transgenesis. We isolated and sequenced 19-29 nt small RNAs from body (abdomen and thorax), thorax and head of adult *w¹¹¹⁸* flies. Sequence reads that perfectly matched the *Drosophila* genome were annotated and discarded. Of the remaining reads, 396,646 (7.8%, body), 237,265 (10.6%, thorax), and 1,099,496 (7.7%, head) matched the published Nora virus sequence (NC_007919.3), indicating that the *w¹¹¹⁸* strain was infected by Nora virus (Table 1). As RNA viruses rapidly evolve, viral small RNA sequences may have been missed in this initial matching step. We therefore reconstituted the Nora virus genome through an iterative alignment/consensus treatment of the viral small RNA sequences in our libraries (21). The reconstituted Nora virus genome (rNora virus) differed at only 3.2% of the nucleotides from the published genome sequence. Aligning small RNAs to the rNora virus genome instead

of the published Nora virus sequence resulted in an increased number of viral reads in the three libraries (~121%, Table 1). We therefore used the reconstituted genome as a reference genome in further analyses.

Table 1. Annotation of small RNA sequences in libraries from body (abdomen and thorax), thorax, and head of Nora virus-infected *w¹¹¹⁸* adult flies

	Body	Thorax	Head
Total library	18,296,275	17,280,520	49,633,458
Match to <i>D. melanogaster</i> *	13,184,119	15,033,831	35,435,546
Unmatched*	5,112,156	2,246,689	14,197,912
Nora virus (NC_007919.3)*	396,646	237,265	1,099,496
Nora virus (reconstituted)*	479,572	291,045	1,329,336

* The number of reads matching the *Drosophila* genome, reads that fail to map to the *Drosophila* genome (unmatched), and reads mapping to the Nora virus genome (isolate Umea 2007) and the reconstituted Nora virus genome are indicated for each library.

In all three libraries, Nora virus-derived small RNAs were predominantly 21-nt long, the typical size of Dcr-2 products. The size distribution of small RNAs derived from the (+) RNA strand, however, were noticeably wider than those derived from the (-) RNA strand (Figure 1A). For 21-nt viral RNA reads, there was only a slight bias towards (+) small RNAs (ratio (+) RNA / total RNA ~0.58), whereas small RNAs of other sizes were predominantly derived from the (+) strand (Figure 1B). In all three libraries, the 21-nt Nora virus-derived RNAs are distributed across the genome, covering both the (+) and (-) viral RNA strands with approximately equal numbers (Figure 1C). These data suggest that dsRNA replication intermediates of Nora virus are processed into 21-nt long siRNAs. The origin of the other size classes of viral small RNAs remains unclear. However, as the predominance of (+) over (-) small RNA reads is reminiscent of the excess of (+) over (-) viral (full-length) RNA that is typically observed in (+) RNA virus infection, they may be due to non-specific RNA degradation.

Drosophila Dcr-2 generates 21-nt duplex siRNAs in which 19 nucleotides are base paired leaving a 2-nt 3' overhang at each end. For each library, we collected the 21-nt RNA reads whose 5' ends overlapped with another 21-nt RNA read on the opposite strand of the Nora virus genome. Then, for each possible overlap of 1 to 21-nt, the numbers of read pairs were counted and converted into Z-scores (Figure 1D). This analysis revealed that 21-nt Nora virus-derived RNAs in body and thorax libraries tend to overlap by 19-nt, which is a typical feature of siRNA duplex precursors. This siRNA duplex signature was observed to a lesser extent in head libraries. Very little Nora virus RNA can be detected in the head (22), yet vsiRNA levels were similar in head, thorax, and body

(Table 1). The origin of the vsiRNAs in the head and the reason for the less pronounced vsiRNA signature of those small RNAs remain unclear. Altogether, our results strongly suggest that Nora virus double-stranded replication intermediates are processed by Dcr-2 into vsiRNAs that trigger an RNAi response in infected flies.

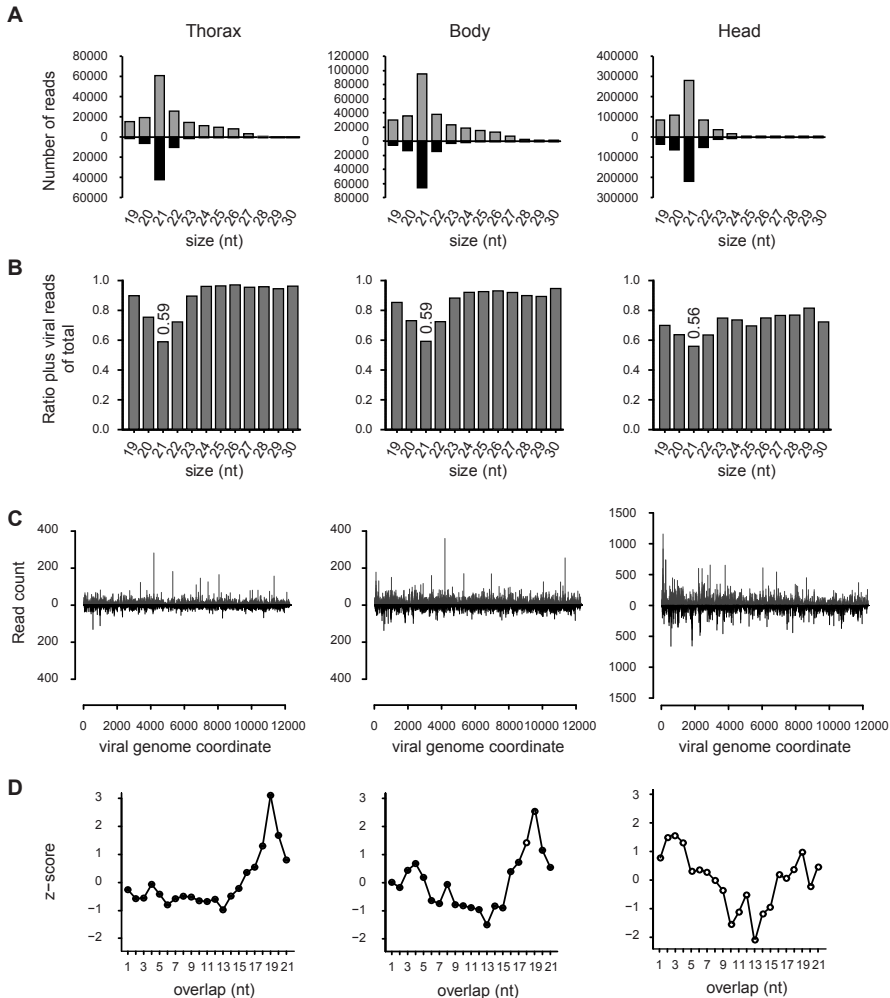


Figure 1. Nora virus is targeted by RNAi in adult flies. (A) Size distribution of Nora virus-derived small RNAs in libraries from thoraxes, bodies and heads of *w¹¹¹⁸* flies. Read counts of small RNAs matching the (+) and (-) viral RNA strands are in gray and black, respectively. (B) Proportion of (+) Nora virus small RNA reads of total viral reads. Frequencies were computed from the distributions in panel A for each size class. (C) Viral siRNA distribution across the viral genome. The abundance of 21-nt small RNAs matching the (+) and (-) viral RNA strands of the reconstituted Nora virus (rNora) reference genome is shown in gray and black, respectively. (D) Z-scores for the number of overlapping pairs of sense and antisense 21-nt Nora virus small RNAs matching the rNora virus reference genome. For each possible overlap of 1 to 21-nt, the number of read pairs was counted and converted into a Z-score.

Nora virus VP1 suppresses RNAi *in vitro*

Our small RNA profiles indicate that Nora virus is targeted by Dcr-2. Nevertheless, the virus efficiently establishes a persistent infection, suggesting that it is able to evade or suppress the antiviral RNAi response. The Nora virus genome contains four open reading frames (ORFs) (Figure 2A). Nora virus ORF2 is predicted to encode the helicase, protease, and polymerase domains that together form a picornavirus-like replication cassette. ORF4 encodes three proteins that make up the Nora virus capsid (VP4A, VP4B, and VP4C) (23). To determine whether the Nora virus genome encodes an RNAi suppressor, we analyzed the four ORFs in an RNAi sensor assay in *Drosophila* cell culture (Figure 2B-2D).

In this assay, S2 cells are transfected with firefly (Fluc) and *Renilla* luciferase (Rluc) reporter plasmids and a plasmid that expresses one of the four viral ORFs. Subsequently, Fluc expression is silenced using specific dsRNA, and Fluc and Rluc activity is monitored. As expected, DCV 1A, a well characterized VSR that binds long dsRNA, efficiently suppressed RNAi, whereas the inactive DCV 1A K73A mutant was unable to do so (Figure 2C and (6)). Cotransfection of the ORF1 expression plasmid also resulted in de-repression of Fluc, suggesting that VP1, the protein product of ORF1, is a suppressor of RNAi. Expression of ORF3 and ORF4 did not affect Fluc activity (Figure 2C). However, since expression of ORF2 and the production of mature capsid proteins from ORF4 were not detectable on Western blot, we cannot exclude the possibility that these protein products are able to suppress RNAi as well (Figure 2B).

Next, we tested whether VP1 inhibits the production of siRNAs by Dcr-2 or a subsequent step in the RNAi pathway. To this end, we repeated the RNAi sensor assay using a synthetic siRNA that does not require Dcr-2 cleavage for its silencing activity. Also under these conditions, Nora virus VP1 suppressed silencing of the Fluc reporter. Furthermore, VP1 suppressed RNAi to a similar extent as CrPV 1A, which was previously shown to suppress the effector stage of the RNAi machinery (13) (Figure 2D).

In *Drosophila*, the microRNA (miRNA) and siRNA pathways are separate processes, with Dcr-1 and AGO1 dedicated to the miRNA pathway and Dcr-2 and AGO2 to the siRNA pathway. Nevertheless, crosstalk between the miRNA and RNAi pathways occurs. Using miRNA sensor assays in S2 cells, in which Fluc expression is silenced by endogenous miRNAs or co-expressed primary miRNAs, we observed that VP1 does not suppress miRNA activity (Text S1 and Figure S1). Together, these data indicate that VP1 is able to suppress the RNAi, but not the miRNA pathway, at a step after dsRNA processing by Dcr-2.

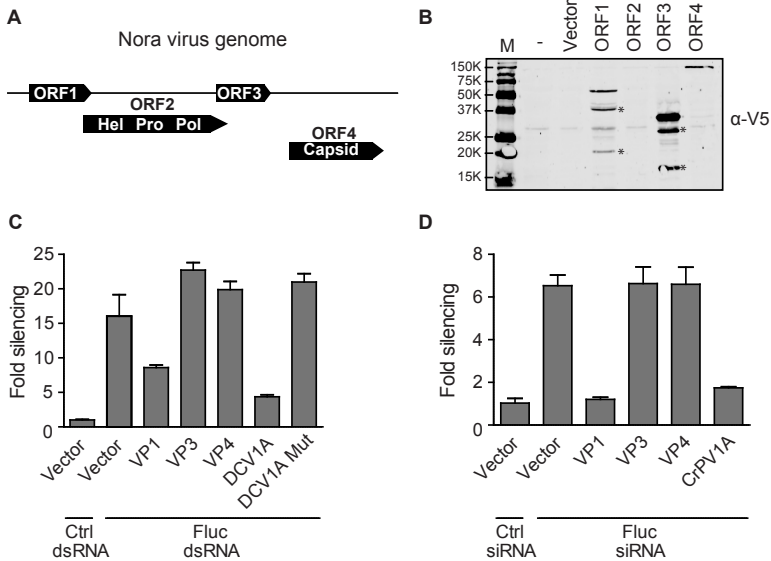


Figure 2. Nora virus VP1 suppresses RNAi *in vitro*. (A) Schematic representation of the Nora virus genome with its four predicted ORFs in three different reading frames. There is a 7-nt overlap between ORF1 and ORF2 and a 26-nt overlap between ORF2 with ORF3. An intergenic region of 85-nt separates ORF3 and ORF4. (B) Western blot analysis of V5-epitope tagged Nora virus expression constructs. Two days after transfection of the indicated plasmids into S2 cells, expression of the constructs was analyzed by Western blot using the V5 antibody (α -V5). Asterisks (*) indicate additional bands that do not correspond to the expected size of the full-length protein product. (C) RNAi reporter assay in *Drosophila* S2 cells. Copper-inducible plasmids encoding Fluc and Rluc were transfected into S2 cells together with a construct expressing Nora virus ORF1, 3, and 4, encoding viral protein 1 (VP1), VP3, and VP4, respectively. Two days after transfection, dsRNA targeting Fluc or GFP (Ctrl) was added to the medium. Seven hours later, expression of Fluc and Rluc was induced and luciferase activity was measured the next day. Fluc counts were normalized to Rluc counts and presented as fold silencing relative to the control GFP dsRNA. Plasmids encoding DCV 1A and the K73A mutant (DCV 1A mut) were used as controls. (D) siRNA-based RNAi reporter assay. The experiment was performed as described in panel C, but 21-nt Fluc siRNAs were cotransfected with the reporter plasmids to silence gene expression. An siRNA targeting the human MDA5 gene was used as a non-silencing control (Ctrl). Bars in panel C represent averages and standard deviations of five independent samples; bars in panel D represent averages and standard deviations of three independent samples. Panel C and D are representative for two and three independent experiments, respectively.

The C-terminus of VP1 is essential for its suppressor activity

VP1 is highly conserved among different Nora virus isolates (Figure S2). We were unable to predict a protein domain in VP1 suggestive of a mechanism of action. Furthermore, we did not obtain a significant alignment to any other protein from the non-redundant protein sequence database. To map the VSR region of VP1, we generated a series of N- and C-terminal (Δ N and Δ C) truncations and tested them in the RNAi reporter assay in S2 cells (Figures 3A and S3). With the exception of the VP1 ^{Δ N390} and VP1 ^{Δ N418} mutants,

in which no protein could be detected on Western blot, all VP1^{ΔN} and VP1^{ΔC} constructs produced proteins of the expected size (Figure 3B). Deletion of 74 amino acids (aa) or more from the C-terminus of VP1 resulted in loss of suppressor activity (Figure 3C). This suggests that the active domain of VP1 resides in its C-terminal region. Indeed, deleting up to 351-aa from the N-terminus (VP1^{ΔN351}), out of a total of 475-aa, did not affect VSR activity. These results show that the RNAi suppressor activity of VP1 maps to the C-terminal 124-aa.

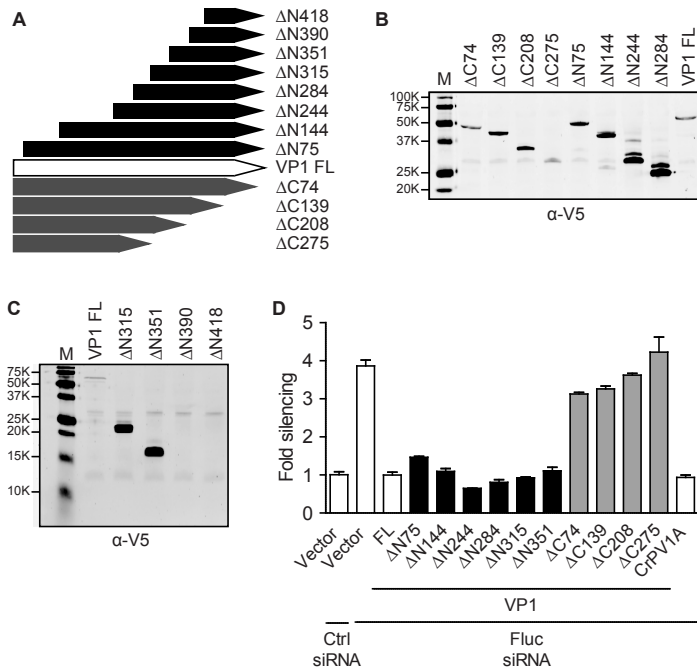


Figure 3. The C-terminus of Nora virus VP1 is essential for RNAi suppressor activity. (A) Schematic presentation of full-length (FL) and N- and C-terminal deletion mutants (ΔN and ΔC) of VP1. (B, C) Western blot analysis of VP1 expression constructs. V5 epitope tagged expression constructs were transfected into *Drosophila* S2 cells and expression of VP1^{FL} and the deletion mutants was analyzed by Western blot using a V5 antibody (α-V5). (D) RNAi reporter assay in S2 cells. The experiment was performed as described in the legend to Figure 2D, using plasmids encoding either CrPV 1A, VP1^{FL} or the VP1 deletion mutants. Bars represent averages and standard deviations of three independent samples. The graph is representative for two independent experiments.

VP1 is an RNAi suppressor *in vivo*

We next evaluated the VSR activity of Nora virus VP1 *in vivo* using transgenic flies in which *thread* (*th*), also known as *Drosophila inhibitor of apoptosis 1*, can be silenced by expression of dsRNA targeting this gene (*th*^{RNAi} (24, 25)) (Figure 4). Eye-specific

expression of th^{RNAi} using the GMR-Gal4 driver leads to severe apoptosis in the developing eye. As a consequence, th^{RNAi} flies display a reduced eye size, loss of eye pigmentation, and roughening of the eye surface (Figure 4A, results are shown for $AGO2^{321}$ heterozygotes; th^{RNAi} in a wildtype background shows the same phenotype, data not shown and ref. 24). Silencing of th in the eye of th^{RNAi} flies is fully dependent on the RNAi pathway, since the phenotype is lost in an $AGO2$ null mutant background (Figure 4B). These results indicate that the th^{RNAi} sensor fly is a robust system to monitor RNAi activity *in vivo*.

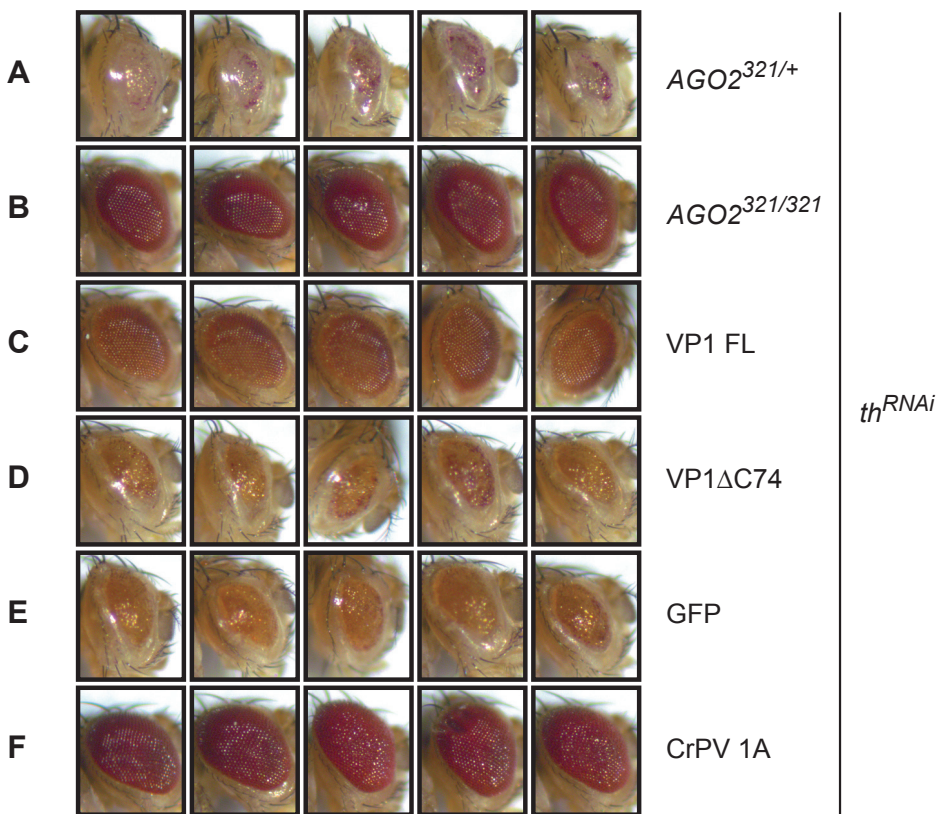


Figure 4. VP1 suppresses RNAi *in vivo*. (A-F) RNAi of *Drosophila Inhibitor of Apoptosis1 / thread (th)* in the eye of adult flies in the indicated genetic background or in the presence of several transgene constructs. RNAi-mediated knockdown of th results in a reduced size and pigmentation of the eye and roughening of the eye surface in $AGO2^{321}$ heterozygotes (A), but not in $AGO2^{321/321}$ homozygotes (B). Eye phenotype of transgenic flies co-expressing the th^{RNAi} construct and Nora virus full-length VP1 (VP1 FL, C), a C-terminal deletion mutant of VP1 (VP1 Δ C74, D), GFP (E) or CrPV 1A (F). Maximum silencing of th was examined in the presence of the GFP control transgene (E). For each line, five representative pictures of eyes of two- to four-day-old male flies are presented. Pictures are representative for three independent experiments.

Consistent with its RNAi suppressive activity in cell culture, expression of full-length VP1 (VP1^{FL}) in *th^{RNAi}* flies resulted in eyes with a normal size and a rescue of the rough eye phenotype (Figure 4C). The phenotype of *th^{RNAi}* flies expressing the VP1^{ΔC74} mutant was similar to that of flies expressing GFP as a negative control, confirming that this mutant is functionally inactive (Figure 4D, E). Notably, while VP1 only partially rescued the RNAi-dependent phenotype, CrPV 1A fully reverted the *th^{RNAi}* induced phenotype (Figure 4F). Whether this difference is due to a more robust RNAi suppressive activity of CrPV 1A or to a difference in expression level remains to be established.

VP1 enhances viral pathogenicity *in vivo*

Having established that VP1 displays RNAi suppressive activity *in vitro* and *in vivo*, we next analyzed the effect of VP1 on viral pathogenicity in adult flies. To this end, we generated recombinant Sindbis virus (SINV) expressing the functional VP1^{ΔN351} (SINV-VP1) or GFP (SINV-GFP) from a second subgenomic promoter (Figure 5A). Although arboviruses are a target of the RNAi pathway during infection in insects (3, 5, 26), we and others have not detected VSR activity in infections with SINV and the related alphavirus Semliki Forest virus (27, 28) (data not shown).

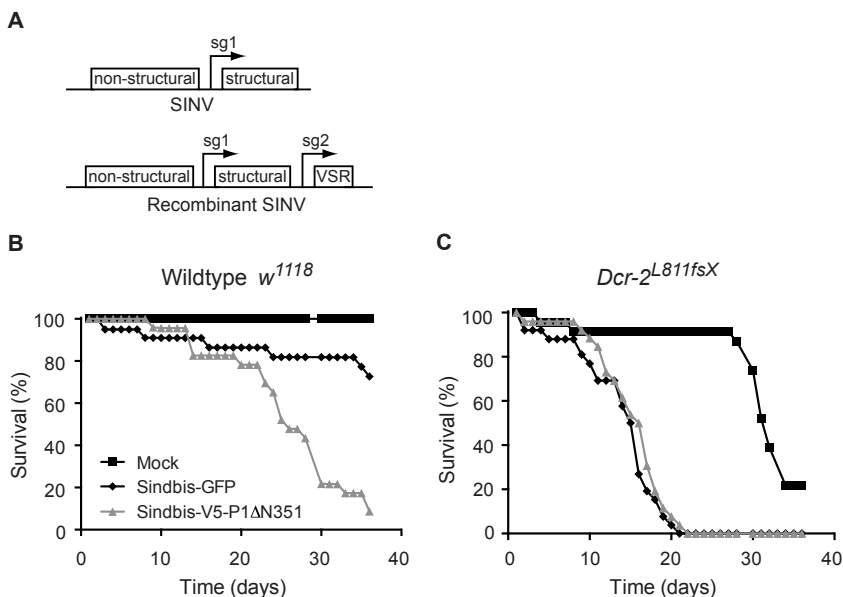


Figure 5. VP1 enhances viral pathogenicity via its RNAi suppressive activity. (A) Schematic representation of Sindbis virus (SINV) and SINV recombinant containing a duplicated subgenomic promoter (sg1 and sg2) driving expression of a viral suppressor of RNAi (VSR). (B and C) Survival curves of *w¹¹¹⁸* wildtype flies (B) and *Dcr-2^{L811fsX}* mutants (C) infected with SINV recombinants expressing either GFP (black diamond) or VP1^{ΔN351} (gray triangle), or mock-infected (black square). Survival curves are representative of two independent experiments.

Indeed, SINV recombinants expressing the viral RNAi suppressors FHV B2 and CrPV 1A were significantly more pathogenic than their controls in mosquitoes and *Drosophila*, respectively (13, 27).

We injected wildtype *w¹¹¹⁸* flies with the SINV recombinants and monitored survival over time. SINV-GFP (and the parental SINV virus, data not shown) induced only modest mortality in these flies with a fully functional RNAi response. After 36 days of infection, 73% of the SINV-GFP-infected flies and all mock-infected flies were still alive. In contrast, SINV-VP1 infection resulted in more severe mortality. SINV-VP1 infected flies died faster and only 9% of the flies survived the 36-days follow up period (Figure 5B). Although these results indicate that VP1 enhances viral pathogenicity, they fail to show that this effect depends on its VSR activity. Viral proteins are often multifunctional and the effect of VP1 on the course of infection might be attributed to another, as yet unknown, activity of VP1. We therefore performed recombinant SINV infections in RNAi deficient *Dcr-2* mutant flies. In this genetic background, an RNAi suppressor is not expected to enhance pathogenicity of the virus. Upon infection with SINV-GFP, the *Dcr-2* mutants died much faster than wildtype flies, confirming that SINV is indeed a target of the RNAi pathway. In contrast to infections in RNAi competent flies, the course of infection of SINV-VP1 and SINV-GFP was remarkably similar in *Dcr-2* mutants, with 100% mortality at 22 days after infection in both cases (Figure 5C). We therefore conclude that VP1 enhances virulence of an RNA virus *in vivo* through its RNAi suppressive activity.

Nora virus VP1 interferes with the effector phase of RNAi

To further characterize the VSR activity of Nora virus VP1, we next analyzed the activity of VP1 in a series of biochemical assays that monitor individual steps of the RNAi pathway. To this end, we fused the active VP1^{ΔN284} mutant to the maltose binding protein (MBP-VP1) and purified it from *Escherichia coli*. We verified that MBP-VP1 fusion proteins are fully functional in VSR assays in S2 cells to exclude the possibility that MBP interferes with VP1 VSR activity (data not shown).

The ability of VP1 to suppress siRNA-initiated RNAi in S2 cells (Figure 2D) suggests that VP1 inhibits a step downstream of siRNA production by Dcr-2. In accordance, recombinant VP1 was unable to bind long dsRNA in gel mobility shift assays and could not interfere with Dcr-2-mediated processing of long dsRNA into siRNAs in S2 cell extract (Figure S4A, B). We next analyzed whether VP1 is able to bind siRNAs in a gel mobility shift assay. As a positive control, we used a fusion protein of MBP and the Rice hoja blanca virus non-structural protein 3 (NS3), which binds duplex siRNAs with high affinity (29). Whereas NS3 efficiently bound siRNAs in our assays, we were unable to observe a shift in mobility of siRNAs after incubation with VP1, even at the highest

concentrations used (Figure 6A).

Since VP1 is incapable of interfering with the initiator phase of the RNAi pathway, we next examined the effect of VP1 on the effector phase of RNAi. For this purpose, we used an *in vitro* RNA cleavage assay (Slicer assay) in *Drosophila* embryo extract (30), in which a sequence-specific siRNA triggers cleavage of a target RNA. Since the 5' cap of the target RNA is radioactively labeled, the 5' cleavage product can be visualized by autoradiography after separation on a denaturing polyacrylamide gel. Indeed, a cleavage product of the expected size was detected if embryo extract was incubated with a target RNA and a specific siRNA. Specific cleavage products were not generated in the presence of a non-specific control siRNA (Figure 6B, lanes 1 and 2). Recombinant VP1 protein, but not control MBP protein, efficiently inhibited the production of cleavage product (Figure 6B, lanes 3 and 4). We note, however, that a minor fraction of the target RNA is still cleaved in the presence of VP1 (Figure 6B, lane 3). Together, these experiments show that VP1 does not affect the initiator phase of the RNAi pathway, but interferes with RISC activity.

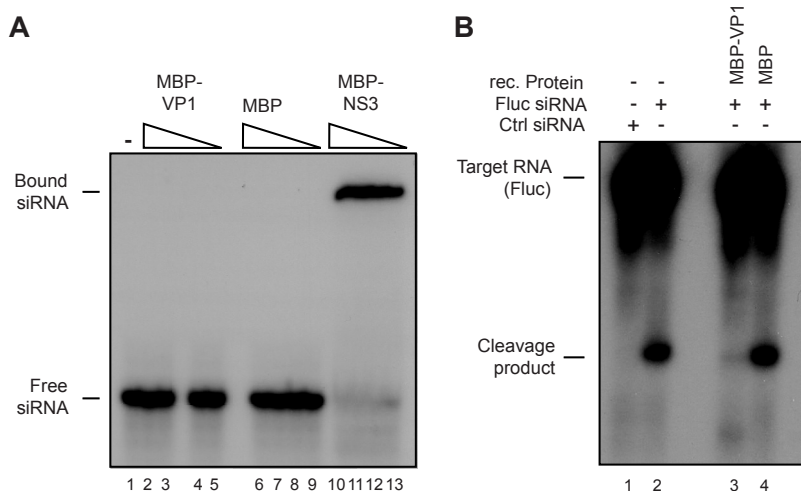


Figure 6. VP1 interferes with the effector phase of the RNAi pathway. (A) Mobility shift assays for binding of viral RNAi suppressor proteins to siRNAs. Radiolabeled siRNAs were incubated in buffer (lane 1) or with decreasing amounts of recombinant MBP-VP1^{ΔN284} (lanes 2-5), MBP (lanes 6-9), and MBP-NS3 (lane 10-13). Ten-fold dilutions were used, starting at 2 μM for MBP-VP1^{ΔN284} (lane 2) and 2.6 μM for MBP (lane 6). MBP-NS3 was tested in two-fold dilutions (highest concentration of 8 μM, lane 10). RNA mobility shifts were analyzed on an 8% native polyacrylamide gel. (B) RISC Slicer assay in *Drosophila* embryo lysate. Lysates were incubated with non-targeting control siRNA (Ctrl, lane 1) or with Fluc siRNA (lanes 2-4) in the absence (lane 2) or presence of recombinant MBP-VP1^{ΔN284} (lane 3) or MBP (lane 4). RISC cleavage products were analyzed on an 8% denaturing polyacrylamide gel. Slicer assay is representative for two independent experiments.

Nora virus VP1 inhibits RISC activity of pre-assembled mature RISC

To discriminate between RISC assembly and target RNA cleavage by a pre-assembled RISC complex, we performed Slicer assays under two experimental conditions (Figure 7A). In the first approach, a purified suppressor protein is added 30 minutes before the

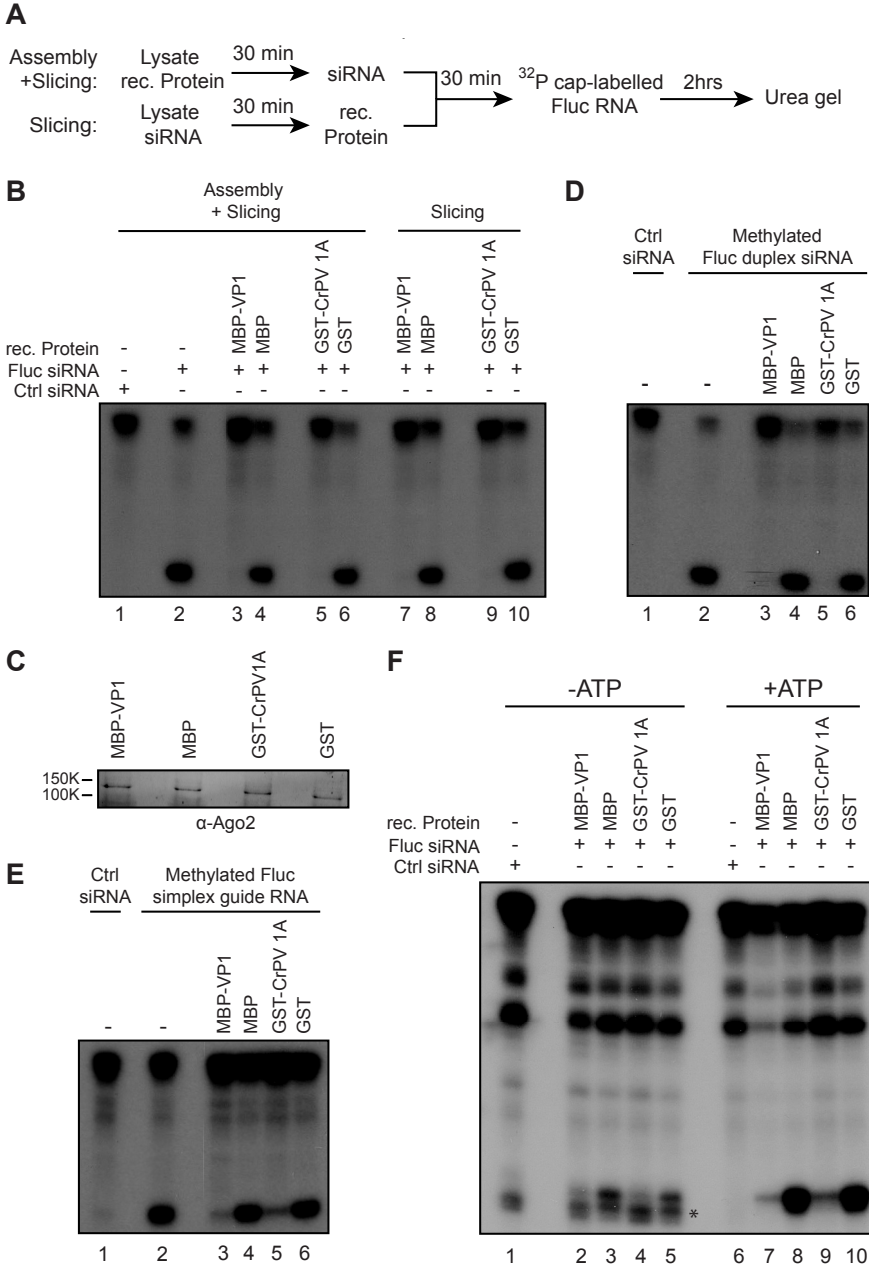


Figure 7. VP1 inhibits Slicer activity of pre-assembled mature RISC. (A) Schematic overview of the two experimental conditions of the Slicer assay designed to monitor the effect of recombinant (rec.) proteins on RISC assembly and Slicer activity (top) or on Slicer activity of pre-assembled RISC (bottom) (B) Slicer assays in *Drosophila* embryo lysates. RISC activity was analyzed in the presence of a non-targeting control siRNA (lane 1) or a specific Fluc siRNA (lane 2-10). Recombinant proteins were added before (lanes 3-6) or after (lanes 7-10) assembly of RISC as indicated. As a control for possible buffer effects, recombinant protein was substituted by protein storage buffer (lanes 1 and 2). (C) Western blot showing the endogenous AGO2 protein levels in embryo lysate after incubation for 2 hours with the indicated recombinant proteins. The blot was developed with AGO2 antibody 4D2. (D) Slicer assay using a siRNA with a 2'-O-methylated guide strand. A non-modified control siRNA (lane 1) or a Fluc siRNA duplex containing a 2'-O-methyl group at the 3' terminal nucleotide of the guide strand (lanes 2-6) was added to embryo lysate 30 minutes prior to the addition of the indicated recombinant proteins. (E) Slicer assay using a 2'-O-methylated simplex guide RNA. A control siRNA duplex (lane 1) or a single-stranded Fluc specific guide strand with a 2'-O-methyl group at the 3' terminal nucleotide (lane 2-6) was added prior to the addition of the indicated recombinant proteins. (F) Slicer assays in the presence or absence of ATP. Embryo lysate was incubated with a control siRNA (lanes 1 and 6) or a specific Fluc siRNA (lanes 2-5 and 7-10). ATP was then depleted (lanes 1-5) or depleted and subsequently regenerated (lanes 6-10) and Slicer activity was monitored. An asterisk (*) indicates a non-specific band appearing in RISC assays under ATP depleted conditions.

siRNA, which allows us to analyze the effect of the VSR on both RISC loading and target cleavage. In the second approach, the embryo extract is incubated with siRNAs for 30 minutes before addition of recombinant protein. This second protocol allows a mature RISC to form prior to the addition of a VSR, thereby allowing us to assess the effect of the VSR on slicing only. As CrPV 1A was previously shown to affect the effector phase of the RNAi pathway (13), we generated recombinant GST-CrPV 1A as well as control GST. These proteins were included in our assays.

Using the first protocol, cleavage of the target RNA was suppressed by VP1 (Figure 7B, lane 3). Strikingly, VP1 was also able to inhibit target cleavage when added to an embryo lysate containing pre-loaded RISC (Figure 7B, lane 7). The observed suppression of slicing was VP1 specific, since MBP alone did not inhibit RNA cleavage (Figure 7B, lane 4 and 8). Recombinant CrPV 1A also suppressed slicing in both experimental procedures (Figure 7B, lanes 5 and 9).

To determine if VP1 affects the protein stability of AGO2, we incubated the recombinant proteins in *Drosophila* embryo extract and analyzed endogenous AGO2 protein levels by Western blot. Neither VP1 nor CrPV 1A affected AGO2 protein levels in embryo lysate, indicating that these two proteins do not mediate RNAi suppression through degradation of AGO2 (Figure 7C).

To further confirm the inhibitory effect of VP1 on Slicer activity rather than RISC assembly, we performed Slicer assays using different siRNA guides. During RISC maturation, guide strands in AGO2 are 2'-O-methylated at their 3' terminal nucleotide by the *Drosophila* methyltransferase Hen1 (31). This modification protects AGO2 associated siRNAs from degradation by trimming and tailing events that occur when there is extensive base pairing of the guide RNA with a target RNA (32). To overcome

2 a requirement for Hen1, an siRNA bearing a 2'-O-methylated 3'-terminal nucleotide on the guide strand was used in Slicer assays. Similar to the non-methylated siRNA, the methylated siRNA produced a specific cleavage product of the expected size (Figure 7D, lane 2). Both Nora virus VP1 and CrPV 1A inhibited the cleavage activity of RISC that was pre-loaded with the methylated siRNA (Figure 7D, lane 3 and 5). Again, the GST and MBP control proteins were unable to affect Slicer activity (Figure 7D, lane 4 and 6). After loading of the siRNA as a duplex, AGO2 cleaves the passenger strand which is then degraded by the C3PO nuclease complex (33). To circumvent canonical loading of RISC, we induced RISC formation with a single-stranded methylated guide RNA. Although less efficient, loading of single-stranded guide strands into AGO2 is possible via a bypass mechanism (34, 35). Indeed, at high concentrations, methylated single-stranded guide RNA induced specific cleavage of cap-labeled target RNA (Figure 7E, lane 2). Interestingly, single-stranded guide RNA-induced target cleavage was specifically inhibited both by Nora virus VP1 and by CrPV 1A (Figure 7E, lanes 3 and 5). These results indicate that both CrPV 1A and Nora virus VP1 inhibit Slicer activity of mature RISC rather than RISC assembly.

Following maturation, RISC binds, cleaves, and releases complementary target RNA, and returns to a Slicer-competent state. *Drosophila* RISC is a multiple turnover complex, in which release of the cleaved target RNA is a rate-limiting step that is greatly enhanced by ATP (36). We therefore analyzed suppression of Slicer activity under ATP-limiting conditions with a 20-fold molar excess of siRNA over target RNA. RISC was loaded in the presence of ATP, after which creatine kinase was inactivated by NEM, and ATP was depleted (-ATP) by addition of hexokinase and glucose (Figure S5). In parallel, ATP levels were restored (+ATP) after NEM treatment by adding back creatine kinase, and omitting hexokinase treatment. As expected, RISC shows a lower cleavage rate in -ATP conditions than in +ATP conditions (Figure 7F, compare lanes 3 and 5 with lanes 8 and 10). Even under -ATP conditions, Nora virus VP1 and CrPV 1A were able to inhibit Slicer activity (Figure 7F, lanes 2 and 4), suggesting that these two VSRs inhibit the catalytic target cleavage by AGO2.

Discussion

The mechanisms by which RNA viruses evade sterilizing immunity and establish chronic persistent infections remain poorly understood (37). Nora virus successfully establishes a persistent infection in *Drosophila*, providing an excellent model to study mechanisms of persistence. We show here that Nora virus is a target of the antiviral RNAi machinery and that it encodes a potent suppressor of RNAi. Of note, Nora virus

RNA levels are unaffected by mutations in the RNAi pathway (38). These observations therefore suggest that dynamic interactions between the antiviral RNAi response and viral counter-defense mechanisms determine viral persistence.

The production of viral siRNAs is a hallmark of an antiviral RNAi response. By detection of Nora virus-derived vsiRNAs in infected fly stocks, we provide direct evidence that Nora virus is a target of Dcr-2. Nora virus vsiRNAs are distributed across the viral genome, with similar amounts derived from the (+) and (-) RNA strands. During (+) RNA virus infection, (+) viral RNA accumulates in large excess over (-) viral RNA (~50-100 fold). Cleavage of structured RNA elements by Dcr-2 is therefore expected to produce viral small RNAs that mirror this asymmetric distribution. Thus, similar to other RNA viruses, our results imply that Dcr-2 targets the dsRNA intermediates in Nora virus replication (2, 4, 39-41).

The current model proposes that the antiviral RNAi response relies on dicing of viral dsRNA and on slicing of viral target RNAs using vsiRNAs as a guide. Genetic analyses support the role of AGO2 in antiviral defense: *AGO2* mutants are hypersensitive to a number of RNA virus infections (3-7, 42). Yet, interpretation of this *AGO2* phenotype is complicated by other cellular functions of AGO2, such as regulation of cellular gene transcription and control of transposon activity (43-45). An alternative model proposes that dicing of double-stranded replication intermediates plays an important role in latent virus infection (46). Dicing of an essential replication intermediate by Dcr-2 should theoretically be sufficient to abort a productive virus replication cycle. The convergent evolution of VSRs that suppress the catalytic activity of AGO2 in two distantly related RNA viruses, Nora virus and CrPV, underlines the essential role of AGO2 Slicer activity in antiviral defense, also in persistent infections *in vivo*. Importantly, these two viruses display a strikingly different course of infection – CrPV causes a lethal infection, whereas Nora virus establishes a non-lethal, persistent infection – suggesting that the interaction between a VSR and the host RNAi machinery is not the main determinant for viral pathogenicity.

Materials and Methods

Small RNA sequencing and analysis

Total RNA was extracted from dissected heads, bodies (abdomens and thoraxes) and thoraxes from *w¹¹¹⁸* male flies using Trizol reagent (Invitrogen), and RNA quality was verified on a Bioanalyzer (Agilent). Small RNAs were then cloned using the DGE-Small RNA Sample Prep Kit and the Small RNA v1.5 Sample Preparation Kit (Illumina) following the manufacturer's instructions. Libraries were sequenced on the Illumina

HiSeq platform.

Sequence reads were clipped from 3' adapters using `fastx_clipper` (http://hannonlab.cshl.edu/fastx_toolkit/). Reads in which the adapter sequence (CTGTAGGCACCATCAATCGT) could not be detected were discarded. Only the clipped 19-30 nt reads were retained. Sequence reads were first matched against the *Drosophila* genome (v5.37) using Bowtie (<http://bowtie-bio.sourceforge.net/index.shtml>). Reads not matching the *Drosophila* genome were then matched against the published Nora virus sequence (NC_007919.3, isolate Umeå 2007), allowing one mismatch during alignment. Viral small RNAs were then used to reconstitute a small RNA-based consensus genome sequence (rNora virus, JX220408) using Papparazzi (21) with NC_007919.3 as a starting viral reference genome. Distributions of Nora virus small RNA sizes were computed by parsing the Bowtie outputs with a python script (available upon request). Small RNA profiles were generated by collecting the 21-nt reads that matched the rNora virus sequence allowing one mismatch, and their frequency relative to their 5' position in the rNora virus (+) or (-) genomic strand was plotted in R. siRNA duplex signatures were calculated according to an algorithm developed to calculate overlap in piRNA sequence reads (47, 48). The distribution of siRNA overlaps was computed by collecting the 21-nt rNora virus RNA reads whose 5' ends overlapped with another 21-nt read on the opposite strand. For each possible overlap of 1 to 21-nt (i), the number of read pairs (O) was counted and converted to a Z-score with the formula $Z(i) = (O(i) - \text{mean}(O)) / \text{standard deviation}(O)$. Small RNA sequences were deposited to the Sequence Read Archive (SRA) at the National Center for Biotechnology Information (NCBI) under accession number SRA054241.

Cell culture and viruses

Drosophila S2 cells were cultured at 25 °C in Schneider's medium (Invitrogen) supplemented with 10% heat inactivated fetal calf serum, 50 U/mL penicillin, and 50 µg/mL streptomycin (Invitrogen). DCV was cultured and titered on S2 cells as described previously (6). For the production of recombinant SINV, the coding sequence of either GFP or the N-terminal V5 epitope tagged VP1^{ΔN351} was cloned into the *Xba*I site of the double subgenomic pTE3'2J vector (49). The resulting plasmids were linearized by *Xho*I restriction, purified and used as template for *in vitro* transcription using the mMMESSAGE mMACHINE SP6 High Yield Capped RNA Transcription kit (Ambion). *In vitro* transcribed RNA was purified using the RNeasy kit (Qiagen) and transfected into BHK cells. Viral titers in the supernatant were determined by plaque assay on BHK cells.

RNAi reporter assay in S2 cells

RNAi reporter assays were performed as described previously using 25 ng pMT-GL3, 6 ng pMT-Ren, and 25 ng suppressor plasmid per well of a 96-well plate (50). Plasmids encoding Nora virus cDNA constructs were generated as described in Protocol S1.

Flies and fly injections

Flies were maintained on standard medium at 25 °C with a light/dark cycle of 12 hours/12 hours. Fly stocks that were used for Sindbis virus infection and for preparation of embryo lysate were cleared of *Wolbachia* and endogenous virus infection (see Protocol S1). We used the following fly stocks and alleles: *UAS-CrPV 1A* (13, 51), *AGO2³²¹* (52), *Dcr-2^{L811fsX}* (53), *tb^{RNAi}* (24, 25). The coding sequences of the full-length VP1 and the inactive VP1^{ΔC74} mutant with an N-terminal V5 epitope tag were cloned into the pUAST vector using the *Sac*II and *Xba*I restriction sites (54). The resulting plasmids were microinjected into *Drosophila w¹¹¹⁸* embryos to generate transgenic fly lines (Bestgene Inc). Virus infections of adult female flies were performed as described previously using 5,000 PFU of recombinant SINV (6). Survival was monitored daily. *In vivo* RNAi experiments were performed by crossing *GMR-Gal4*, *UAS-tb^{RNAi}/CyO* virgins (24) with *UAS-VSR/TM3 Sb* flies. The eye phenotype was monitored in two- to four-day-old male F1 offspring lacking the *CyO* and *TM3 Sb* balancers.

Production of recombinant proteins in *E. coli*

The GST and MBP fusion proteins were purified from *E. coli* as described in Protocol S1. Purified recombinant proteins were dialyzed against dialysis buffer (20 mM Tris-HCl, 0.5 mM EDTA, 5 mM MgCl₂, 1 mM DTT, 140 mM NaCl, 2.7 mM KCl). Recombinant proteins were stored as aliquots at -80 °C in dialysis buffer containing 30% glycerol.

Gel mobility shift, Dicer and Slicer assays

Gel mobility shift assays were performed as described (6). Briefly, uniformly radio-labeled 113-nt long dsRNA (50 cps/reaction) or end-labeled siRNAs (200 cps/reaction) were incubated with purified recombinant protein for 30 minutes at room temperature. Samples were then separated on an 8% native polyacrylamide gel and exposed to a Kodak Biomax XAR film.

Dicer and Slicer assays were performed according to the protocol of Haley and colleagues with minor modifications, described in Protocol S1 (30). For Slicer assays with the methylated duplex, Fluc guide strand 5'- UCG AAG UAC UCA GCG UAA GU[mU] and passenger strand 5'- CUU ACG CUG AGU ACU UCG AUU were annealed by incubating 20 μM of each siRNA strand in annealing buffer (100 mM potassium

acetate, 30 mM HEPES-KOH at pH 7.4, 2 mM magnesium acetate) for 1 min at 90 °C, followed by incubation for 1 hour at 37 °C. For guide strand loading of RISC, embryo lysates were incubated with Fluc single-stranded guide strand RNA at a final concentration of 10 μM. Radiolabeled probes and target RNA for gel shift and Slicer assays are described in Protocol S1.

Acknowledgements

We thank members of the Van Rij laboratory, members of the Van Kuppeveld laboratory, and Darren Obbard for discussions. We thank Koen van Cleef for critical reading of the manuscript and Pascal Miesen for bioinformatics support. We thank P. Zamore for providing fly stocks and a generous supply of embryo lysate; M. Siomi for providing AGO2 antibody; E. Schnettler for recombinant NS3 protein and miR1 sensor plasmids; A. Müller for fly stocks, A. Schenck and J. Kramer for fly stocks, discussions and advice; and M.C. Saleh for hosting Sindbis injections. Furthermore, we thank J. Koenderink for experimental support and Minh Nguyen for technical support. Small RNA data were generated as part of the NeuomiR project of the laboratories of Hervé Tricoire, Magalie Lecourtois, Serge Birman, and Christophe Antoniewski.

References

1. Ding SW & Voinnet O (2007) Antiviral immunity directed by small RNAs. *Cell* 130:413-426.
2. Van Rij RP & Berezikov E (2009) Small RNAs and the control of transposons and viruses in *Drosophila*. *Trends Microbiol* 17:139-178.
3. Keene KM, Foy BD, Sanchez-Vargas I, Beaty BJ, Blair CD, & Olson KE (2004) From the Cover: RNA interference acts as a natural antiviral response to O'nyong-nyong virus (Alphavirus; Togaviridae) infection of *Anopheles gambiae*. *Proc Natl Acad Sci U S A* 101:17240-17245.
4. Mueller S, Gausson V, Vodovar N, Deddouche S, Troxler L, Perot J, Pfeffer S, Hoffmann JA, Saleh MC, & Imler JL (2010) RNAi-mediated immunity provides strong protection against the negative-strand RNA vesicular stomatitis virus in *Drosophila*. *Proc.Natl.Acad.Sci.U.S.A* 107:19390-19395.
5. Sanchez-Vargas I, Scott JC, Poole-Smith BK, Franz AW, Barbosa-Solomieu V, Wilusz J, Olson KE, & Blair CD (2009) Dengue virus type 2 infections of *Aedes aegypti* are modulated by the mosquito's RNA interference pathway.

- PLoS Pathog* 5:e1000299.
6. Van Rij RP, Saleh MC, Berry B, Foo C, Houk A, Antoniewski C, & Andino R (2006) The RNA silencing endonuclease Argonaute 2 mediates specific antiviral immunity in *Drosophila melanogaster*. *Genes Dev* 20:2985-2995.
 7. Zambon RA, Vakharia VN, & Wu LP (2006) RNAi is an antiviral immune response against a dsRNA virus in *Drosophila melanogaster*. *Cell Microbiol* 8:880-889.
 8. Aliyari R, Wu Q, Li HW, Wang XH, Li F, Green LD, Han CS, Li WX, & Ding SW (2008) Mechanism of induction and suppression of antiviral immunity directed by virus-derived small RNAs in *Drosophila*. *Cell Host Microbe* 4:387-397.
 9. Li HW, Li WX, & Ding SW (2002) Induction and suppression of RNA silencing by an animal virus. *Science* 296:1319-1321.
 10. Chao JA, Lee JH, Chapados BR, Debler EW, Schneemann A, & Williamson JR (2005) Dual modes of RNA-silencing suppression by Flock House virus protein B2. *Nat Struct Mol Biol* 12:952-957.
 11. Lakatos L, Csorba T, Pantaleo V, Chapman EJ, Carrington JC, Liu YP, Dolja VV, Calvino LF, Lopez-Moya JJ, & Burgyan J (2006) Small RNA binding is a common strategy to suppress RNA silencing by several viral suppressors. *Embo J* 25:2768-2780.
 12. Merai Z, Kerenyi Z, Kertesz S, Magna M, Lakatos L, & Silhavy D (2006) Double-stranded RNA binding may be a general plant RNA viral strategy to suppress RNA silencing. *J Virol* 80:5747-5756.
 13. Nayak A, Berry B, Tassetto M, Kunitomi M, Acevedo A, Deng C, Krutchinsky A, Gross J, Antoniewski C, & Andino R (2010) Cricket paralysis virus antagonizes Argonaute 2 to modulate antiviral defense in *Drosophila*. *Nat. Struct. Mol. Biol.* 17:547-554.
 14. Moore NF, Pullin JS, Crump WA, & Plus N (1982) The proteins expressed by different isolates of *Drosophila C* virus. *Arch Virol* 74:21-30.
 15. Plus N, Croizier G, Jousset FX, & David J (1975) Picornaviruses of laboratory and wild *Drosophila melanogaster*: geographical distribution and serotypic composition. *Annales de microbiologie* 126:107-117.
 16. Scotti PD, Dearing S, & Mossop DW (1983) Flock House virus: a nodavirus isolated from *Costelytra zealandica* (White) (Coleoptera: Scarabaeidae). *Arch Virol* 75:181-189.
 17. Reinganum C, O'Loughlin GT, & Hogan TW (1970) A Nonoccluded Virus of Field Crickets *Teleogryllus-Oceanicus* and *T-Commodus* (Orthoptera-Gryllidae). *J Invertebr Pathol* 16:214-220.

18. Dasgupta R, Free HM, Zietlow SL, Paskewitz SM, Aksoy S, Shi L, Fuchs J, Hu C, & Christensen BM (2007) Replication of flock house virus in three genera of medically important insects. *J Med Entomol* 44:102-110.
19. Plus N, Croizier G, Reinganum C, & Scott PD (1978) Cricket paralysis virus and drosophila C virus: serological analysis and comparison of capsid polypeptides and host range. *J.Invertebr.Pathol.* 31:296-302.
20. Habayeb MS, Ekengren SK, & Hultmark D (2006) Nora virus, a persistent virus in *Drosophila*, defines a new picorna-like virus family. *J Gen Virol* 87:3045-3051.
21. Vodovar N, Goic B, Blanc H, & Saleh MC (2011) In silico reconstruction of viral genomes from small RNAs improves virus-derived small interfering RNA profiling. *J Virol* 85:11016-11021.
22. Habayeb MS, Cantera R, Casanova G, Ekstrom JO, Albright S, & Hultmark D (2009) The *Drosophila* Nora virus is an enteric virus, transmitted via feces. *J.Invertebr.Pathol.* 101:29-33.
23. Ekstrom JO, Habayeb MS, Srivastava V, Kieselbach T, Wingsle G, & Hultmark D (2011) *Drosophila* Nora virus capsid proteins differ from those of other picorna-like viruses. *Virus Res* 160:51-58.
24. Meyer WJ, Schreiber S, Guo Y, Volkmann T, Welte MA, & Muller HA (2006) Overlapping functions of argonaute proteins in patterning and morphogenesis of *Drosophila* embryos. *PLoS.Genet.* 2:e134.
25. Huh JR, Guo M, & Hay BA (2004) Compensatory proliferation induced by cell death in the *Drosophila* wing disc requires activity of the apical cell death caspase Dronc in a nonapoptotic role. *Curr Biol* 14:1262-1266.
26. Campbell CL, Keene KM, Brackney DE, Olson KE, Blair CD, Wilusz J, & Foy BD (2008) *Aedes aegypti* uses RNA interference in defense against Sindbis virus infection. *BMC Microbiol* 8:47.
27. Cirimotich CM, Scott JC, Phillips AT, Geiss BJ, & Olson KE (2009) Suppression of RNA interference increases alphavirus replication and virus-associated mortality in *Aedes aegypti* mosquitoes. *BMC Microbiol* 9:49.
28. Attarzadeh-Yazdi G, Fragkoudis R, Chi Y, Siu RW, Ulper L, Barry G, Rodriguez-Andres J, Nash AA, Bouloy M, Merits A, *et al.* (2009) Cell-to-cell spread of the RNA interference response suppresses Semliki Forest virus (SFV) infection of mosquito cell cultures and cannot be antagonized by SFV. *J Virol* 83:5735-5748.
29. Hemmes H, Kaaij L, Lohuis D, Prins M, Goldbach R, & Schnettler E (2009) Binding of small interfering RNA molecules is crucial for RNA interference suppressor activity of rice hoja blanca virus NS3 in plants. *J.Gen. Virol.* 90:1762-

- 1766.
30. Haley B, Tang G, & Zamore PD (2003) In vitro analysis of RNA interference in *Drosophila melanogaster*. *Methods* 30:330-336.
 31. Horwich MD, Li C, Matranga C, Vagin V, Farley G, Wang P, & Zamore PD (2007) The *Drosophila* RNA methyltransferase, DmHen1, modifies germline piRNAs and single-stranded siRNAs in RISC. *Curr Biol* 17:1265-1272.
 32. Ameres SL, Horwich MD, Hung JH, Xu J, Ghildiyal M, Weng Z, & Zamore PD (2010) Target RNA-directed trimming and tailing of small silencing RNAs. *Science* 328:1534-1539.
 33. Liu Y, Ye X, Jiang F, Liang C, Chen D, Peng J, Kinch LN, Grishin NV, & Liu Q (2009) C3PO, an endoribonuclease that promotes RNAi by facilitating RISC activation. *Science* 325:750-753.
 34. Martinez J, Patkaniowska A, Urlaub H, Luhrmann R, & Tuschl T (2002) Single-stranded antisense siRNAs guide target RNA cleavage in RNAi. *Cell* 110:563-574.
 35. Iwasaki S, Kobayashi M, Yoda M, Sakaguchi Y, Katsuma S, Suzuki T, & Tomari Y (2010) Hsc70/Hsp90 chaperone machinery mediates ATP-dependent RISC loading of small RNA duplexes. *Mol. Cell* 39:292-299.
 36. Haley B & Zamore PD (2004) Kinetic analysis of the RNAi enzyme complex. *Nat. Struct. Mol. Biol.* 11:599-606.
 37. Virgin HW, Wherry EJ, & Ahmed R (2009) Redefining chronic viral infection. *Cell* 138:30-50.
 38. Habayeb MS, Ekstrom JO, & Hultmark D (2009) Nora virus persistent infections are not affected by the RNAi machinery. *PLoS One* 4:e5731.
 39. Wu Q, Luo Y, Lu R, Lau N, Lai EC, Li WX, & Ding SW (2010) Virus discovery by deep sequencing and assembly of virus-derived small silencing RNAs. *Proc. Natl. Acad. Sci. U.S.A* 107:1606-1611.
 40. Brackney DE, Beane JE, & Ebel GD (2009) RNAi targeting of West Nile virus in mosquito midguts promotes virus diversification. *PLoS Pathog.* 5:e1000502.
 41. Myles KM, Wiley MR, Morazzani EM, & Adelman ZN (2008) Alphavirus-derived small RNAs modulate pathogenesis in disease vector mosquitoes. *Proc. Natl. Acad. Sci. U.S.A* 105:19938-19943.
 42. Galiana-Arnoux D, Dostert C, Schneemann A, Hoffmann JA, & Imler JL (2006) Essential function in vivo for Dicer-2 in host defense against RNA viruses in *drosophila*. *Nat Immunol* 7:590-597.
 43. Cernilogar FM, Onorati MC, Kothe GO, Burroughs AM, Parsi KM, Breiling A, Lo Sardo F, Saxena A, Miyoshi K, Siomi H, *et al.* (2011) Chromatin-associated RNA interference components contribute to transcriptional regulation in

- Drosophila. *Nature* 480:391-395.
44. Fagegaltier D, Bouge AL, Berry B, Poisot E, Sismeiro O, Coppee JY, Theodore L, Voinnet O, & Antoniewski C (2009) The endogenous siRNA pathway is involved in heterochromatin formation in *Drosophila*. *Proc Natl Acad Sci U S A* 106:21258-21263.
 45. Ghildiyal M, Seitz H, Horwich MD, Li C, Du T, Lee S, Xu J, Kittler EL, Zapp ML, Weng Z, *et al.* (2008) Endogenous siRNAs Derived from Transposons and mRNAs in *Drosophila* Somatic Cells. *Science* 320:1077-1081.
 46. Flynt A, Liu N, Martin R, & Lai EC (2009) Dicing of viral replication intermediates during silencing of latent *Drosophila* viruses. *Proc.Natl.Acad. Sci.U.S.A* 106:5270-5275.
 47. Khurana JS, Wang J, Xu J, Koppetsch BS, Thomson TC, Nowosielska A, Li C, Zamore PD, Weng Z, & Theurkauf WE (2011) Adaptation to P element transposon invasion in *Drosophila melanogaster*. *Cell* 147:1551-1563.
 48. Muerdter F, Olovnikov I, Molaro A, Rozhkov NV, Czech B, Gordon A, Hannon GJ, & Aravin AA (2012) Production of artificial piRNAs in flies and mice. *RNA* 18:42-52.
 49. Hahn CS, Hahn YS, Braciale TJ, & Rice CM (1992) Infectious Sindbis virus transient expression vectors for studying antigen processing and presentation. *Proc.Natl.Acad.Sci.U.S.A* 89:2679-2683.
 50. van Cleef KW, van Mierlo JT, van den Beek M, & Van Rij RP (2011) Identification of viral suppressors of RNAi by a reporter assay in *Drosophila* S2 cell culture. *Methods Mol.Biol.* 721:201-213.
 51. Berry B, Deddouche S, Kirschner D, Imler JL, & Antoniewski C (2009) Viral suppressors of RNA silencing hinder exogenous and endogenous small RNA pathways in *Drosophila*. *PLoS.One.* 4:e5866.
 52. Hain D, Bettencourt BR, Okamura K, Csorba T, Meyer W, Jin Z, Biggerstaff J, Siomi H, Hutvagner G, Lai EC, *et al.* (2010) Natural variation of the amino-terminal glutamine-rich domain in *Drosophila argonaute2* is not associated with developmental defects. *PLoS One* 5:e15264.
 53. Lee YS, Nakahara K, Pham JW, Kim K, He Z, Sontheimer EJ, & Carthew RW (2004) Distinct roles for *Drosophila* Dicer-1 and Dicer-2 in the siRNA/miRNA silencing pathways. *Cell* 117:69-81.
 54. Brand AH & Perrimon N (1993) Targeted gene expression as a means of altering cell fates and generating dominant phenotypes. *Development* 118:401-415.
 55. Chapman EJ, Prokhnevsky AI, Gopinath K, Dolja VV, & Carrington JC (2004) Viral RNA silencing suppressors inhibit the microRNA pathway at an

- intermediate step. *Genes Dev.* 18:1179-1186.
56. Jay F, Wang Y, Yu A, Taconnat L, Pelletier S, Colot V, Renou JP, & Voinnet O (2011) Misregulation of AUXIN RESPONSE FACTOR 8 underlies the developmental abnormalities caused by three distinct viral silencing suppressors in Arabidopsis. *PLoS.Pathog.* 7:e1002035.
 57. Ghildiyal M, Xu J, Seitz H, Weng Z, & Zamore PD (2010) Sorting of Drosophila small silencing RNAs partitions microRNA* strands into the RNA interference pathway. *RNA.* 16:43-56.
 58. Okamura K, Liu N, & Lai EC (2009) Distinct mechanisms for microRNA strand selection by Drosophila Argonautes. *Mol. Cell* 36:431-444.
 59. Eulalio A, Rehwinkel J, Stricker M, Huntzinger E, Yang SF, Doerks T, Dorner S, Bork P, Boutros M, & Izaurralde E (2007) Target-specific requirements for enhancers of decapping in miRNA-mediated gene silencing. *Genes Dev.* 21:2558-2570.
 60. Schnettler E, Hemmes H, Huismann R, Goldbach R, Prins M, & Kormelink R (2010) Diverging affinity of tospovirus RNA silencing suppressor proteins, NSs, for various RNA duplex molecules. *J. Virol.* 84:11542-11554.
 61. Teixeira L, Ferreira A, & Ashburner M (2008) The bacterial symbiont Wolbachia induces resistance to RNA viral infections in Drosophila melanogaster. *PLoS Biol* 6:e2.

Supporting Information

Text S1.

Nora virus VP1 is unable to suppress the miRNA pathway

Several plant virus RNAi suppressors influence the miRNA pathway, thereby inducing strong developmental defects in transgenic plants that express RNAi suppressors during development (55, 56). This effect may be due to convergence of the antiviral RNAi and miRNA pathways on Argonaute-1 (AGO1) in plants. In *Drosophila*, the miRNA and siRNA pathways are parallel pathways. Nevertheless, there is crosstalk between these pathways with miRNA and miRNA-star sequences being loaded into AGO2 and, conversely, with siRNAs being loaded into AGO1 (57, 58). To determine whether VP1 suppresses the miRNA pathway, we used a miRNA sensor assay in S2 cells (Protocol S1). In this assay, an Fluc reporter containing the 3'UTR of the *Drosophila par6* gene (Fluc-par6), a target for miRNA1, is co-transfected with a plasmid expressing the primary miRNA1 (pri-miR1), or a control plasmid expressing pri-miR12 (59, 60). Co-transfection of pri-miR1 led to specific silencing of the Fluc-par6 gene (Figure S1). We verified whether the reporter was suppressed in an AGO1-dependent manner, by cotransfection of dsRNA targeting *AGO1* or, as a control, *AGO2*. As expected, the miRNA reporter assay monitors the canonical miRNA pathway, since knock-down of the *AGO1* gene by dsRNA led to de-repression of Fluc-par6 expression (although this did not reach statistical significance, $p=0.09$). In contrast, co-transfection of *AGO2* dsRNA did not lead to de-repression, but even enhanced silencing of the miRNA reporter, perhaps reflecting more efficient AGO1 loading under conditions in which *AGO2* is depleted. Expression of Nora virus VP1 did not de-repress the Fluc-par6 construct, indicating that VP1 does not suppress the miRNA pathway. Similarly, VP1 did not affect silencing of a miRNA sensor consisting of a luciferase construct containing two perfect complementary target sites for the endogenous miR2 in its 3'UTR (data not shown) (6). In addition, transgenic flies expressing VP1 driven by a strong ubiquitous promoter (Tubulin-Gal4) are viable and fertile, lending further support to the conclusion that VP1 does not inhibit miRNA biogenesis and function (data not shown).

Protocol S1.

Extended Experimental Procedures and Supplemental Methods **Molecular cloning**

To construct plasmids encoding C-terminal V5 epitope tagged proteins of Nora virus, cDNA prepared from Nora virus-infected flies was amplified using primers 5'-AGT GGT ACC AAC ATG ATT AAC AAT CAA ACA AAC and 5'-GGT GGG CCC TTG ACA TTG TTG TTT CTG CG for ORF1, primers 5'-AGT GGT ACC AAC ATG

TTA ATT GAA GCT TTC ATC and 5'-GGT GGG CCC TCC AAG ATC TCC TCT TTT AAT G for ORF2, primers 5'-AGT GGT ACC AAC ATG GCA TTA AAA GAG GAG ATC and 5'-GGT GGG CCC TTG CAT AGA GTC ATA AAT TAC for ORF3, and primers 5'-AGT GGT ACC AAC ATG CAG AAT CCA ACA CAA ACC and 5'-GGT GGG CCC CTG CTG CCT CAC GGA AGG GAA for ORF4. Amplified products were cloned as *KpnI* and *Apal* fragments into pAc5.1-V5-His-A (Invitrogen). For the expression of VP1 mutants tagged at the N-terminus with the V5-His epitopes, the pAc5.1-V5-His-Ntag plasmid was constructed. This plasmid was created by annealing and cloning the oligonucleotides 5'-CAA CAT GGG TAA GCC TAT CCC TAA CCC TCT CCT AGG TCT CGA TTC TAC GCG TAC CGG TCA TCA TCA CCA TCA CCA TG and 5'-AAT TCA TGG TGA TGG TGA TGA TGA CCG GTA CGC GTA GAA TCG AGA CCT AGG AGA GGG TTA GGG ATA GGC TTA CCC ATG TTG GTA C into the *EcoRI* and *KpnI* restriction sites of pAc5.1-V5-His-A. The sequences of all VP1 deletion mutants were cloned into pAc5.1-V5-His-Ntag using the *EcoRI* and *SacI* restriction sites. For mutant sequences see supplemental Figure S3.

miRNA sensor assay

The miRNA sensor assay and its plasmids were described previously (59, 60). Briefly, 5×10^4 S2 cells were seeded per well in a 96-well plate one day before transfection. Subsequently, the cells were transfected with 54.5 ng suppressor plasmid, 6.8 ng pMT-Fluc-par6, 1.6 ng pMT-Ren, and 2.7 ng pMT-miR1 or pMT-miR12 using the Effectene transfection reagent (Qiagen) according to the manufacturer's protocol. To knockdown *AGO1* or *AGO2* expression, 5.4 ng of dsRNA was cotransfected with the plasmids. Expression of the reporter constructs was induced with CuSO_4 at 48 hrs post-transfection and luciferase activities were measured at 72 hrs post-transfection.

Clearance of *Wolbachia* and endogenous viruses from fly stocks

Fly stocks used for Sindbis virus infection and preparation of embryo lysates were cleared from endogenous viruses by collecting eggs on apple-juice agar plates, followed by a treatment with 50% household bleach for 5 minutes. Subsequently, the bleached eggs were washed three times in a large volume of water, after which they were transferred to clean vials containing standard fly food. After culturing the fly stocks for two generations we confirmed the absence of Nora virus and Drosophila C virus (DCV) by RT-PCR. Fly stocks were then cleared from *Wolbachia* infection by raising the flies for two generations on standard fly food supplemented with 0.05 mg/mL tetracycline hydrochloride (Sigma). To verify the clearance of *Wolbachia* infection, PCR amplification was performed with *Wolbachia* specific primers on DNA extracts of adult flies, as described earlier (61).

Production of recombinant proteins in *E. coli*

To fuse the VP1^{ΔN284} protein to the C-terminus of maltose binding protein (MBP), the coding sequence of the VP1^{NΔ284} mutant was cloned as an *EcoRI-Sall* fragment into the pMal-C2X vector (New England Biolabs). The resulting pMal-C2X-VP1^{NΔ284} and parental pMal-C2X plasmids were transformed into the *E. coli* BL21 (DE3) strain. Expression of the recombinant fusion proteins was induced at 1.0 OD₆₀₀ by adding 0.2 mM IPTG followed by incubation at 37 °C for 3 hours. MBP and MBP-VP1^{NΔ284} fusion proteins were purified using amylose resin (New England Biolabs) according to the manufacturer's protocol.

The coding sequence of CrPV 1A (amino acids 1-148) was amplified using primers 5'- CGG GAA TTC ATG TCT TTT CAA CAA ACA AAC AAC and 5'- AGA GTC GAC TTA GAA GGC TCT GCA TT and cloned into the pGEX-4T-1 plasmid (GE healthcare) as an *EcoRI-Sall* fragment. After transformation of the *E. coli* BL21 (DE3) strain with the resulting pGEX-CrPV 1A plasmid, expression was induced at 1.0 OD₆₀₀ using 0.2 mM IPTG. Protein production was allowed to continue overnight at 20 °C. The GST-CrPV 1A fusion protein was purified using glutathione sepharose 4 fast flow (GE healthcare) according to the manufacturer's protocol. GST (pGEX-4T-1) and GST-DCV 1A (pGEX-DCV 1A) fusion proteins were purified using the same method, after induction of protein expression at 37 °C for 3 hours (6).

Radioactively labeled probes and target RNA

Uniformly radio-labeled 113-bp long dsRNA was generated by *in vitro* transcription in the presence of α-[³²P]-UTP using a T7 promoter flanked firefly luciferase (GL3) PCR product as a template. T7 promoter flanked PCR products were generated with primers 5'-TAA TAC GAC TCA CTA TAG GGA GAT ATG AAG AGA TAC GCC CTG GTT and 5'-TAA TAC GAC TCA CTA TAG GGA GAA TAG CTT CTG CCA ACC GAA C. Unincorporated nucleotides were removed using a G-25 sephadex column (Roche) followed by purification of the dsRNA from an 8% polyacrylamide gel. Gl3 siRNAs (Dharmacon) were ³²P end-labeled using T4 polynucleotide kinase (Roche) after which unincorporated nucleotides were removed using a G-25 sephadex column (Roche).

To generate target RNA for the Slicer assay, a 492-bp region of the GL3 luciferase gene was PCR amplified using the primers 5'-TAA TAGAC TCA CTA TAG GGA GAA TGG AAG ACG CCA AAA ACA T and 5'-CAT CGA CTG AAA TCC CTG GT. The GL3 PCR product was used as a template for *in vitro* transcription using the Ampliscribe T7 flash transcription kit (Epicentre). After purification from an 8% urea-polyacrylamide gel, the RNA was cap-radiolabeled with the Scriptcap m⁷G capping system (Epicentre) according to the manufacturer's protocol. The capped RNA was purified from an 8% Urea-polyacrylamide gel before use in the Slicer assay.

Dicer assay

Dicer assays were performed in a final volume of 12 μL containing 4 μL S2 cell extract, 3 μL dicer buffer, 1 μL uniformly labeled dsRNA (200 cps), and 4 μL purified recombinant protein. Dicer buffer contained 0.175 $\mu\text{g}/\mu\text{L}$ creatine kinase (Roche), 16.7 mM DTT, 0.02 mg/ μL creatine monophosphate (Roche), 3.3 mM MgAc, 50 mM Hepes-KOH, 33.3% glycerol, 0.67 U/ μL RNasin (Roche), and 3.3 mM ATP. Reactions were incubated for 3 hrs at 27 $^{\circ}\text{C}$ after which they were deproteinized by proteinase K and phenol extracted (30). After precipitation, the RNA was dissolved in Ambion loading buffer II and loaded on a 12% denaturing polyacrylamide gel. Dicer products were visualized by exposing the polyacrylamide gel to a Kodak Biomax XAR film.

Slicer assay

Drosophila embryo lysates were produced from *w¹¹¹⁸* flies as described (30). Slicer reactions contained 5 μL embryo lysate, 3 μL cleavage buffer, 100 nM siRNA, 0.3 μM recombinant protein, and 1 μL capped target RNA (-1000 cps) in a final volume of 11 μL . The GL3 siRNA (Dharmacon) was used to induce cleavage of the firefly luciferase target RNA, whereas the control siRNA (Qiagen) was used as a negative control. After assembly of the reaction, samples were incubated for 2 hours at 25 $^{\circ}\text{C}$. Samples were then treated with proteinase K, extracted with phenol, and precipitated as described (30). Precipitated RNA was dissolved in Loading buffer II (Ambion) and analyzed on an 8% urea-polyacrylamide gel. Slicer products in ATP depleting conditions were analyzed on a 6% urea-polyacrylamide gel. Kodak Biomax XAR films were used to visualize the radioactive Slicer products.

Supplemental Figures

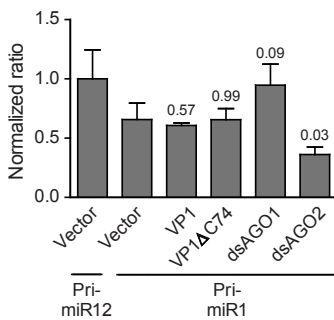


Figure S1. VP1 is unable to suppress the miRNA pathway. A firefly luciferase (Fluc) construct containing the par6 3'UTR, a target for miRNA1 (Fluc-par6), was co-transfected with plasmids encoding *Renilla* luciferase (Rluc) and either Nora virus VP1 or the inactive VP1 Δ C74 mutant. Fluc-par6 expression was silenced by co-transfecting a plasmid encoding pri-miRNA1, whereas a pri-miRNA12 expressing construct was used as a negative control. *AGO1* or *AGO2* gene expression was knocked down by co-transfection of dsRNA targeting these genes (dsAGO1 and dsAGO2, respectively). Expression of Fluc and Rluc was induced 2 days after transfection, and reporter activities were measured 3 days after transfection. Rluc activity was used to normalize Fluc activity within each sample, and data were normalized to the pri-miR12 treated sample. Bars represent averages and standard deviations of biological triplicates. A representative graph of two independent experiments is shown. The numbers represent p-values relative to pri-miR1 treated vector control samples in a two-tailed Student's t-test assuming equal variances.

2

```

NoraV Umea 2007      MINNQTNKKGQPLERVHFGSTQVVGKSTKRRQRGTKLDIEYTVRRNDAPKEQKFLISEIF 60
NoraV NL1           MINNQTNKKGQPLERVHFGSTQVVGKSTKRRQRGTKLDIEYTVRRNDAPKEQKFLISEIF 60
NoraV NL2           MINNQTNKKGQPLERVHFGSAQVVGKSTKRRQRGTKLDIEYTVKRNDAPKEQKFLVSEIF 60
NoraV reconstituted FR1 MINNQTNKKGQPLERVHFGSAQVVGKSTKRRQRGTKFDIEYTVKRNDAPKEQKFLVSEIF 60
*****:*****:*****:*****:*****

NoraV Umea 2007      DEKLDKQIKYEKKQNHTFIKPKLNLVIKEEQHITKKVLRGKERAATHAFMKEMVESNKIQ 120
NoraV NL1           DEKLDKQIKYEKKQNHTFIKPKLNLVIKEEQHIKKVLRGKERAATHAFMKEMVESNKIQ 120
NoraV NL2           DEKLDKQIKYEKKQNHTFIKPKLNLVTRREEQHMTKKVLRGKERAATHAFMKEMVESNKIQ 120
NoraV reconstituted FR1 DEKLDKQIKYEKKQNHTFIKPKLNLVTRREEQHVTKKVLRGKERAATHAFMKEMVESNKIQ 120
*****:****:*****

NoraV Umea 2007      PSWNVEYEKEIDEVDLFFMKKTKPFSGFSIKELRDSLIVQSDDKNMAQPTVMSSIDEIV 180
NoraV NL1           PSWNVEYEKEIDEVDLFFMKKTKPFSGFSIKELRDSLIVQSDDKNMAQPTVMSSIDEIV 180
NoraV NL2           PSWNVEYEKEIDEVDLFFMKKTKPFSGFSIKELRDSLIVQSDDKNMAQPTVMSSINEIV 180
NoraV reconstituted FR1 PSWNVEYEKEIDEVDLFFMKKTKPFSGFSIKELRDSLIVQSDDKNMAQPTVMSSSTNEIV 180
*****:***

NoraV Umea 2007      TPREEISVSAISEQLASLMERVDKLEKMNAALEEENKQLKKEREATIKSVKKEAKKIKQE 240
NoraV NL1           TPREEISVSAISEQLASLMERVDKLEKMNAALEEENKQLKKEREATIKSVKKEAKKIKQE 240
NoraV NL2           TPREEISVSAISEQLASLMERVDKLEKMNAALEEENKQLKKEREATIESVKKEAKRTKQE 240
NoraV reconstituted FR1 TPREEISVSAISEQLASLMERVDKLEKMNAALEEENKQLKKEREATIKSVKKEAKRTKQE 240
*****:*****:***

NoraV Umea 2007      KPQIVKKTQHKSGLVNLKITKTKVVGQEQCLEIENTQHKKFVEKPSMPLKVSKKMTEHQL 300
NoraV NL1           KPQIVKKTQHKSGLVNLKITKTKVVGQEQCLEIENTQHKKFVEKPSMPLKVSKKMTEHQL 300
NoraV NL2           KPQIAKKTQHKSGLVNLKITKIKVVGQEQCLEIENTQHKKFVEKPSMPSKVSKKMKGQQL 300
NoraV reconstituted FR1 KPQIAKKTQHKSGLVNLKITKTKVVGQEQCLEIENTQHKKFVEKPSMPSKVSKKMKGQQL 300
*****:*****:*****

NoraV Umea 2007      KKTIRTWYEFDPKSLVQHQKEVLNSVVTNTTFADKVRETGIPKQKIRYVAKPPAEKRSI 360
NoraV NL1           KKTIRTWYEFDPKSLVQHQKEVLNSVVTNTTFADKVRETGIPKQKIRYIAKPPAEKRSI 360
NoraV NL2           KKTIRTWYEFDPKSLVQHQKEVLNSVVTNTTFADKVRETGIPKQKIRYTAKPPAEKRSI 360
NoraV reconstituted FR1 KKTIRTWYEFDPKSLVQHQKEVLNSVVTNTTFADKVRETGIPKQKIRYVAKPPAEKRSI 360
*****

NoraV Umea 2007      HFYGYKPKGIPNKVWVNWVTTGTAMDAYEKADRYLYHQFKREMMIYRNKWKVFSKEFNYPY 420
NoraV NL1           HFYGYKPKGIPNKVWVNWVTTGTAMDAYEKADRYLYHQFKREMMIYRNKWKVFSKEFNYPY 420
NoraV NL2           HFYGYKPKGIPNKVWVNWVTTGTAMDAYEKADRYLYHQFKREMMVYRNKWKVFSKEFNYPY 420
NoraV reconstituted FR1 HFYGYKPKGIPNKVWVNWVTTGTAMDAYEKADRYLYHQFKREMMVYRNKWKVFSKEFNYPY 420
*****:*****:*****

NoraV Umea 2007      LSKPKMVWEENTWEYKYKTDVPYNFILKWRQLVQTYKPNTPIQADWYKISQKQQC 475
NoraV NL1           LSKPKMVWEENTWEYKYKTDVPYNFILKWRQLVQTYKPNTPIQADWYKISQKQQC 475
NoraV NL2           LSEPKMVWEENTWEYKYKTDVPYNFILKWRQLVQTYKPNTPIQADWYKISQKQQC 475
NoraV reconstituted FR1 LSEPKMVWEENTWEYKYKTDVPYNFILKWRQLVQTYKPNTPIQADWYKISQKQQC 475
**:*:*****

```

Figure S2. Alignment of VP1 sequences from different Nora virus isolates. Alignment of VP1 sequences of Nora virus isolate Umea 2007 (accession number GQ257737) and Nora virus sequences from infected fly stocks from our own laboratory (isolates NL1 and NL2, GenBank accession number JQ288019 and JQ288020). We analyzed VP1 sequences in a total of eight Nora virus-infected fly stocks. Five VP1 sequences were identical to NL1, one was the NL2 sequence, and two stocks contained a mixed population of Nora virus sequences. These eight stocks were obtained from five different laboratories or stock centers. However, they have been maintained in our laboratory before we tested them for Nora virus infection, and we cannot exclude the possibility that they became infected in our laboratory. Although we therefore cannot infer overall virus diversity from these data, they do indicate that VP1 is a conserved protein. The FR1 isolate is the Nora virus genome that was reconstituted from small RNA sequences from wildtype *w¹¹¹⁸* flies from a laboratory based in France (GenBank accession number JX220408).

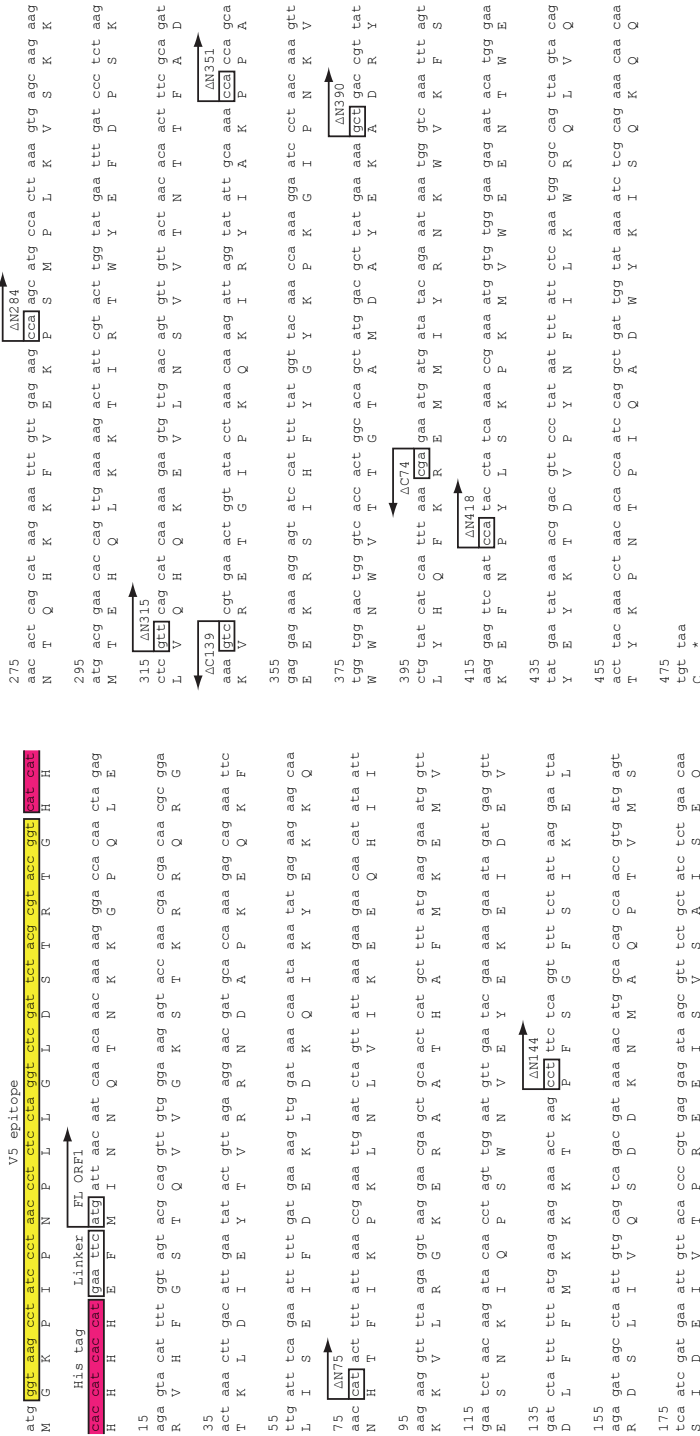


Figure S3. Nucleotide and protein sequence of full-length and VP1 mutants fused to V5-His tag at the N-terminus. Nucleotide and amino acid sequence of V5 epitope and Histidine (His) tagged full-length VP1 sequence (VP1^{FL}). A linker sequence between the His tag and VP1 was created to facilitate cloning. Start and stop sites of the respective N- and C-terminal deletion mutants of VP1 are indicated. The VP1 deletion mutants were fused to the V5-His tag in an identical way as the VP1^{FL} construct.

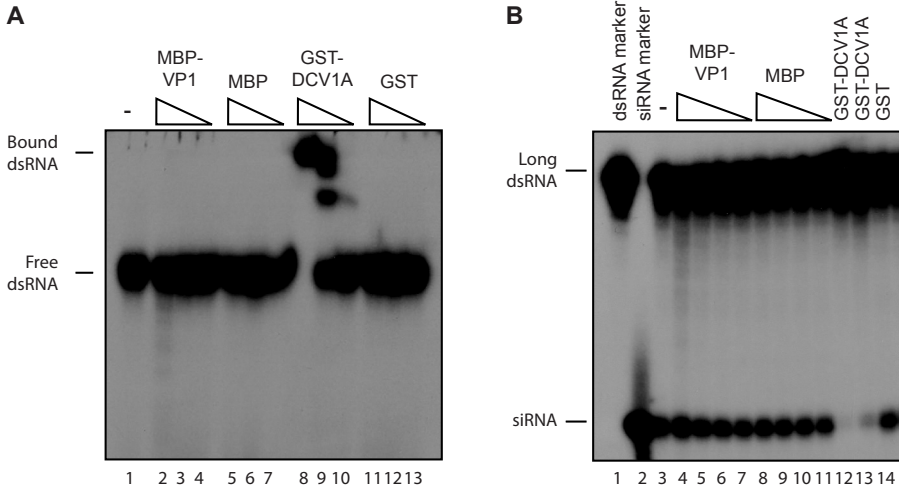


Figure S4. Nora virus VP1 is unable to bind long dsRNA or to interfere with Dcr-2 activity. (A) Mobility shift assay of suppressor proteins with long dsRNA. Uniformly radiolabeled long dsRNA was incubated for 30 minutes with buffer (lane 1) or recombinant MBP-VP1^{ΔN284} (lanes 2-4), MBP (lanes 5-7), GST-DCV 1A (lanes 8-10) or GST (lanes 11-13). Ten-fold dilutions of recombinant protein were used starting from the following concentrations: MBP-VP1^{ΔN284} (2 μM, lane 2), MBP (2.6 μM, lane 5), GST-DCV 1A (1 μM, lane 8), and GST (2.24 μM, lane 11). RNA mobility shifts were analyzed on an 8 % native polyacrylamide gel. (B) Dicer activity in S2 cell extract in the presence of viral suppressors. Uniformly radiolabeled long dsRNA was incubated in S2 cell extract for 3 hours with buffer (lane 3) or the indicated recombinant proteins. Two-fold dilutions were used for MBP-VP1^{ΔN284} (lanes 4-7, highest concentration 1.1 μM) and MBP (lanes 8-11, highest concentration 4.2 μM). Two independent preparations of GST-DCV 1A were used (lane 12, concentration of 0.54 μM and lane 13, concentration of 0.03 μM). GST was used at a concentration of 1.2 μM (lane 14). As size markers, dsRNA input (lane 1) and end-labelled siRNAs (lane 2) were used. Dicer products were analyzed on a 12% denaturing polyacrylamide gel.

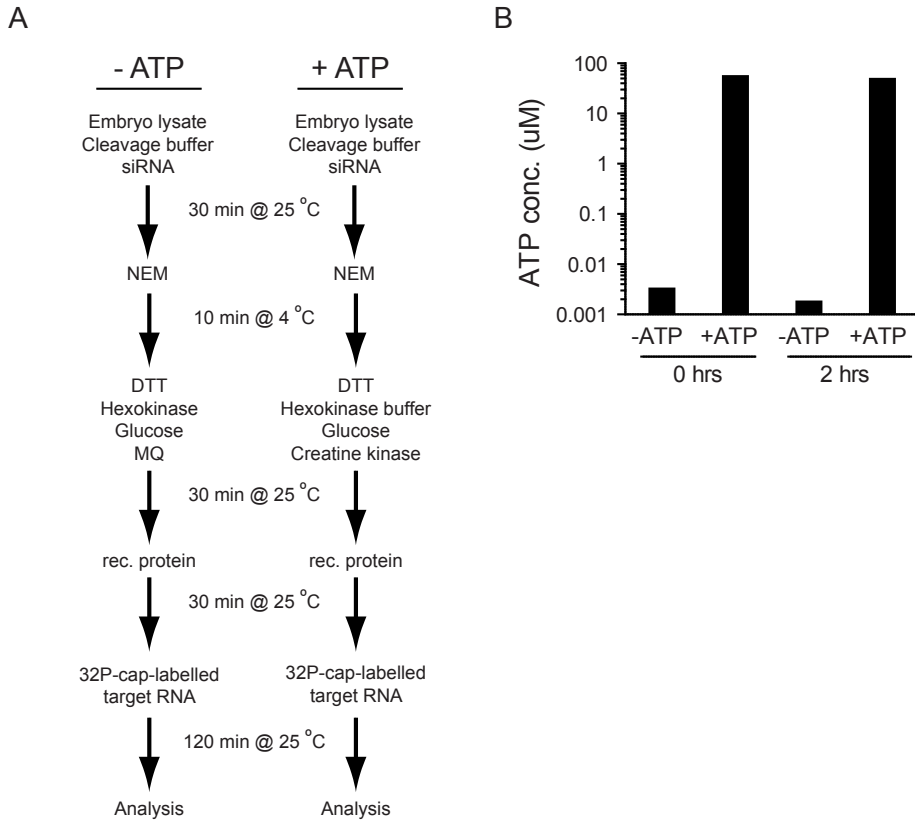


Figure S5. ATP depletion during Slicer assay. (A) Schematic representation of the protocol used to deplete (-ATP) or to regenerate ATP after initial depletion (+ATP) for Slicer assays of Figure 7F. For RISC loading, *Drosophila* embryo lysate was incubated with an siRNA for 30 minutes under standard conditions. Subsequently, N-ethylmaleimide (NEM) was added in both conditions to inhibit the ATP regenerating activity of creatine kinase. After incubating the reactions for 10 minutes on ice, DTT was added to quench the NEM in both conditions. Hexokinase, glucose, and milliQ water (MQ) were added in the -ATP protocol to deplete the pool of ATP. For the +ATP condition, Hexokinase was substituted by hexokinase buffer, and MQ was substituted for Creatine kinase to restore the ATP regenerating activity. Subsequently, the reactions were incubated for 30 minutes after which recombinant protein (rec. protein) was added. Following another 30 minutes incubation period, the ³²P-cap-labelled RNA was added to the reaction, after which the incubation was continued for another 2 hours. Subsequently, reactions were analyzed on a polyacrylamide gel. (B) ATP concentrations before and after the Slicer assay under -ATP and +ATP conditions. ATP levels were measured at the moment of target RNA addition (0 hrs) or after 2 hours of incubation with target RNA. For ATP concentration measurements, recombinant protein was substituted for protein storage buffer, and target RNA was substituted for MQ. ATP levels were measured using the Celltiter-Glo Luminescent Cell Viability Assay (Promega) according to the manufacturer's protocol.

Chapter 3

The DNA virus Invertebrate iridescent virus 6 is a target of the *Drosophila* RNAi machinery

Alfred W. Bronkhorst*, Koen W.R. van Cleef*, Nicolas Vodovar, İkbal Agah İnce, Hervé Blanc, Just M. Vlak, Maria-Carla Saleh and Ronald P. van Rij

Proc Natl Acad Sci U S A 2012, 109:E3604-3613

*These authors contributed equally to this manuscript

Abstract

RNA viruses in insects are targets of an RNA interference (RNAi)-based antiviral immune response, in which viral replication intermediates or viral dsRNA genomes are processed by Dicer-2 (Dcr-2) into viral small interfering RNAs (vsiRNAs). Whether dsDNA virus infections are controlled by the RNAi pathway remains to be determined. Here, we analyzed the role of RNAi in DNA virus infection using *Drosophila melanogaster* infected with Invertebrate iridescent virus 6 (IIV-6) as a model. We show that Dcr-2 and Argonaute-2 mutant flies are more sensitive to virus infection, suggesting that vsiRNAs contribute to the control of DNA virus infection. Indeed, small RNA sequencing of IIV-6-infected WT and RNAi mutant flies identified abundant vsiRNAs that were produced in a Dcr-2-dependent manner. We observed a highly uneven distribution with strong clustering of vsiRNAs to small defined regions (hotspots) and modest coverage at other regions (coldspots). vsiRNAs mapped in similar proportions to both strands of the viral genome, suggesting that long dsRNA derived from convergent overlapping transcripts serves as a substrate for Dcr-2. In agreement, strand-specific RT-PCR and Northern blot analyses indicated that antisense transcripts are produced during infection. Moreover, we show that vsiRNAs are functional in silencing reporter constructs carrying fragments of the IIV-6 genome. Together, our data indicate that RNAi provides antiviral defense against dsDNA viruses in animals. Thus, RNAi is the predominant antiviral defense mechanism in insects that provides protection against all major classes of viruses.

Introduction

Double-stranded RNA (dsRNA) is a danger signal: It cannot be detected in healthy, non-infected cells, but it is produced during infection by many RNA and DNA viruses (1). It is thus not surprising that dsRNA is a central trigger of innate immune responses. In vertebrates, recognition of dsRNA by the cytosolic sensors RIG-I and MDA-5 initiates a cascade of events culminating in the production of type I IFN and the subsequent induction of an antiviral state (2). Likewise, dsRNA triggers a sequence-independent antiviral response in penaeid shrimp that is distinct from the vertebrate IFN pathway (3). In plants, fungi, and arthropods, viral dsRNA triggers an antiviral RNAi response (4, 5).

Studies in insects like *Drosophila melanogaster* and mosquitoes support a model in which viral dsRNA is processed by Dicer-2 (Dcr-2) into viral small interfering RNAs (vsiRNAs). These vsiRNAs are then incorporated into Argonaute-2 (AGO2) in the RNA induced silencing complex (RISC), where they guide the recognition and endonucleic cleavage of viral target RNAs (6-8). Indeed, early seminal work in mosquitoes and *Drosophila* cells directly detected viral small RNAs by Northern blot analysis and demonstrated that knockdown of core RNAi genes resulted in an increase in virus replication (8-10). In accordance, in the genetic model organism *D. melanogaster*, flies with defects in *Dcr-2*, *R2D2*, or *AGO2* are unable to control RNA virus replication and, consequently, are hypersensitive to virus infection and succumb more rapidly than their wildtype (WT) controls (11-14).

Small RNA cloning and next-generation sequencing provides detailed insights into vsiRNA biogenesis. In several studies in insects, the polarity of the vsiRNA population deviates strongly from the highly skewed distribution of positive strand (+) over negative (-) viral RNAs that is generally observed in (+) RNA virus infection. Indeed, vsiRNAs mapped in similar proportions to (+) and (-) viral RNA strands in *Aedes aegypti*, *A. albopictus* and *Culex pipiens* mosquitoes infected with a number of arthropod-borne viruses including Sindbis virus, Semliki Forest virus, West Nile virus, Dengue virus and Chikungunya virus, as well as in *Drosophila* infected with (+) RNA viruses from different families (5, 15-24). In addition, in infections of *Drosophila* with the negative strand RNA virus vesicular stomatitis virus similar numbers of (+) over (-) vsiRNAs were recovered (14). These results, together with the distribution of vsiRNAs all along the viral genome, imply that viral replication intermediates of RNA viruses are the main targets for Dcr-2. Also in dsRNA virus infections, similar amounts of vsiRNAs of both polarities were generated, most likely by Dcr-2-dependent processing of viral genomic dsRNA (18). Thus, different classes of viruses seem to be processed by a similar vsiRNA biogenesis pathway. These studies have focused on RNA viruses, because all well-

established model viruses of *Drosophila* and all known mosquito-transmitted viruses are RNA viruses. More recently, a next-generation sequencing approach identified small RNAs derived from a novel densovirus, a single-stranded (ss) DNA virus, in wild-caught *C. pipiens molestus* (25). These observations suggest that ssDNA viruses are a target for Dicer in mosquitoes, although the biogenesis and function of the viral small RNAs remain unclear.

dsDNA viruses produce dsRNA during their replication, presumably due to base pairing of convergent overlapping transcripts from both strands of the DNA genome (26-28). Whether such dsRNA is a *bona fide* target for Dcr-2 remains to be established. Although a dsDNA virus has recently been identified in wild-caught *Drosophila innubila* (29), a dsDNA virus that naturally infects *D. melanogaster* has yet to be discovered. Invertebrate iridescent virus 6 (IIV-6), a member of the *Iridovirus* genus within the *Iridoviridae* family, has a broad host range; under experimental conditions it replicates in a number of Dipteran species, including *D. melanogaster* (30-32). We therefore used IIV-6, also known as Chilo iridescent virus, as a model to analyze the RNAi response against dsDNA viruses in *Drosophila*. IIV-6 is a large, complex virus with a dsDNA genome of 212,482-bp that encodes 211 putative open reading frames (ORFs) distributed along the two strands of the viral genome (33, 34). Here, we report that IIV-6 is a target of the RNAi machinery. We demonstrate that *Dcr-2* and *AGO2* mutant flies are more sensitive to IIV-6 infection. Moreover, we identified *Dcr-2*-dependent vsiRNAs that map to both strands of the viral genome, show an uneven distribution across the viral genome, but are remarkably conserved between independent libraries. In accordance, we showed that both sense and antisense transcripts are generated *in vivo* and *in vitro* during IIV-6 replication, supporting a model in which viral dsRNA that is produced by bidirectional overlapping transcription is a target for Dcr-2. Together, our results indicate that RNAi provides antiviral defense against DNA viruses in *Drosophila*.

Results

IIV-6 as a model to study antiviral immunity against DNA viruses in *Drosophila*

We investigated the replication kinetics of IIV-6 in *w¹¹¹⁸* and Oregon-R (OR) WT flies. We inoculated adult flies intra-abdominally with IIV-6 and monitored survival and viral titers over time. IIV-6 established a productive infection as revealed by iridescence in eyes, thorax and abdomen, which is the result of light reflection by assemblies of paracrystalline arrays of IIV-6 particles (35) (Figure 1A). Accordingly, IIV-6 virion coat proteins were detected by Western blot analysis in total lysates of IIV-6-infected

flies (Figure 1B, lanes 2 and 4). The specificity of the IIV-6 antibody was verified by lack of signal in mock-infected flies (lanes 1 and 3). IIV-6 replicated efficiently with a rapid 6- to 7-log increase in viral titer over the first 6 days, and a relatively stable titer thereafter (Figure 1C). However, despite these high and stable titers, virus infection did not efficiently kill WT flies over the course of 31 days (Figure 1D, over 60% survival after follow-up). These results establish IIV-6 as a model to study DNA virus infection in *Drosophila*.

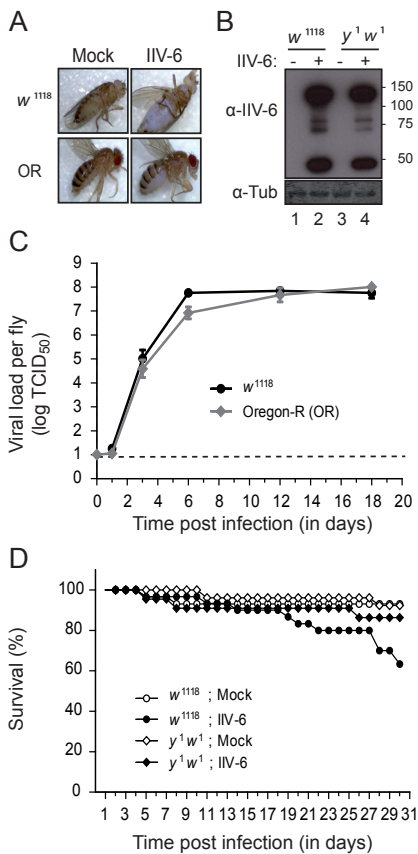


Figure 1. IIV-6 as a model to study antiviral immunity against DNA viruses in *D. melanogaster*. (A) IIV-6 infection of w^{1118} and Oregon-R (OR) WT flies results in iridescence in eyes, thorax and abdomen. Female flies were inoculated in the abdomen with 14,000 TCID₅₀ units of IIV-6 or with Tris buffer as a control (mock). Representative images of flies at 30 days post-infection are shown. Iridescence becomes apparent as of day 9. (B) Western blot analysis of viral proteins in IIV-6 or mock-infected w^{1118} and $y^1 w^1$ WT flies. Female flies were harvested at 12 days post-infection. Polyclonal anti-IIV-6 antibodies were used to visualize virion coat proteins. A polyclonal anti- α -tubulin (α -Tub) antibody was used as loading control. Molecular mass (kDa) is indicated to the right of the autoradiograph. (C) Viral titers in w^{1118} (black) and OR (gray) female flies after infection with IIV-6. Three pools of four flies were collected and homogenized at each indicated time point and viral titer in the homogenate was determined by end-point dilution. Titers represent averages and SEMs of three independent pools of four flies. The dashed line represents the detection limit of the assay. (D) Survival curve of *D. melanogaster* WT flies after IIV-6 infection. Survival rate of w^{1118} (circles) and $y^1 w^1$ (diamonds) female flies was monitored daily after virus infection (filled symbols) or mock infection (open symbols). A representative of three independent experiments is shown.

RNAi mutant flies are more susceptible to IIV-6 infection

To examine the role of the antiviral RNAi machinery on IIV-6 replication *in vivo*, we analyzed the outcome of IIV-6 infection in flies that lack core RNAi components. First, we analyzed whether *Dcr-2* mutant flies were more sensitive to IIV-6 infection. After an initial stable survival, *Dcr-2* mutants died from 18 days post-infection onwards, with 100% mortality at 29 days after infection. In contrast, over 85% of $y^1 w^1$ controls survived

3

over the same time course (Figure 2A). Survival after inoculation with UV-inactivated IIV-6 was similar to that of mock-infected flies (about 85% survival after follow-up), indicating that mortality is the result of active virus replication (Figure 2B). To further analyze whether RNAi controls IIV-6 infection *in vivo*, we monitored survival rates of *AGO2* mutant flies. *AGO2* homozygous mutants (*AGO2*^{414/414}) and their heterozygous controls (*AGO2*^{414/+}) were challenged with IIV-6. Although heterozygous controls were resistant to IIV-6 infection, *AGO2* homozygotes were more sensitive to virus infection with 35% mortality after follow-up for 31 days (Figure 2C). To exclude the possibility that the susceptibility of *AGO2* homozygous mutant flies was due to second-site mutations in the genome of *AGO2*⁴¹⁴ flies, we analyzed survival of flies that carried a combination of two different *AGO2* null alleles and thus do not express *AGO2* (*AGO2*^{414/454}, *AGO2*^{414/321} and *AGO2*^{321/454} transheterozygotes) and their *AGO2* heterozygous controls (*AGO2*^{414/+} and *AGO2*^{321/+}). Because *AGO2*³²¹ and *AGO2*⁴⁵⁴ were reported to be true null alleles (36), we first analyzed survival of these *AGO2* transheterozygous mutants in the well-studied Drosophila C virus (DCV) and Cricket paralysis virus (CrPV) models of infection. *AGO2* transheterozygous flies are equally sensitive to DCV challenge as *AGO2*⁴¹⁴ homozygous mutant flies, whereas their heterozygous controls displayed a slower mortality rate (Figure S1A). Similar results were obtained upon CrPV challenge (Figure S1B). These results establish *AGO2* transheterozygous mutant flies as a reliable genetic model to analyze survival following virus infection. We observed that *AGO2* transheterozygous mutants died more rapidly after IIV-6 challenge (40-65% survival after follow-up) compared to their heterozygous controls (over 85% survival) (Figure 2D) and with their mock-infected controls (over 88% survival). To analyze whether the increased lethality correlates with an increase in viral titers, we analyzed the viral load in RNAi mutant and WT flies. We observed a modest increase in viral titers in RNAi mutant flies compared to WT controls at 3 days post-infection (Figure 2E). However, viral titers were similar at 12 days after infection. Our results thus imply that RNAi controls IIV-6 infection in *Drosophila*, but that it only modestly affects viral titers.

IIV-6 infection triggers the production of Dcr-2-dependent viral siRNAs

dsDNA viruses are known to produce dsRNA during infection (1), presumably as a result of convergent overlapping transcription from both strands of the viral genome. The IIV-6 genome is predicted to encode 211 ORFs, of which 45% and 55% derive from the upper and lower strands, respectively (34). We refer to the viral strand that is transcribed from left to right on the conventional map as the R (upper) strand and to its complement as the L (lower) strand.

To investigate whether viral dsRNA is processed into vsiRNAs, we sequenced the small RNAs from WT and RNAi mutant flies at 12 days after infection with IIV-6. Small

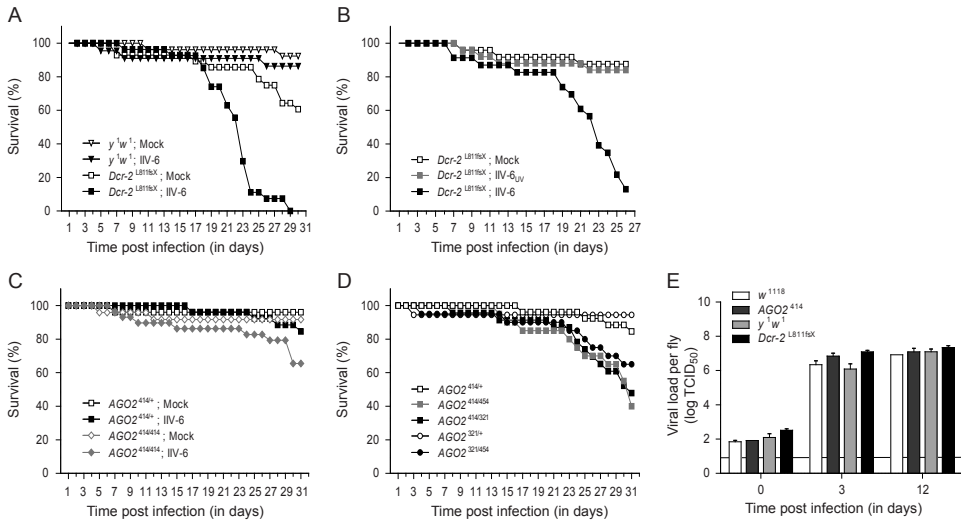


Figure 2. *D. melanogaster* RNAi mutant flies are susceptible to IIV-6 infection. (A) Survival of *Dcr-2* mutant flies after IIV-6 challenge. The survival rate of female *Dcr-2*^{L811fsX} (squares) and *y*¹*w*¹ control (triangles) flies was monitored daily after IIV-6 (filled symbols) or mock infection (open symbols). A representative of three independent experiments is shown. (B) Survival assay of *Dcr-2*^{L811fsX} female flies injected with UV-inactivated IIV-6 (IIV-6_{UV}, gray squares), IIV-6 (black squares) or Tris buffer (white squares). (C) Survival of *AGO2*⁴¹⁴ homozygous (diamonds) and *AGO2*^{414/+} heterozygous controls (squares) infected with IIV-6 (filled symbols) or Tris buffer (open symbols). A representative of two independent experiments is shown. (D) Survival of IIV-6-infected *AGO2*-null mutant flies. *AGO2*^{414/454} (gray squares), *AGO2*^{414/321} (black squares), and *AGO2*^{321/454} (black circles) transheterozygous flies, as well as *AGO2*^{414/+} (white squares) and *AGO2*^{321/+} (white circles) heterozygous controls were infected with IIV-6, and survival was monitored daily. A representative of two independent experiments is shown. The experiments in C and D were run in parallel; the survival curve of IIV-6-infected *AGO2*^{414/+} flies is depicted in both panels. (E) Viral load in RNAi mutant and WT flies after IIV-6 infection. *Dcr-2*^{L811fsX}, *AGO2*⁴¹⁴ and their WT controls *y*¹*w*¹ and *w*¹¹¹⁸, respectively, were infected with IIV-6, and virus production in the flies was monitored over time. At each time point, three pools of four flies were homogenized, and the viral titer in the homogenate was determined by end-point dilution. Bars represent averages and SEMs of three independent pools of four flies. The horizontal line represents the detection limit of the titration.

RNAs ranging in size from 19 to 30-nt were cloned and deep-sequenced on an Illumina Genome Analyzer. Two independent libraries of IIV-6-infected WT and *AGO2* mutant flies were analyzed (datasets 1 and 2). Small RNAs were first mapped to the *Drosophila* genome; nonmapping small RNAs were then mapped to the IIV-6 genome (Table 1). The vast majority of IIV-6-derived small RNAs in WT and *AGO2* mutant flies was 21-nt long (Figure 3). These small RNAs were *Dcr-2*-dependent vsRNAs, because the normalized levels of vsRNAs decreased >875-fold in *Dcr-2* mutant flies compared with WT flies (Table 1).

Table 1. Descriptions of small RNA libraries

	<i>w¹¹¹⁸</i>		<i>AGO2¹¹⁴</i>		<i>Dcr-2^{LS1fix}</i>
	Dataset 1	Dataset 2	Dataset 1	Dataset 2	Dataset 1
<i>Drosophila</i> genome, reads	1,647,783	10,588,690	7,664,970	14,758,882	5,371,641
rRNA, %*	49.0	49.9	27.7	32.1	21.5
miRNA, %*	44.7	38.4	65.5	55.9	67.5
IIV-6: 0 mismatch, %*	8.3	8.2	2.8	10.1	0.03
IIV-6: 1 mismatch, %*	0.4	0.3	0.2	0.5	0.001
IIV-6, % to miRNAs [†]	17.4	20.0	3.5	17.5	0.02

*Descriptions of small RNAs in the size range of 19-25 nt; percentage relative to reads mapping to the *Drosophila* genome.

[†]Normalized 21-nt viral reads mapping to the IIV-6 genome, allowing 0 or 1 mismatch during alignment; percentage viral reads relative to total cellular miRNA reads.

Dcr-2 generates 21-nt duplex siRNAs in which 19 nucleotides are base paired, leaving 2-nt 3' overhangs at each end. We thus analyzed 21-nt viral small RNAs for the presence of this Dcr-2 signature, as previously described (37). In contrast to our observations in infections with Nora virus, a (+) RNA virus (37), we did not observe enrichment for a 19-nt overlap among viral small RNAs mapping to opposite strands of the IIV-6 genome (Figure S2A). Asymmetric RISC loading preferentially retains one of the two strands of an siRNA duplex (38). Our results thus suggest that the majority of IIV-6-derived vsiRNAs do not exist as siRNA duplexes, but that they are associated with RISC. Although the size distribution of viral small RNAs was similar between *AGO2* mutant and WT flies, the size distribution of the viral small RNAs in *Dcr-2* mutants was vastly different. In contrast to the sharp 21-nt peak in WT flies and *AGO2* mutants, small RNAs in *Dcr-2* mutants showed a broader size distribution, with only a minor enrichment at 21-nt. A similar shift toward small RNAs with sizes other than 21-nt was noted before in *Dcr-2* mutant flies infected with vesicular stomatitis virus (14). Recombinant and immunoprecipitated Dicer-1 (Dcr-1) is able to process long dsRNA into siRNA in *in vitro* assays, albeit with low efficiency (39-41). Moreover, small RNAs derived from an inverted repeat transgene could be detected by Northern blot analysis in *Dcr-2* null mutants (42). We thus hypothesize that in the absence of Dcr-2, another nuclease, presumably Dcr-1, processes low levels of viral dsRNA to generate viral small RNAs. The lack of a prominent 22-nt viral RNA peak in *Dcr-2* mutants (Figure 3) suggests that IIV-6 does not produce viral microRNAs (miRNAs). Together, our data indicate that IIV-6 infection results in the production of vsiRNAs in a Dcr-2-dependent manner.

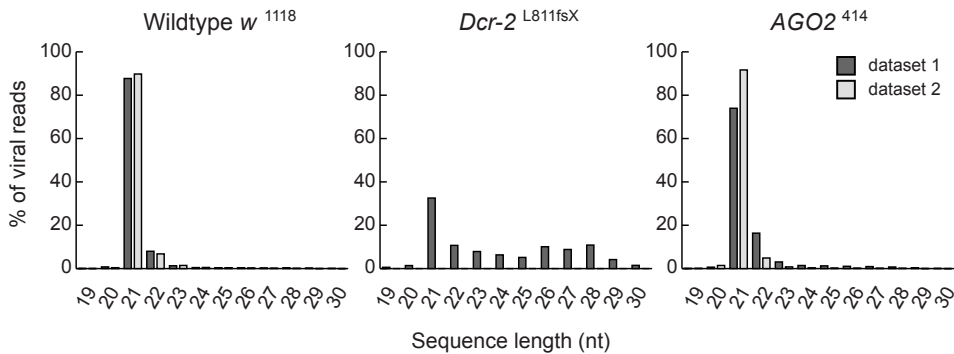


Figure 3. Production of Dcr-2-dependent viral siRNAs in IIV-6 infection. Size profiles of viral small RNAs mapping to the IIV-6 genome, allowing one mismatch during alignment, in *w*¹¹¹⁸ WT (Left), *Dcr-2*^{L811fsX} (Center) and *AGO2*⁴¹⁴ (Right) flies are shown. Small RNA libraries were generated from a pool of 15 female flies at 12 days post-infection. Two independent libraries of IIV-6-infected WT flies and *AGO2* mutants were analyzed (datasets 1 and 2; dark gray and light gray, respectively).

Uneven distribution of viral siRNA profiles across the IIV-6 genome

We next analyzed the distribution of vsiRNAs across the viral genome in WT and *AGO2* mutant flies (Figure 4A and B). A global presentation of vsiRNA coverage over the viral genome indicates that vsiRNAs are derived from both strands of the viral genome. In *Dcr-2* mutants (Figure 4C), the low number of viral small RNAs also mapped to both strand of the viral genome, which is in line with our hypothesis that low level of viral dsRNA processing may occur in a Dcr-2-independent manner. Although vsiRNAs mapped along the entire viral genome in WT and *AGO2* mutant flies, a highly uneven distribution of vsiRNAs with strong clustering in small defined genomic regions (hotspots) and only modest coverage in other regions (coldspots) was observed (Figure 4 A and B, Figure S2B). The uneven coverage of vsiRNAs across the genome was highly reproducible between experiments, with a strong correlation between vsiRNA densities in the two independent datasets of WT and *AGO2* mutant flies ($r=0.975$, $P < 0.001$ and $r=0.967$, $P < 0.001$, respectively, Figure S3). Furthermore, the distribution of vsiRNAs across the genome was highly similar between WT and *AGO2* mutant flies (Figure 4A and B). Indeed, a remarkable congruence of vsiRNA profiles in both genetic backgrounds was apparent in more detailed views of highly covered regions of the genome (representative examples are shown in Figure 4D and E). To substantiate the congruence between small RNA profiles in WT and *AGO2* mutant flies further, we divided the viral genome into 500-bp bins and compared the number of small RNAs in each bin between these genotypes (Figure 4F). Indeed, we observed a strong correlation between vsiRNA densities in WT and *AGO2* mutant libraries in both independent datasets ($r=0.939$, $P < 0.001$ and $r=0.959$, $P < 0.001$ for dataset 1 and 2 respectively).

The concordance of vsiRNA profiles in flies with different genetic backgrounds suggests that the uneven distribution of vsiRNAs and the presence of vsiRNA hotspots in the genome are caused by factors intrinsic to the virus, such as the relative expression of viral transcripts.

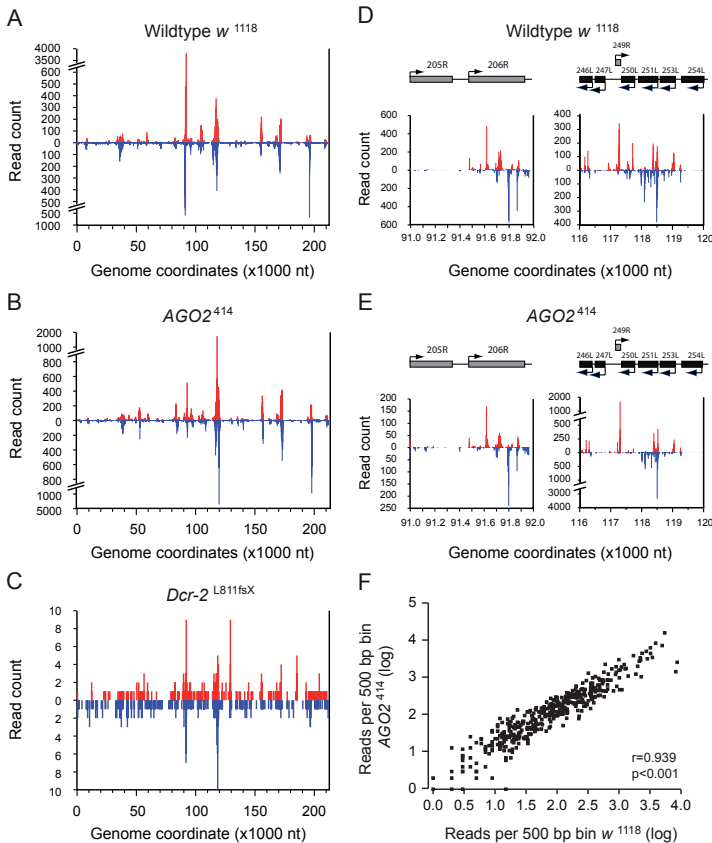


Figure 4. Uneven distribution of viral siRNA profiles across the IIV-6 genome. (A-C) Profile of IIV-6-derived vsiRNAs across the IIV-6 genome. Viral siRNAs were aligned to the IIV-6 genome allowing one mismatch during alignment. The genome coordinates of the 5' end of each vsiRNA in *w*¹¹¹⁸ WT (A), *AGO2*⁴¹⁴ (B), and *Dcr-2*^{L811fsX} (C) flies were plotted. (D-E) Profile of IIV-6-derived vsiRNAs in *w*¹¹¹⁸ WT (D) and *AGO2*⁴¹⁴ (E) flies mapping to genome coordinates 91,000-92,000 (Left) and 116,000-120,000 (Right) that contain regions with a high density of vsiRNAs are shown. ORFs located in the genome region are depicted above the plot, drawn to scale. Viral siRNAs that mapped to the R and L strand of the IIV-6 genome are shown in red and blue, respectively. Small RNA libraries were generated from a pool of 15 female flies at 12 days post-infection. Profiles from dataset 1 are presented; profiles from dataset 2 are provided in Figure S3. (F) The IIV-6 genome was divided into 500-bp bins and the number of vsiRNAs per bin in *w*¹¹¹⁸ WT and *AGO2*⁴¹⁴ mutant flies was analyzed in a scatter plot (log-transformed data, dataset 1; $r = 0.939$, $P < 0.001$, Pearson's correlation test).

Convergent transcripts as a source of viral double-stranded RNA in IIV-6 infection

To identify the dsRNA substrate for vsiRNA biogenesis, we analyzed the distribution of the vsiRNAs corresponding to the L and R strands of IIV-6. We found that 47% and 43% of the vsiRNAs mapped to the R strand in WT and *AGO2* mutant flies, respectively (Figure 5A), closely mimicking the distribution of the ORFs over the viral genome strands (45% R strand ORFs). When restricting our analyses to individual ORFs, we also observed that vsiRNAs are derived from both the L and R strands. Moreover, the density of vsiRNAs that map to the L strand strongly correlated with the density of reads mapping to the R strand of individual ORFs (Figure 5B, $r=0.78$, $P<0.001$). Thus, individual ORFs produced vsiRNAs that map to both strands of the genome, irrespective of the L or R orientation of the ORF. These results suggest that vsiRNAs predominantly derive from overlapping sense and antisense transcripts, rather than from intramolecular stem-loop structures in single-stranded viral transcripts. To analyze the occurrence of antisense transcription during IIV-6 infection, we performed strand-specific RT-PCRs on infected w^{1118} WT flies. To avoid possible false-positive

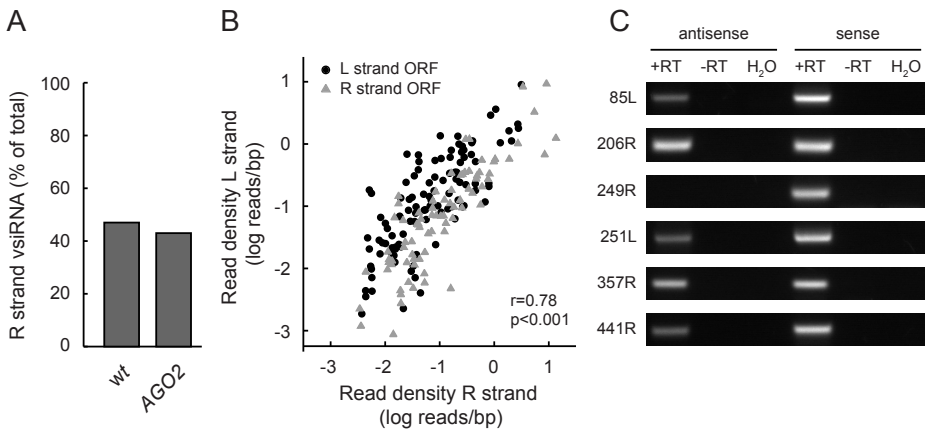


Figure 5. Convergent transcripts are a source of dsRNA during IIV-6 infection. (A) Percentage of the total vsiRNAs that map to the viral R strand in w^{1118} WT (wt) and *AGO2*¹¹⁴ mutant flies. (B) Scatter plot of the vsiRNAs from individual ORFs that map to the viral L and R strand in w^{1118} WT flies. For each ORF, the total number of vsiRNAs derived from each strand was divided by the length of the ORF. The data were log transformed and presented in a scatter plot. Circles and triangles indicate ORFs on the viral L and R strand, respectively. Correlation between both read densities was evaluated with a Pearson's correlation test. (C) Ethidium bromide-stained gels of strand-specific RT-PCR assays for the detection of sense and antisense transcripts from the indicated IIV-6 ORFs in infected w^{1118} WT flies. RT-PCR assays were performed in either the presence (+RT) or absence (-RT) of reverse transcriptase. H₂O was included as nontemplate control during PCR amplification. 85L, 206R, 249R, 251L and 441R represent ORFs with a high coverage of vsiRNA reads per base pair (bp), whereas 357R represents an ORF with a low coverage of vsiRNAs per bp.

3

results due to mispriming during cDNA synthesis, we used strand-specific primers containing a nonviral tag sequence (T7 promoter) at the 5' end, thereby generating tagged cDNA that can be PCR-amplified using a combination of a virus-specific primer with a T7 primer (43-46). We selected five ORFs with a high density of vsiRNA reads (85L, 206R, 249R, 251L and 441R) and one ORF with a low vsiRNA density (357R). For five out of six selected ORFs, we readily detected sense and antisense transcripts; for ORF 249R we could not detect antisense transcripts using this method (Figure 5C). All gene-specific primers efficiently amplified fragments of the selected ORFs in control PCR reactions using viral DNA as a template (Figure S4), excluding inefficient primer binding as an explanation for our inability to detect antisense ORF 249R transcripts. These results further support the existence of bidirectional overlapping transcription in the IIV-6 genome. Because antisense transcription also occurs in genomic regions with low vsiRNA coverage (ORF 357R), these results suggest that other factors, such as the relative amounts of viral sense and antisense transcripts, may contribute to differences in vsiRNA coverage across the genome.

To confirm the presence of sense and antisense transcripts, we performed Northern blot analysis on mock and IIV-6-infected *Drosophila* S2 cells using oligonucleotide probes that specifically recognize either viral RNA strand (Figure S5). For all tested ORFs (85L, 206R, and 441R), sense transcripts that matched the predicted size of the selected ORFs were readily detected. Northern blot analyses using probes that detect antisense transcripts revealed the presence of high molecular weight (>9 kb) antisense transcripts for all three ORFs as well as a small antisense transcript for ORF 441R. The origin and biogenesis of these antisense transcripts awaits further investigation.

Together, the small RNA profiles, strand-specific RT-PCR, and Northern blot analyses indicate that both sense and antisense transcripts are generated during IIV-6 infection. We propose that these viral transcripts form dsRNA that activates the RNAi pathway, resulting in the production of Dcr-2-dependent vsiRNAs.

IIV-6 derived vsiRNAs mediate gene silencing

To analyze whether IIV-6 derived vsiRNAs are functional in mediating target gene silencing, we designed luciferase reporter plasmids. To this end, the IIV-6 genome was divided into 500-bp bins, from which we selected 10 hotspot regions that produced the highest number of vsiRNAs (Figure S2B). These fragments, as well as a non-specific GFP control sequence, were cloned in the 3' UTR of a firefly luciferase (Fluc) reporter plasmid (Figure 6A). *Drosophila* S2 cells were transfected with these reporter plasmids together with a plasmid encoding *Renilla* luciferase (Rluc) as a normalization control. We then infected these cells with IIV-6 and monitored luciferase activity. If vsiRNAs are incorporated in a functional RISC complex, it is expected that IIV-6 infection

will induce specific silencing of the IIV-6 reporters, but not the GFP control plasmid. Indeed, we observed significant silencing of six IIV-6 reporters (Figure 6B). The extent of silencing did not seem to correlate with vsiRNA density. For example, the reporter for hotspot 8 was silenced most efficiently, whereas the reporter for the hotspot with the highest density (hotspot 1) was silenced to a lesser extent. These results are in line with observations in *Nicotiana benthamiana*, in which no clear correlation was observed between vsiRNA density and efficiency of silencing of a sensor construct (47). Strikingly, in mosquito cells, hotspot vsiRNAs were found to be less efficient at mediating antiviral RNAi than coldspot vsiRNA, which was hypothesized to reflect a decoy strategy to evade the antiviral RNAi response (22). Whether a similar mechanism plays a role in IIV-6 infection remains to be established.

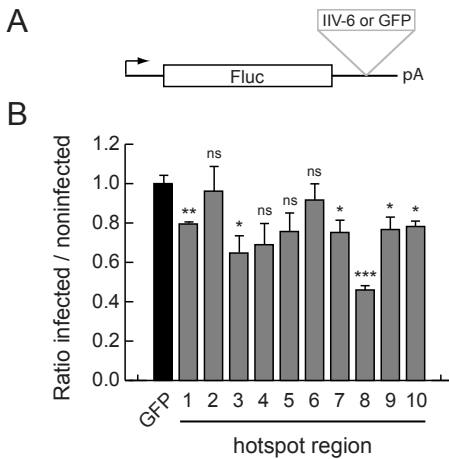


Figure 6. IIV-6 derived vsiRNAs mediate gene silencing. (A) Schematic representation of reporter plasmids. Sequences (500-bp) of IIV-6 genome or GFP (control) were cloned into the 3' UTR of a copper-inducible firefly luciferase (Fluc) plasmid to generate IIV-6 and GFP reporter plasmids. (B) RNAi reporter assay in *Drosophila* S2 cells. IIV-6 or control reporter plasmids were transfected together with a *Renilla* luciferase (Rluc) plasmid 1 day before mock or IIV-6 infection. Two days after transfection, expression of Fluc and Rluc was induced and luciferase activity was measured the day thereafter. Fluc expression was normalized to Rluc expression and presented as ratio of infected over noninfected cells relative to the values for GFP control plasmid (set at 1). Bars represent averages and SEMs of three independent experiments. *P* values were calculated using Student's *t* test; * *P* < 0.05; ** *P* < 0.01; *** *P* < 0.001; ns, not significant.

Having established that IIV-6-derived vsiRNAs are incorporated into a functional RISC complex, we analyzed their effect on viral gene expression. To this end, we compared viral transcript levels in IIV-6-infected *w*¹¹¹⁸ WT and *AGO2*⁴¹⁴ mutant flies. We selected 5 ORFs with a high coverage of vsiRNA reads per base pair and analyzed expression levels using strand-specific quantitative RT-PCR (qRT-PCR). Although we observed a modest, but not statistically significant, 1.6-1.8 fold increase in antisense and sense transcripts for one ORF (227L), we were unable to detect a general increase in viral transcript levels in *AGO2* mutant flies (Figure S6). Because we analyzed viral transcript levels at a single time point and viral gene expression is likely to be under tight temporal control, we cannot exclude the possibility that the pathology in RNAi mutant flies is due

to an early disequilibrium of transcripts levels (i.e. high levels of specific viral transcripts in *AGO2* mutants at a specific time in infection). Future genome-wide transcriptome analyses will be required to analyze the dynamics of viral gene expression and the role of the RNAi machinery in post-transcriptional regulation thereof.

Discussion

RNA viruses in insects are targets of an RNAi-based antiviral immune response, in which viral replication intermediates or viral dsRNA genomes are processed by Dcr-2 into vsiRNAs. In this study, we established IIV-6 as a model to study the role of RNAi in a productive but nonlethal infection by a dsDNA virus. Our results demonstrate that RNAi targets dsDNA viruses *in vivo*, further extending the role of RNAi as an antiviral defense mechanism.

The production of vsiRNAs upon RNA virus infection is a key feature of an antiviral RNAi response. The detection of Dcr-2-dependent vsiRNAs in infected flies provides direct evidence that IIV-6 is a target of the *Drosophila* RNAi machinery. We observed a highly uneven distribution of vsiRNAs across the IIV-6 genome, with similar levels of vsiRNAs mapping to both strands of the viral genome. Accordingly, analysis of individual ORFs revealed a strong correlation in vsiRNA reads derived from the R and L strands of the viral genome. Furthermore, using strand-specific (q)RT-PCR and Northern blot analysis, we demonstrate the presence of sense and antisense viral transcripts derived from different regions in the IIV-6 genome. Finally, we show that IIV-6-derived vsiRNAs mediate gene silencing in reporter assays in S2 cells. These results support a model in which dsRNA that is generated by bidirectional overlapping transcription is the major substrate for vsiRNA biogenesis during dsDNA virus infection.

Antisense transcription is prevalent among different families of DNA viruses, and has been suggested to affect viral gene expression (48-52). Antisense transcripts have the potential to form dsRNA by base pairing with sense transcripts. Indeed dsRNA can readily be detected in infections by DNA viruses in mammalian cells (1). However, although mammalian DNA viruses encode microRNAs, they do not seem to produce Dicer-dependent vsiRNAs (53, 54). For example, a recent report detected widespread antisense transcription in lytic Kaposi's sarcoma-associated herpesvirus infection, but failed to identify abundant vsiRNAs (51). Similarly, antisense transcription is very abundant throughout the genome of human cytomegalovirus (50). However, deep sequencing of the small RNAs in infected cells readily identified viral miRNAs, but detected only a limited number of other viral small RNAs. These small RNAs mapped to a restricted number of defined genomic loci and whether they are *bona fide* Dicer

products remains unclear (55). In plants (*Arabidopsis*), the pararetrovirus Cauliflower mosaic virus (CaMV) also produces long antisense transcripts (56, 57). Furthermore, CaMV vsRNAs mapped to both strands of the genome, indicating that antisense transcripts base pair with sense transcripts to produce dsRNA substrates for members of the Dicer-like protein family. Formation of dsRNA by convergent transcription in Cassava mosaic virus, a single-stranded DNA virus of the *Geminiviridae* family, was also postulated to be the source of vsRNA production in tobacco (*N. benthamiana*) and cassava (*Manihot esculenta*) plants (58, 59).

Thus, DNA viruses in plants, insects and mammals have an enormous potential to form dsRNA, but only in plants and insects this dsRNA is processed into vsRNAs. The reason for this discrepancy is not obvious because *in vitro* and *in vivo* studies imply that mammalian Dicer is capable of processing long stretches of dsRNA into siRNAs (60-63). Strikingly, humans only encode a single Dicer protein, whereas plants and *Drosophila* encode multiple Dicer family members (two and four in *Drosophila* and *Arabidopsis*, respectively). Perhaps, the diversification of the Dicer gene family in plants and insects allowed the functional specialization and more efficient processing of viral dsRNA for antiviral defense.

Another remarkable difference between vertebrate DNA viruses and IIV-6 is the notable absence of viral miRNAs in IIV-6. Mammalian DNA viruses, including herpesviruses and polyomaviruses, produce viral miRNAs that are capable of modulating viral or host gene expression (64). Individual herpesviruses may encode multiple miRNAs; for example, human cytomegalovirus encodes 22 miRNAs in its 230-kb genome (55). In *Drosophila*, miRNA biogenesis involves the sequential processing of primary miRNA transcripts into pre-miRNAs by Drosha and its cofactor Pasha (together known as the Microprocessor complex) in the nucleus and the cleavage of pre-miRNA into mature miRNAs by cytoplasmic Dcr-1. Mature miRNAs are then incorporated into an Argonaute-1-containing RISC, where they trigger translational repression or degradation of the target mRNA (65). Iridoviruses are nucleocytoplasmic viruses with an initial stage of replication in the nucleus, where early viral transcripts are generated from the input virion DNA template by host RNA Polymerase II (30). These viral transcripts may follow the canonical miRNA processing pathway of cellular miRNAs. Indeed, 11 viral miRNAs were identified in Singapore grouper iridovirus, a member of the *Iridoviridae* family (*Ranavirus* genus) that infects fish (66). Analysis of our deep sequencing data revealed the lack of a prominent 22-nt RNA peak in *Dcr-2* mutants. Furthermore, we were unable to computationally predict pre-miRNA-like stem-loop structures in regions of the viral genome that gives rise to the most abundant viral small RNAs. Together, these results suggest that IIV-6 does not produce viral miRNAs. However, the lack of viral miRNAs is not a general attribute to insect DNA viruses, because miRNAs have

been identified in other large invertebrate DNA viruses, *Heliothis virescens* ascovirus and *Bombix mori* nucleopolyhedrosis virus (67, 68).

Our model postulates that base pairing of overlapping converging transcripts generates the viral dsRNA substrates for vsiRNA production by Dcr-2. Consequently, vsiRNAs are 100% complementary to viral transcripts and should be able to target them for degradation. Indeed, we observed an enhanced susceptibility of RNAi mutant flies to IIV-6 infection and observed that vsiRNAs mediate silencing of reporter constructs. Nevertheless, we only observed a modest increase in viral load at early time points in RNAi mutant flies. Several hypotheses could explain this apparent paradox. First, vsiRNAs may target viral genes that are involved in viral pathogenesis, but not viral replication per se. Consequently, in the absence of a functional RNAi response, expression of these putative pathogenicity factors will be increased, resulting in a more rapid onset of disease. Second, the observed IIV-6-associated mortality may be due to invasion or high-level replication in specific critical tissues. Perhaps RNAi-pathway components have tissue-specific functions during IIV-6 replication that could explain the observed mild differences in viral titers in whole flies. Third, the susceptibility of RNAi mutant flies could also be attributed to additional (direct or indirect) functions of Dcr-2 and AGO2, other than controlling viral RNA levels. For example, the putative antiviral effector *Vago* is induced upon RNA virus infection in a Dcr-2-dependent, but AGO2-independent manner (69). We note that *Dcr-2* mutants seem to be more severely affected by IIV-6 infection than *AGO2* mutants, which would fit a Dcr-2-dependent induction of a disease modifying activity.

It is well established that the RNAi machinery targets endogenous retroviruses, dsRNA viruses as well as viruses with (+) or (-) RNA genomes. We now show that dsDNA virus-derived siRNAs are produced by Dcr-2 and that these vsiRNAs provide defense against infection. Thus RNAi in insects is the predominant antiviral defense mechanism that provides protection against all major classes of viruses.

Materials and Methods

Virus titration

IIV-6 was kindly supplied by C. Joel Funk (US Department of Agriculture-Agricultural Research Service Western Cotton Research Laboratory, Phoenix, Arizona) and was propagated in *Galleria mellonella* (greater wax moth) larvae and purified by 25-65% (wt/vol) sucrose density gradient centrifugation as described previously (70, 71). IIV-6 UV-inactivated virus was produced by exposing the virus stock to a total of 12,000 mJ UV light in four intervals of 3 min (72).

Viral titers were determined by end-point dilution. *Drosophila* S2 cells (Invitrogen) were seeded in 96-well plates at a density of 2.5×10^4 cells per well. Subsequently, cells were infected with 10-fold serial dilutions of fly homogenate or virus suspension. Each infection was performed in quadruplicate. IIV-6 infection was scored by a lack of proliferation of cells and by the presence of cell debris and large cells, presumably syncytia. Viral titers were calculated according to the method of Reed and Muench (73). For titration of infectious virus in adult flies, three pools of four flies were harvested and stored at -70°C until further processing. Each pool of flies was homogenized in 150 μL of PBS, and fly debris was removed by centrifugation for 10 min at $16,000 \times g$ at 4°C . The supernatant was transferred to a fresh tube and, prior to titration, centrifuged again for 5 min at $16,000 \times g$ at room temperature.

Clearance of *Wolbachia*- and virus-infected flies and validation by PCR

To clean fly stocks from persistent viruses, eggs were collected on apple-juice agar plates and treated with 50% (vol/vol) household bleach for 5 min. After three extensive washes with water, eggs were transferred to fresh vials containing standard fly food. After culturing for two subsequent generations, we verified the absence of Nora virus and DCV by RT-PCR assay.

For RT-PCR assays, total RNA was extracted from pools of 15 flies using Isol-RNA Lysis Reagent (5 Prime) according to manufacturer's recommendations. cDNA synthesis was performed on 1 μg of DNase-I (Invitrogen)-treated total RNA using random hexamers and Taqman reverse transcriptase (Roche). Primers used for PCR amplification of Nora virus were NoV 1370F (5'-ATGGCGCCAGTTAGTGCAGACCT-3') and NoV 1780R (5'-CCTGTTGTTCCAGTTGGGTTCTGA-3'). DCV primers were DCV 1947F (5'-TTGATCTAGATACTGAAACCGCAAATCGTG-3') and DCV 2528R (5'-TCGCCCATACGATTAAAGAAA-3'). As positive control for RNA extraction, we used Act42A 19F (5'-GCGTCGGTCAATTCAATCTT-3') and Act42A 386R (5'-CTTCTCCATGTCGTCCCAGT-3'). The PCR program used was: 94°C for 5 min; 35 cycles of 94°C for 30 s, 57°C for 30 s, and 72°C for 50 s; 72°C for 10 min. To clear fly stocks from *Wolbachia* infection, flies were raised for two generations in standard fly food containing 0.05 mg/ml of tetracycline hydrochloride (Sigma). Clearance of *Wolbachia* infection was validated by PCR amplification of *Wolbachia*-specific genes from DNA extracts of adult flies, as described previously (32).

Fly stocks and virus infections

Virus- and *Wolbachia*-cleared flies were reared on standard medium at 25°C with a light/dark cycle of 12 h/12 h. We used the following alleles: *AGO2*⁴¹⁴ (74), *AGO2*³²¹, *AGO2*⁴⁵⁴ (36), and *Dcr-2*^{L811fsX} (42). We used *w*¹¹¹⁸ and *y*^{1w1} flies were used as WT

controls for *AGO2* and *Dcr-2* mutant flies, respectively. For generation of *AGO2* transheterozygous mutant flies, *AGO2*⁴¹⁴ homozygous flies were crossed with *AGO2*⁴⁵⁴/*TM3Sb* or *AGO2*³²¹/*TM3Sb* flies, and the F1 progeny was selected based on the absence of the balancer. Likewise, for generation of *AGO2*^{321/454} transheterozygous flies, *AGO2*³²¹/*TM3Sb* flies were crossed with *AGO2*⁴⁵⁴/*TM3Sb* flies. Heterozygous controls were generated by crossing *AGO2* flies with *w*¹¹¹⁸ flies.

Female flies (2-4 days of age) were injected with 50 nL of the appropriate virus dilution [containing 14,000 median (50%) tissue culture infectious dose (TCID₅₀) units of IIV-6, 500 TCID₅₀ units of DCV or 2,500 TCID₅₀ units of CrPV] in 10 mM Tris-HCl (pH 7.5) or with 10 mM Tris-HCl (pH 7.5) as a mock infection, as described previously (13). Flies were injected in the anterior ventral abdomen near the dorsal-ventral boundary while anesthetized with CO₂ (75). Flies were cultured at 25 °C, and mortality was monitored daily. Every 3 to 4 days, the flies were transferred to fresh food. Fly mortality at day 1 was attributed to damage invoked by the injection procedure and was excluded from survival analysis. In all survival experiments, 20-30 female flies per genotype were injected.

Western blots

Pools of five IIV-6-infected or mock-infected female flies were homogenized in lysis buffer [50 mM Tris (pH 7.4), 150 mM NaCl, 1 mM EDTA, 1% (vol/vol) Nonidet P-40, 0.05% (wt/vol) SDS, 1 mM DTT, 0.5 mM PMSF and complete protease inhibitor mixture (Roche)] for 30 min at 4 °C. Fly lysates were centrifuged for 10 min at 16,000 × *g* at 4 °C. The supernatant was transferred to a fresh tube and centrifuged again for 5 min at 16,000 × *g* at room temperature. For Western blot analysis, SDS-solubilized proteins were separated on a 10% (wt/vol) denaturing polyacrylamide gel and transferred to a nitrocellulose membrane for detection. For the detection of virus-specific proteins, polyclonal rabbit antibodies raised against IIV-6 virion coat proteins were diluted (1:2,000) in blocking buffer [5% (wt/vol) skimmed milk, 0.1% (vol/vol) Tween 20 in PBS]. The blot was incubated for 1 h at room temperature with the primary antibody. Subsequently, the blot was incubated with a secondary antibody, HRP-conjugated polyclonal goat anti-rabbit IgG (Dako), for 1 h in blocking buffer (1:5,000 dilution). Bound antibodies were detected using chemiluminescence (Roche). As a loading control, the same blot was probed with a rat anti- α -tubulin antibody (1:1,000 dilution; AbD Serotec) as a primary antibody. Goat anti-rat-IRDye680 antibody (1:15,000 dilution; Invitrogen) was used as a secondary antibody. Bound antibodies were visualized on an Odyssey infrared imager (LI-COR Biosciences).

Small RNA library preparation and analysis

Total RNA was extracted from pools of 15 IIV-6-infected female flies harvested at 12 days post-infection, using Isol-RNA Lysis reagent. Small RNA libraries were prepared as previously described (76) and sequenced on a Genome Analyzer *Iix* (Illumina). Small RNA libraries were analyzed as described previously (77). Briefly, small RNA reads were first mapped to the *D. melanogaster* genome allowing no mismatches during alignment. Nonmapping reads were then aligned to the IIV-6 reference genome (National Center for Biotechnology Information database, accession no. AF303741), allowing one mismatch. The IIV-6 genome annotation as proposed by Eaton *et al.* (34) was used to analyze read density per ORF. Correlations were evaluated using Pearson's correlation test as implemented in the statistical package SPSS (IBM SPSS). Sequences were submitted to the Sequence Read Archive at the National Center for Biotechnology Information (accession no. SRA048623).

Strand-specific RT-PCR assays

For strand-specific RT-PCR assays, a pool of 10 IIV-6-infected *w*¹¹¹⁸ flies (14,000 TCID₅₀ units) was harvested at 12 days post-infection. RNA was isolated from the flies using Isol-RNA Lysis Reagent and treated with DNase-I (Ambion). cDNA synthesis was performed on 400 ng of DNase-I-treated RNA using the TaqMan Reverse Transcription Reagents in a 20- μ L reaction according to the manufacturer's instructions (Applied Biosystems) utilizing strand-specific primers tagged with a 5' T7 promoter sequence at a final concentration of 0.2 μ M (Table S1). Following cDNA synthesis, PCR analysis was performed using a combination of an IIV-6-specific primer and a primer specific for the T7 promoter sequence (Table S1). One microliter of the cDNA product was used in a 20- μ L PCR assay containing 2.5 mM MgCl₂, 1 \times reaction buffer, 0.2 mM dNTPs, 0.5 μ M of each primer and 0.625 U/ μ L Thermopertect DNA polymerase (Integro). The PCR program was as follows: 95 °C for 5 min; 40 cycles of 95 °C for 30 s, 55 °C for 30 s, and 72 °C for 30 s; 72 °C for 10 min. RT-PCR products were analyzed on 2% (wt/vol) agarose gels. Several control reactions were run in parallel for each sample. cDNA synthesis without reverse transcriptase and PCR amplification without cDNA template were performed to verify the absence of contaminating DNA in RNA preparations and PCR reagents, respectively. A control PCR assay was performed on proteinase K (Qiagen)-treated virus stock to verify primer efficiency (Figure S4).

For strand-specific qRT-PCR assays, RNA was isolated from three pools of 25 IIV-6-infected *w*¹¹¹⁸ and *AGO2*⁴¹⁴ flies at 12 days post-infection. RNA isolation, DNase-I treatment and cDNA synthesis with T7 promoter-tagged primers were performed as described above. qPCR analysis using a combination of T7 promoter and IIV-6-specific primers were performed on a LightCycler 480 using LightCycler 480 SYBR Green I

Master (Roche). The PCR program was as follows: 95 °C for 5 min; 45 cycles of 95 °C for 5 s, 60 °C for 10 s, and 72 °C for 20 s. The data were normalized to Rp49, for which qRT-PCR assays were run in parallel. The entire experiment was performed three times.

Northern blots

S2 cells were either mock-infected or infected with 4.23×10^6 TCID₅₀ units of IIV-6. At 3 days post-infection, RNA was isolated from the cells using Isol-RNA Lysis Reagent. The RNA (10 µg per lane) was separated on 1.5% (wt/vol) agarose/formaldehyde gel and transferred onto Nytran SuPerCharge nylon membranes (Whatman). Blots were hybridized with ³²P end-labeled oligonucleotide DNA probes for specific detection of sense and antisense transcripts of selected ORFs. Probes for ORF 85L were 85L antisense (5'-tggcttgccgggatatttggatgcagatggctgcgctc-3') and 85L sense (5'-gacgcagccatctgcatcctaataatcccgaagcca-3'). ORF 206R probes were 206R antisense (5'-gggaaactcagaagaaaaggaaagtggcgcgagtacg-3') and 206R sense (5'-cgtactcgccactttccttttcttctgagtttccc-3'). Probes for ORF 441R were 441 antisense (5'-cctcttatagagacttggcaagtttggcgcgactcgt-3') and 441R sense (5'-caggatcgccaaactttgccaaagtctcataagagg-3'). Blots were hybridized in ULTRAhyb-Oligo hybridization buffer (Ambion) according to the manufacturer's instructions and visualized by autoradiography. Blots of gels with *in vitro* transcribed RNA (25 ng per lane) were run in parallel as positive controls (Table S2).

IIV-6 sensor assay in S2 cells

To generate IIV-6 sensor plasmids, we amplified ten 500-bp regions of the IIV-6 genome from proteinase K-treated virus stock by PCR assay using the primers from Table S3. PCR fragments were cloned in the 3' UTR of the Fluc gene in the pMT-GL3 plasmid (13) using the PspOMI and PmeI restriction sites. As a nonspecific control, a 500-bp fragment of GFP (nucleotides 192-691) was amplified from the pEGFP-N1 plasmid (Clontech) and cloned in a similar manner. The pMT-Ren plasmid (13) was used as a transfection control.

For the RNAi reporter assay, 1.5×10^5 S2 cells were seeded in a 24-well plate. Twenty-four hours post-seeding, cells were transfected with 12 ng pMT-Ren and 50 ng of an IIV-6 sensor or GFP control plasmid, as described (78). Twenty-four hours after transfection cells were mock-infected or infected with 21,000 TCID₅₀ units of IIV-6. Expression of the Fluc and Rluc reporters was induced at 24 h after infection by adding CuSO₄ at a final concentration of 500 µM to the culture supernatant. After incubation for an additional 18 h, luciferase activities were measured using the Dual Luciferase reporter system (Promega).

Acknowledgements

We thank Lionel Frangeul for bioinformatic support; and P. Zamore, A. Müller, and the Bloomington *Drosophila* Stock Center for providing fly stocks. This work was financially supported by a VIDI fellowship (project number 864.08.003), the Open Program of the Division for Earth and Life Sciences (project number 821.02.028) from the Netherlands Organization for Scientific Research, a Horizon Breakthrough fellowship from the Netherlands Genomics Initiative (project number 93519018), and a fellowship from the Nijmegen Centre for Molecular Life Sciences (to R.P.v.R), as well as by Grant ANR-09-394 JCJC-0045-01 from the French Agence Nationale de la Recherche and Grant FP7/2007-2013 ERC 242703 from the European Research Council (to M.-C.S).

References

1. Weber F, Wagner V, Rasmussen SB, Hartmann R, & Paludan SR (2006) Double-stranded RNA is produced by positive-strand RNA viruses and DNA viruses but not in detectable amounts by negative-strand RNA viruses. *J Virol* 80:5059-5064.
2. Kato H, Takahasi K, & Fujita T (2011) RIG-I-like receptors: cytoplasmic sensors for non-self RNA. *Immunol Rev* 243:91-98.
3. Robalino J, Browdy CL, Prior S, Metz A, Parnell P, Gross P, & Warr G (2004) Induction of antiviral immunity by double-stranded RNA in a marine invertebrate. *J Virol* 78:10442-10448.
4. Ding SW & Voinnet O (2007) Antiviral immunity directed by small RNAs. *Cell* 130:413-426.
5. Van Rij RP & Berezikov E (2009) Small RNAs and the control of transposons and viruses in *Drosophila*. *Trends Microbiol* 17:139-178.
6. Kawamata T & Tomari Y (2010) Making RISC. *Trends Biochem.Sci.* 35:368-376.
7. Carthew RW & Sontheimer EJ (2009) Origins and Mechanisms of miRNAs and siRNAs. *Cell* 136:642-655.
8. Blair CD (2011) Mosquito RNAi is the major innate immune pathway controlling arbovirus infection and transmission. *Future Microbiol* 6:265-277.
9. Sanchez-Vargas I, Travanty EA, Keene KM, Franz AW, Beaty BJ, Blair CD, & Olson KE (2004) RNA interference, arthropod-borne viruses, and mosquitoes. *Virus Res* 102:65-74.

10. Li HW, Li WX, & Ding SW (2002) Induction and suppression of RNA silencing by an animal virus. *Science* 296:1319-1321.
11. Galiana-Arnoux D, Dostert C, Schneemann A, Hoffmann JA, & Imler JL (2006) Essential function in vivo for Dicer-2 in host defense against RNA viruses in drosophila. *Nat Immunol* 7:590-597.
12. Wang XH, Aliyari R, Li WX, Li HW, Kim K, Carthew R, Atkinson P, & Ding SW (2006) RNA interference directs innate immunity against viruses in adult *Drosophila*. *Science* 312:452-454.
13. Van Rij RP, Saleh MC, Berry B, Foo C, Houk A, Antoniewski C, & Andino R (2006) The RNA silencing endonuclease Argonaute 2 mediates specific antiviral immunity in *Drosophila melanogaster*. *Genes Dev* 20:2985-2995.
14. Mueller S, Gausson V, Vodovar N, Deddouche S, Troxler L, Perot J, Pfeffer S, Hoffmann JA, Saleh MC, & Imler JL (2010) RNAi-mediated immunity provides strong protection against the negative-strand RNA vesicular stomatitis virus in *Drosophila*. *Proc.Natl.Acad.Sci.U.S.A* 107:19390-19395.
15. Brackney DE, Beane JE, & Ebel GD (2009) RNAi targeting of West Nile virus in mosquito midguts promotes virus diversification. *PLoS.Pathog.* 5:e1000502.
16. Brackney DE, Scott JC, Sagawa F, Woodward JE, Miller NA, Schilkey FD, Mudge J, Wilusz J, Olson KE, Blair CD, *et al.* (2010) C6/36 *Aedes albopictus* cells have a dysfunctional antiviral RNA interference response. *PLoS.Negl.Trop.Dis.* 4:e856.
17. Myles KM, Wiley MR, Morazzani EM, & Adelman ZN (2008) Alphavirus-derived small RNAs modulate pathogenesis in disease vector mosquitoes. *Proc. Natl.Acad.Sci.U.S.A* 105:19938-19943.
18. Wu Q, Luo Y, Lu R, Lau N, Lai EC, Li WX, & Ding SW (2010) Virus discovery by deep sequencing and assembly of virus-derived small silencing RNAs. *Proc. Natl.Acad.Sci.U.S.A* 107:1606-1611.
19. Aliyari R, Wu Q, Li HW, Wang XH, Li F, Green LD, Han CS, Li WX, & Ding SW (2008) Mechanism of induction and suppression of antiviral immunity directed by virus-derived small RNAs in *Drosophila*. *Cell Host Microbe* 4:387-397.
20. Flynt A, Liu N, Martin R, & Lai EC (2009) Dicing of viral replication intermediates during silencing of latent *Drosophila* viruses. *Proc.Natl.Acad.Sci.U.S.A* 106:5270-5275.
21. Scott JC, Brackney DE, Campbell CL, Bondu-Hawkins V, Hjelle B, Ebel GD, Olson KE, & Blair CD (2010) Comparison of dengue virus type 2-specific small RNAs from RNA interference-competent and -incompetent mosquito cells. *PLoS.Negl.Trop.Dis.* 4:e848.

22. Siu RW, Fragkoudis R, Simmonds P, Donald CL, Chase-Topping ME, Barry G, Attarzadeh-Yazdi G, Rodriguez-Andres J, Nash AA, Merits A, *et al.* (2011) Antiviral RNA interference responses induced by Semliki Forest virus infection of mosquito cells: characterization, origin, and frequency-dependent functions of virus-derived small interfering RNAs. *J Virol* 85:2907-2917.
23. Morazzani EM, Wiley MR, Murreddu MG, Adelman ZN, & Myles KM (2012) Production of virus-derived ping-pong-dependent piRNA-like small RNAs in the mosquito soma. *PLoS Pathog* 8:e1002470.
24. Vodovar N, Bronkhorst AW, van Cleef KW, Miesen P, Blanc H, van Rij RP, & Saleh MC (2012) Arbovirus-Derived piRNAs Exhibit a Ping-Pong Signature in Mosquito Cells. *PLoS One* 7:e30861.
25. Ma M, Huang Y, Gong Z, Zhuang L, Li C, Yang H, Tong Y, Liu W, & Cao W (2011) Discovery of DNA viruses in wild-caught mosquitoes using small RNA high throughput sequencing. *PLoS One* 6:e24758.
26. Kumar M & Carmichael GG (1998) Antisense RNA: function and fate of duplex RNA in cells of higher eukaryotes. *Microbiol Mol Biol Rev* 62:1415-1434.
27. Jacobs BL & Langland JO (1996) When two strands are better than one: the mediators and modulators of the cellular responses to double-stranded RNA. *Virology* 219:339-349.
28. Friesen PD & Miller LK (1986) The regulation of baculovirus gene expression. *Curr Top Microbiol Immunol* 131:31-49.
29. Unckless RL (2011) A DNA virus of *Drosophila*. *PLoS One* 6:e26564.
30. Williams T, Barbosa-Solomieu V, & Chinchar VG (2005) A decade of advances in iridovirus research. *Adv Virus Res* 65:173-248.
31. Constantino M, Christian P, Marina CF, & Williams T (2001) A comparison of techniques for detecting Invertebrate iridescent virus 6. *J Virol Methods* 98:109-118.
32. Teixeira L, Ferreira A, & Ashburner M (2008) The bacterial symbiont *Wolbachia* induces resistance to RNA viral infections in *Drosophila melanogaster*. *PLoS Biol* 6:e2.
33. Jakob NJ, Muller K, Bahr U, & Darai G (2001) Analysis of the first complete DNA sequence of an invertebrate iridovirus: coding strategy of the genome of Chilo iridescent virus. *Virology* 286:182-196.
34. Eaton HE, Metcalf J, Penny E, Tcherepanov V, Upton C, & Brunetti CR (2007) Comparative genomic analysis of the family Iridoviridae: re-annotating and defining the core set of iridovirus genes. *Virology* 361:11-21.
35. Williams T (2008) Iridoviruses of invertebrates. *Encyclopedia of Virology*, eds

- Mahy BWJ & Van Regenmortel MHV (Elsevier, Oxford, UK.), Third Ed, pp 161-167.
36. Hain D, Bettencourt BR, Okamura K, Csorba T, Meyer W, Jin Z, Biggerstaff J, Siomi H, Hutvagner G, Lai EC, *et al.* (2010) Natural variation of the amino-terminal glutamine-rich domain in *Drosophila argonaute2* is not associated with developmental defects. *PLoS One* 5:e15264.
 37. van Mierlo JT, Bronkhorst AW, Overheul GJ, Sadanandan SA, Ekstrom JO, Heestermans M, Hultmark D, Antoniewski C, & van Rij RP (2012) Convergent evolution of argonaute-2 slicer antagonism in two distinct insect RNA viruses. *PLoS Pathog* 8:e1002872.
 38. Schwarz DS, Hutvagner G, Du T, Xu Z, Aronin N, & Zamore PD (2003) Asymmetry in the assembly of the RNAi enzyme complex. *Cell* 115:199-208.
 39. Jiang F, Ye X, Liu X, Fincher L, McKearin D, & Liu Q (2005) Dicer-1 and R3D1-L catalyze microRNA maturation in *Drosophila*. *Genes Dev* 19:1674-1679.
 40. Saito K, Ishizuka A, Siomi H, & Siomi MC (2005) Processing of pre-microRNAs by the Dicer-1-Loquacious complex in *Drosophila* cells. *PLoS Biol* 3:e235.
 41. Cenik ES, Fukunaga R, Lu G, Dutcher R, Wang Y, Tanaka Hall TM, & Zamore PD (2011) Phosphate and R2D2 restrict the substrate specificity of Dicer-2, an ATP-driven ribonuclease. *Mol Cell* 42:172-184.
 42. Lee YS, Nakahara K, Pham JW, Kim K, He Z, Sontheimer EJ, & Carthew RW (2004) Distinct roles for *Drosophila* Dicer-1 and Dicer-2 in the siRNA/miRNA silencing pathways. *Cell* 117:69-81.
 43. Purcell MK, Hart SA, Kurath G, & Winton JR (2006) Strand-specific, real-time RT-PCR assays for quantification of genomic and positive-sense RNAs of the fish rhabdovirus, Infectious hematopoietic necrosis virus. *J Virol Methods* 132:18-24.
 44. Plaskon NE, Adelman ZN, & Myles KM (2009) Accurate strand-specific quantification of viral RNA. *PLoS One* 4:e7468.
 45. Lanford RE, Sureau C, Jacob JR, White R, & Fuerst TR (1994) Demonstration of in vitro infection of chimpanzee hepatocytes with hepatitis C virus using strand-specific RT/PCR. *Virology* 202:606-614.
 46. Komurian-Pradel F, Perret M, Deiman B, Sodoyer M, Lotteau V, Paranhos-Baccala G, & Andre P (2004) Strand specific quantitative real-time PCR to study replication of hepatitis C virus genome. *J Virol Methods* 116:103-106.
 47. Szittyta G, Moxon S, Pantaleo V, Toth G, Rusholme Pilcher RL, Moulton V, Burgyan J, & Dalmy T (2010) Structural and functional analysis of viral

- siRNAs. *PLoS.Pathog.* 6:e1000838.
48. Bego M, Maciejewski J, Khaiboullina S, Pari G, & St Jeor S (2005) Characterization of an antisense transcript spanning the UL81-82 locus of human cytomegalovirus. *J Virol* 79:11022-11034.
 49. Prang N, Wolf H, & Schwarzmann F (1999) Latency of Epstein-Barr virus is stabilized by antisense-mediated control of the viral immediate-early gene BZLF-1. *J Med Virol* 59:512-519.
 50. Zhang G, Raghavan B, Kotur M, Cheatham J, Sedmak D, Cook C, Waldman J, & Trgovcich J (2007) Antisense transcription in the human cytomegalovirus transcriptome. *J Virol* 81:11267-11281.
 51. Lin YT, Kincaid RP, Arasappan D, Dowd SE, Hunicke-Smith SP, & Sullivan CS (2010) Small RNA profiling reveals antisense transcription throughout the KSHV genome and novel small RNAs. *RNA* 16:1540-1558.
 52. Munroe SH & Zhu J (2006) Overlapping transcripts, double-stranded RNA and antisense regulation: a genomic perspective. *Cell Mol Life Sci* 63:2102-2118.
 53. Umbach JL & Cullen BR (2009) The role of RNAi and microRNAs in animal virus replication and antiviral immunity. *Genes Dev* 23:1151-1164.
 54. Pfeffer S, Zavolan M, Grasser FA, Chien M, Russo JJ, Ju J, John B, Enright AJ, Marks D, Sander C, *et al.* (2004) Identification of virus-encoded microRNAs. *Science* 304:734-736.
 55. Stark TJ, Arnold JD, Spector DH, & Yeo GW (2012) High-resolution profiling and analysis of viral and host small RNAs during human cytomegalovirus infection. *J Virol* 86:226-235.
 56. Blevins T, Rajeswaran R, Shivaprasad PV, Beknazariants D, Si-Ammour A, Park HS, Vazquez F, Robertson D, Meins F, Jr., Hohn T, *et al.* (2006) Four plant Dicers mediate viral small RNA biogenesis and DNA virus induced silencing. *Nucleic Acids Res* 34:6233-6246.
 57. Blevins T, Rajeswaran R, Aregger M, Borah BK, Schepetilnikov M, Baerlocher L, Farinelli L, Meins F, Jr., Hohn T, & Pooggin MM (2011) Massive production of small RNAs from a non-coding region of Cauliflower mosaic virus in plant defense and viral counter-defense. *Nucleic Acids Res* 39:5003-5014.
 58. Akbergenov R, Si-Ammour A, Blevins T, Amin I, Kutter C, Vanderschuren H, Zhang P, Gruissem W, Meins F, Jr., Hohn T, *et al.* (2006) Molecular characterization of geminivirus-derived small RNAs in different plant species. *Nucleic Acids Res* 34:462-471.
 59. Chellappan P, Vanitharani R, Pita J, & Fauquet CM (2004) Short interfering RNA accumulation correlates with host recovery in DNA virus-infected hosts,

- and gene silencing targets specific viral sequences. *J Virol* 78:7465-7477.
60. Zhang H, Kolb FA, Brondani V, Billy E, & Filipowicz W (2002) Human Dicer preferentially cleaves dsRNAs at their termini without a requirement for ATP. *Embo J* 21:5875-5885.
 61. Zhang H, Kolb FA, Jaskiewicz L, Westhof E, & Filipowicz W (2004) Single processing center models for human Dicer and bacterial RNase III. *Cell* 118:57-68.
 62. Billy E, Brondani V, Zhang H, Muller U, & Filipowicz W (2001) Specific interference with gene expression induced by long, double-stranded RNA in mouse embryonal teratocarcinoma cell lines. *Proc Natl Acad Sci U S A* 98:14428-14433.
 63. Paddison PJ, Caudy AA, & Hannon GJ (2002) Stable suppression of gene expression by RNAi in mammalian cells. *Proc Natl Acad Sci U S A* 99:1443-1448.
 64. Cullen BR (2011) Viruses and microRNAs: RISCy interactions with serious consequences. *Genes Dev* 25:1881-1894.
 65. Bartel DP (2009) MicroRNAs: target recognition and regulatory functions. *Cell* 136:215-233.
 66. Yan Y, Cui H, Jiang S, Huang Y, Huang X, Wei S, Xu W, & Qin Q (2011) Identification of a novel marine fish virus, Singapore grouper iridovirus-encoded microRNAs expressed in grouper cells by Solexa sequencing. *PLoS One* 6:e19148.
 67. Singh J, Singh CP, Bhavani A, & Nagaraju J (2010) Discovering microRNAs from Bombyx mori nucleopolyhedrosis virus. *Virology* 407:120-128.
 68. Hussain M, Taft RJ, & Asgari S (2008) An insect virus-encoded microRNA regulates viral replication. *J. Virol.* 82:9164-9170.
 69. Deddouche S, Matt N, Budd A, Mueller S, Kemp C, Galiana-Arnoux D, Dostert C, Antoniewski C, Hoffmann JA, & Imler JL (2008) The DExD/H-box helicase Dicer-2 mediates the induction of antiviral activity in drosophila. *Nat Immunol* 9:1425-1432.
 70. Ince IA, Boeren SA, van Oers MM, Vervoort JJ, & Vlask JM (2010) Proteomic analysis of Chilo iridescent virus. *Virology* 405:253-258.
 71. Marina CF, Arredondo-Jiménez JI, Castillo A, & Williams T (1999) Sublethal effects of iridovirus disease in a mosquito. *Oecologia* 119:383-388.
 72. Hedges LM & Johnson KN (2008) Induction of host defence responses by Drosophila C virus. *J Gen Virol* 89:1497-1501.
 73. Reed LJ & Muench H (1938) A simple method of estimating fifty percent endpoints. *Am J Hyg* 27:493-497.

74. Okamura K, Ishizuka A, Siomi H, & Siomi MC (2004) Distinct roles for Argonaute proteins in small RNA-directed RNA cleavage pathways. *Genes Dev* 18:1655-1666.
75. Cherry S & Perrimon N (2004) Entry is a rate-limiting step for viral infection in a *Drosophila melanogaster* model of pathogenesis. *Nat Immunol* 5:81-87.
76. Gausson V & Saleh MC (2011) Viral small RNA cloning and sequencing. *Methods Mol.Biol.* 721:107-122.
77. Vodovar N, Goic B, Blanc H, & Saleh MC (2011) In silico reconstruction of viral genomes from small RNAs improves virus-derived small interfering RNA profiling. *J Virol* 85:11016-11021.
78. van Cleef KW, van Mierlo JT, van den Beek M, & Van Rij RP (2011) Identification of viral suppressors of RNAi by a reporter assay in *Drosophila* S2 cell culture. *Methods Mol.Biol.* 721:201-213.

Supporting Information

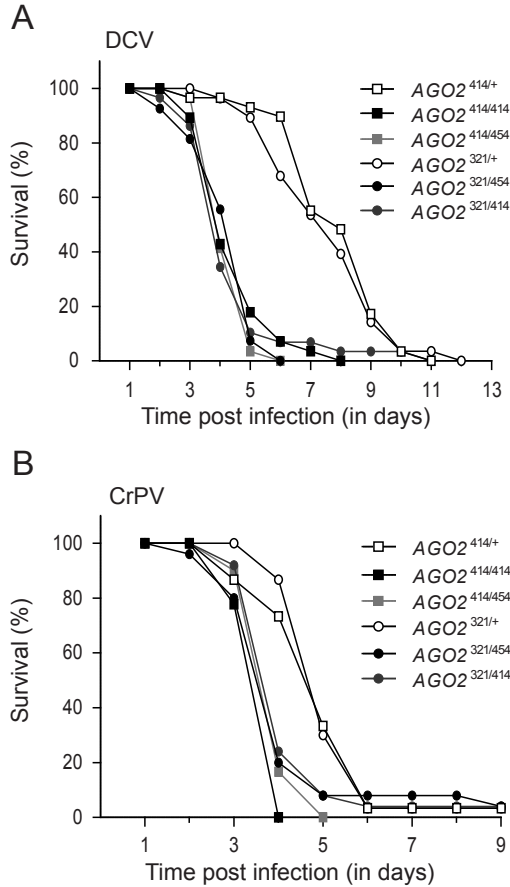


Figure S1. Enhanced susceptibility of *Argonaute-2* (*AGO2*) transheterozygous mutant flies to RNA virus infection. $AGO2^{414/414}$ homozygous flies (black squares), $AGO2^{414/454}$ transheterozygous flies (gray squares), $AGO2^{321/454}$ transheterozygous flies (black circles), and $AGO2^{321/414}$ transheterozygous flies (gray circles), as well as $AGO2^{414/+}$ (white squares) and $AGO2^{321/+}$ (white circles) heterozygous controls were infected with 500 median (50%) tissue culture infectious dose ($TCID_{50}$) units of *Drosophila C* virus (A) or with 2,500 $TCID_{50}$ units of Cricket paralysis virus (CrPV) (B), and survival was monitored daily.

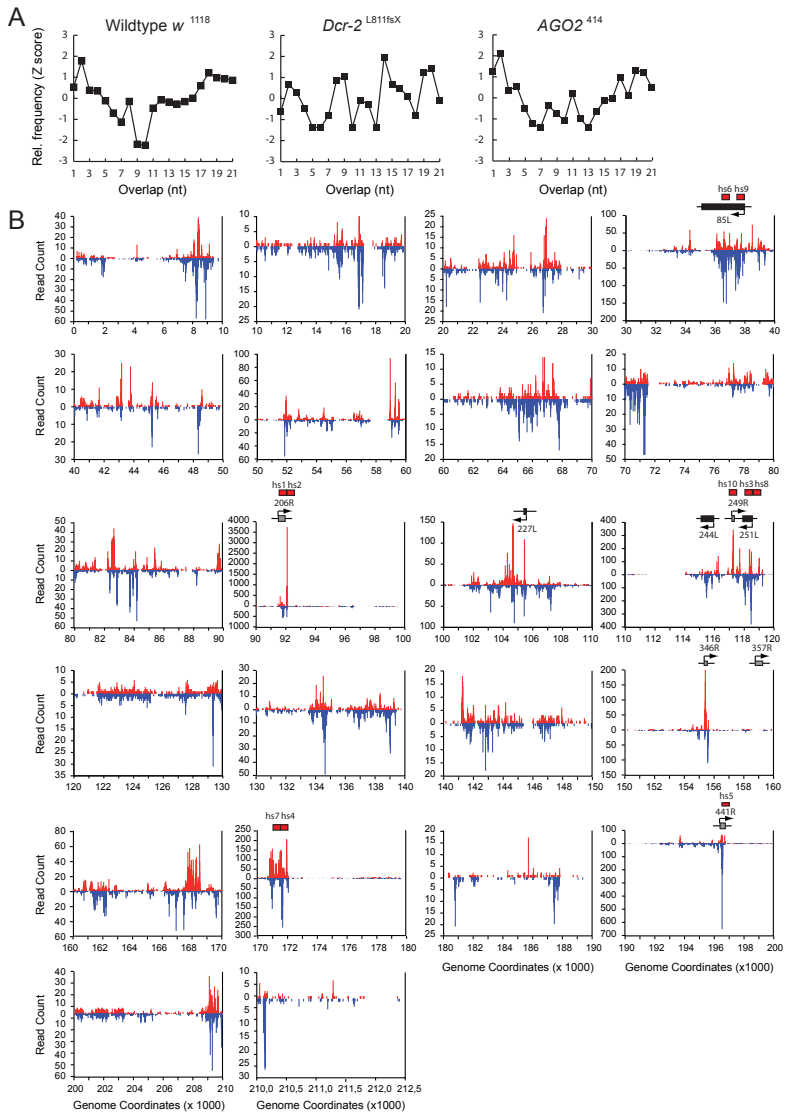


Figure S2. Profile of Invertebrate iridescent virus 6 (IIV-6)-derived viral small interfering RNAs (vsiRNAs). (A) Relative (Rel.) frequencies of 5' overlap between 21-nt small RNAs that map to opposite strands of the viral genome in IIV-6-infected *w¹¹¹⁸* (Left), *Dcr-2^{L811fsX}* (Center), and *AGO2⁴¹⁴* (Right) flies. For each possible overlap of 1-21 nt, the number of read pairs was quantified and converted into a Z-score. (B) Viral siRNAs in *w¹¹¹⁸* WT flies were aligned to the IIV-6 genome allowing one mismatch during alignment, and genome coordinates of the 5' end of vsiRNAs are plotted in 10,000-bp regions. vsiRNAs that mapped to the upper (R) and lower (L) strands of the IIV-6 genome are shown in red and blue, respectively. Note that the scale of the y axes differs between the individual plots. The ten 500-bp bins [hotspots, (hs)] that contained the highest density of vsiRNA reads and were used in the sensor assay of Figure 6B are presented above the plots. ORFs that were analyzed for the presence of sense and antisense are depicted above the plots, drawn to scale. Small RNA profiles are from dataset 1.

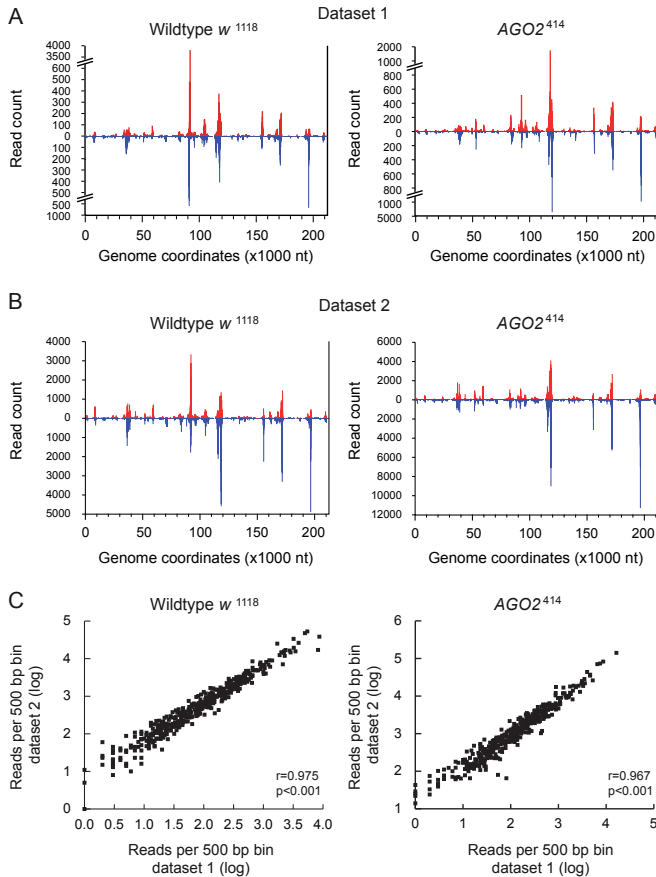


Figure S3. Small RNA profiles from two independent libraries from Invertebrate iridescent virus 6 (IIV-6)-infected flies. Profile of IIV-6-derived viral small interfering RNAs (vsiRNAs) across the IIV-6 genome from dataset 1 (A) and dataset 2 (B). Viral siRNAs were aligned to the IIV-6 genome, allowing one mismatch during alignment. The genome coordinates of the 5' end of vsiRNAs in w^{1118} WT (Left) and Argonaute-2 ($AGO2$)⁴¹⁴ (Right) flies were plotted. vsiRNAs that mapped to the upper (R) and lower (L) strands of the IIV-6 genome are shown in red and blue, respectively. Small RNA libraries were generated from a pool of 15 female flies at 12 days post-infection. Small RNA libraries of dataset 1 and dataset 2 were prepared at different times from independent batches of infected flies and analyzed on different runs on a Genome Analyzer (Illumina). Note the profiles from dataset 1 are also presented in Figure 4A and 4B; they are shown here to allow direct comparison of both datasets. (C) The IIV-6 genome was divided into 500-bp bins, and the correlation between vsiRNA densities in the two datasets was analyzed in a scatter plot (log-transformed data) for w^{1118} WT (Left; $r=0.975$, $P<0.001$, Pearson's correlation test) and $AGO2^{414}$ mutant flies (Right; $r=0.967$, $P<0.001$).

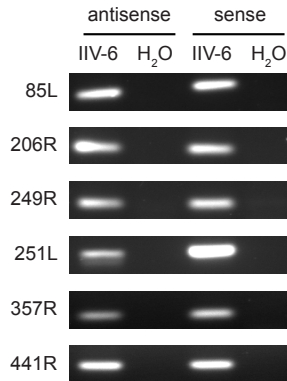


Figure S4. Control PCR assay on viral DNA. Ethidium bromide-stained gels of a PCR assay on proteinase K-treated Invertebrate iridescent virus 6 (IIV-6) virus stock are shown to demonstrate amplification efficiency of the primers used for Figure 5C. H₂O was included as nontemplate control during PCR amplification. In strand-specific RT-PCR assays, a T7-tagged IIV-6-specific primer was used for cDNA synthesis, and a nontagged IIV-6-specific primer in combination with a T7 primer was used in PCR assays. Note that this primer combination cannot be tested on viral DNA. We therefore verified PCR efficiency of the non-tagged IIV-6 specific primer in PCR reactions with the T7-tagged IIV-6-specific primer in combination with the nontagged IIV-6 specific primer (Table S1).

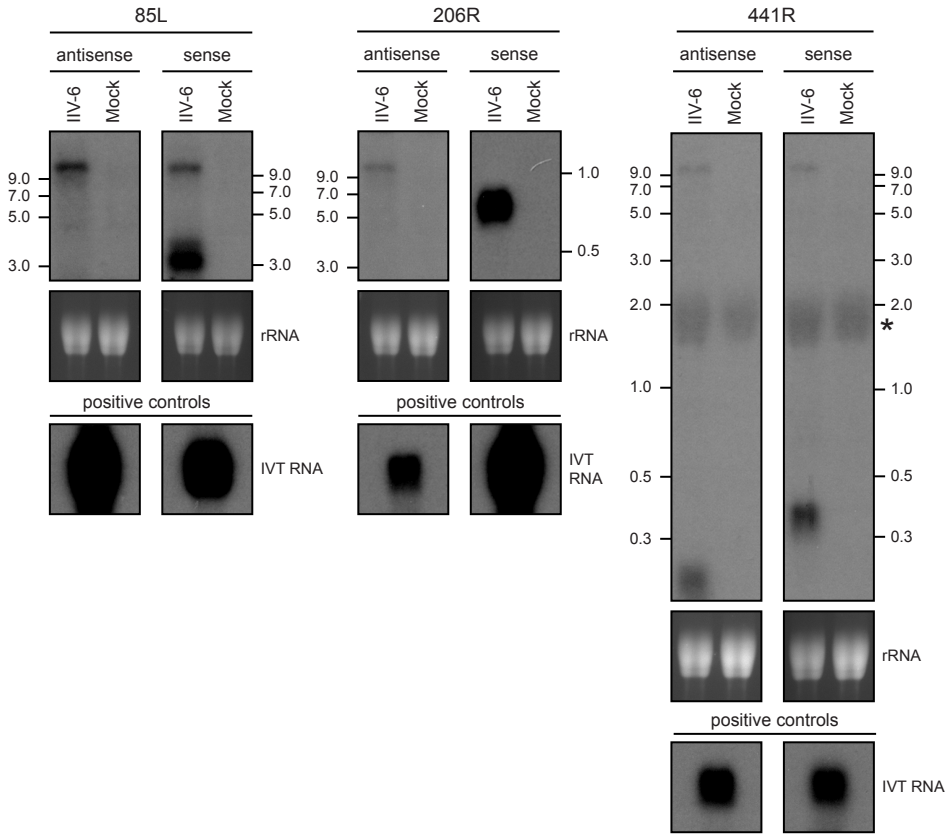


Figure S5. Northern blot analysis for the detection of sense and antisense Invertebrate iridescent virus 6 (IIV-6) transcripts. Northern blots for the detection of sense and antisense transcripts of the indicated IIV-6 ORFs in mock- or IIV-6-infected *Drosophila* S2 cells. The position and sizes of the RNA markers are indicated. The rRNA bands on the ethidium bromide-stained gels before blotting are shown to indicate equal loading. Hybridization of the probes to *in vitro* transcribed (IVT) sense and antisense RNA was used as a positive control to verify the ability of the probes to detect the indicated transcripts. Equal exposures were used for detection of sense and antisense transcripts of 85L and 441R. Exposure times for 206R sense and antisense were 1 h and 16 days, respectively. The asterisk indicates cross-hybridization to *Drosophila* rRNA. Sizes of the predicted ORFs are: 85L, 2,880-nt; 206R, 459-nt; 441R, 351-nt. Transcription start and stop sites for IIV-6 genes remain unknown; thus, the size of the UTRs and the actual expected size of the viral transcript cannot be accurately predicted.

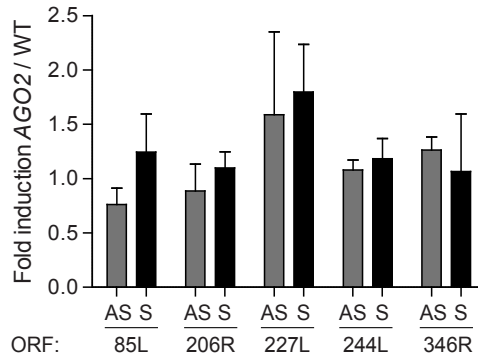


Figure S6. Viral transcript levels in Invertebrate iridescent virus 6 (IIV-6)-infected w^{1118} WT and *Argonaute-2* (*AGO2*)⁴¹⁴ flies. Five ORFs that were among the 10 ORFs with the highest density of viral small interfering RNAs (vsiRNA) reads were selected, and sense (s) and antisense (as) transcript levels were analyzed using strand-specific qRT-PCR at 12 days post-infection. Transcript levels were normalized to Rp49 levels and are presented as the fold induction of *AGO2* mutant over WT flies. Values represent averages and SEMs of three independent experiments.

Table S1. Primers used for strand-specific RT-PCR assays

ORF	Orientation	cDNA synthesis primer (5'-3')*	(quantitative) PCR primer (5'-3')*
85L	Antisense	<u>taatacgaactcactatagggaga</u> tgacgtacgaacctgacaggact	gcattccaaatatccccgaagccat
85L	Sense	<u>taatacgaactcactatagggaga</u> gcattccaaatatccccgaagccat	tgacgtacgaacctgacaggact
206R	Antisense	<u>taatacgaactcactatagggaga</u> gcaagtaaagcattgggtgatgatg	gcaagtaaagcattgggtgatgatg
206R	Sense	<u>taatacgaactcactatagggaga</u> gtttccctcttgggaatgacagg	gtttccctcttgggaatgacagg
227L	Antisense	<u>taatacgaactcactatagggaga</u> gagcctgaaattaaaacatttgc	ccaatttctaccataaaaagttttcc
227L	Sense	<u>taatacgaactcactatagggaga</u> ccaatttctaccataaaaagttttcc	gagcctgaaattaaaacatttgc
244L	Antisense	<u>taatacgaactcactatagggaga</u> acctcccggaagattttagaagc	acctctgttgactctatcgacc
244L	Sense	<u>taatacgaactcactatagggaga</u> acctctgttgactctatcgacc	acctcccggaagattttagaagc
249R	Antisense	<u>taatacgaactcactatagggaga</u> ggtgtttcttotaaaacaaagacct	ccaattagttaatccacatcctccc
249R	Sense	<u>taatacgaactcactatagggaga</u> ccaattagttaatccacatcctccc	ggtgtttcttotaaaacaaagacct
251L	Antisense	<u>taatacgaactcactatagggaga</u> aaacagtcgtttccactcctgg	tttctgtttgtgtttctatattgga
251L	Sense	<u>taatacgaactcactatagggaga</u> tttctgtttgtgtttctatattgga	aaacagtcgtttccactcctgg
346R	Antisense	<u>taatacgaactcactatagggaga</u> gatgaatcgctctatgagtcctcaagctaa	tttctcttcgctagcatcac
346R	Sense	<u>taatacgaactcactatagggaga</u> tttctcttcgctagcatcac	gatgaatcgctctatgagtcctcaagctaa
357R	Antisense	<u>taatacgaactcactatagggaga</u> tttaaattgcaaagaaggaactgg	aattatgttctggaccaatcc
357R	Sense	<u>taatacgaactcactatagggaga</u> aattatgttctggaccaatcc	tttaaattgcaaagaaggaactgg
441R	Antisense	<u>taatacgaactcactatagggaga</u> caaagtttgcgatcctgtatgt	tgcagatattgctagtgtgttct
441R	Sense	<u>taatacgaactcactatagggaga</u> tgcagatattgctagtgtgttct	caaagtttgcgatcctgtatgt
RP49 [†]	Sense	ctgcatgagcaggacctcca	atgaccatccgccagcatac

L, Left, lower strand; R, right, upper strand

*T7 promoter tag sequences are underlined; (quantitative) PCR primers were used in combination with a T7 primer (5'-taatacgaactcactataggg-3').

[†]For amplification of Rp49, the cDNA synthesis primer was also used as the reverse primer in qPCR assays.

Table S2. Primers used to generate 500-bp PCR templates for *in vitro* transcription of RNA

ORF	Orientation	Forward primer (5'-3')*	Reverse primer (5'-3')*
85L	Sense	<u>taatacgactcactatagggaga</u> tatcatgcactcccg	agtgggcccaaatctaaatgtatacac
85L	Antisense	ggtgtttaaactatcatgcactcccg	<u>taatacgactcactatagggaga</u> aaaatctaaatgtatacac
206R	Sense	<u>taatacgactcactatagggaga</u> tacaatacatgtgaa	ggtgtttaaactatagatttatagatttttaaatataatatt
206R	Antisense	agtgggcctacaatacatgtgaa	<u>taatacgactcactatagggaga</u> tatagatttatagatttttaaatataatatt
441R	Sense	<u>taatacgactcactatagggaga</u> taaaagcacttcatag	ggtgtttaaacagatcctatggaaactgg
441R	Antisense	agtgggcctaaaagcacttcatag	<u>taatacgactcactatagggaga</u> agatcctatggaaactgg

L, left; R, right

*T7 promoter sequences are underlined. PspOMI and PmeI restriction sites are in italic.

Table S3. Primers used for cloning of IIV-6 sensor plasmids

Sensor plasmid	Nucleotide positions	Forward primer (5'-3')*	Reverse primer (5'-3')*
pMT-GL3_HS1	91,501–92,000	agtgggcctacaatacatgtgaa	ggtgtttaaactatagatttatagatttttaaatataatatt
pMT-GL3_HS2	92,001–92,500	agtgggcccaaatctataaatatatt ttttaaggtttcttaacacc	ggtgtttaaacggttgaatttttaatatat ttttagccaac
pMT-GL3_HS3	118,001–118,500	agtgggccccatttattttgttc	ggtgtttaaacatttgaagggtgtgataag
pMT-GL3_HS4	171,501–172,000	agtgggccagttgaagatcg	ggtgtttaaactacaccgcttttcaacc
pMT-GL3_HS5	196,501–197,000	agtgggcctaaaagcacttcatag	ggtgtttaaacagatcctatggaaactgg
pMT-GL3_HS6	36,501–37,000	agtgggcccaaatctaaatgtatacac	ggtgtttaaactatcatgcactcccg
pMT-GL3_HS7	171,001–171,500	agtgggcccgacagctact	ggtgtttaaacgaatatctaattttcac
pMT-GL3_HS8	118,501–119,000	agtgggccactattaaaagaccac	ggtgtttaaactttattcacttctacatt aagaag
pMT-GL3_HS9	37,501–38,000	agtgggcccggtggttattatt	ggtgtttaaacataaagaagtaaacatgagc
pMT-GL3_HS10	117,001–117,500	agtgggccttcaaaattatttaatac	ggtgtttaaacaattgtaacaattgaag
pMT-GL3_eGFP ₅₀₀	192-691	agtgggccccctgacctacg	ggtgtttaaactgatcccggcg

*PspOMI and PmeI restriction sites are in italic.

Chapter 4

Small RNAs tackle large viruses: RNA interference-based antiviral defense against DNA viruses in insects

Alfred W. Bronkhorst, Pascal Miesen and Ronald P. van Rij

Fly 2014, 7:216-223

Extra View to:

Bronkhorst AW, van Cleef KW, Vodovar N, Ince IA, Blanc H, Vlak JM, Saleh MC, and Van Rij RP. The DNA virus Invertebrate iridescent virus 6 is a target of the *Drosophila* RNAi machinery. Proc Natl Acad Sci U S A 2012, 109:E3604-3613.

Abstract

The antiviral RNA interference (RNAi) pathway processes viral double-stranded RNA (dsRNA) into viral small interfering RNAs (vsiRNA) that guide the recognition and cleavage of complementary viral target RNAs. In RNA virus infections, viral replication intermediates, dsRNA genomes or viral structured RNAs have been implicated as Dicer-2 substrates. In a recent publication, we demonstrated that a double-stranded DNA virus, Invertebrate iridescent virus 6, is a target of the *Drosophila* RNAi machinery, and we proposed that overlapping converging transcripts base pair to form the dsRNA substrates for vsiRNA biogenesis. Here, we discuss the role of RNAi in antiviral defense to DNA viruses in *Drosophila* and other invertebrate model systems.

Introduction

Viruses can infect all living organisms and are a major cause of infectious diseases. Survival of an infected host depends on an effective immune response that limits viral replication and minimizes virus-induced damage (1). A critical attribute of the innate immune system is its ability to recognize ongoing virus infection and to distinguish non-self molecular patterns from those of the host (self). An effective mechanism to sense virus infection is by the specific recognition of viral nucleic acids based on non-self signatures or on their subcellular localization. Double-stranded RNA (dsRNA) is a strong non-self pattern; it is present at high levels in virus-infected cells, whereas healthy cells normally do not produce detectable amounts of dsRNA (2).

In mammals, viral nucleic acids are sensed by innate pattern recognition receptors, such as Toll-like receptors (TLRs), retinoic acid-inducible gene I (RIG-I)-like receptors (RLRs) and nucleotide oligomerization domain (NOD)-like receptors (NLRs). For example, the transmembrane receptors TLR3 and TLR7/8 mediate the recognition of double-stranded (ds) RNA and single-stranded (ss) RNA in endosomal and lysosomal compartments, whereas endolysosomal TLR9 detects virus derived DNA (3). The RLR family members RIG-I and melanoma differentiation-associated gene 5 (MDA5) sense replicating RNA viruses in the cytoplasm based on non-self RNA signatures. MDA5 detects dsRNA replication intermediates that are generated during the viral life cycle of positive strand RNA viruses (4, 5), and the protein is also believed to mediate the recognition of viral genomic RNA of dsRNA viruses (6). RIG-I recognizes short dsRNA as well as RNAs with a 5' triphosphate moiety that is present on RNAs of specific virus families, but absent from highly abundant cellular RNAs, such as mRNAs and tRNAs (6). Activation of intracellular signaling cascades by the TLR and RLR receptor families leads to the induction of the transcription factors nuclear factor- κ B (NF- κ B) and interferon-regulatory factor 3 (IRF3) and/or 7 (IRF7), which induce expression of type I interferon (IFN) and other inflammatory cytokines that in turn establish an antiviral state of the cell (3).

DNA viruses are also known to induce production of type I IFNs. Viral dsDNA can be sensed directly by a variety of cytosolic DNA-binding proteins that activate downstream signaling cascades (7, 8). Interestingly, two recent reports show that the cyclic guanosine monophosphate-adenosine monophosphate (cGAMP) synthase enzyme binds viral cytoplasmic DNA and induces the production of the second messenger molecule cGAMP, which subsequently triggers STING (stimulator of interferon genes)-dependent IFN signaling (9, 10). More indirect detection of cytoplasmic DNA may occur via host DNA-dependent RNA polymerase III that transcribes viral cytoplasmic AT-rich dsDNA into 5' triphosphate containing dsRNA, which is subsequently detected by RIG-I (11).

Lacking the adaptive and interferon-based innate responses of vertebrates, insects rely on other mechanisms for antiviral defense. Over the last few years it has become increasingly clear that RNA interference (RNAi) is a major mechanism for the defense against RNA viruses (12-14). This gene-silencing pathway is primed by dsRNA, thus providing a strong basis for self-nonself discrimination. However, it was not clear how insects defend themselves from infections by DNA viruses. In a recent publication, we demonstrated that RNAi is also involved in the defense against dsDNA virus infection in flies (15). Here, we discuss our results in light of other recent observations in *Drosophila* and other invertebrate model systems.

The antiviral RNA interference pathway in insects

In plants, fungi, nematodes, and arthropods, viral dsRNA triggers an antiviral RNAi response (Figure 1) (12, 13). Several studies in *Drosophila melanogaster* and mosquitoes

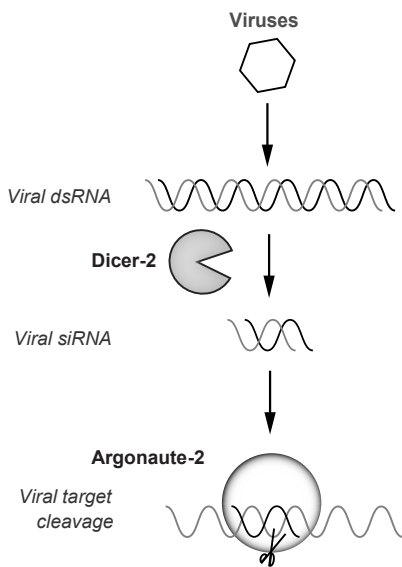


Figure 1. Virus infection triggers an antiviral RNA interference response in insects. The endoribonuclease Dicer-2 processes viral double-stranded (dsRNA) substrates into viral small interfering RNAs (siRNA) of 21-nt in size. The guide strand that remains incorporated in RISC directs Argonaute-2 onto fully complementary RNA sequences to mediate viral target cleavage.

demonstrated that viral small RNAs are produced during infections with different classes of RNA viruses (14, 16, 17). These virus-derived small interfering RNAs (vsiRNAs) are RNA duplexes of 21-nt with 2-nt 3' overhangs that are generated by cleavage of viral dsRNA by the RNase III enzyme Dicer-2 (Dcr-2). After incorporation of vsiRNA duplexes into an Argonaute-2 (AGO2) containing RNA-induced silencing complex (RISC), one of the strands (the passenger strand) is excluded from RISC. The guide strand remains associated with the mature RISC and mediates recognition of complementary viral target RNAs. Upon recognition of a fully complementary sequence, AGO2 cleaves the viral target RNA. Thus, the RNAi pathway may exert its antiviral activity at two different levels: by Dicer-mediated cleavage of essential dsRNA replication intermediates or viral dsRNA genomes and by AGO2-mediated

cleavage (slicing) of viral genomes and transcripts (Figure 1).

Fly mutants with defects in the core RNAi genes *Dcr-2* and *AGO2* are highly susceptible to RNA virus infection (18-22). The inability of these RNAi-deficient flies to control RNA virus replication is also evident from higher viral RNA copy numbers and higher viral titers in RNAi mutants. The hypersensitivity to virus infection of *R2D2* and *AGO2* mutants (19, 20, 22), which have defects in RISC loading and RISC activity but are fully competent in *Dcr-2* activity, implies that slicing of viral target RNAs contributes to the antiviral potential of the RNAi machinery. This notion is further supported by the observation that 2 unrelated RNA viruses encode RNAi antagonists that inhibit the catalytic activity of the RISC complex (23, 24).

The antiviral RNAi pathway controls DNA virus infection in *Drosophila*

We used Invertebrate iridescent virus 6 (IIV-6), a member of the *Iridoviridae* family, as a model to study antiviral immunity against DNA viruses in *Drosophila* (15). Although IIV-6 is not a natural pathogen of *Drosophila*, it is known to experimentally infect a broad range of Dipteran species including *Drosophila* (25-27). IIV-6 replicated efficiently in wildtype flies, with a rapid increase in viral titers over the first 6 days after inoculation and stable titers thereafter. Despite the stable high titers, infected flies survived for prolonged periods of time (> 30 days), suggesting that IIV-6 establishes a productive non-lethal infection. To monitor whether the RNAi pathway controls DNA virus infection *in vivo*, we next analyzed survival of *Dcr-2* and *AGO2* mutants upon IIV-6 infection. IIV-6 infection dramatically decreased survival of *Dcr-2* null mutant flies compared with wildtype controls and mock-infected flies. Similarly, flies that do not encode a functional *AGO2* protein were also more susceptible to IIV-6 infection. *Dcr-2* mutants seem to be more severely affected than *AGO2* mutants. However, the reduced stress-resistance and shorter life span of non-infected *Dcr-2* mutants (28) complicates the interpretation of this apparent difference. Our results were further supported by a recent study of Kemp et al. who show that *Dcr-2*, *R2D2* and *AGO2* null mutants die more rapidly upon IIV-6 challenge than wildtype controls (29). Moreover, Kemp et al. observed that the increased lethality in RNAi mutant flies correlates well with an increase in viral load at 10 days post-infection (29). We, however, only observed mild differences in viral titers in *AGO2* and *Dcr-2* mutant flies early in infection, whereas viral load was not affected at a later time point (12 days post-infection). The reason for this difference between the two studies remains unclear.

Dcr-2-dependent vsiRNA are produced from overlapping transcripts

Having determined that the RNAi pathway controls DNA virus infection *in vivo*, we next analyzed whether vsiRNAs are produced during IIV-6 infection. Using small RNA cloning and next-generation sequencing technology, we readily detected viral small RNAs in wildtype and *AGO2* mutant flies, the majority of which were 21-nt in size. A strong decrease in normalized levels of 21-nt viral small RNAs in *Dcr-2* mutant flies indicates that these RNAs are indeed Dcr-2-dependent vsiRNAs. Using a similar approach, Kemp and colleagues also demonstrated Dcr-2-dependent vsiRNA biogenesis in IIV-6 infection (29).

Viral dsRNA replication intermediates or structured elements in single-stranded viral RNAs are potential targets for Dcr-2-dependent vsiRNA production. Several studies reported similar ratios of positive strand (+) over negative strand (-) vsiRNAs in invertebrate hosts infected with dsRNA viruses or positive strand RNA viruses (30, 31). In addition, (+) and (-) vsiRNAs are present in approximately equal ratios in flies infected with the (-) RNA virus vesicular stomatitis virus (VSV) (22, 32). Moreover, viral siRNAs from these different classes of RNA viruses generally cover the entire viral genome. This is further exemplified by the finding that vsiRNAs can be used to deduce up to full-length genomes of known and novel (+) RNA and dsRNA viruses (24, 30, 33). Together, these results imply that viral replication intermediates or viral dsRNA genomes serve as the Dcr-2 substrates for vsiRNA biogenesis in RNA virus infection (13, 31).

Nevertheless, for several RNA viruses structured RNA elements seem to be preferentially processed by Dcr-2, indicating that vsiRNA biogenesis may be more complex. For example, in small RNA profiles of 2 (+) RNA viruses, *Drosophila C* virus (DCV) and Flock House virus (FHV), there is an over-representation of (+) strand vsiRNAs (32, 33). This bias reflects the higher abundance of viral genomic (+) RNA strands over antigenomic (-) RNA strands that is generally observed in (+) RNA virus infection. It was thus suggested that structured elements in viral genomic RNA become the predominant target for Dcr-2 when dsRNA replication intermediates are shielded from Dcr-2 cleavage by a viral RNAi suppressor (32, 34). This hypothesis was supported by the observation that vsiRNA reads are heavily biased toward the (+) strand in wildtype FHV infections, whereas similar numbers of (+) and (-) vsiRNAs were derived from infections with RNAi suppressor-deficient virus (34, 35). DCV encodes an RNAi antagonist that binds dsRNA (20) and may similarly skew vsiRNAs towards (+) viral strands (32).

DNA viruses do not replicate via a dsRNA replication intermediate and other dsRNA

sources must therefore be processed by Dcr-2 for vsiRNA biogenesis. In mammalian cells, dsRNA can be detected upon dsDNA virus infection, (2) which is probably generated by base pairing of convergent overlapping transcripts of both strands of the viral genome or derives from secondary structures in viral transcripts (36).

To identify the dsRNA substrate for vsiRNA biogenesis during IIV-6 replication, we analyzed the distribution of vsiRNAs across the IIV-6 genome. Viral open reading frames (ORFs) in IIV-6 are oriented in both directions in the viral genome. Nevertheless, irrespective of the orientation of the viral ORFs, vsiRNAs mapped in similar proportions to the upper and lower strand of the viral genome (Figure 2A). These data suggest that vsiRNAs are derived from overlapping sense and antisense transcripts. Indeed, sense and antisense transcripts that cover highly targeted ORFs (i.e. ORFs with high density of vsiRNA reads) could readily be detected by strand-specific RT-PCR assays and Northern blot analyses. These bidirectional transcripts have the potential to base pair and form long dsRNA molecules that trigger the antiviral RNAi machinery via Dcr-2-dependent vsiRNA biogenesis (Figure 3A).

Uneven distribution of vsiRNAs across the IIV-6 genome

IIV-6 derived vsiRNAs display a highly uneven distribution along the viral genome, with some regions in the genome producing high numbers of vsiRNAs (hotspots) and other regions only producing few vsiRNAs. The uneven coverage of vsiRNAs across the genome was very similar between wildtype and *AGO2* mutant flies and between 2 independent datasets from our study. Strikingly, the distribution of vsiRNAs along the viral genome in our study is highly similar to that of Kemp et al. (Figure 2A and B). To further substantiate this observation, we divided the IIV-6 genome in non-overlapping 500-bp bins and counted the number of vsiRNAs mapping to individual bins in both datasets. Indeed, we observed a strong correlation between vsiRNA mapping between the two studies (Figure 2C, $r = 0.894$, $P < 0.001$). Nevertheless, when zooming in on highly targeted regions, it becomes apparent that vsiRNA profiles are not fully identical in the 2 studies, with some highly targeted sequences from one study being markedly less abundant in the other study (Figure 2B). It has been reported that vsiRNA cloning procedures may induce cloning biases. Such biases are introduced during the ligation steps that are used to link the small RNAs to 3' end 5' adaptor sequences, with small RNA sequences that more stably anneal to the adapters producing higher read numbers (37). As the 2 studies used different adaptor sequences, slight differences in vsiRNA profiles, such as observed in Figure 2B, may be due to cloning/sequencing biases.

How do the major vsiRNA hotspot regions in the viral genome arise? Since the 2

independent studies used different sequencing platforms and adaptor sequences but display highly similar profiles, we deem it unlikely that cloning biases explain the observed IIV-6 vsRNA hotspots. Another putative source for biases could be differential stability of RISC-loaded small RNAs, as siRNAs that possess a cytidine at their 5' termini seem to be preferentially loaded into AGO2 (38, 39). IIV-6 derived siRNA profiles are highly similar between wildtype and *AGO2* mutant flies that lack a functional RISC (15). Thus the observed uneven distribution of vsRNA profiles cannot be explained by differences in stability within RISC.

Viral siRNA hotspots often map to regions in the genome that correspond to predicted ORFs (Figure 2B). It is likely that vsRNA hotspots derive from regions in the genome in which there is high bidirectional transcriptional activity. We thus propose a model in which highly abundant transcripts base pair with low-level antisense transcripts to generate dsRNA substrates for Dcr-2. Alternatively, there may be particularly high level of antisense transcription in hotspot regions. At this point, the transcriptional landscape of IIV-6 remains poorly defined; thus, the temporal regulation of transcription, transcription start and stop sites, as well as the extent of antisense transcription throughout the viral genome remains unclear. Future studies using strand-specific next generation cDNA sequencing (RNA-seq) may provide a high-resolution map of transcriptional activity across the IIV-6 genome. Once these data become available, our model can be more robustly tested.

DNA virus-derived vsRNA profiles in other model systems

A number of recent publications have now analyzed vsRNA profiles in DNA virus infections in different invertebrate model systems. These studies further underscore that DNA viruses are targets of an antiviral RNAi response, but that the mechanism for vsRNA biogenesis may differ from that in IIV-6-infected flies. In a recent study, Dcr-2-dependent vsRNAs were recovered from a *Drosophila* cell line infected with Vaccinia virus (VACV), a dsDNA virus of the poxvirus family (32). Abundant vsRNAs were particularly recovered from tandem repeats located at the covalently closed genomic termini. Computational predictions indicated that transcripts of these repetitive sequences have the ability to fold into hairpin RNA structures (Figure 3B). Indeed, knockdown experiments indicated that these RNA structures are targets of Dcr-2, and to a lesser extent of the microRNA processing enzyme Dcr-1. Base paired bidirectional transcripts or structured regions of single-stranded transcripts were proposed to be Dcr-2 substrates in other regions of the VACV genome, but these hypotheses remain to be experimentally tested. Moreover, *Drosophila* cells do not support a full VACV replication

cycle, and the full extent of vsiRNA production in poxvirus infection remains to be established.

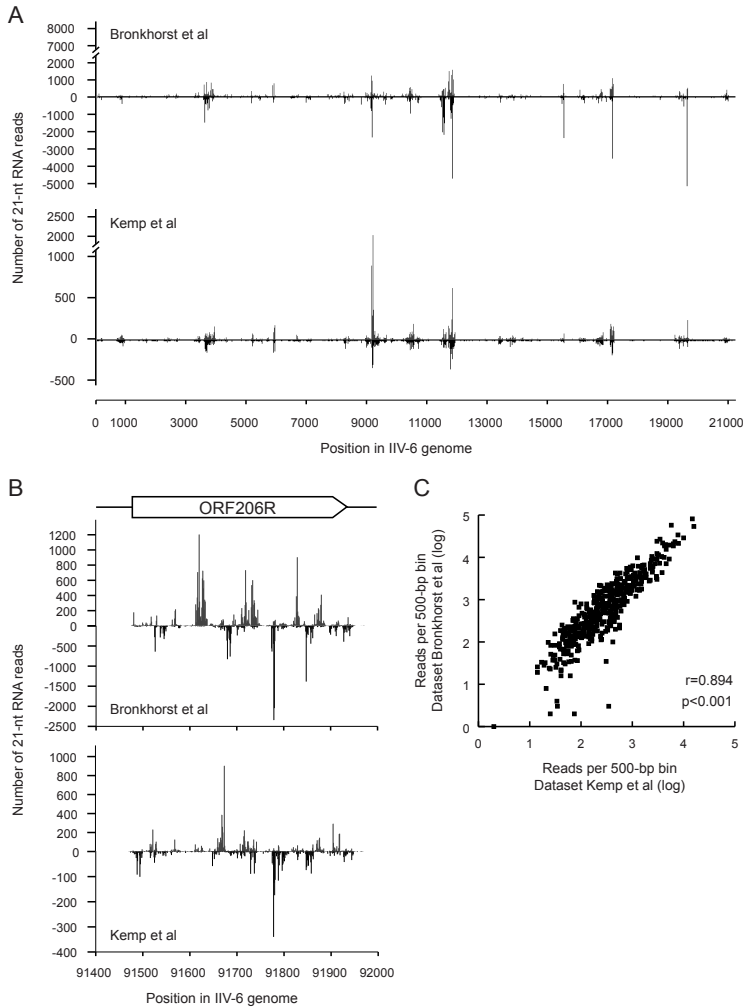


Figure 2. Viral small RNA profiles from 2 independent studies of IIV-6-infected *Drosophila*. (A) Viral siRNAs (21-nt) were aligned to the IIV-6 genome, allowing one mismatch during alignment. The genome coordinates of the 5' end of vsiRNAs in the study of Bronkhorst et al. (upper panel; w^{1118} control flies) and of Kemp et al. (lower panel; $y^1 w^1$ control flies) were plotted. vsiRNAs that map to the upper and lower strands of the IIV-6 genome are shown in gray and black, respectively. Data from Bronkhorst et al. are the sum of 2 independent data sets of IIV-6-infected w^{1118} flies. (B) Detailed profile of IIV-6 derived vsiRNAs (21-nt) mapping to genome coordinates 91,400 to 92,000 is shown for the 2 independent studies. ORF 206R, which is located in this region, is depicted above the plot (drawn to scale). (C) The IIV-6 genome was divided into non-overlapping 500-bp bins, and the correlation between vsiRNAs densities in the studies of Bronkhorst et al. and Kemp et al. was analyzed in a scatter plot (log-transformed data; $r = 0.894$, $P < 0.001$, Pearson's correlation test).

Structured RNA elements were also implied as Dcr-2 substrates in *Culex tritaeniorhynchus* densovirus, a novel, single-stranded DNA virus of the *densovirus* genus virus that was recently identified in wild-caught mosquitoes (40). Two inverted repeat sequences at the non-coding genomic termini, which were previously not known to be transcribed, gave rise to abundant viral small RNAs. This observation suggests that these termini are transcribed and fold into dsRNA structures that are processed into small RNAs. Indeed, *in silico* predictions suggest that putative transcripts of these regions have the potential to fold into Y-shaped RNA structures with extensive perfectly base paired stems of 35- and 68-bp for the 5' terminal inverted repeat 1 (IR1, Figure 3C) and the 3' terminal inverted repeat 2 (IR2, not shown), respectively. To explore whether these structures are putative Dicer substrates, we analyzed the published small RNA sequences to determine the size profiles of the viral small RNAs. 74.3% and 79.8% of the small RNAs that map to IR1 and IR2, respectively, were 21 or 22-nt in size. Moreover, these small RNAs mapped to the stem, but not to the two arms of the predicted Y-shaped RNA structures (data not shown). These results suggest that IR-derived small RNAs are *bona fide* Dicer products, but this remains to be experimentally demonstrated. Densoviral terminal stem-loop structures likely play a role in genome replication and/or packaging (41). It remains to be investigated how transcription of the inverted repeats and Dicer-mediated processing of the resulting transcripts affect these processes. Another source of viral small RNAs in this study were the protein coding transcripts of the viral genome (40). These small RNAs predominantly derive from the sense transcripts of the viral genome and have a broad distribution of sizes, ranging from 18 to 30-nt, with only a minor enrichment at 21 or 22-nt (32.3%, data not shown). The majority of these small RNAs are therefore unlikely to be generated in a Dicer-dependent manner.

Like our observations in IIV-6-infected flies, convergent transcripts also seem to be the source of vsiRNAs in other insect species infected with complex dsDNA viruses. In a recent study, the antiviral RNAi response to the baculovirus *Helicoverpa armigera* single nucleopolyhedrovirus (HaSNPV) was analyzed in larvae of the cotton bollworm moth (*Helicoverpa armigera*) (42). Similar to vsiRNAs in IIV-6-infected flies, small RNAs displayed an uneven distribution across the viral genome, with some hotspot regions generating abundant amounts of small RNAs, and other regions generating few small RNAs. Moreover, in most hotspots, vsiRNAs map to both strands of the viral genome, consistent with base paired overlapping transcripts as a Dicer substrate. For a number of highly targeted ORFs, small RNAs were enriched for those derived from only one strand of the viral genome. The substrates for the biogenesis of these small RNAs remain unclear. When *Dcr-2* was depleted in *Helicoverpa zea* derived fat body cells, higher expression levels were detected for 2 highly targeted ORFs, but not for 2 ORFs that did not give rise to vsiRNAs. Moreover, a modest increase in viral DNA replication was

observed upon *Dcr-2* knockdown. It was thus proposed that RNAi-mediated silencing of essential viral genes restricts virus replication (42).

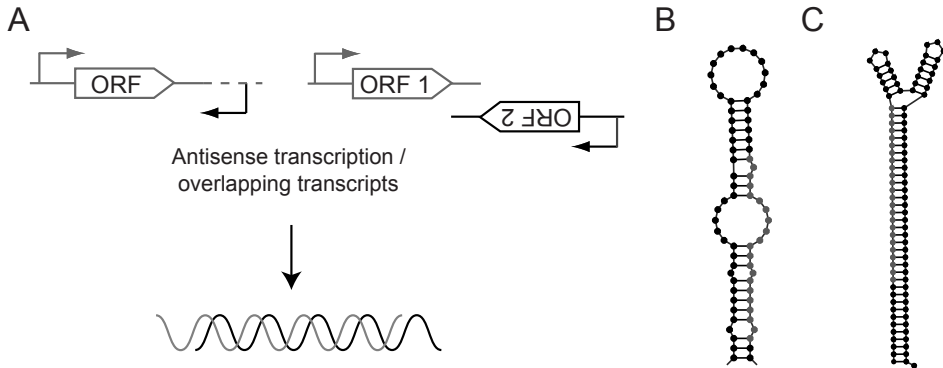


Figure 3. Proposed substrates for vsiRNA biogenesis in DNA virus infection of insects. (A) Converging overlapping transcripts base pair to generate dsRNA substrates for Dicer-2 in iridovirus, Vaccinia virus, and baculovirus infection. (B) Transcripts of repeats at the genomic termini of vaccinia virus are predicted to fold into hairpin RNA structures that give rise to Dicer-dependent small RNAs (in gray). (C) Putative transcripts of the 5' terminal inverted repeat sequence (IR1) of *Culex tritaeniorhynchus* densovirus are predicted to fold into a Y-shaped RNA structure. Small RNAs of 21-22 nt in size map to the stem, but not the arms, of the structure (in gray). It is not possible to unambiguously map the small RNAs to either the 5' or 3' stem sequence, since the stem is a perfectly base paired sequence and the orientation in which the region is transcribed is unknown. Transcripts of the 3' terminal inverted repeat sequence (IR2) are predicted to fold in a similarly Y-shaped shaped structure with a longer, 68-bp stem. IR2-derived 21-22 nt small RNAs map along the dsRNA stem, without evidence for phasing.

The antiviral potential of RNAi to control DNA virus infection was recently also confirmed in another invertebrate system. Knockdown of *Dcr-2* expression in white spot syndrome virus (WSSV)-infected shrimp resulted in an increase in virus replication, suggesting that this circular dsDNA virus is a target of the invertebrate RNAi machinery (43). Unfortunately, the authors only monitored the production of a single viral siRNA by Northern blot. This particular siRNA was indeed produced in a *Dcr-2*-dependent manner. Future studies using small RNA deep sequencing may provide more detailed insights into the *Dcr-2* substrates in this virus and into the mechanism of vsiRNA biogenesis.

Seminal studies have established that RNA viruses are processed into vsiRNAs in plants (12, 44). Interestingly, DNA viruses are also targets of the RNAi machinery in plants. Like DNA viruses in insects, vsiRNA may arise from processing of structured RNA elements (45) or from dsRNA generated by base pairing of sense and antisense

transcripts (46, 47). Indeed, vsiRNAs of both sense and antisense polarity are generated upon infection with Gemini viruses (ssDNA virus) and the pararetrovirus Cauliflower mosaic virus (circular dsDNA virus) (46-49).

Concluding remarks

Together, these studies demonstrate that an antiviral RNAi response is mounted against distinct DNA viruses in different invertebrate hosts. Our study implies that base paired, overlapping sense and antisense transcripts are the major Dcr-2 substrates in IIV-6 infection; in other viruses (VACV and densovirus) structured RNA elements may be additional substrates for Dcr-2. Important questions remain. For example, are vsiRNAs incorporated in RISC and functional in directing target RNA cleavage? Using sensor assays, we demonstrated that some IIV-6-derived vsiRNAs are indeed functional, but that the efficiency of silencing is modest. Moreover, for 5 selected ORFs that contained a high density of vsiRNA reads, we did not observe a general increase in viral transcript levels in *AGO2* mutant flies. Further genome-wide transcriptome analyses are required to establish if and to what extent RNAi regulates IIV-6 viral gene expression. Strikingly, in HaSNPV infection an increase in transcript levels upon *Dcr-2* knockdown was observed, suggesting that vsiRNAs are RISC-associated and functional in silencing viral gene expression (42).

Other questions pertain to the function of vsiRNAs in DNA virus infection. Is dsRNA produced as an inevitable by-product of a densely packed genome that is transcribed in 2 directions? Does the RNAi machinery exploit this feature for antiviral defense? Alternatively, the virus may exploit the antiviral RNAi machinery to regulate expression of viral genes. RNAi-mediated regulation of expression of essential viral genes may contribute to the fine-tuning of viral replication and pathogenesis. In this respect, it would be of interest to see whether antisense transcription (and thus the potential for dsRNA formation) is dynamically regulated. For some ORFs of HaSNPV, sense transcripts seem to be the major origin of small RNAs (42). These small RNAs by definition cannot target coding transcripts as they have the same orientation. Perhaps these highly abundant transcripts are decoy Dcr-2 substrates that saturate the RNAi machinery, thereby preventing other essential viral genes from being targeted. Dedicated non-coding transcripts may have a similar function in large complex DNA viruses. Finally, as was reported for the plant DNA virus cauliflower mosaic virus, (45) viral small RNAs may regulate the expression of cellular genes, in functional analogy to virus-encoded miRNAs (50). A striking similarity between VACV and *Culex tritaeniorhynchus* densovirus is that both viruses produce small RNAs from putative RNA structures

encoded by non-coding genomic termini. How these small RNAs affect the viral life cycle is an open question for future investigation.

In several organisms, small RNAs mediate gene silencing at the transcriptional level. For example, small RNAs guide RNA-mediated DNA methylation in plants (*Arabidopsis thaliana*) or induce heterochromatin formation by guiding the deposition of repressive marks on histone proteins in yeast (*S. pombe*) and in *D. melanogaster* (51, 52). During nuclear replication of geminiviruses in plants, viral dsDNA intermediates associate with cellular histone proteins, thus forming viral minichromosomes. Interestingly, it was proposed that viral small RNAs guide *de novo* cytosine methylation of the geminivirus genome as an antiviral defense strategy (53). DNA viruses in mammals also form chromatin-like structures that are subject to epigenetic regulation (54, 55). Whether vsiRNAs guide transcriptional silencing of DNA viruses in insects remains an open question.

A final important question is whether there are alternative mechanisms for antiviral defense against DNA viruses. Several cytoplasmic DNA sensors have been identified in mammals over the last few years. While insects lack the interferon response of mammals that are induced by these sensors, direct cytoplasmic DNA sensing could also play a role in activating immune or stress responses in insects. Altogether, recent studies reveal that DNA viruses produce *bona fide* Dcr-2 substrates that elicit antiviral RNAi responses in invertebrates; nevertheless, the identification of several atypical Dcr-2 substrates suggests that the interaction between DNA viruses and the host RNAi machinery may be highly complex.

Acknowledgements

We thank members of the Van Rij laboratory, Carla Saleh, and Sassan Asgari for discussions. This work was financially supported by a VIDI fellowship (Project 864.08.003) from the Netherlands Organization for Scientific Research and a fellowship from the Nijmegen Centre for Molecular Life Sciences to van Rij RP and by a PhD fellowship from Radboud University Nijmegen Medical Centre to Miesen P.

References

1. Medzhitov R, Schneider DS, & Soares MP (2012) Disease tolerance as a defense strategy. *Science* 335:936-941.
2. Weber F, Wagner V, Rasmussen SB, Hartmann R, & Paludan SR (2006)

- Double-stranded RNA is produced by positive-strand RNA viruses and DNA viruses but not in detectable amounts by negative-strand RNA viruses. *J Virol* 80:5059-5064.
3. Takeuchi O & Akira S (2010) Pattern recognition receptors and inflammation. *Cell* 140:805-820.
 4. Feng Q, Hato SV, Langereis MA, Zoll J, Virgen-Slane R, Peisley A, Hur S, Semler BL, van Rij RP, & van Kuppeveld FJ (2012) MDA5 detects the double-stranded RNA replicative form in picornavirus-infected cells. *Cell reports* 2:1187-1196.
 5. Triantafyllou K, Vakakis E, Kar S, Richer E, Evans GL, & Triantafyllou M (2012) Visualisation of direct interaction of MDA5 and the dsRNA replicative intermediate form of positive strand RNA viruses. *J Cell Sci* 125:4761-4769.
 6. Kato H, Takahashi K, & Fujita T (2011) RIG-I-like receptors: cytoplasmic sensors for non-self RNA. *Immunol Rev* 243:91-98.
 7. Keating SE, Baran M, & Bowie AG (2011) Cytosolic DNA sensors regulating type I interferon induction. *Trends Immunol* 32:574-581.
 8. Cavlar T, Ablasser A, & Hornung V (2012) Induction of type I IFNs by intracellular DNA-sensing pathways. *Immunol Cell Biol* 90:474-482.
 9. Wu J, Sun L, Chen X, Du F, Shi H, Chen C, & Chen ZJ (2013) Cyclic GMP-AMP is an endogenous second messenger in innate immune signaling by cytosolic DNA. *Science* 339:826-830.
 10. Sun L, Wu J, Du F, Chen X, & Chen ZJ (2013) Cyclic GMP-AMP synthase is a cytosolic DNA sensor that activates the type I interferon pathway. *Science* 339:786-791.
 11. O'Neill LA (2009) DNA makes RNA makes innate immunity. *Cell* 138:428-430.
 12. Ding SW & Voinnet O (2007) Antiviral immunity directed by small RNAs. *Cell* 130:413-426.
 13. Van Rij RP & Berezikov E (2009) Small RNAs and the control of transposons and viruses in *Drosophila*. *Trends Microbiol* 17:139-178.
 14. Blair CD (2011) Mosquito RNAi is the major innate immune pathway controlling arbovirus infection and transmission. *Future Microbiol* 6:265-277.
 15. Bronkhorst AW, van Cleef KW, Vodovar N, Ince IA, Blanc H, Vlak JM, Saleh MC, & van Rij RP (2012) The DNA virus Invertebrate iridescent virus 6 is a target of the *Drosophila* RNAi machinery. *Proc Natl Acad Sci U S A* 109:E3604-3613.
 16. Sanchez-Vargas I, Travanty EA, Keene KM, Franz AW, Beaty BJ, Blair CD, & Olson KE (2004) RNA interference, arthropod-borne viruses, and mosquitoes.

- Virus Res* 102:65-74.
17. van Mierlo JT, van Cleef KW, & van Rij RP (2011) Defense and counterdefense in the RNAi-based antiviral immune system in insects. *Methods in molecular biology* 721:3-22.
 18. Galiana-Arnoux D, Dostert C, Schneemann A, Hoffmann JA, & Imler JL (2006) Essential function in vivo for Dicer-2 in host defense against RNA viruses in drosophila. *Nat Immunol* 7:590-597.
 19. Wang XH, Aliyari R, Li WX, Li HW, Kim K, Carthew R, Atkinson P, & Ding SW (2006) RNA interference directs innate immunity against viruses in adult *Drosophila*. *Science* 312:452-454.
 20. Van Rij RP, Saleh MC, Berry B, Foo C, Houk A, Antoniewski C, & Andino R (2006) The RNA silencing endonuclease Argonaute 2 mediates specific antiviral immunity in *Drosophila melanogaster*. *Genes Dev* 20:2985-2995.
 21. Zamboni RA, Vakharia VN, & Wu LP (2006) RNAi is an antiviral immune response against a dsRNA virus in *Drosophila melanogaster*. *Cell Microbiol* 8:880-889.
 22. Mueller S, Gausson V, Vodovar N, Deddouche S, Troxler L, Perot J, Pfeffer S, Hoffmann JA, Saleh MC, & Imler JL (2010) RNAi-mediated immunity provides strong protection against the negative-strand RNA vesicular stomatitis virus in *Drosophila*. *Proc.Natl.Acad.Sci.U.S.A* 107:19390-19395.
 23. Nayak A, Berry B, Tassetto M, Kunitomi M, Acevedo A, Deng C, Krutchinsky A, Gross J, Antoniewski C, & Andino R (2010) Cricket paralysis virus antagonizes Argonaute 2 to modulate antiviral defense in *Drosophila*. *Nat. Struct.Mol.Biol.* 17:547-554.
 24. van Mierlo JT, Bronkhorst AW, Overheul GJ, Sadanandan SA, Ekstrom JO, Heestermans M, Hultmark D, Antoniewski C, & van Rij RP (2012) Convergent evolution of argonaute-2 slicer antagonism in two distinct insect RNA viruses. *PLoS Pathog* 8:e1002872.
 25. Constantino M, Christian P, Marina CF, & Williams T (2001) A comparison of techniques for detecting Invertebrate iridescent virus 6. *J Virol Methods* 98:109-118.
 26. Williams T, Barbosa-Solomieu V, & Chinchar VG (2005) A decade of advances in iridovirus research. *Adv Virus Res* 65:173-248.
 27. Teixeira L, Ferreira A, & Ashburner M (2008) The bacterial symbiont *Wolbachia* induces resistance to RNA viral infections in *Drosophila melanogaster*. *PLoS Biol* 6:e2.
 28. Lim DH, Oh CT, Lee L, Hong JS, Noh SH, Hwang S, Kim S, Han SJ, & Lee YS (2011) The endogenous siRNA pathway in *Drosophila* impacts stress resistance

- and lifespan by regulating metabolic homeostasis. *FEBS Lett* 585:3079-3085.
29. Kemp C, Mueller S, Goto A, Barbier V, Paro S, Bonnay F, Dostert C, Troxler L, Hetru C, Meignin C, *et al.* (2013) Broad RNA interference-mediated antiviral immunity and virus-specific inducible responses in *Drosophila*. *J Immunol* 190:650-658.
 30. Wu Q, Luo Y, Lu R, Lau N, Lai EC, Li WX, & Ding SW (2010) Virus discovery by deep sequencing and assembly of virus-derived small silencing RNAs. *Proc. Natl.Acad.Sci.U.S.A* 107:1606-1611.
 31. van Mierlo JT, van Cleef KWR, & Van Rij RP (2010) Small Silencing RNAs: Piecing Together a Viral Genome. *Cell Host & Microbe* 7:87-89.
 32. Sabin LR, Zheng Q, Thekkat P, Yang J, Hannon GJ, Gregory BD, Tudor M, & Cherry S (2013) Dicer-2 processes diverse viral RNA species. *PLoS One* 8:e55458.
 33. Vodovar N, Goic B, Blanc H, & Saleh MC (2011) In silico reconstruction of viral genomes from small RNAs improves viral-derived siRNA profiling. *J Virol* 85:11016-11021.
 34. Han YH, Luo YJ, Wu Q, Jovel J, Wang XH, Aliyari R, Han C, Li WX, & Ding SW (2011) RNA-based immunity terminates viral infection in adult *Drosophila* in the absence of viral suppression of RNA interference: characterization of viral small interfering RNA populations in wild-type and mutant flies. *J Virol* 85:13153-13163.
 35. Aliyari R, Wu Q, Li HW, Wang XH, Li F, Green LD, Han CS, Li WX, & Ding SW (2008) Mechanism of induction and suppression of antiviral immunity directed by virus-derived small RNAs in *Drosophila*. *Cell Host Microbe* 4:387-397.
 36. Jacobs BL & Langland JO (1996) When two strands are better than one: the mediators and modulators of the cellular responses to double-stranded RNA. *Virology* 219:339-349.
 37. Sorefan K, Pais H, Hall AE, Kozomara A, Griffiths-Jones S, Moulton V, & Dalmay T (2012) Reducing ligation bias of small RNAs in libraries for next generation sequencing. *Silence* 3:4.
 38. Ghildiyal M, Seitz H, Horwich MD, Li C, Du T, Lee S, Xu J, Kittler EL, Zapp ML, Weng Z, *et al.* (2008) Endogenous siRNAs Derived from Transposons and mRNAs in *Drosophila* Somatic Cells. *Science* 320:1077-1081.
 39. Marques JT, Kim K, Wu PH, Alleyne TM, Jafari N, & Carthew RW (2010) Loqs and R2D2 act sequentially in the siRNA pathway in *Drosophila*. *Nat. Struct.Mol.Biol.* 17:24-30.
 40. Ma M, Huang Y, Gong Z, Zhuang L, Li C, Yang H, Tong Y, Liu W, & Cao W

- (2011) Discovery of DNA viruses in wild-caught mosquitoes using small RNA high throughput sequencing. *PLoS One* 6:e24758.
41. Carlson J, Suchman E, & Buchatsky L (2006) Densoviruses for control and genetic manipulation of mosquitoes. *Adv Virus Res* 68:361-392.
 42. Jayachandran B, Hussain M, & Asgari S (2012) RNA interference as a cellular defense mechanism against the DNA virus baculovirus. *J Virol* 86:13729-13734.
 43. Huang T & Zhang X (2013) Host defense against DNA virus infection in shrimp is mediated by the siRNA pathway. *Eur J Immunol* 43:137-146.
 44. Hamilton AJ & Baulcombe DC (1999) A species of small antisense RNA in posttranscriptional gene silencing in plants. *Science* 286:950-952.
 45. Moissiard G & Voinnet O (2006) RNA silencing of host transcripts by cauliflower mosaic virus requires coordinated action of the four Arabidopsis Dicer-like proteins. *Proc Natl Acad Sci U S A* 103:19593-19598.
 46. Blevins T, Rajeswaran R, Aregger M, Borah BK, Schepetilnikov M, Baerlocher L, Farinelli L, Meins F, Jr., Hohn T, & Pooggin MM (2011) Massive production of small RNAs from a non-coding region of Cauliflower mosaic virus in plant defense and viral counter-defense. *Nucleic Acids Res* 39:5003-5014.
 47. Blevins T, Rajeswaran R, Shivaprasad PV, Beknazariants D, Si-Ammour A, Park HS, Vazquez F, Robertson D, Meins F, Jr., Hohn T, *et al.* (2006) Four plant Dicers mediate viral small RNA biogenesis and DNA virus induced silencing. *Nucleic Acids Res* 34:6233-6246.
 48. Chellappan P, Vanitharani R, Pita J, & Fauquet CM (2004) Short interfering RNA accumulation correlates with host recovery in DNA virus-infected hosts, and gene silencing targets specific viral sequences. *J Virol* 78:7465-7477.
 49. Akbergenov R, Si-Ammour A, Blevins T, Amin I, Kutter C, Vanderschuren H, Zhang P, Gruissem W, Meins F, Jr., Hohn T, *et al.* (2006) Molecular characterization of geminivirus-derived small RNAs in different plant species. *Nucleic Acids Res* 34:462-471.
 50. Kincaid RP & Sullivan CS (2012) Virus-encoded microRNAs: an overview and a look to the future. *PLoS Pathog* 8:e1003018.
 51. Fagegaltier D, Bouge AL, Berry B, Poisot E, Sismeiro O, Coppee JY, Theodore L, Voinnet O, & Antoniewski C (2009) The endogenous siRNA pathway is involved in heterochromatin formation in *Drosophila*. *Proc Natl Acad Sci U S A* 106:21258-21263.
 52. Castel SE & Martienssen RA (2013) RNA interference in the nucleus: roles for small RNAs in transcription, epigenetics and beyond. *Nat Rev Genet* 14:100-112.

53. Raja P, Wolf JN, & Bisaro DM (2010) RNA silencing directed against geminiviruses: post-transcriptional and epigenetic components. *Biochim Biophys Acta* 1799:337-351.
54. Tempera I & Lieberman PM (2010) Chromatin organization of gammaherpesvirus latent genomes. *Biochim Biophys Acta* 1799:236-245.
55. Knipe DM, Lieberman PM, Jung JU, McBride AA, Morris KV, Ott M, Margolis D, Nieto A, Nevels M, Parks RJ, *et al.* (2013) Snapshots: chromatin control of viral infection. *Virology* 435:141-156.

Chapter 5

A dsRNA-binding protein of a complex invertebrate DNA virus suppresses the *Drosophila* RNAi response

Alfred W. Bronkhorst, Koen W.R. van Cleef, Hanka Venselaar
and Ronald P. van Rij

Nucleic Acids Res 2014, in press

Abstract

Invertebrate RNA viruses are targets of the host RNA interference (RNAi) pathway, which limits virus infection by degrading viral RNA substrates. Several insect RNA viruses encode suppressor proteins to counteract this antiviral response. We recently demonstrated that the dsDNA virus Invertebrate iridescent virus 6 (IIV-6) induces an RNAi response in *Drosophila*. Here, we show that RNAi is suppressed in IIV-6-infected cells and we mapped RNAi suppressor activity to the viral protein 340R. Using biochemical assays, we reveal that 340R binds long dsRNA and prevents Dicer-2-mediated processing of long dsRNA into small interfering RNAs (siRNAs). We demonstrate that 340R additionally binds siRNAs and inhibits siRNA loading into the RNA-induced silencing complex. Finally, we show that 340R is able to rescue a Flock House virus replicon that lacks its viral suppressor of RNAi. Together, our findings indicate that, in analogy to RNA viruses, DNA viruses antagonize the antiviral RNAi response.

Introduction

Recognition of double-stranded (ds) RNA is critical for many cellular processes, including gene regulation, RNA transport, and RNA editing. Most dsRNA-protein interactions are established by proteins that contain a canonical dsRNA-binding domain (dsRBD), which binds dsRNA in a sequence-independent manner (1,2). RNA interference (RNAi) is a dsRNA-initiated mechanism for post-transcriptional gene silencing that is guided by small interfering RNAs (siRNAs) and requires dsRBD-containing proteins at several stages (3,4).

The RNAi pathway serves as a cellular defense mechanism that destroys viral RNA in diverse eukaryotes, including plants, fungi, nematodes, insects, and mammals (5-8). In *Drosophila*, cytoplasmic Dicer-2 (Dcr-2), which contains two RNase III motifs and a single dsRBD, recognizes viral dsRNA as non-self and processes it into viral small interfering RNAs (vsiRNAs), RNA duplexes of 21-nt that contain 2-nt 3' overhangs (5,9). A heterodimer composed of the dsRBD adaptor protein R2D2 and Dcr-2 subsequently binds vsiRNA duplexes to mediate their loading into Argonaute-2 (AGO2) in the RNA-induced silencing complex (RISC). Within RISC, vsiRNAs guide the recognition and cleavage of fully complementary viral target RNA by AGO2 (9,10). Several insect RNA viruses have evolved viral suppressors of RNAi (VSRs) to antagonize the initiation phase of the antiviral RNAi pathway (9). For example, the 1A protein of *Drosophila C virus* (DCV) contains a canonical dsRBD that binds long dsRNA and prevents Dcr-2-mediated vsiRNA biogenesis (11). The B2 protein of Flock House virus (FHV) and the VP3 proteins of *Drosophila X virus* and the mosquito-specific *Culex Y virus* interfere with the insect RNAi pathway by sequestering long dsRNA as well as siRNAs (12-16). These VSRs may thus inhibit the production of vsiRNAs and prevent their incorporation into RISC.

In RNA virus-infected plants, viral dsRNA is processed by the Dicer-like (DCL) proteins DCL2, DCL3, and DCL4, which generate viral small RNAs of 22, 24, and 21-nt in size, respectively (5). The P19 protein of tombusviruses is one of the best-characterized VSRs in plants. P19 specifically binds 21-nt sized siRNAs (17-20) and thereby prevents siRNA incorporation into RISC (21). A similar strategy is used by several other plant RNA viruses (22,23). Sweet potato chlorotic stunt virus prevents siRNA loading into RISC via an alternative mechanism. This single-stranded RNA virus encodes a viral RNase III protein that processes siRNAs into 14-bp small RNA duplexes, which are non-functional in RNAi (24). Likewise, the RNase III of the dsDNA virus *Heliothis virescens* ascovirus-3e cleaves long dsRNA in the tobacco budworm (*Heliothis virescens*) (25). Thus, the RNase III proteins of two unrelated viruses interfere with RNAi, either by inhibiting vsiRNA production through destruction of Dcr-2 substrates or by preventing

the incorporation of functional vsiRNAs into RISC.

Importantly, some insect and plant RNA viruses inhibit the RNAi pathway at the effector phase (9,23). For example, the Cricket paralysis virus (CrPV) 1A and Nora virus VP1 proteins antagonize the enzymatic activity of AGO2 in *Drosophila* (26,27). Similarly, the Cucumber mosaic virus 2b protein inhibits the endonuclease activity of AGO1 in plants (28). Plant AGO1 function is also suppressed by the P0 and P38 proteins of Beet western yellows virus and Turnip crinkle virus, respectively (29-32). These studies indicate that unrelated viruses have evolved VSRs that inhibit the catalytic activity of RISC and thus highlight the critical role of Argonaute proteins in antiviral defense.

Over the last years, several studies revealed that different classes of RNA viruses are both targets and suppressors of RNAi in *Drosophila* (11,13,33,34). Recently, we and others showed that RNAi also provides antiviral defense against DNA viruses *in vivo* (35,36). Indeed, Dcr-2-dependent vsiRNAs were generated in Invertebrate iridescent virus 6 (IIV-6)-infected flies and, accordingly, *AGO2* and *Dcr-2* mutant flies were more susceptible to IIV-6 infection than wildtype flies. However, it remained unknown whether DNA viruses antagonize the *Drosophila* antiviral RNAi response.

In the present study, we investigated whether IIV-6 suppresses RNAi. We demonstrate that the IIV-6 340R protein inhibits RNA silencing when RNAi is induced by long dsRNA as well as by siRNA duplexes. In a series of biochemical assays, we further demonstrate that 340R binds RNA duplexes to prevent siRNA biogenesis and to inhibit RISC loading. Our findings indicate that DNA viruses are targets and suppressors of the antiviral RNAi response.

Results

RNAi is suppressed in IIV-6-infected cells

We and others recently reported that the dsDNA virus IIV-6 triggers an antiviral RNAi response in *Drosophila* (35,36). To investigate whether IIV-6 antagonizes the host RNAi response, we performed RNAi reporter assays in *Drosophila* S2 cells. In these well-established assays, RNAi-mediated silencing of a Fluc reporter gene is induced by Fluc-specific long dsRNA or siRNAs (11,38).

We first tested whether RNAi is suppressed in IIV-6-infected S2 cells. As a positive control, we included the positive-sense RNA virus DCV, which encodes a VSR and inhibits RNAi in infection (11). Co-transfection of reporter plasmids along with Fluc-specific long dsRNA resulted in efficient silencing of the Fluc reporter in mock-infected cells (240-fold, Figure 1A). In contrast, in IIV-6-infected cells, silencing of the Fluc reporter was suppressed in an MOI (multiplicity of infection)-dependent manner, to

118-fold at an MOI of 0.01 and to 28-fold at an MOI of 0.1 (Figure 1A; $P = 0.061$ and $P = 0.004$, respectively). As observed before (11), DCV also suppressed RNAi in an MOI-dependent manner (Figure 1A). Together, these results indicate that the RNAi pathway is suppressed in IIV-6-infected cells.

The IIV-6 340R protein is a suppressor of RNAi

IIV-6 is a large, complex virus with a 212-kb genome that contains 211 predicted open reading frames (ORFs) (45,46). We therefore browsed the IIV-6 genome for ORFs that encode proteins with predicted domains or motifs that might account for the observed RNAi suppressor activity. A candidate is ORF 142R, which encodes a putative RNase III that might degrade siRNAs or long dsRNA substrates for Dcr-2, as was observed for RNase III proteins of other viruses (24,25). Another candidate VSR is 340R, which contains a predicted canonical dsRBD. Such domains have also been observed in other VSRs (11,47). The 142R and 340R proteins are conserved in different genera within the *Iridoviridae* family (46,48), suggesting that these proteins have important functions in the viral life cycle.

To analyze whether 142R and 340R inhibit the RNAi pathway, we cloned the individual ORFs into expression plasmids for RNAi reporter assays. S2 cells were transfected with the expression plasmids along with the reporter plasmids. Two days after transfection, dsRNA was added to the culture supernatant to induce RNAi, thus allowing expression of viral proteins before induction of RNAi. The CrPV 1A protein, which suppresses the RNAi pathway by antagonizing RISC enzymatic activity, served as a positive control (26). The dsRBD protein 340R suppressed RNAi to background levels (compared with 12-fold silencing for the empty control vector, $P \leq 0.001$), similar to CrPV 1A (Figure 1B, $P \leq 0.001$). In contrast, we did not observe VSR activity for the predicted RNase III 142R (Figure 1B). Although we readily detected protein expression of 142R and 340R in transfected S2 cells by Western blot analysis (Figure 1C), 142R was expressed at lower levels than 340R. Increasing the amount of transfected 142R expression plasmid led to a mild increase in protein levels. However, also under these conditions, we could not detect VSR activity for 142R (Figure S1A). To confirm these results, we performed an RNAi reporter assay in which a *Renilla* luciferase (Rluc) reporter is silenced by an Rluc-specific hairpin RNA expressed from a copper-inducible promoter. Also in this assay, 340R efficiently suppressed RNAi (Figure 1D, $P = 0.003$), whereas 142R was unable to do so.

To investigate whether 340R inhibits the RNAi pathway downstream of siRNA production, we performed an assay in which we induced RNAi with siRNAs instead of long dsRNA. We found that 340R efficiently inhibited siRNA-induced RNAi (Figure 1E; 7.7-fold silencing compared with 27-fold for the empty control plasmid, $P \leq$

0.001), indicating that this VSR is capable of suppressing the RNAi pathway at a stage downstream of Dcr-2-dependent siRNA production.

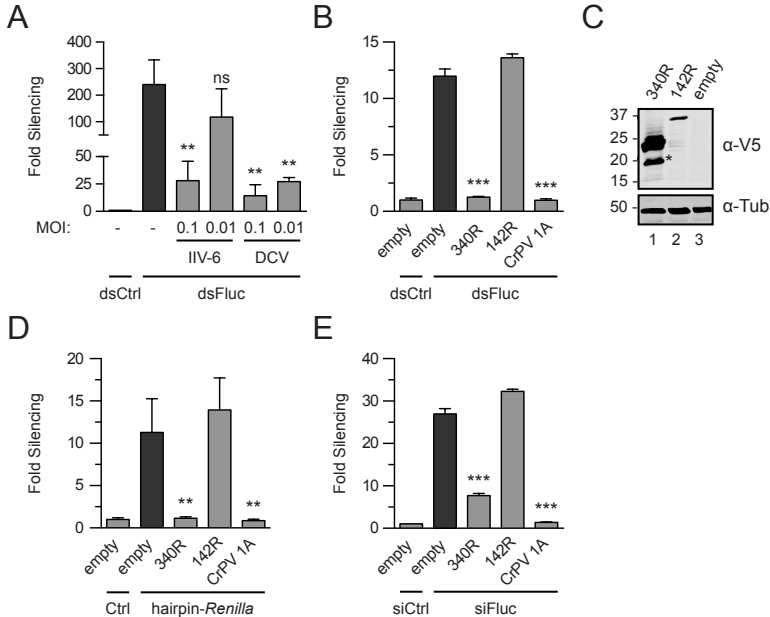


Figure 1. IIV-6 encodes a suppressor of RNAi. (A) dsRNA-induced RNAi reporter assay in virus-infected *Drosophila* S2 cells. S2 cells were mock-infected (-) or infected with either IIV-6 or DCV at the indicated MOI. Fluc and *Renilla* luciferase (Rluc) reporter plasmids were transfected along with dsRNA targeting Fluc (dsFluc) or a non-specific control sequence (dsCtrl) and 3 days after transfection, luciferase activities were measured. (B) RNAi reporter assay in S2R⁺ cells expressing individual viral proteins. Cells were transfected with luciferase reporter plasmids along with control plasmid (empty) or expression plasmids encoding the indicated viral proteins. CrPV 1A was included as a positive control. Two days post-transfection, RNAi was induced by adding long dsRNA to the culture supernatant. (C) Western blot analysis of V5 epitope-tagged 340R and 142R in transfected S2 cells. Viral proteins were detected using anti-V5 antibodies (α-V5); polyclonal anti-α-tubulin (α-Tub) antibody was used as a loading control. Molecular mass (in kDa) is indicated on the left of the image. The predicted molecular weights for 340R and 142R are 23 kDa and 37 kDa, respectively. The asterisk (*) indicates a 340R-specific processing or degradation product. (D) *Renilla* hairpin-induced RNAi reporter assay. S2 cells were transfected with luciferase reporter plasmids, expression plasmids for the indicated viral proteins, and either a plasmid that encodes a *Renilla* hairpin RNA (hairpin-*Renilla*) or an empty plasmid control (Ctrl). (E) siRNA-induced RNAi reporter assay in S2 cells. Cells were transfected with plasmids encoding the indicated viral proteins followed by transfection of luciferase reporter plasmids along with siRNAs that target the Fluc reporter (siFluc) or non-silencing control siRNAs (siCtrl). For all reporter assays in which Fluc expression was silenced, Fluc counts were normalized to Rluc counts and expressed as fold silencing relative to control treatment, and vice versa when Rluc expression was silenced. Fold silencing in the non-silencing controls (dsCtrl or siCtrl) was set to one for all panels. Bars in all panels represent the means and standard deviations of three independent samples. Difference in RNAi efficiency compared to controls (dark gray bars) was analyzed by one-way ANOVA followed by a *post-hoc* Dunnett's test. * $P \leq 0.05$; ** $P \leq 0.01$; *** $P \leq 0.001$; ns, not significant.

The dsRBD of 340R is required for RNAi suppression

The IIV-6 340R gene encodes a 23-kDa protein that contains a 70-aa dsRBD flanked by a 30-aa N-terminal sequence and a 73-aa C-terminal sequence. Alignment of the the dsRBD of 340R to the dsRBDs of DCV 1A and cellular proteins from different model organisms shows that conserved amino acids are present throughout the motif (Figure 2A). Homology modeling suggests that the dsRBD of 340R adopts the expected abbba topology, in which two α helices are packed along a three-stranded antiparallel β sheet, and that the dsRBD is preceded by an N-terminal helical structure (Figure 2B). Based on these analyses, we selected for site-directed mutagenesis four highly conserved residues (L35Y, F63A and AA92LL) and two residues within a region expected to interact with dsRNA (K86A and K89A) (Figure 2A and 2B and S2). In addition, we generated a C-terminally truncated version of 340R, consisting of the N-terminal 100-aa that contains the complete dsRBD (dsRBD¹⁰⁰).

Western blot analysis verified that all mutant proteins were expressed in transfected S2 cells, albeit at different levels relative to the wildtype (WT) protein (Figure 2C). We subsequently analyzed VSR activity of WT and mutant 340R in reporter assays in which RNAi was induced by feeding of long dsRNA. In these assays, WT 340R almost completely blocked RNAi (Figure 2D; 1.4-fold silencing compared with 11-fold for the empty control vector, $P \leq 0.001$). All tested mutants lost VSR activity relative to WT 340R (Figure 2D). Mutation of residues predicted to be involved in dsRNA binding reduced silencing to 3.6-fold (K86A, $P \leq 0.001$) and 8.2-fold (K89A, $P = 0.074$) (Figure 2D). Loss of VSR activity of the conserved residue mutants AA92LL and L35Y might result from reduced expression levels (Figure 2C), perhaps due to destabilizing effects of the substitutions on the local protein structure (Figure S2).

To increase VSR protein levels in our RNAi reporter assays, we increased the amount of transfected L35Y and AA92LL expression plasmids (Figure S2B and S2C, respectively). L35Y expression was increased to WT 340R levels under several conditions, but this did not result in detectable VSR activity (Figure S2B). For the AA92LL mutant, we only observed a slight increase in protein levels, which was not sufficient for suppression of RNAi (Figure S2C). Similar to the 340R point mutants, dsRBD¹⁰⁰ did not suppress RNAi (Figure 2D). Since this construct was expressed at lower levels than WT 340R, we repeated the assay with increasing amounts of plasmid. However, although dsRBD¹⁰⁰ reached similar protein levels as WT 340R under these conditions, dsRBD¹⁰⁰ did not inhibit silencing of the reporter, indicating that the dsRBD by itself is insufficient to exert VSR activity (Figure S1D).

We next performed an RNAi reporter assay in which RNAi is induced by siRNA transfection and included dsRBD¹⁰⁰ as well as the K89A mutant (Figure 2E). As observed before (Figure 1E), WT 340R, as well as the positive control CrPV 1A, efficiently

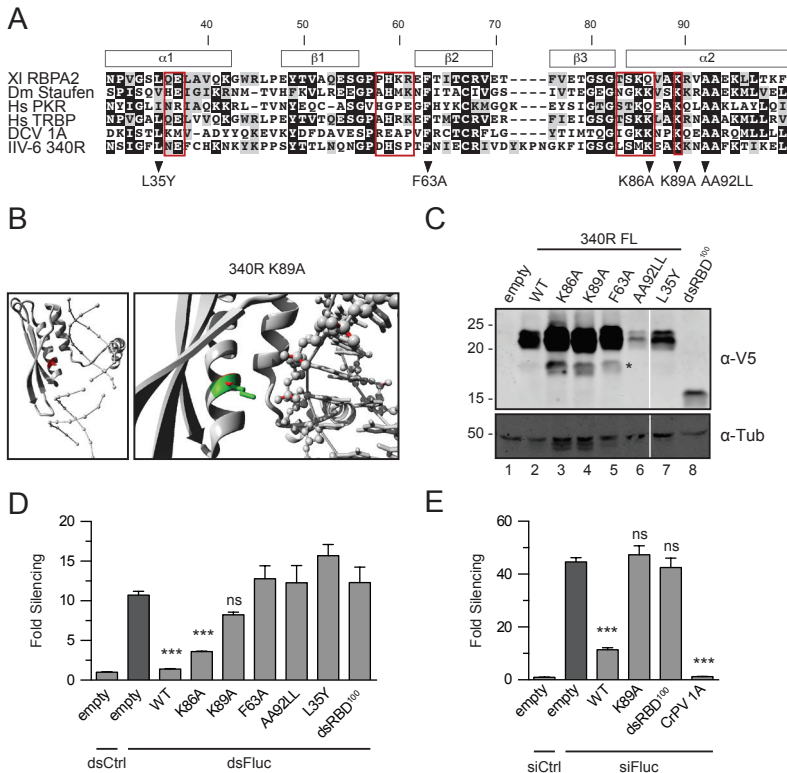


Figure 2. Viral protein 340R requires a functional dsRBD to suppress RNAi. (A) Alignment of the dsRBD of 340R (aa 30-100) to the dsRBDs of proteins from different model organisms and to the dsRBD of DCV 1A. Red boxes indicate residues that interact with dsRNA in structural analyses of the second dsRBD of *Xenopus laevis* RNA-binding protein A (XI RBP2) (56). Residues predicted to be involved in RNA binding or conserved amino acids were selected for site-directed mutagenesis. Position of secondary structures are indicated above the alignment. (B) Homology model of 340R in complex with dsRNA. The protein is shown in cartoon-view with the WT residue K89 shown in red (left panel) or with the WT residue shown in green and the mutant residue (Alanine) shown in red (right panel). The RNA is shown in ball-and-stick view, without atomic details (left) and with all atoms (right). The side-chain of residue K89 is positioned towards the phosphate backbone of the RNA and likely binds dsRNA through an electrostatic interaction of the positively charged Lysine with the negatively charged phosphates. The substitution of this Lysine into the small and hydrophobic Alanine is likely to abolish the interaction. See Figure S2 for other residues selected for site-directed mutagenesis. (C) Western blot analysis of V5 epitope-tagged WT and mutant 340R from transfected S2 cells. Proteins were detected using anti-V5 antibodies (α -V5) or, as a loading control, using anti- α -tubulin (α -Tub) antibodies. Molecular mass (in kDa) is indicated on the left of the image. The predicted molecular weight for dsRBD¹⁰⁰ is 14.7 kDa. FL, full-length. The asterisk (*) indicates a 340R-specific processing or degradation product. (D) dsRNA-induced RNAi reporter assay. The experiment was performed as described in the legend to Figure 1B, using expression plasmids for WT and mutant 340R. (E) siRNA-induced RNAi reporter assay. Sequential transfection was performed as described in the legend to Figure 1E, using expression plasmids for WT and mutant 340R and CrPV 1A. Difference in RNAi efficiency compared to controls (dark gray bars) was analyzed by one-way ANOVA followed by a *post-hoc* Dunnett's test. * $P \leq 0.05$; ** $P \leq 0.01$; *** $P \leq 0.001$; ns, not significant.

suppressed siRNA-induced RNAi (11-fold and 1.2-fold silencing, respectively, compared with 44-fold for the empty vector). The K89A and dsRBD¹⁰⁰ mutants completely lost VSR activity (47-fold and 43-fold silencing, respectively), suggesting that suppression of siRNA-induced RNAi requires the dsRNA-binding activity of 340R as well as its 73-aa C-terminal domain.

340R binds long dsRNA and siRNA duplexes

To directly analyze dsRNA binding by 340R, we performed electrophoretic mobility shift assays (EMSAs) using different dsRNA substrates. Full-length WT 340R and the VSR-defective mutants K89A and dsRBD¹⁰⁰ were fused to maltose-binding protein (MBP) and affinity-purified from *E. coli*. We first tested whether these recombinant proteins can bind radioactively-labeled, 126-bp long dsRNA. As positive control, we included recombinant MBP-DCV 1A. As expected, no shift in mobility of long dsRNA on native polyacrylamide gels was observed with increasing concentrations of MBP (Figure 3A, compare lanes 2-4 with lane 1). By contrast, addition of DCV 1A resulted in protein-dsRNA complex formation (Figure 3A, lane 5), which is in line with previous observations (11,27). Similarly, WT 340R bound dsRNA in a dose-dependent manner (Figure 3A, lanes 6-10). Interestingly, the K89A mutant could still bind long dsRNA, although 8-fold higher protein concentrations were required for a complete dsRNA shift (Figure 3A, lanes 11-15). Indeed, WT 340R had a ~12-fold higher affinity for long dsRNA than the K89A mutant (dissociation constants of 138.8 ± 34.0 nM and 1626 ± 412.2 nM, respectively, Figure 3B). No dsRNA-binding activity was detected for dsRBD¹⁰⁰, even when a 25-fold higher protein concentration was tested (Figure 3A, lanes 16-18). These results are in line with the results from the RNAi reporter assay, in which we observed slight VSR activity for the K89A mutant and a lack of VSR activity for dsRBD¹⁰⁰ (Figure 2D).

We next used EMSAs to analyze whether 340R has binding affinity for siRNA duplexes. Synthetic 21-nt siRNA duplexes that contain 2-nt 3' overhangs shifted after incubation with increasing amounts of WT 340R (Figure 3C, lanes 3-8) and the K89A mutant (Figure 3C, lanes 9-13), indicating that these proteins are able to bind siRNAs. No protein-siRNA complexes were formed with either MBP (Figure 3C, lane 2) or dsRBD¹⁰⁰ (Figure 3C, lanes 14-18). Similar to the long dsRNA binding assay, higher concentrations of the K89A mutant were required to observe an siRNA shift. Accordingly, WT 340R had higher affinity for siRNA duplexes than the K89A mutant (dissociation constants of 717.7 ± 97.8 nM and 6353 ± 699.5 nM, respectively, Figure 3D).

To analyze whether the 3' overhangs are required for efficient siRNA binding, we used a 19-nt blunt dsRNA probe in EMSAs (Figure 3E). These experiments revealed that both WT and K89A mutant 340R bind 19-nt blunt dsRNA in a dose-dependent

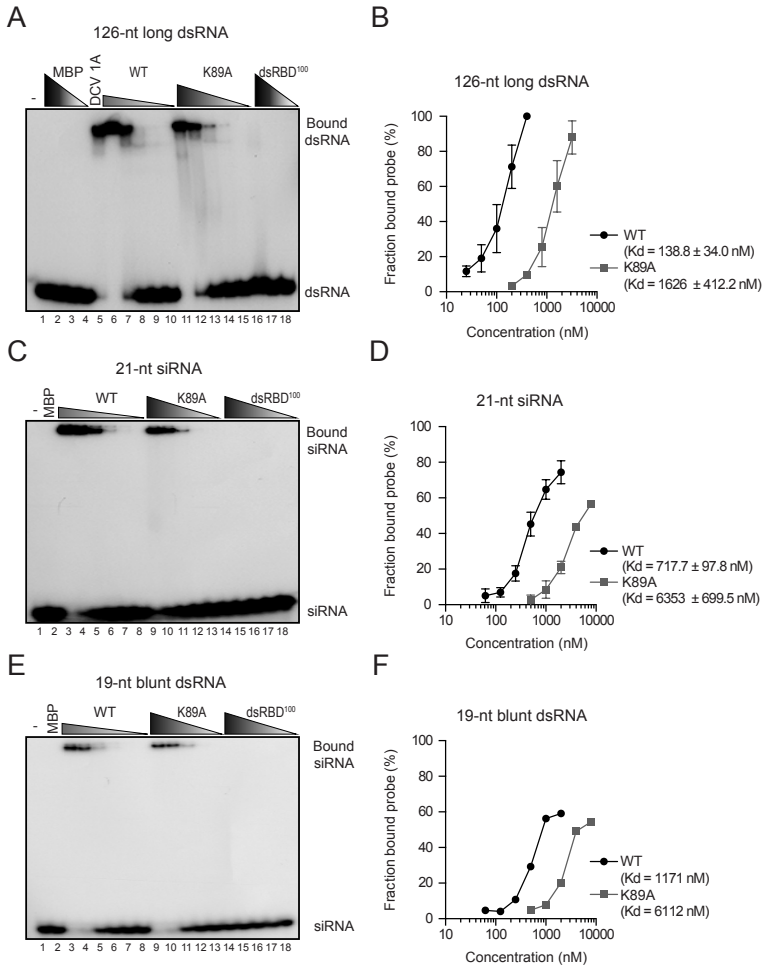


Figure 3. 340R binds long dsRNA and duplex siRNAs. (A) EMSA of 126-nt blunt dsRNA with WT 340R and the K89A and dsRBD¹⁰⁰ mutants. Buffer only (-, lane 1) and decreasing concentrations of MBP were included as negative controls (lanes 2-4; 10 μM, 3.2 μM and 0.4 μM). An MBP-DCV 1A fusion protein was included as positive control (lane 5; 0.1 μM). WT and K89A 340R were tested in 2-fold serial dilutions starting at 0.4 μM (WT, lanes 6-10) and 3.2 μM (K89A, lanes 11-15). dsRBD¹⁰⁰ 340R protein was tested in 10-fold dilutions starting at 10 μM (lanes 16-18). (B) Quantification of the fraction bound probe at different protein concentrations for WT 340R (black line) and the K89A mutant (gray line). Data represent means and standard deviations of three independent experiments. (C) EMSA of 21-nt siRNAs containing 2-nt 3' overhangs with MBP (lane 2; 8 μM) and 2-fold serial dilutions of WT 340R (lanes 3-8; starting at 2 μM), and the K89A and dsRBD¹⁰⁰ mutants (lanes 9-13 and 14-18, respectively; starting at 8 μM). A representative experiment of three independent experiments is shown in panels A and C. (D) Quantification of the fraction bound siRNA at different protein concentrations for WT 340R (black line) and the K89A mutant (gray line). Data represent means and standard deviations of three independent experiments. (E) EMSA of 19-nt blunt dsRNA with decreasing amounts of recombinant proteins. Protein concentrations are as described in panel (C). (F) Quantification of the fraction bound 19-nt blunt dsRNA probe at different protein concentrations for WT 340R (black line) and the K89A mutant (gray line).

manner (Figure 3E, lanes 3-8 and 9-13, respectively), with dissociation constants of 1171 and 6112 nM, respectively (Figure 3F). The observation that both WT and K89A mutant 340R had similar binding affinities for siRNAs and 19-nt blunt dsRNA (Figure S3), indicate that the 2-nt 3'overhangs of siRNAs are not essential for efficient siRNA binding. Taken together, these results show that WT 340R efficiently binds both long and short dsRNA, as well as siRNA duplexes.

340R inhibits Dcr-2-dependent dsRNA processing

Our data show that 340R interacts with dsRNA and that the dsRBD and C-terminus are required for its VSR activity. The dsRNA-binding activity of 340R may inhibit RNAi at two stages. First, by binding to dsRNA, it may shield long dsRNA from processing by Dcr-2. Second, by sequestering siRNAs, it may prevent incorporation of small RNAs into RISC. We performed *in vitro* Dicer assays to test whether dsRNA processing is inhibited in lysates of IIV-6-infected cells. In these assays, we analyzed cleavage of a radiolabeled 126-nt dsRNA substrate into 21-nt siRNAs on denaturing polyacrylamide gels. In mock-infected cell lysates, dsRNA was efficiently processed into siRNAs (Figure 4A, lane 3), whereas siRNA production was completely blocked in lysates from IIV-6-infected cells (MOI of 1.0) (Figure 4A, lane 7). Using a mixture of IIV-6 and mock-infected cell lysates at different ratios, dsRNA processing was inhibited in a dose-dependent manner (Figure 4A, lanes 4-6). Similar results were observed in lysates from cells that were infected with IIV-6 at an MOI of 0.1 (Figure 4A, lanes 9-13), albeit that Dicer activity was not completely blocked at this lower MOI (Figure 4A, compare lane 13 with lane 7). Together, these results indicate that IIV-6 encodes an inhibitor of dsRNA processing.

We next tested our hypothesis that the 340R protein interferes with Dcr-2-mediated dsRNA processing. Long dsRNA was efficiently processed into siRNAs in non-supplemented S2 cell extracts and in extracts supplemented with recombinant MBP (Figure 4B, lanes 3 and 4). WT 340R inhibited processing of long dsRNA in a dose-dependent manner (Figure 4B, lanes 6-8). Likewise, the addition of recombinant DCV 1A, a VSR that is known to bind long dsRNA (11), completely blocked dsRNA cleavage (Figure 4B, lane 5). In contrast, the K89A or dsRBD¹⁰⁰ mutants could not prevent the production of siRNAs, even at the highest concentration tested (Figure 4B, lanes 9-11 and 12-14, respectively). It is worthwhile noting that the K89A mutant does show dsRNA-binding activity in EMSAs (Figure 3A, lanes 11-14), but that it does not protect dsRNA from Dicer-mediated processing (Figure 4B, lanes 9-11). Altogether, these data indicate that WT 340R interferes with Dcr-2-dependent siRNA biogenesis and that efficient dsRNA binding is required to prevent Dcr-2 processing activity.

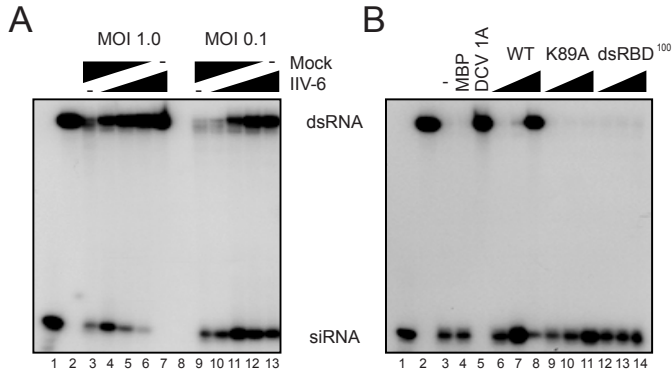


Figure 4. 340R inhibits Dicer-dependent production of siRNAs. (A) Processing of radiolabeled long dsRNA into siRNAs in cytoplasmic extracts of S2 cells that were mock-infected or infected with IIV-6 at the indicated MOI. siRNA production was analyzed in lysates of mock-infected cells (lanes 3 and 9), IIV-6-infected cells (lanes 7 and 13), and in mixtures of infected and non-infected lysates at different ratios (1:3; 1:1; 3:1; lanes 4-6 and 10-12). Synthetic siRNA and unprocessed dsRNA were loaded on gel as size markers (lanes 1 and 2, respectively). (B) Processing of dsRNA into siRNAs was analyzed in non-supplemented S2 cell extract (lane 3), and in cell extracts supplemented with recombinant MBP (lane 4; 1 μ M), DCV 1A (lane 5; 1 μ M), and increasing concentrations of WT 340R (lanes 6-8), and the K89A (lanes 9-11) and dsRBD¹⁰⁰ (lanes 12-14) mutants (0.01 μ M, 0.1 μ M and 1 μ M). Size markers for siRNA and dsRNA were loaded in lanes 1 and 2, respectively.

340R does not inhibit AGO2 slicing activity

Having shown that 340R interferes with the initiation steps of the RNAi pathway, we wondered whether 340R also inhibits the effector phase of the RNAi response. We thus monitored slicing of a radioactively 5' cap-labeled target RNA (44) in the presence or absence of 340R. *Drosophila* embryo lysates were incubated with a 492-nt Fluc target RNA sequence and a Fluc-specific siRNA that triggers target RNA cleavage into a 164-nt 5' cleavage product (Figure 5A, lane 2). This specific cleavage product was not detected after incubation with a non-specific control siRNA (Figure 5A, lane 1). In a first approach, we analyzed whether 340R interferes with RISC assembly and subsequent target RNA cleavage. To this end, we incubated recombinant proteins with embryo lysate before the addition of siRNAs (27). Using this approach, we observed that WT 340R efficiently inhibited target RNA cleavage (Figure 5A, lane 4). In contrast, the K89A and dsRBD¹⁰⁰ mutants did not suppress slicing (Figure 5A, lanes 5 and 6), similar to MBP alone (lane 3). To differentiate between the effect of 340R on RISC assembly and target slicing, we next tested whether WT 340R affects slicing by interfering with a pre-assembled RISC. To allow mature RISC formation, we pre-incubated embryo extracts with siRNAs before the addition of 340R. Neither MBP alone (Figure 5B, lane 3) nor WT or mutant 340R (lanes 4-6) inhibited target RNA cleavage under these conditions. In contrast, the positive control Nora virus VP1 efficiently inhibited

AGO2-mediated target cleavage in both experimental approaches (Figure 5A and 5B, lane 7) (27). These results demonstrate that 340R does not inhibit the activity of a pre-assembled mature RISC. Because 340R binds siRNAs (Figure 3C and 3D), we propose that 340R interferes with the RISC assembly process by preventing siRNA loading into AGO2.

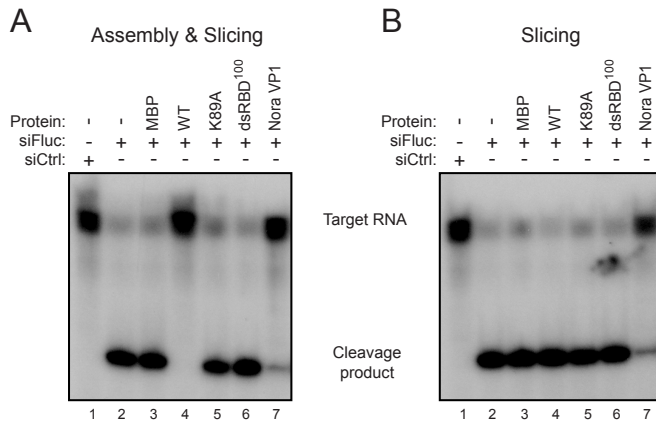


Figure 5. 340R does not inhibit Slicer activity of pre-assembled RISC. (A) *In vitro* RNA cleavage (Slicer) assay in *Drosophila* embryo lysates to analyze the effect of 340R on RISC assembly and subsequent AGO2 catalytic activity. Embryo lysates were pre-incubated for 30 min with recombinant proteins (lanes 3-8) or protein storage buffer (lanes 1 and 2), followed by the addition of Fluc-specific siRNAs (siFluc, lanes 2-8) or non-specific control siRNAs (siCtrl, lane 1). After another 30-min incubation, a radioactive cap-labeled Fluc target RNA was added to the reaction mixture. Target cleavage was analyzed on a denaturing gel after a further 2-h incubation. (B) Slicer assay to monitor the effect of WT 340R on Slicer activity of a pre-assembled RISC. Recombinant proteins (lanes 3-8) were added after RISC assembly for 30 min with siFluc (lanes 2-4) or siCtrl (lane 1). After a further 30-min incubation, target RNA was added and the reaction was allowed to proceed for 2 h before analysis. Nora virus VP1 was analyzed at a concentration of 0.3 μ M, all other proteins at 1.5 μ M.

IIV-6 340R rescues replication of a VSR-defective FHV replicon

To analyze whether the 340R-mediated VSR activity is sufficient to suppress an antiviral RNAi response, we investigated whether 340R can rescue replication of a VSR-defective FHV replicon (12,34). The WT replicon consists of RNA1 of FHV, which encodes the viral RNA-dependent RNA polymerase (RdRP) and expresses the B2 suppressor protein that antagonizes RNAi by binding dsRNA and siRNA duplexes (Figure 6A) (12,14,15). In the VSR-defective FHV replicon (FHV Δ B2), two point mutations were introduced that abolish B2 expression, resulting in an RNAi-dependent replication defect (Figure 6A) (12,43,49).

We first analyzed whether CrPV 1A can rescue the replication defect of the FHV Δ B2 replicon. We performed RT-qPCR analysis to determine FHV RNA levels and observed

that the FHV Δ B2 replicon replicates efficiently when CrPV 1A is expressed (\sim 170-fold increase over the empty vector control, Figure 6B), confirming that the FHV Δ B2 replicon is restricted by an AGO2-dependent antiviral RNAi response. Next, we tested whether WT 340R and the K89A mutant can rescue FHV Δ B2 replication. Upon expression of WT 340R, FHV RNA levels were 20-fold higher than in cells transfected with the empty vector control (Figure 6B, $P = 0.018$), whereas the K89A mutant was unable to rescue FHV Δ B2 replication (\sim 2-fold increase). In line with the results of the RNAi reporter assays (Figure 1), the putative RNase III 142R did not rescue FHV Δ B2 replication. Together, our results show that 340R suppresses the antiviral RNAi pathway.

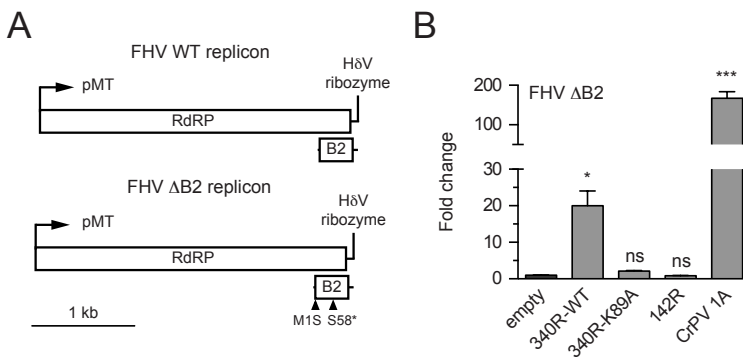


Figure 6. 340R rescues VSR-deficient FHV replication. (A) Schematic representation of the WT and Δ B2 FHV replicons. FHV RNA1 is self-replicating and encodes the RNA-dependent RNA polymerase (RdRP). B2, the viral suppressor of RNAi, is expressed from a subgenomic RNA (upper panel). The FHV Δ B2 replicon lacks B2 expression due to point mutations (triangles) that disrupt the start codon (M1S) and introduce a premature stop codon (S58*) (bottom panel) (49). pMT, metallothionein promoter; HdV, Hepatitis delta virus. (B) FHV RNA levels in S2 cells co-transfected with the FHV Δ B2 replicon and expression plasmids encoding the indicated viral proteins. FHV RNA levels were analyzed by qRT-PCR, normalized to Rp49 and presented as fold change relative to the empty vector control. Bars represent the means and standard deviations of three independent samples. Viral RNA levels were compared to the control (empty plasmid) with one-way ANOVA followed by a *post-hoc* Dunnett's test. * $P \leq 0.05$; ** $P \leq 0.01$; *** $P \leq 0.001$; ns, not significant.

Discussion

In recent years, it has become clear that different classes of RNA viruses are targets of the RNAi pathway in *Drosophila*. The antiviral activity of the RNAi machinery is mediated by Dcr-2-dependent cleavage of viral dsRNA into vsiRNAs that guide AGO2-dependent slicing of viral single-stranded RNA (9,11,13,26,33,34,50). During the ongoing arms race between viruses and their hosts, viruses have evolved sophisticated mechanisms

to suppress or evade host-based immune responses. The best-studied examples of viral antagonism of RNAi in *Drosophila* come from studies on RNA viruses, which encode VSRs that interfere with the initiation and effector phases of the RNAi pathway (9). DNA viruses also induce an RNAi response in *Drosophila*, which is initiated by processing of viral dsRNA substrates derived from overlapping convergent transcripts (35,36) or from structured regions within viral transcripts (51,52). However, it remained unclear whether DNA viruses inhibit this small RNA-based immune response in *Drosophila*. In this study, we show that the dsRBD-containing protein 340R from the DNA virus IIV-6 suppresses RNAi.

IIV-6 is a nucleocytoplasmic virus that can infect *Drosophila*-derived cells as well as adult flies (35,36,53,54). This linear dsDNA virus contains 211 putative ORFs, which are transcribed from either strand of the viral genome (45,46). We show that RNAi is inhibited in IIV-6-infected cells and demonstrate that the IIV-6-encoded 340R protein inhibits Dcr-2 processing and RISC loading through duplex RNA binding. However, we cannot exclude the possibility that IIV-6 produces additional VSRs that contribute to RNAi antagonism. The plant RNA virus Citrus tristeza virus, for example, encodes three distinct VSRs to inhibit the antiviral RNAi response at different levels (55). Studies on *Xenopus laevis* RNA-binding protein (Xlrpb) and *Drosophila* Staufen revealed that their dsRBDs alone are sufficient to bind dsRNA (56-58). Surprisingly however, the C-terminal deletion mutant dsRBD¹⁰⁰, which contains the entire dsRBD, was unable to bind RNA duplexes and did not exert VSR activity. How the C-terminal region of 340R contributes to VSR activity remains an open question for further studies.

Viral RNase III proteins are conserved amongst all genera within the *Iridoviridae* family, suggesting that this protein has important functions within the viral life cycle (46). However, under our experimental conditions, the putative RNase III 142R did not show VSR activity in reporter assays and was not able to rescue FHV Δ B2 replication. These observations suggest that the IIV-6-encoded RNase III is not involved in suppression of the RNAi response. This is in contrast to the proposed VSR activity of the RNase III proteins from *Heliothis virescens* ascovirus-3e, a DNA virus that infects moths, and from the plant RNA virus Sweet potato chlorotic stunt virus (24,25). 142R is structurally similar to bacterial RNase III proteins that are involved in the processing of structured, non-coding RNAs and specific mRNAs (59). Similarly, Iridovirus-encoded RNase III proteins may be involved in the processing of viral or cellular RNAs, rather than suppression of RNAi.

Viral dsRNA triggers a sequence-specific RNAi response in invertebrates, but may additionally induce a sequence-independent antiviral response in marine shrimp (*Litopenaeus vannamei*) and honey bees (*Apis mellifera*) (60,61). Notably, IIV-6 infects a broad range of invertebrate hosts under natural and experimental conditions, including

honey bees and penaeid shrimp (53,62,63). Therefore, it will be interesting to analyze whether 340R (and perhaps 142R) antagonizes putative dsRNA-induced transcriptional responses in invertebrates.

In this study, we used RNAi reporter assays to detect VSR activity for candidate proteins. However, these assays have their limitations, since they may fail to identify *cis*-acting VSRs (64) and host-species specific VSRs (65). Moreover, these assays could identify VSR activity of dsRNA binding proteins that are unlikely to suppress RNAi under natural conditions (66). To analyze whether viral dsRNA-binding proteins function as VSRs *in vivo*, it is important to study replication of VSR-defective virus mutants in an RNAi competent host as well as in an RNAi-deficient host. Since no strategies are yet available to genetically manipulate IIV-6, the role of 340R in infection remains to be established. Nevertheless, we demonstrated that RNAi is suppressed in IIV-6-infected cells and that 340R, like other VSRs, rescues replication of FHV Δ B2 (12,13,34,43,47,67-69), suggesting that 340R is a *bona fide* VSR. We and others previously reported that the DNA virus IIV-6 is restricted by an antiviral RNAi response (35,36). Our finding that IIV-6 340R antagonizes RNAi provides further support for an antiviral RNAi response to DNA virus infection in insects.

Materials and Methods

5

Cells and viruses

Drosophila melanogaster S2 cells were cultured as described previously (27). DCV and IIV-6 were propagated and titered as described previously (11,35).

Plasmids

A proteinase K-treated IIV-6 virus stock was used as a template to amplify the 340R and 142R coding sequences, using primers that contain flanking XbaI restriction sites and introduce a *Drosophila* Kozak sequence (Table S1). PCR products were subsequently cloned into the XbaI site of pAc5-V5-His B (Life Technologies), yielding plasmids that encode C-terminal V5 epitope-tagged proteins. ORF 340R mutant plasmids were generated by site-directed mutagenesis using the primers from Table S1. The orientation and sequence of the selected clones was confirmed by DNA sequencing. Plasmids pAWH CrPV-1A, pMT-Luc and pMT-Ren were described previously (11,26). The pMT *Renilla* hairpin plasmid was kindly provided by R. Zhou (37). Plasmids encoding FHV replicons were described previously (16).

Plasmids encoding maltose-binding protein (MBP) fusion proteins were generated for the production of recombinant protein in *E. coli*. The sequences coding for DCV 1A,

WT 340R and the 340R mutants K89A and dsRBD¹⁰⁰ were PCR amplified and cloned as EcoRI-SalI fragments into pMAL-C2X (New England Biolabs) (see Table S1 for primer sequences).

RNAi reporter assays in S2 cells

The ability of IIV-6 to suppress RNAi-mediated silencing of firefly luciferase (Fluc) expression was analyzed as previously described for DCV (11). Briefly, 2.5×10^4 S2 cells were seeded in a 96-well plate and mock-infected or infected with IIV-6 or DCV at a multiplicity of infection (MOI) of 0.1 or 0.01. Twenty-four hours after infection, cells were co-transfected with 12.5 ng pMT-Luc, 3 ng pMT-Ren, 50 ng empty pAc5-V5-His B plasmid and 10 ng dsRNA targeting either Fluc (dsFluc) or green fluorescent protein (GFP) (non-specific control, dsCtrl), using Effectene Transfection Reagent (Qiagen). Twenty-four hours after transfection, expression of the Fluc and *Renilla* luciferase (Rluc) reporters was induced by addition of 0.5 mM CuSO₄ to the culture supernatant. Cell lysates were prepared after an additional 18-h incubation and luciferase activities were measured using the Dual luciferase reporter system (Promega).

Reporter assays in which RNAi was induced by dsRNA feeding were performed in S2R+ cells in a 96-well format. 3.0×10^4 S2R+ cells were seeded and transfected the next day with 12.5 ng pMT-Luc, 3 ng pMT-Ren, and with either 50 ng pAc-VSR to express one of the viral proteins or with the empty pAc vector. Two days after transfection, 400 ng dsRNA was added to the culture medium. Expression of reporter genes was induced at 8 h after dsRNA treatment and luciferase activities were measured the next day (38). RNAi reporter assays in which RNAi was induced by *Renilla* hairpin RNA were performed in S2 cells. 3.0×10^5 S2 cells were seeded in a 24-well plate and transfected the next day with 12 ng pMT-Ren, 50 ng pMT-Luc, 200 ng pAc-VSR plasmid, and either with 75 ng of copper-inducible pMT hairpin-*Renilla* plasmid or, as non-silencing control, empty pMT plasmid. Expression of the *Renilla* hairpin RNA and the luciferase reporters was induced 2 days post-transfection by addition of copper sulfate to the culture supernatant and luciferase activities were measured at 18 h post-induction.

For the sequential co-transfection, 3.0×10^5 S2 cells were seeded in 24-well plates. The next day, S2 cells were transfected with 100 ng pCoBlast (Life Technologies) and 300 ng of pAc-VSR plasmid. Forty-eight hours after transfection, the cells were transferred to 96-well plates in medium containing 25 µg/mL of blasticidin S (Life Technologies) to select for cells that express the viral proteins. The next day, a second transfection was performed with 12.5 ng pMT-Luc, 3 ng pMT-Ren, 50 ng pAc-empty carrier plasmid, and 2 pmol of Fluc-specific siRNA (siFluc) or non-silencing control siRNA (siCtrl). The reporters were induced 24 h post-transfection and luciferase activities were measured the next day. For all reporter assays in which Fluc expression was silenced, Fluc counts were

normalized to Rluc counts and expressed as fold silencing relative to control (empty vector) treatment, and vice versa when Rluc expression was silenced (38).

Western blot analysis

To analyze protein expression from VSR expression plasmids, 3.0×10^5 S2 cells were seeded in a 24-well plate. Twenty-four hours after seeding, cells were transfected with 500 ng of a VSR expression plasmid or an empty control plasmid using Effectene Transfection Reagent (Qiagen) and harvested at 3 days post-transfection. To analyze protein expression from VSR expression plasmids in our RNAi reporter assays, we pooled the cell lysates of 10 individual wells of a 96-well plate. Proteins were separated on a 12.5% denaturing polyacrylamide gel and transferred to an 0.2- μ m nitrocellulose membrane (Bio-Rad). The membrane was stained by subsequent incubations in anti-V5 mouse monoclonal antibodies (Life Technologies) and Alexa Fluor 680-conjugated goat anti-mouse antibodies (LI-COR Biosciences). As a loading control, the same membrane was probed with anti- α -tubulin antibodies (AbD Serotec) and Alexa Fluor 800-conjugated goat anti-rat antibodies (LI-COR Biosciences). Bound antibodies were visualized on an Odyssey infrared imager (LI-COR Biosciences).

Homology modeling

To predict the protein structure of 340R, we generated a homology model using the YASARA & WHAT IF Twinset under default settings (39,40). The experimentally solved protein structure of TRBP2 (Protein database accession 3ADL) and *Aquifex aeolicus* RNase III (PDB 2NUG) were used as a template (41,42). The model contained residues 1-112 of 340R (out of a total length of 173 aa), of which residues 1-37 were modeled after Aa-RNase III and residues 20-112 after TRBP2.

Production and purification of recombinant proteins

Plasmids encoding MBP fusion proteins were transformed into the *E. coli* BL21 (DE3) strain and expression of recombinant proteins was induced with 1 mM IPTG at an OD₆₀₀ of 1.2. The cultures were incubated for 3 h at 37 °C for pMAL-empty and pMAL-DCV 1A and for 4.5 h at 25 °C for pMAL-340R. Fusion proteins were affinity-purified using amylose resin according to the manufacturer's protocol (New England Biolabs). Recombinant proteins were transferred to a dialysis membrane (molecular weight cut-off 12-14 kDa) and dialyzed to buffer (20 mM Tris-HCl, 0.5 mM EDTA, 5 mM MgCl₂, 1 mM DTT, 140 mM NaCl, 2.7 mM KCl). Recombinant proteins were stored as aliquots at -80 °C in dialysis buffer containing 30% glycerol. Protein concentrations were determined by a Bradford assay (Bio-Rad).

Electrophoretic mobility shift assays

Radiolabeled probes for EMSAs were generated as described before (43). Uniformly-labeled 126-nt blunt dsRNA was generated by *in vitro* transcription of T7 promoter-flanked PCR fragments using T7 RNA polymerase in the presence of α -³²P-[UTP]. After annealing of the two radiolabeled RNA strands, unincorporated nucleotides were removed using a G-25 Sephadex column (Roche) and dsRNA was purified from an 8% native polyacrylamide gel. Synthetic 21-nt siRNAs containing 2-nt 3' overhangs and 19-nt blunt dsRNAs (43) were end-labeled with α -³²P-[ATP] using T4 polynucleotide kinase (Roche) and purified on a G-25 Sephadex column.

EMSAs were performed as described previously (11). Briefly, radiolabeled 126-nt long dsRNA (5 ng), 19-nt dsRNA or siRNA duplexes (1 nM) were incubated with different concentrations of recombinant proteins for 1 h at room temperature. Long dsRNA and siRNA EMSAs were analyzed on 6% and 12% native polyacrylamide gels, respectively. Gels were exposed to a Kodak Biomax XAR film and radioactive signals were quantified with ImageJ software.

Dicer and Slicer assays

To analyze processing of long dsRNA into siRNA, we performed *in vitro* Dicer assays in *Drosophila* S2 cell lysate as described before (27,44). 11×10^6 S2 cells were seeded in T75 flasks and one day after seeding, cells were either mock-infected or infected with IIV-6 at an MOI of 1.0 or 0.1. Two days post-infection, cells were harvested and homogenized in lysis buffer [30 mM HEPES-KOH, 100 mM KOAc, 2 mM Mg(OAc)₂, 5 mM DTT and complete protease inhibitor mixture (Roche)] for 1 h on ice. Protein concentrations of S2 cell extracts were analyzed by a Bradford assay (Bio-Rad) and lysates were frozen at -80 °C. Before analyzing Dicer activity, cell extracts were thawed on ice and centrifuged for 30 min at $16,000 \times g$ at 4 °C to remove cell debris.

To analyze AGO2 target RNA cleavage, we performed *in vitro* Slicer assays in *Drosophila* embryo lysates as described previously (27,44).

FHV replicon assay

S2 cells were seeded in a 24-well plate at a density of 3.0×10^5 cells per well. The next day, cells were transfected with 100 ng of plasmid encoding either the WT FHV replicon or the B2-deficient replicon (FHV Δ B2) along with either 300 ng of pAc-VSR plasmid or empty control plasmid. Two days after transfection, 0.5 mM CuSO₄ was added to the culture medium to induce transcription of the FHV replicon. The following day, cells were harvested and total RNA was isolated using Isol-RNA Lysis reagent. RNA was treated with DNase-I (Life Technologies) and cDNA synthesis was performed using TaqMan Reverse Transcription Reagents (Life Technologies) and a strand-specific FHV

primer tagged with a 5' T7 promoter sequence (43). Following cDNA synthesis, qPCR analysis was performed using a combination of a T7 promoter primer and an FHV-specific forward primer. Data were normalized to Rp49 (RpL32), for which strand-specific qRT-PCR assays were run in parallel (43), and presented as fold change relative to empty vector control.

Acknowledgements

We thank members of the Van Rij laboratory for discussions and Agah Ince for providing IIV-6.

References

1. Tian, B., Bevilacqua, P.C., Diegelman-Parente, A. and Mathews, M.B. (2004) The double-stranded-RNA-binding motif: interference and much more. *Nat Rev Mol Cell Biol*, **5**, 1013-1023.
2. Chang, K.Y. and Ramos, A. (2005) The double-stranded RNA-binding motif, a versatile macromolecular docking platform. *Febs J*, **272**, 2109-2117.
3. Meister, G. and Tuschl, T. (2004) Mechanisms of gene silencing by double-stranded RNA. *Nature*, **431**, 343-349.
4. Van Rij, R.P. and Berezikov, E. (2009) Small RNAs and the control of transposons and viruses in *Drosophila*. *Trends Microbiol*, **17**, 139-178.
5. Ding, S.W. and Voinnet, O. (2007) Antiviral immunity directed by small RNAs. *Cell*, **130**, 413-426.
6. Ding, S.W. (2010) RNA-based antiviral immunity. *Nat Rev Immunol*, **10**, 632-644.
7. Maillard, P.V., Ciaudo, C., Marchais, A., Li, Y., Jay, F., Ding, S.W. and Voinnet, O. (2013) Antiviral RNA interference in mammalian cells. *Science*, **342**, 235-238.
8. Li, Y., Lu, J., Han, Y., Fan, X. and Ding, S.W. (2013) RNA interference functions as an antiviral immunity mechanism in mammals. *Science*, **342**, 231-234.
9. Bronkhorst, A.W. and van Rij, R.P. (2014) The long and short of antiviral defense: small RNA-based immunity in insects. *Current opinion in virology*, **7C**, 19-28.
10. Kawamata, T. and Tomari, Y. (2010) Making RISC. *Trends Biochem.Sci.*, **35**,

- 368-376.
11. Van Rij, R.P., Saleh, M.C., Berry, B., Foo, C., Houk, A., Antoniewski, C. and Andino, R. (2006) The RNA silencing endonuclease Argonaute 2 mediates specific antiviral immunity in *Drosophila melanogaster*. *Genes Dev*, **20**, 2985-2995.
 12. Li, H.W., Li, W.X. and Ding, S.W. (2002) Induction and suppression of RNA silencing by an animal virus. *Science*, **296**, 1319-1321.
 13. Wang, X.H., Aliyari, R., Li, W.X., Li, H.W., Kim, K., Carthew, R., Atkinson, P. and Ding, S.W. (2006) RNA interference directs innate immunity against viruses in adult *Drosophila*. *Science*, **312**, 452-454.
 14. Lu, R., Maduro, M., Li, F., Li, H.W., Broitman-Maduro, G., Li, W.X. and Ding, S.W. (2005) Animal virus replication and RNAi-mediated antiviral silencing in *Caenorhabditis elegans*. *Nature*, **436**, 1040-1043.
 15. Chao, J.A., Lee, J.H., Chapados, B.R., Debler, E.W., Schneemann, A. and Williamson, J.R. (2005) Dual modes of RNA-silencing suppression by Flock House virus protein B2. *Nat Struct Mol Biol*, **12**, 952-957.
 16. van Cleef, K.W., van Mierlo, J.T., Miesen, P., Overheul, G.J., Fros, J.J., Schuster, S., Marklewitz, M., Pijlman, G.P., Junglen, S. and van Rij, R.P. (2014) Mosquito and *Drosophila* entomobirnaviruses suppress dsRNA- and siRNA-induced RNAi. *Nucleic Acids Res*, **42**, 8732-8744.
 17. Silhavy, D., Molnar, A., Lucioli, A., Szittyá, G., Hornyik, C., Tavazza, M. and Burgyan, J. (2002) A viral protein suppresses RNA silencing and binds silencing-generated, 21- to 25-nucleotide double-stranded RNAs. *EMBO J*, **21**, 3070-3080.
 18. Lakatos, L., Szittyá, G., Silhavy, D. and Burgyan, J. (2004) Molecular mechanism of RNA silencing suppression mediated by p19 protein of tombusviruses. *EMBO J*, **23**, 876-884.
 19. Vargason, J.M., Szittyá, G., Burgyan, J. and Tanaka Hall, T.M. (2003) Size selective recognition of siRNA by an RNA silencing suppressor. *Cell*, **115**, 799-811.
 20. Ye, K., Malinina, L. and Patel, D.J. (2003) Recognition of small interfering RNA by a viral suppressor of RNA silencing. *Nature*, **426**, 874-878.
 21. Lakatos, L., Csorba, T., Pantaleo, V., Chapman, E.J., Carrington, J.C., Liu, Y.P., Dolja, V.V., Calvino, L.F., Lopez-Moya, J.J. and Burgyan, J. (2006) Small RNA binding is a common strategy to suppress RNA silencing by several viral suppressors. *Embo J*, **25**, 2768-2780.
 22. Li, F. and Ding, S.W. (2006) Virus counterdefense: diverse strategies for evading the RNA-silencing immunity. *Annu Rev Microbiol*, **60**, 503-531.

23. Burgyan, J. and Havelda, Z. (2011) Viral suppressors of RNA silencing. *Trends in plant science*, **16**, 265-272.
24. Cuellar, W.J., Kreuze, J.F., Rajamaki, M.L., Cruzado, K.R., Untiveros, M. and Valkonen, J.P. (2009) Elimination of antiviral defense by viral RNase III. *Proc Natl Acad Sci U S A*, **106**, 10354-10358.
25. Hussain, M., Abraham, A.M. and Asgari, S. (2010) An Ascovirus-encoded RNase III autoregulates its expression and suppresses RNA interference-mediated gene silencing. *J Virol*, **84**, 3624-3630.
26. Nayak, A., Berry, B., Tassetto, M., Kunitomi, M., Acevedo, A., Deng, C., Krutchinsky, A., Gross, J., Antoniewski, C. and Andino, R. (2010) Cricket paralysis virus antagonizes Argonaute 2 to modulate antiviral defense in *Drosophila*. *Nat.Struct.Mol.Biol.*, **17**, 547-554.
27. van Mierlo, J.T., Bronkhorst, A.W., Overheul, G.J., Sadanandan, S.A., Ekstrom, J.O., Heestermans, M., Hultmark, D., Antoniewski, C. and van Rij, R.P. (2012) Convergent evolution of argonaute-2 slicer antagonism in two distinct insect RNA viruses. *PLoS Pathog*, **8**, e1002872.
28. Zhang, X., Yuan, Y.R., Pei, Y., Lin, S.S., Tuschl, T., Patel, D.J. and Chua, N.H. (2006) Cucumber mosaic virus-encoded 2b suppressor inhibits Arabidopsis Argonaute1 cleavage activity to counter plant defense. *Genes Dev*, **20**, 3255-3268.
29. Baumberger, N., Tsai, C.H., Lie, M., Havecker, E. and Baulcombe, D.C. (2007) The Pterovirus Silencing Suppressor P0 Targets Argonaute Proteins for Degradation. *Curr Biol*, **17**, 1609-1614.
30. Bortolamiol, D., Pazhouhandeh, M., Marrocco, K., Genschik, P. and Ziegler-Graff, V. (2007) The Pterovirus F box protein P0 targets ARGONAUTE1 to suppress RNA silencing. *Curr.Biol.*, **17**, 1615-1621.
31. Csorba, T., Lozsa, R., Hutvagner, G. and Burgyan, J. (2010) Pterovirus protein P0 prevents the assembly of small RNA-containing RISC complexes and leads to degradation of ARGONAUTE1. *Plant J.*, **62**, 463-472.
32. Azevedo, J., Garcia, D., Pontier, D., Ohnesorge, S., Yu, A., Garcia, S., Braun, L., Bergdoll, M., Hakimi, M.A., Lagrange, T. *et al.* (2010) Argonaute quenching and global changes in Dicer homeostasis caused by a pathogen-encoded GW repeat protein. *Genes Dev.*, **24**, 904-915.
33. Mueller, S., Gausson, V., Vodovar, N., Deddouche, S., Troxler, L., Perot, J., Pfeffer, S., Hoffmann, J.A., Saleh, M.C. and Imler, J.L. (2010) RNAi-mediated immunity provides strong protection against the negative-strand RNA vesicular stomatitis virus in *Drosophila*. *Proc.Natl.Acad.Sci.U.S.A*, **107**, 19390-19395.
34. Galiana-Arnoux, D., Dostert, C., Schneemann, A., Hoffmann, J.A. and Imler,

- J.L. (2006) Essential function in vivo for Dicer-2 in host defense against RNA viruses in drosophila. *Nat Immunol*, **7**, 590-597.
35. Bronkhorst, A.W., van Cleef, K.W., Vodovar, N., Ince, I.A., Blanc, H., Vlak, J.M., Saleh, M.C. and van Rij, R.P. (2012) The DNA virus Invertebrate iridescent virus 6 is a target of the Drosophila RNAi machinery. *Proc Natl Acad Sci U S A*, **109**, E3604-3613.
36. Kemp, C., Mueller, S., Goto, A., Barbier, V., Paro, S., Bonnay, F., Dostert, C., Troxler, L., Hetru, C., Meignin, C. *et al.* (2013) Broad RNA interference-mediated antiviral immunity and virus-specific inducible responses in Drosophila. *J Immunol*, **190**, 650-658.
37. Zhou, R., Hotta, I., Denli, A.M., Hong, P., Perrimon, N. and Hannon, G.J. (2008) Comparative analysis of argonaute-dependent small RNA pathways in Drosophila. *Mol Cell*, **32**, 592-599.
38. van Cleef, K.W., van Mierlo, J.T., van den Beek, M. and Van Rij, R.P. (2011) Identification of viral suppressors of RNAi by a reporter assay in Drosophila S2 cell culture. *Methods Mol. Biol.*, **721**, 201-213.
39. Krieger, E., Koraimann, G. and Vriend, G. (2002) Increasing the precision of comparative models with YASARA NOVA--a self-parameterizing force field. *Proteins*, **47**, 393-402.
40. Vriend, G. (1990) WHAT IF: a molecular modeling and drug design program. *Journal of molecular graphics*, **8**, 52-56, 29.
41. Yang, S.W., Chen, H.Y., Yang, J., Machida, S., Chua, N.H. and Yuan, Y.A. (2010) Structure of Arabidopsis HYPOASTIC LEAVES1 and its molecular implications for miRNA processing. *Structure*, **18**, 594-605.
42. Gan, J., Shaw, G., Tropea, J.E., Waugh, D.S., Court, D.L. and Ji, X. (2008) A stepwise model for double-stranded RNA processing by ribonuclease III. *Molecular microbiology*, **67**, 143-154.
43. van Cleef, K.W., van Mierlo, J.T., Miesen, P., Overheul, G.J., Fros, J.J., Schuster, S., Marklewitz, M., Pijlman, G.P., Junglen, S. and van Rij, R.P. (2014) Mosquito and Drosophila entomobirnaviruses suppress dsRNA- and siRNA-induced RNAi. *Nucleic Acids Res.*, **42**, 8732-8744.
44. Haley, B., Tang, G. and Zamore, P.D. (2003) In vitro analysis of RNA interference in Drosophila melanogaster. *Methods*, **30**, 330-336.
45. Jakob, N.J., Muller, K., Bahr, U. and Darai, G. (2001) Analysis of the first complete DNA sequence of an invertebrate iridovirus: coding strategy of the genome of Chilo iridescent virus. *Virology*, **286**, 182-196.
46. Eaton, H.E., Metcalf, J., Penny, E., Tcherepanov, V., Upton, C. and Brunetti, C.R. (2007) Comparative genomic analysis of the family Iridoviridae: re-

- annotating and defining the core set of iridovirus genes. *Virology*, **4**, 11.
47. Li, W.X., Li, H., Lu, R., Li, F., Dus, M., Atkinson, P., Brydon, E.W., Johnson, K.L., Garcia-Sastre, A., Ball, L.A. *et al.* (2004) Interferon antagonist proteins of influenza and vaccinia viruses are suppressors of RNA silencing. *Proc Natl Acad Sci U S A*, **101**, 1350-1355.
 48. Wong, C.K., Young, V.L., Kleffmann, T. and Ward, V.K. (2011) Genomic and proteomic analysis of invertebrate iridovirus type 9. *J Virol*, **85**, 7900-7911.
 49. Ball, L.A. (1995) Requirements for the self-directed replication of flock house virus RNA 1. *J Virol*, **69**, 720-727.
 50. Marques, J.T., Wang, J.P., Wang, X., de Oliveira, K.P., Gao, C., Aguiar, E.R., Jafari, N. and Carthew, R.W. (2013) Functional specialization of the small interfering RNA pathway in response to virus infection. *PLoS Pathog*, **9**, e1003579.
 51. Sabin, L.R., Zheng, Q., Thekkat, P., Yang, J., Hannon, G.J., Gregory, B.D., Tudor, M. and Cherry, S. (2013) Dicer-2 processes diverse viral RNA species. *PLoS One*, **8**, e55458.
 52. Bronkhorst, A.W., Miesen, P. and van Rij, R.P. (2013) Small RNAs tackle large viruses: RNA interference-based antiviral defense against DNA viruses in insects. *Fly*, **7**, 216-223.
 53. Williams, T., Barbosa-Solomieu, V. and Chinchar, V.G. (2005) A decade of advances in iridovirus research. *Adv Virus Res*, **65**, 173-248.
 54. Teixeira, L., Ferreira, A. and Ashburner, M. (2008) The bacterial symbiont *Wolbachia* induces resistance to RNA viral infections in *Drosophila melanogaster*. *PLoS Biol*, **6**, e2.
 55. Lu, R., Folimonov, A., Shintaku, M., Li, W.X., Falk, B.W., Dawson, W.O. and Ding, S.W. (2004) Three distinct suppressors of RNA silencing encoded by a 20-kb viral RNA genome. *Proc Natl Acad Sci U S A*, **101**, 15742-15747.
 56. Ryter, J.M. and Schultz, S.C. (1998) Molecular basis of double-stranded RNA-protein interactions: structure of a dsRNA-binding domain complexed with dsRNA. *Embo J*, **17**, 7505-7513.
 57. Ramos, A., Grunert, S., Adams, J., Micklem, D.R., Proctor, M.R., Freund, S., Bycroft, M., St Johnston, D. and Varani, G. (2000) RNA recognition by a Staufen double-stranded RNA-binding domain. *EMBO J*, **19**, 997-1009.
 58. St Johnston, D., Brown, N.H., Gall, J.G. and Jantsch, M. (1992) A conserved double-stranded RNA-binding domain. *Proc Natl Acad Sci U S A*, **89**, 10979-10983.
 59. Court, D.L., Gan, J., Liang, Y.H., Shaw, G.X., Tropea, J.E., Costantino, N., Waugh, D.S. and Ji, X. (2013) RNase III: Genetics and function; structure and

- mechanism. *Annu Rev Genet*, **47**, 405-431.
60. Robalino, J., Browdy, C.L., Prior, S., Metz, A., Parnell, P., Gross, P. and Warr, G. (2004) Induction of antiviral immunity by double-stranded RNA in a marine invertebrate. *J Virol*, **78**, 10442-10448.
 61. Flenniken, M.L. and Andino, R. (2013) Non-specific dsRNA-mediated antiviral response in the honey bee. *PLoS One*, **8**, e77263.
 62. Bromenshenk, J.J., Henderson, C.B., Wick, C.H., Stanford, M.F., Zulich, A.W., Jabbour, R.E., Deshpande, S.V., McCubbin, P.E., Seccomb, R.A., Welch, P.M. *et al.* (2010) Iridovirus and microsporidian linked to honey bee colony decline. *PLoS One*, **5**, e13181.
 63. Lightner, D.V. and Redman, R.M. (1993) A Putative Iridovirus from the Penaeid Shrimp *Protrachypene-Precipua* Burkenroad (Crustacea, Decapoda). *J Invertebr Pathol*, **62**, 107-109.
 64. Mari-Ordóñez, A., Marchais, A., Etcheverry, M., Martin, A., Colot, V. and Voinnet, O. (2013) Reconstructing de novo silencing of an active plant retrotransposon. *Nat Genet*, **45**, 1029-1039.
 65. van Mierlo, J.T., Overheul, G.J., Obadia, B., van Cleef, K.W., Webster, C.L., Saleh, M.C., Obbard, D.J. and van Rij, R.P. (2014) Novel Drosophila Viruses Encode Host-Specific Suppressors of RNAi. *PLoS Pathog*, **10**, e1004256.
 66. Lichner, Z., Silhavy, D. and Burgyan, J. (2003) Double-stranded RNA-binding proteins could suppress RNA interference-mediated antiviral defences. *J Gen Virol*, **84**, 975-980.
 67. Han, Y.H., Luo, Y.J., Wu, Q., Jovel, J., Wang, X.H., Aliyari, R., Han, C., Li, W.X. and Ding, S.W. (2011) RNA-based immunity terminates viral infection in adult Drosophila in the absence of viral suppression of RNA interference: characterization of viral small interfering RNA populations in wild-type and mutant flies. *J Virol*, **85**, 13153-13163.
 68. Aliyari, R., Wu, Q., Li, H.W., Wang, X.H., Li, F., Green, L.D., Han, C.S., Li, W.X. and Ding, S.W. (2008) Mechanism of induction and suppression of antiviral immunity directed by virus-derived small RNAs in Drosophila. *Cell Host Microbe*, **4**, 387-397.
 69. Berry, B., Deddouche, S., Kirschner, D., Imler, J.L. and Antoniewski, C. (2009) Viral suppressors of RNA silencing hinder exogenous and endogenous small RNA pathways in Drosophila. *PLoS One*, **4**, e5866.
 70. Krovat, B.C. and Jantsch, M.F. (1996) Comparative mutational analysis of the double-stranded RNA binding domains of *Xenopus laevis* RNA-binding protein A. *J Biol Chem*, **271**, 28112-28119.

Supporting Information

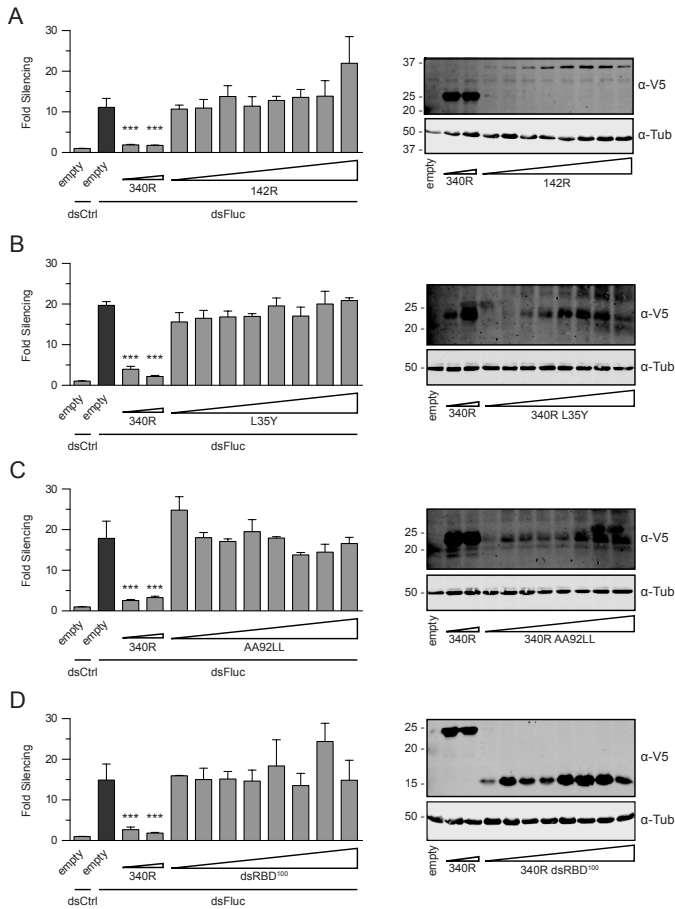


Figure S1. Increasing the expression of 142R, 340R L35Y, 340R AA92LL, and 340R dsRBD¹⁰⁰ does not result in detectable VSR activity. Left panels, RNAi reporter assays in S2R⁺ cells transfected with luciferase reporter plasmids and either a control plasmid (empty) or increasing amounts (50 to 400 ng) of expression plasmids encoding 142R (A), the 340R point mutants L35Y (B) and AA92LL (C), or 340R dsRBD¹⁰⁰ (D). In all panels, WT 340R (25 and 50 ng) was included as a positive control. RNAi was induced by addition of long Fluc dsRNA (dsFluc) to the culture supernatant. Fluc counts were normalized to Rluc counts and expressed as fold silencing relative to control treatment (dsCtrl). Bars in all panels represent the means and standard deviations of three independent samples. Difference in RNAi efficiency compared to controls (dark gray bars) was analyzed by one-way ANOVA followed by a *post-hoc* Dunnett's test. * $P \leq 0.05$; ** $P \leq 0.01$; *** $P \leq 0.001$. Right panels, Western blot analyses of V5 epitope-tagged VSR constructs from cell lysates of the corresponding RNAi reporter assays. Proteins were detected using anti-V5 antibodies (α -V5). A polyclonal anti- α -tubulin (α -Tub) antibody was used as a loading control. Molecular mass (in kDa) is indicated on the left of the image. The predicted molecular weights for 340R WT and the point mutants L35Y and AA92LL are 23 kDa. The predicted molecular weights for 340R dsRBD¹⁰⁰ and 142R are 14.7 kDa and 37 kDa, respectively.

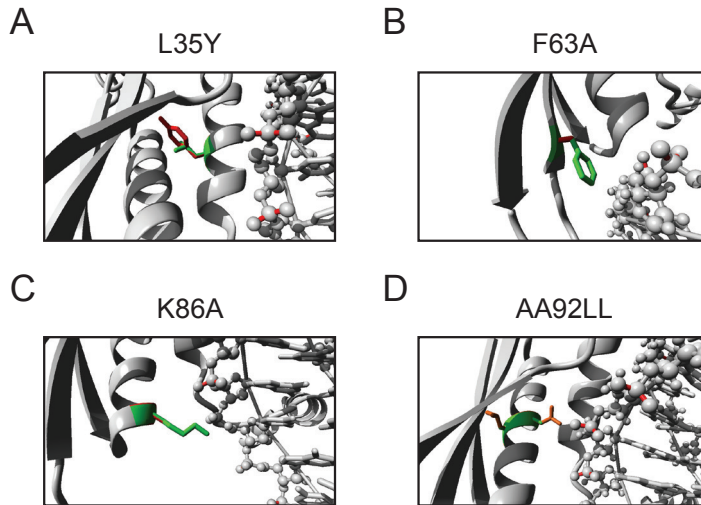


Figure S2. Homology models of WT and mutant 340R in complex with dsRNA. In all panels, the WT residue is shown in green and the mutant residue in red. The RNA is presented in ball-and-stick view with all atoms shown. (A) The conserved residue L35 is located in alpha helix 1 ($\alpha 1$), with its side-chain buried in the core of the protein. Putative RNA interacting residues are located in $\alpha 1$, on the opposite side of L35. The L to Y substitution is likely to disturb the local structure, thereby affecting RNA interactions. (B) The highly conserved residue F63 is surface-exposed, with its side-chain positioned towards the dsRNA, and was proposed to properly position the long flexible dsRNA-interacting Lysine side-chains in Xlrpba (56). Indeed, mutational analysis of Xlrpba F145, which corresponds to F63 in 340R, revealed that this residue is required for efficient RNA binding (70). (C) As for K89 (Figure 2B), the side-chain of residue K86 is positioned towards the phosphate backbone of the RNA. The K86A substitution is likely to abolish the interaction between the positively-charged Lysine and the negatively-charged phosphates. (D) The AA92LL substitutions are located in the core of the protein and are expected to severely disturb the local structure and thereby affect the interaction with dsRNA-binding region 3.

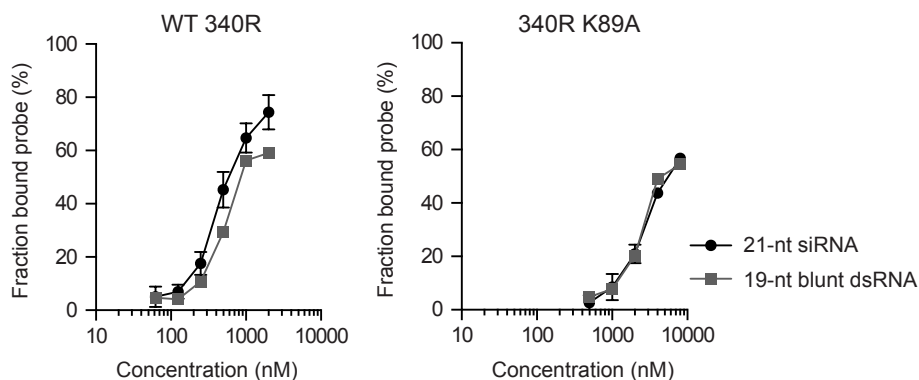


Figure S3. 340R binds 21-nt siRNAs and 19-nt blunt dsRNA with similar affinities. Quantification of the fraction bound 21-nt siRNA (black line) and 19-nt blunt dsRNA (gray line) at different protein concentrations of WT 340R (A) and the K89A mutant (B). Data points for siRNA shifts (black lines) represent means and standard deviations of three independent experiments. Please note that both panels are merged images of Figure 3D and 3E.

Table S1. Primers used for cloning and site-directed mutagenesis

Cloning into pAc5.1-V5-HIS B & site-directed mutagenesis		
Construct	Forward primer (5'-3')	Reverse primer (5'-3')
142R	AGT <u>CTAG</u> AACATGGAAAAACAATATTGAAAATTTTGATC	GGT <u>CTAG</u> ATTACATAAAAGCTTTAAACCTGTCTGG
340R-WT	AGT <u>CTAG</u> AACATGGAAAAACAAAAGATAACGTAACCTC	GGT <u>CTAG</u> ATTAATAATCGTCTATATCAACAGAGTCTC
340R-dsRBD ¹⁰⁰	AGT <u>CTAG</u> AACATGGAAAAACAAAAGATAACGTAACCTC	GGT <u>CTAG</u> ATAATCTTTAATAGTTTTAAATGCTGC
340R-K86A	GGTAGCGGTTTATCCATGGCCGAAGCCAAAAAATGTC	GCATTTTTTTGGCTTCGGCCATGGATAAACCCGTACC
340R-K89A	CATGAAAGAAGCCGCAAAAAATGCAGC	GTCGCATTTTTTGGCGCTTCTTTTCATG
340R-F63A	GATCATTCTCCAACGGCTAATATTGAATGTGC	CGACATCAATATTAGCCGTTGGAGAATGATC
340R-AA92LL	CCATGAAAGAAGCCAAAAAATCTCCTCTTTAAACTAT	ATAGTTTTTAAAGAGGAGATTTTTTTGGCTTCTTTCATGG
340R-L35Y	CAATTGGATTTTACAACGAATTTTGTGTC	GACAAAATTCGTTGTAATAATCCAATTG
Cloning into pMAL-C2X		
Construct	Forward primer (5'-3')	Reverse primer (5'-3')
DCV 1A	AGTGAATTTCATGGAAATCTGATAAAAGTATGGCC	GGTGTCCGACTTAAACGGGTCCAGGGTTAGTCTC
340R-WT	AGTGAATTTCATGGAAAAACAAAAGATAACGTAACCTC	GGTGTCCGACTTAAATATCGTCTATATCAACAGAGTCTC
340R-K89A	AGTGAATTTCATGGAAAAACAAAAGATAACGTAACCTC	GGTGTCCGACTTAAATATCGTCTATATCAACAGAGTCTC
340R-dsRBD ¹⁰⁰	AGTGAATTTCATGGAAAAACAAAAGATAACGTAACCTC	GGTGTCCGACTTATAATCTTTAATAGTTTTAAATGCTGC

Introduced restriction sites of XbaI, EcoRI and SalI are underlined.

Chapter 6

Arbovirus-derived piRNAs exhibit a ping-pong signature in mosquito cells

Nicolas Vodovar, Alfred W. Bronkhorst, Koen W.R. van Cleef, Pascal Miesen, Hervé Blanc, Ronald P. van Rij and Maria-Carla Saleh

PLoS One 2012, 7:e30861

Abstract

The siRNA pathway is an essential antiviral mechanism in insects. Whether other RNA interference pathways are involved in antiviral defense remains unclear. Here, we report in cells derived from the two main vectors for arboviruses, *Aedes albopictus* and *Aedes aegypti*, the production of viral small RNAs that exhibit the hallmarks of ping-pong derived piwi-associated RNAs (piRNAs) after infection with positive or negative sense RNA viruses. Furthermore, these cells produce endogenous piRNAs that mapped to transposable elements. Our results show that these mosquito cells can initiate *de novo* piRNA production and recapitulate the ping-pong-dependent piRNA pathway upon viral infection. The mechanism of viral-piRNA production is discussed.

Introduction

Arboviruses are maintained in a transmission cycle between hematophagous arthropod vectors and vertebrate hosts. Within their arthropod vector, arboviruses encounter several anatomical and immunological barriers that determine the potential of the virus to be transmitted. RNA interference (RNAi) is a major antiviral defense mechanism in insects (1-8). A hallmark of the insect antiviral RNAi response is the activation of the pathway by cleavage of viral double-stranded RNA (dsRNA) into 21 nucleotides (nt) viral small interfering RNAs (vsiRNA) by Dicer-2 (Dcr-2). Once produced, vsiRNAs guide the sequence-specific recognition and cleavage of viral target RNAs by an Argonaute-2 (AGO-2) containing RNA induced silencing complex.

The siRNA and piRNA (piwi-interacting RNA) pathways are both gene regulatory mechanisms guided by small silencing RNAs in association with an Argonaute family member. piRNAs differ from siRNAs in several aspects (9): i) piRNAs are generated in a Dicer-independent manner from single-stranded precursors and display a broader size range of ~25-30 nt; ii) piRNAs associate with the PIWI subclass of the Argonaute family, in flies consisting of piwi, Argonaute-3 (AGO3) and aubergine (aub); iii) PIWI proteins and their associated piRNAs are highly enriched in gonadal tissues, where they protect the germline from activation of transposable elements (TE). Nevertheless, piRNA expression in somatic tissues has recently been reported (10).

Two mechanisms have been proposed for the biogenesis of piRNAs (9). First, a pool of piRNAs is processed from single-stranded RNA precursors transcribed by chromosomal loci that consist of remnants of TEs. This generates primary piRNAs with a 5' uridine bias (U_1) that are usually antisense to TE transcripts. Cleavage of complementary transposon RNA by primary piRNAs initiates the second biogenesis pathway: the ping-pong amplification cycle that involves AGO3 and aub (9). This amplification loop gives rise to the signature of ping-pong-dependent piRNAs: a strong U_1 bias for aub-associated piRNAs and a bias for adenosine at the tenth position (A_{10}) of AGO3-associated piRNAs. PIWI-associated piRNAs have a strong strand bias: AGO3 associates with sense TE piRNAs, whereas piwi and aub associate with antisense TE piRNAs (11, 12).

While the siRNA pathway is well characterized as an antiviral defense mechanism in insects, the involvement of the piRNA pathway has been recently suggested. Indeed, the potential of the primary piRNA pathway to recognize and process viral RNAs was shown in *Drosophila* ovarian somatic sheet cells (OSS cell line) (13) where in addition to the typical Dcr-2-dependent 21-nt siRNAs, a broader peak of ~25 to 30-nt piRNAs with a U_1 bias was observed. These cells are capable of producing primary piRNAs but are incapable of ping-pong amplification, due to the lack of aub and AGO3 expression

(14). The existence of viral piRNAs has also been suggested in mosquito, but only based on the size range of the viral small RNAs population (15-17).

Here, we show for the first time that mosquito cells infected with (+) and (-) RNA arboviruses produce viral small RNAs with the hallmarks of ping-pong amplification. These results show that mosquito tissue culture faithfully recapitulates the piRNA pathway from an exogenous trigger and may combine RNAi pathways to control a viral infection. These observations have important implications for our understanding of insect innate immunity.

Results

Multiple viral small RNAs species in mosquito cells

The C6/36 (18) and U4.4 (19) cell lines were cloned from the same cell population isolated from *Aedes albopictus* larvae (20). C6/36 cells are devoid of Dcr-2 activity (17), but produce virus-derived small RNA that are longer than vsRNAs, which were proposed to be viral-derived piRNAs (vpiRNAs) (15, 17). Nevertheless, the absence of functional Dcr-2 activity in C6/36 (17) may have biased these results. To study whether Dcr-2 competent mosquito cells naturally produce vpiRNAs, we analyzed viral small RNAs following infection of U4.4 cells. In contrast to C6/36 cells, the U4.4 cells exhibit a functional Dcr-2 activity (Figure 1). Synthetic ³²P-labelled dsRNA was effectively processed into 21-nt small RNA in U4.4 cell extracts (Figure 1A), and dsRNA directed against firefly luciferase efficiently silenced plasmid-driven luciferase expression (Figure 1B). Altogether, these data show that U4.4 cells possess a functional siRNA pathway that should be able to produce vsRNAs upon virus infection.

To analyze the impact of Dcr-2 activity on the overall virus-derived small RNA population in *A. albopictus* cells, we infected U4.4 cells with Sindbis virus (SINV), a (+) RNA arbovirus, expressing GFP as a reporter of viral replication. Small RNAs ranging from 19 to 30-nt in length were recovered from infected cells and deep-sequenced. Consistent with the Dcr-2 activity detected, the size distribution of virus-derived small RNAs displayed a sharp peak at 21-nt (Figure 1C) that corresponds to vsRNAs. In addition, a broader Gaussian distribution that peaks at 27-28 nt was observed (Figure 1C), which has previously also been reported in C6/36 cells (15, 17).

Aedes albopictus cells produce vpiRNA through a ping-pong mechanism

We next analyzed the viral small RNA population that peaks at 27-28 nt. Similar to vsRNAs (Figure 2A), these small RNAs are distributed across the viral genome, but with an enrichment at the 5' end of the highly expressed SINV-GFP subgenomic RNA

(Figure 2B). They display a strand bias, with more than 69% of the reads mapping to the sense strand of the viral genome.

OSS cells only produced sense primary vpiRNAs that display a strong U_1 bias. In contrast, 25 to 29-nt viral small RNAs from SINV-GFP-infected U4.4 cells originate from both viral RNA strands and display the following nucleotide bias (Figure 2C): vpiRNAs that mapped on the sense strand exhibit a strong A_{10} bias, while vpiRNAs that mapped on the antisense strand displayed a strong U_1 bias. Furthermore, the 5' ends of complementary vpiRNAs are most frequently separated by 10-nt (Figure 2D), which is characteristic of the ping-pong mechanism for piRNA generation (11). We therefore propose that these viral small RNAs represent ping-pong derived vpiRNAs.

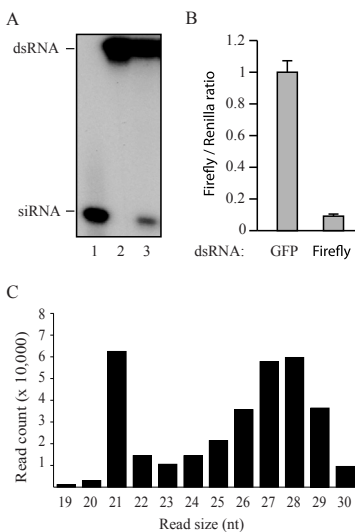


Figure 1. *Aedes albopictus* U4.4 cells are Dcr-2 competent and produce two populations of viral small RNAs. (A) Dicer assay in uninfected U4.4 cells. Lane 3 shows processing of a 113-bp dsRNA substrate into 21-nt siRNAs after incubation in a U4.4 cell extract. Synthetic siRNA (21-nt) and input dsRNA (113-nt) are used as size markers in lanes 1 and 2, respectively. (B) RNAi reporter assay. Co-transfection of firefly luciferase specific dsRNA with reporter plasmids encoding firefly and *Renilla* luciferase into U4.4 cells results in silencing of the firefly luciferase reporter. GFP dsRNA was used as non-specific dsRNA control. *Renilla* luciferase activity was used as internal control to normalize the firefly luciferase activity. Error bars represent the standard deviations of three individual samples. (C) Size distribution of the small RNA reads that match the genome of SINV-GFP with 0 mismatches.

Viral small RNA profiles from SINV-infected C6/36 cells display a similar profile with a size ranging from 19 to 30-nt (15, 17). We therefore infected C6/36 with SINV-GFP and sequenced the viral small RNA population. Similar to the U4.4 cells, SINV-derived small RNAs from infected C6/36 cells exhibited all the hallmarks of ping-pong amplification (data not shown). Furthermore, the 25-29 nt vpiRNA in C6/36 were

Table 1. vpiRNAs are resistant to beta-elimination

	C6/36 + SINV-GFP	C6/36 + SINV-GFP
	No treatment	Beta-elimination
Total number of reads*	916,504	1,028,574
miRNA reads* (22nt)	286,711	146,225
25-29 nt viral reads	23,737	242,762

*Numbers of reads matching the *Drosophila melanogaster* genome available at flybase and miRNA sequences available at mirBase.

resistant to β -elimination, suggesting that they are associated with a PIWI protein and 2'-O-methylated at their 3' terminal nucleotide (Table 1), similar to piRNAs in *Drosophila* and *Bombyx mori* (21, 22). Altogether, these results show that upon virus infection U4.4 and C6/36 cells produce vpiRNA through a ping-pong amplification mechanism. Furthermore, as C6/36 cells are deficient in Dcr-2 activity, these results suggest that the piRNA pathway is not a backup mechanism when the antiviral siRNA pathway is defective.

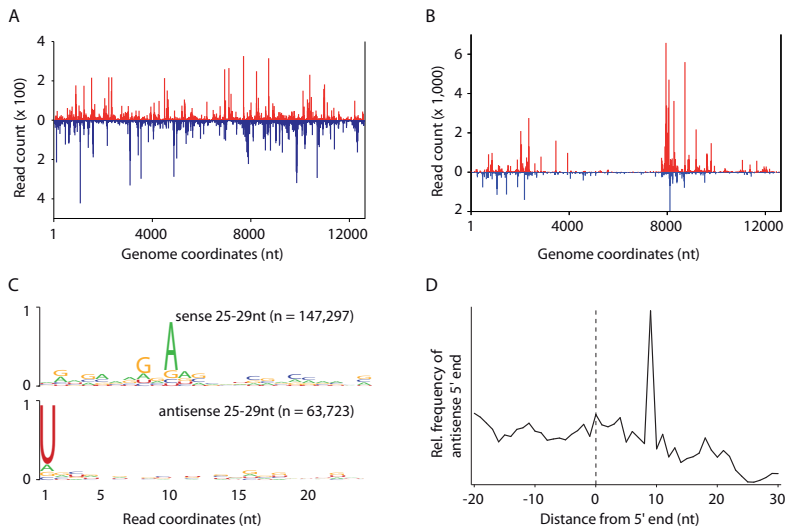


Figure 2. U4.4 cells produce vsRNAs and vpiRNAs through a ping-pong mechanism upon (+) ssRNA arbovirus infection. Profile of 21-nt vsRNAs (A) and 25-29 nt (B) SINV-GFP-derived small RNAs allowing 0 mismatch during alignment. Viral small RNAs that mapped to the sense and antisense strand of the SINV-GFP genome are shown in red and blue, respectively. (C) Conservation and relative nucleotide frequency per position of 25-29 nt SINV-GFP-derived reads that mapped to the sense (top) and the antisense (bottom) strands of the SINV-GFP genome. The overall height of the nucleotide stack indicates the sequence conservation; the height of the nucleotides within each stack represents their relative frequency at that position. n indicates the number of reads used to generate each logo. (D) Frequency map of the distance between 25-29 nt small RNAs that mapped to opposite strands of the SINV-GFP genome. The peak at position 9 on the sequence (the first nucleotide being position 0) indicates the position of maximal probability of finding the 5' end of a complementary small RNA.

Ping-pong derived vpiRNAs in (-) RNA virus infection

Given the fundamental differences in replication strategies of (+) and (-) RNA viruses, we next analyzed a published dataset from C6/36 cells infected with La Crosse virus (LACV) (15), an arbovirus with a tri-segmented single-stranded (-) RNA genome (23). The viral RNA segments serve as templates for transcription of viral mRNAs and for the synthesis of full-length viral complementary RNA. Transcripts from the three segments,

Large (L), Medium (M) and Small (S), accumulate at different levels (S>M>L) (24). The absolute number of 25-29 nt virus-derived small RNAs did not follow the differential accumulation of each transcript; however, the number of reads normalized for the length of the segments did mirror the much greater mRNA levels of the S segment [20] (S segment 257.3 reads/nt >> L segment 37.5 > M segment 19.5). The relative amounts of vpiRNA mapping on each strand of the viral segments differed among the three segments, with ratios of sense over antisense vpiRNAs of 20.3, 4.3, and 0.7 for S, M and L, respectively (Figure 3A-C). This strand bias of vpiRNA followed the previously estimated gradient of mRNA over viral genome ratios from highly (S) to lower (L) expressed transcripts [20].

Analysis of the nucleotide biases indicated that all segments presented a U₁ bias on the genomic (-) strand and an A₁₀ bias for the antigenomic (+) RNA strand (Figure 3A-C). In addition, complementary vpiRNAs are enriched for those in which the 5' ends are separated by exactly 10 nucleotides (Figure 3D-F). Thus similar to the (+) RNA virus SINV, LACV viral RNAs are targets for ping-pong-dependent vpiRNA biogenesis with U₁ vpiRNAs originating from the negative strand, regardless of viral genome polarity and relative abundance of transcript.

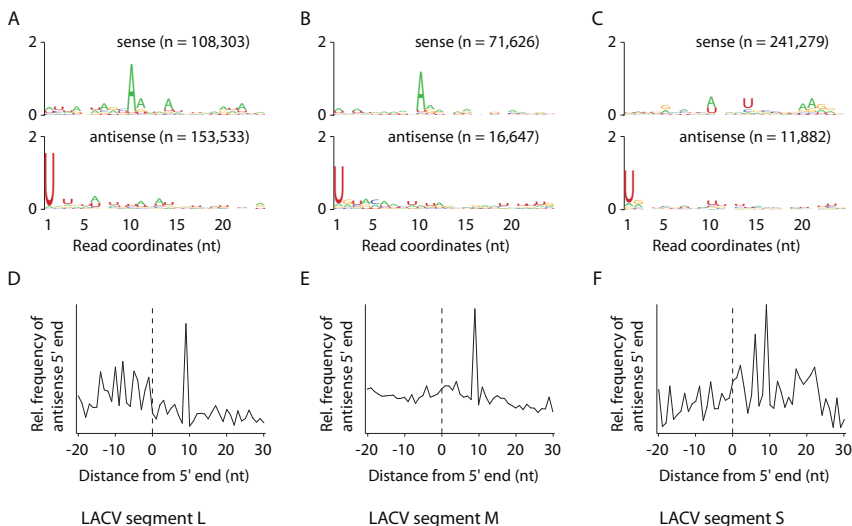


Figure 3. *Aedes albopictus* C6/36 cells produce ping-pong-dependent vpiRNA upon (-) RNA virus infection. (A), (B), and (C) Conservation and relative nucleotide frequency per position of the 25-29 nt LACV-derived reads that mapped to the antigenomic sense (top) and genomic antisense (bottom) strands of the LACV genome segments L, M and S, respectively. n indicates the number of reads used to generate each logo. (D), (E), and (F). Frequency map of the distance between 25-29 nt reads that mapped to opposite strands of the LACV genome segments L, M and S, respectively. The peak at position 9 on the sequence (the first nucleotide being position 0) indicates the position of maximal probability of finding the 5' end of a complementary small RNA.

***Aedes aegypti* Aag2 cells produce vsiRNA and vpiRNA with a ping-pong signature**

A. albopictus and *A. aegypti* are the major vectors for arboviruses within the *Aedes* genus of culicine mosquitoes. To test whether vpiRNA production also occurs in cells from *A. aegypti*, we analyzed small RNAs in the Aag2 cell line (25) after infection with SINV-GFP.

We observed a size distribution of virus-derived small RNAs with a sharp peak at 21-nt and a broader Gaussian distribution that peaks at 28-nt (Figure 4A). Similar to previous observations of Alphavirus-infected Aag2 cells (26), the 21-nt vsiRNAs mapped across the viral genome in similar proportions over viral sense and antisense strands (Figure 4B). The viral small RNAs of 25 to 29-nt are distributed across the viral genome, but enriched at the 5' end of the highly expressed SINV subgenomic RNA (Figure 4C). Furthermore, these small RNAs display the hallmarks of ping-pong-dependent piRNAs (Figure 4D-E) as observed in *A. albopictus* cells. Together, our results show that three different cell lines derived from the two major mosquito vectors for arboviruses have a functional PIWI pathway and produce ping-pong derived piRNAs after infection with Sindbis virus.

The PIWI gene family has greatly expanded in *A. aegypti*. In addition to a single *Ago3* orthologue, the *A. aegypti* genome encodes seven *Piwi/Aub* orthologues (27). Based on their clustering with *Anopheles gambiae Ago4* and *Ago5*, *A. aegypti Piwi1* through *Piwi4* belong to the *Ago4* clade, whereas *Piwi5* to *Piwi7* belong to the *Ago5* clade. Our observation of ping-pong derived vpiRNAs in mosquito cells implies that PIWI proteins from the different clades are expressed in these cells. Indeed, we readily detected in Aag2 cells transcripts from multiple PIWI family members, including *Piwi4*, *Piwi5*, *Piwi6*, and *Ago3* (Figure 4F).

To address a potential germline source of the Aag2 cells, we analyzed the expression of *Nanos* in Aag2 cells, but we were unable to detect any transcripts by RT-PCR (data not shown). While this result does not rule out a germline origin of the cell line, we do note that the identification of piRNAs with a ping-pong signature in somatic tissues in flies implies that a functional PIWI pathway is present in the soma of insects (10).

***Aedes aegypti* Aag2 cells produce transposon-derived piRNAs with a ping-pong signature**

Our results imply that the piRNA pathway targets replicating RNA viruses in mosquito cells. The majority of piRNAs in *Drosophila* and other animals were described to map to transposable elements. As the genome sequence of *A. aegypti* is available (28), we analyzed whether Aag2 cells engage in ping-pong-dependent amplification of TE derived piRNAs. We mapped the non-viral small RNAs to a dataset that contain full-length

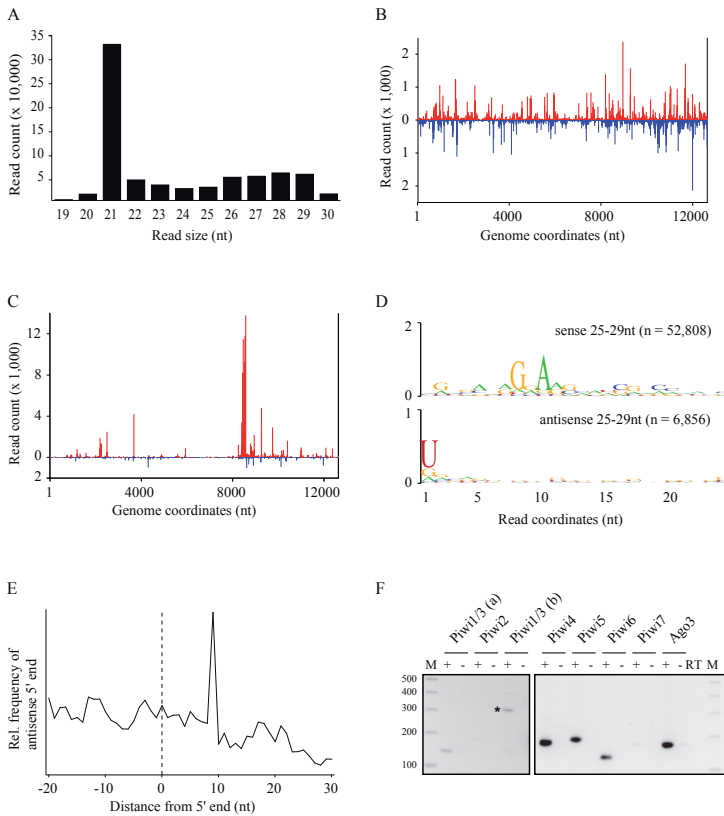


Figure 4. *Aedes aegypti* Aag2 cells produce vsRNA and vpiRNA with a ping-pong signature upon arbovirus infection. (A) Size distribution of the small RNA reads that match the genome of SINV-GFP with 0 mismatches. Profile of 21-nt vsRNAs (B) and 25-29 nt (C) SINV-GFP-derived small RNAs allowing 0 mismatch during alignment. Viral small RNA that mapped to the sense and antisense strand of the SINV-GFP genome are shown in red and blue, respectively. (D) Conservation and relative nucleotide frequency per position of 25-29 nt SINV-GFP-derived reads that mapped to the sense (top) and antisense (bottom) strands of the SINV-GFP genome. n indicates the number of reads used to generate each logo. (E) Frequency map of the distance between 25-29 nt small RNAs that mapped to opposite strands of the SINV-GFP genome. The peak at position 9 on the sequence (the first nucleotide being position 0) indicates the position of maximal probability of finding the 5' end of a complementary small RNA. (F) Expression of PIWI family members in Aag2 cells analyzed by RT-PCR. cDNA synthesis was performed in the presence (+) or absence (-) of reverse transcriptase (RT). The -RT samples are included as controls for contamination of RNA preparations with chromosomal DNA. The coding sequences of Piwi1 and Piwi3 are 95% identical at the nucleotide level. Two different primer sets that amplify both Piwi1 and Piwi3 were used (a and b). A higher exposure was used for the gel image with Piwi1 to Piwi3. A 100-bp ladder was used as a size marker (M). The asterisk indicates a non-specific PCR amplification product.

non-composite transposons sequences (<http://tefam.biochem.vt.edu/tefam/index.php>). TE-derived small RNAs display a sharp 21-nt peak and a broader peak centering around 27-nt, which is suggestive of TE targeting by the *Aedes* siRNA and piRNA

pathways (Figure 5A). In contrast to TE-derived endo-siRNAs, the vast majority of TE piRNAs derive from retrotransposons and not from DNA transposons (Figure 5A). For most retrotransposons, the 25-29 nt TE RNAs display a strong over-representation of antisense reads (Figure 5B-C). The sequence depth of our library did not allow us to analyze ping-pong signatures in individual TEs. We therefore analyzed sequence logos of 25-29 nt small RNAs of the entire retrotransposon dataset (Figure 5D). A strong U₁

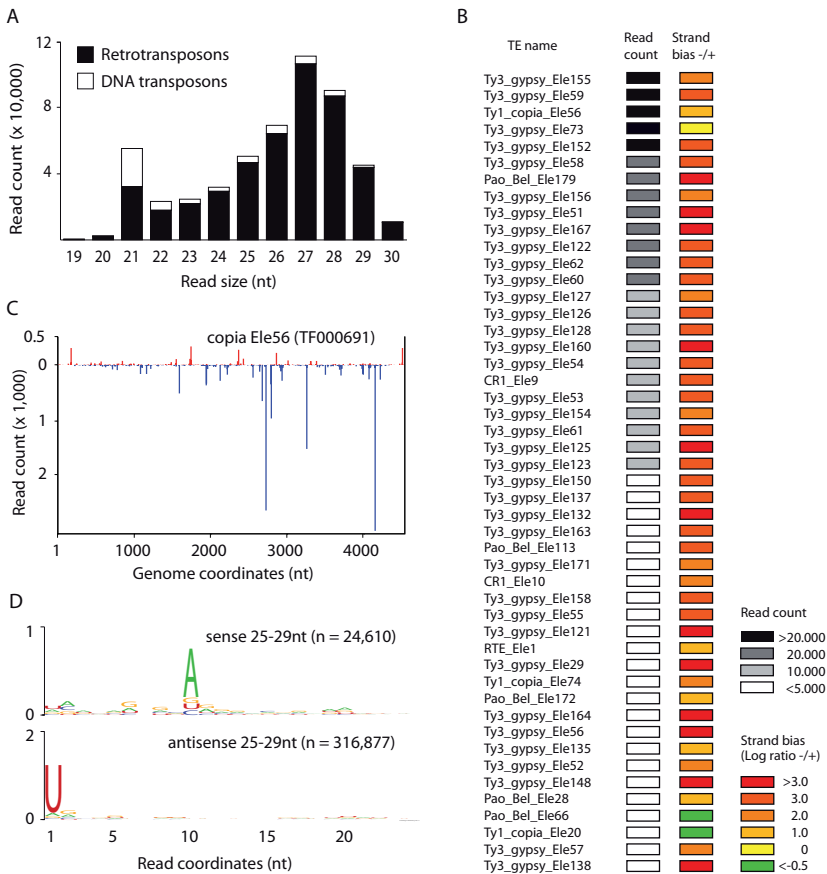


Figure 5. *Aedes aegypti* Aag2 cells produce transposon-derived piRNAs with a ping-pong signature. (A) Size distribution of the small RNA reads that match with 0 mismatches against an *Aedes aegypti* transposon dataset that contain full-length non-composite transposons sequences (TEfam: <http://tefam.biochem.vt.edu/tefam/index.php>). (B) Heat map for 25-29 nt small RNAs that mapped to individual retrotransposons with more than 1000 reads. Read count and log-transformed ratios of antisense/sense small RNAs are presented. (C) Profile of 25-29 nt reads that mapped to the transposon Copia Ele56 (TF000691) allowing 0 mismatch during alignment. Transposon-derived piRNAs that mapped to the sense and antisense strand of the transposon sequence are shown in red and blue, respectively. (D) Conservation and relative nucleotide frequency per position of 25-29 nt reads that mapped to the sense (top) and the antisense (bottom) strands of the entire transposon dataset. n indicates the number of reads used to generate each logo.

bias for antisense small RNAs and an enrichment of A_{10} in sense small RNAs imply that, similar to *Drosophila*, TEs are processed by the piRNA pathway in a ping-pong-dependent manner in Aag2 cells.

Discussion

Antiviral RNAi activity in insects has thus far only been attributed to the siRNA pathway. The identification of vpiRNAs in *Drosophila* OSS cells (13) and in *A. aegypti* and *A. albopictus* cells (this study) strongly suggests that the piRNA pathway constitutes another facet of the antiviral RNAi response in insects. Unlike the siRNA pathway, the piRNA pathway is highly enriched in the gonads where it plays a critical role in the control of transposition in the germ line. Because arboviruses can be transmitted vertically in arthropod vectors (29), an antiviral piRNA response in the gonads may constitute an antiviral mechanism to limit vertical transmission of arboviruses in insect vectors. In addition, a putative somatic piRNA pathway may represent an important aspect of vector competence. While the relevance of the piRNA pathway in controlling virus infections awaits experimental validation, it is likely that a pathway that efficiently cleaves viral RNA affects virus replication. Hence, the piRNA pathway should be considered as an intrinsic component of the antiviral RNAi response in insects. Moreover, U4.4 and Aag2 cells emerge as an attractive model to dissect piRNA biogenesis and the interplay between siRNA and piRNA pathways.

Contrary to the OSS cell line that only produces primary vpiRNAs (13), U4.4, Aag2 and C6/36 cells produce primary and secondary vpiRNAs through a ping-pong mechanism. In OSS cells, vpiRNAs map predominantly to the positive strand of the genome of (+) RNA viruses and display the expected U_1 bias for primary piRNAs. In U4.4, Aag2 and C6/36 cells however, the nucleotide bias signature is inverted, regardless the polarity of the viral genome. The vpiRNAs that derive from the (-) strand (i.e. the antigenomic strand of SINV and the genomic RNA strand of LACV) present a U_1 bias, whereas those that derive from the (+) strand display an A_{10} bias. This disparity between OSS cells and mosquito cells is unlikely to be due to differences in piRNA biogenesis, as our results on TE piRNAs in Aag2 and observations in *Bombyx Mori* BmN4 cells (30) suggest that basic features of piRNA biogenesis are conserved among insects. It is then most likely that this inversion is based on intrinsic features of the viral lifecycle.

The +/- strand ratio is uneven in ssRNA viruses. In (+) RNA viruses, the (+) strand is over-represented compared to the negative strand that serves as template for the production of progeny viral RNA. In many (-) RNA viruses, the (+) viral RNA strand that corresponds to viral transcript is over-represented compared to the genomic (-) strand, although

the relative amounts of transcripts are variable. In LACV, there is a gradient of +/- strand ratio between highly (S segment) and slightly (L segment) expressed transcripts. In both (+) and (-) RNA viruses, the genome and the intermediates of replication are shielded from cytoplasmic components, contrary to viral RNAs that engage in translation. Interestingly, primary vpiRNAs are produced from the (-) strand, regardless viral genome polarity. Moreover, in most cases, the ratio between U_1 and secondary A_{10} vpiRNAs follows strand stoichiometry. According to these observations, we propose two non-mutually exclusive hypotheses for the production of vpiRNAs through a ping-pong mechanism. The first hypothesis is based on the relative amounts of (+) and (-) strands during viral replication. For primary vpiRNAs that are produced from the abundant (+) strand, the generation of secondary vpiRNAs from the (-) strand is limited due to the relative limited amount of viral (-) RNA strands. Conversely, the production of primary vpiRNAs from the (-) strand may allow the generation of abundant secondary vpiRNAs from the abundant (+) strand. According to this hypothesis, as the (+) strand is more abundant than the (-) strand, the second ping-pong mechanism supersedes the first one. As a second hypothesis, the production of primary vpiRNAs from the (-) strand may result for a differential accessibility of the viral RNAs by piRNA pathway components. We propose that the PIWI protein that is responsible for primary piRNA biogenesis can better access viral (-) RNAs, and that the PIWI proteins that are responsible for secondary piRNA biogenesis can mostly access viral (+) RNAs. This may be due to spatial restriction of piRNA pathway proteins or to a differential accessibility of PIWI proteins to the viral RNAs engaged in replication and in translation. Finally, we show that viruses trigger the piRNA and the siRNA pathways in a similar way as transposons. This suggests that the RNAi pathways only discriminate common features of parasitic nucleic acids rather than their origin.

Materials and Methods

Cell culture, virus production and infection

A. albopictus U4.4 cells and *A. aegypti* Aag2 cells ((19, 25), kindly provided by G.P. Pijlman, Wageningen University, the Netherlands) were cultured at 28 °C in Leibovitz L-15 medium (Invitrogen) supplemented with 10% heat inactivated fetal calf serum (FCS, Invitrogen), 2% Tryptose Phosphate Broth Solution (Sigma) and 1% Non-Essential Amino Acids (Invitrogen). BHK-21 cells (American Type Culture Collection) were cultured in DMEM medium (Invitrogen) supplemented with 10% FCS (Invitrogen), and maintained at 37 °C in 5% CO₂. *In vitro* transcribed RNA from recombinant SINV expressing the Green Fluorescent Protein (31) was transfected into

BHK-21 cells. Virus titer was determined by plaque assay on BHK-21 cells. 2×10^6 U4.4 were infected with SINV-GFP for 2 hours in culture medium at a multiplicity of infection of 1. Cells were harvested 2 days post-infection, when 80-90% of the cells were positive for GFP expression.

RNAi reporter and Dicer assays

RNAi reporter assays were adapted from (32), using 3×10^5 U4.4 cells per well of a 24-well plate, 156 ng of pMT-Luc and pMT-Ren plasmids (6), and 0.625 ng of either firefly luciferase or GFP dsRNA. Dicer activity was determined in cell extracts from uninfected U4.4 cells as previously described (33), using 100 counts per seconds of an uniformly ^{32}P -radiolabeled 113-bp dsRNA substrate.

Small RNA library preparation and analysis

Small RNA libraries were prepared as described (34) and sequenced on a Genome Analyzer *Iix* (Illumina). Virus-derived small RNAs were analyzed using Paparazzi (35). piRNA signatures were calculated using in-house Perl scripts from 25-29 nucleotide-long virus-derived small RNA as previously described (11). Nucleotide frequencies per position were displayed using the WebLogo program (36). 19-30 nt reads from the Aag2 small RNA library were aligned with 0 mismatch against the *Aedes aegypti* transposon dataset available at Tefam (<http://tefam.biochem.vt.edu/tefam/>). The aligned reads were processed similarly to the virus-derived small RNA with in-house Perl scripts. Sequences were submitted to the Sequence Read Archive at the National Center for Biotechnology Information under accession number SRA047263.

RT-PCR

Total RNA was isolated from a confluent 75 cm² flask of Aag2 cells using Isol-RNA Lysis Reagent (5 Prime) according to manufacturer's recommendations. cDNA synthesis was performed on 1 µg of DNase-I (Invitrogen)-treated total RNA using an oligo-dT primer and TaqMan reverse transcriptase (Roche). PCR was performed using the following primers: F-AaeNanos, CAAACGTGAAGCGGAAGATT; R-AaeNanos, AATCAACGATGGATCGGATT; F-AaePIWI1/3a, TGTAGGGGAAGTAATGCATCG; R-AaePIWI1/3a, TCTACGGCAATGGTATCTGCT; F-AaePIWI1/3b, GGCCGTTAGCGAGTCTCAT; R-AaePIWI1/3b, GGCAGAACCTTCGTGGTAAG; F-AaePIWI2, ATGAAAGCCGGGAAGGTC; R-AaePIWI2, CTGCTACCATTGC-CATTTCC; F-AaePIWI4, TGACCGTTACTCTCAAGGGCGCTACCGT; R-AaePIWI4, GACCGTTCACGGCCACCTGCCGAT; F-AaePIWI5, GCCATACATCGGGTCAAAT; R-AaePIWI5, TGAGGTTGTTGCTTCTGAGGT; F-AaePIWI6, TAATCCACAGGAAGGCTCCA; R-AaePIWI6, CTCCTCCATTGTCCGATCCT;

F-AaePIWI7, GGAGGTCGTGGAGGTAACAA; R-AaePIWI7, CCTTCCAATCAC-GATTGCTT; F-AaeAgo3, TCGGTTTACCGCCAGCTGGGAGTTTTG; R-AaeAgo3, AGGTTATCTCAGCGGGAAAATCATGTCGCT

References

1. Campbell CL, Keene KM, Brackney DE, Olson KE, Blair CD, Wilusz J, & Foy BD (2008) *Aedes aegypti* uses RNA interference in defense against Sindbis virus infection. *BMC Microbiol* 8:47.
2. Galiana-Arnoux D, Dostert C, Schneemann A, Hoffmann JA, & Imler JL (2006) Essential function in vivo for Dicer-2 in host defense against RNA viruses in drosophila. *Nat Immunol* 7:590-597.
3. Keene KM, Foy BD, Sanchez-Vargas I, Beaty BJ, Blair CD, & Olson KE (2004) RNA interference acts as a natural antiviral response to O'nyong-nyong virus (Alphavirus; Togaviridae) infection of *Anopheles gambiae*. *Proc Natl Acad Sci U S A* 101:17240-17245.
4. Myles KM, Wiley MR, Morazzani EM, & Adelman ZN (2008) Alphavirus-derived small RNAs modulate pathogenesis in disease vector mosquitoes. *Proc. Natl.Acad.Sci.U.S.A* 105:19938-19943.
5. Sanchez-Vargas I, Scott JC, Poole-Smith BK, Franz AW, Barbosa-Solomieu V, Wilusz J, Olson KE, & Blair CD (2009) Dengue virus type 2 infections of *Aedes aegypti* are modulated by the mosquito's RNA interference pathway. *PLoS Pathog* 5:e1000299.
6. Van Rij RP, Saleh MC, Berry B, Foo C, Houk A, Antoniewski C, & Andino R (2006) The RNA silencing endonuclease Argonaute 2 mediates specific antiviral immunity in *Drosophila melanogaster*. *Genes Dev* 20:2985-2995.
7. Wang XH, Aliyari R, Li WX, Li HW, Kim K, Carthew R, Atkinson P, & Ding SW (2006) RNA interference directs innate immunity against viruses in adult *Drosophila*. *Science* 312:452-454.
8. Zambon RA, Vakharia VN, & Wu LP (2006) RNAi is an antiviral immune response against a dsRNA virus in *Drosophila melanogaster*. *Cell Microbiol* 8:880-889.
9. Siomi MC, Sato K, Pezic D, & Aravin AA (2011) PIWI-interacting small RNAs: the vanguard of genome defence. *Nat.Rev.Mol.Cell Biol.* 12:246-258.
10. Yan Z, Hu HY, Jiang X, Maierhofer V, Neb E, He L, Hu Y, Hu H, Li N, Chen W, *et al.* (2011) Widespread expression of piRNA-like molecules in somatic tissues. *Nucleic Acids Res* 39:6596-6607.

11. Brennecke J, Aravin AA, Stark A, Dus M, Kellis M, Sachidanandam R, & Hannon GJ (2007) Discrete small RNA-generating loci as master regulators of transposon activity in *Drosophila*. *Cell* 128:1089-1103.
12. Gunawardane LS, Saito K, Nishida KM, Miyoshi K, Kawamura Y, Nagami T, Siomi H, & Siomi MC (2007) A slicer-mediated mechanism for repeat-associated siRNA 5' end formation in *Drosophila*. *Science* 315:1587-1590.
13. Wu Q, Luo Y, Lu R, Lau N, Lai EC, Li WX, & Ding SW (2010) Virus discovery by deep sequencing and assembly of virus-derived small silencing RNAs. *Proc. Natl. Acad. Sci. U.S.A* 107:1606-1611.
14. Lau NC, Robine N, Martin R, Chung WJ, Niki Y, Berezikov E, & Lai EC (2009) Abundant primary piRNAs, endo-siRNAs, and microRNAs in a *Drosophila* ovary cell line. *Genome Res* 19:1776-1785.
15. Brackney DE, Scott JC, Sagawa F, Woodward JE, Miller NA, Schilkey FD, Mudge J, Wilusz J, Olson KE, Blair CD, *et al.* (2010) C6/36 *Aedes albopictus* cells have a dysfunctional antiviral RNA interference response. *PLoS.Negl. Trop. Dis.* 4:e856.
16. Hess AM, Prasad AN, Pritsyn A, Ebel GD, Olson KE, Barbacioru C, Monighetti C, & Campbell CL (2011) Small RNA profiling of Dengue virus-mosquito interactions implicates the PIWI RNA pathway in anti-viral defense. *BMC. Microbiol.* 11:45.
17. Scott JC, Brackney DE, Campbell CL, Bondu-Hawkins V, Hjelle B, Ebel GD, Olson KE, & Blair CD (2010) Comparison of dengue virus type 2-specific small RNAs from RNA interference-competent and -incompetent mosquito cells. *PLoS.Negl. Trop. Dis.* 4:e848.
18. Igarashi A (1978) Isolation of a Singh's *Aedes albopictus* cell clone sensitive to Dengue and Chikungunya viruses. *J Gen Virol* 40:531-544.
19. Condreay LD & Brown DT (1986) Exclusion of superinfecting homologous virus by Sindbis virus-infected *Aedes albopictus* (mosquito) cells. *J Virol* 58:81-86.
20. Singh KRP (1967) Cell Cultures Derived from Larvae of *Aedes Albopictus* (Skuse) and *Aedes Aegypti* (L). *Curr Sci India* 36:506-508.
21. Kawaoka S, Izumi N, Katsuma S, & Tomari Y (2011) 3' End Formation of PIWI-Interacting RNAs In Vitro. *Mol. Cell* 43:1015-1022.
22. Horwich MD, Li C, Matranga C, Vagin V, Farley G, Wang P, & Zamore PD (2007) The *Drosophila* RNA methyltransferase, DmHen1, modifies germline piRNAs and single-stranded siRNAs in RISC. *Curr Biol* 17:1265-1272.
23. Borucki MK, Kempf BJ, Blitvich BJ, Blair CD, & Beaty BJ (2002) La Crosse virus: replication in vertebrate and invertebrate hosts. *Microbes and Infection*

- 4:341-350.
24. Rossier C, Raju R, & Kolakofsky D (1988) LaCrosse virus gene expression in mammalian and mosquito cells. *Virology* 165:539-548.
 25. Peleg J (1968) Growth of Arboviruses in Monolayers from Subcultured Mosquito Embryo Cells. *Virology* 35:617-619.
 26. Siu RW, Fragkoudis R, Simmonds P, Donald CL, Chase-Topping ME, Barry G, Attarzadeh-Yazdi G, Rodriguez-Andres J, Nash AA, Merits A, *et al.* (2011) Antiviral RNA interference responses induced by Semliki Forest virus infection of mosquito cells: characterization, origin, and frequency-dependent functions of virus-derived small interfering RNAs. *J Virol* 85:2907-2917.
 27. Campbell CL, Black WC, Hess AM, & Foy BD (2008) Comparative genomics of small RNA regulatory pathway components in vector mosquitoes. *BMC Genomics* 9:425.
 28. Nene V, Wortman JR, Lawson D, Haas B, Kodira C, Tu ZJ, Loftus B, Xi ZY, Megy K, Grabherr M, *et al.* (2007) Genome sequence of *Aedes aegypti*, a major arbovirus vector. *Science* 316:1718-1723.
 29. Hanley KA & Weaver SC (2008) Arbovirus evolution. *Origin and evolution of viruses*, eds Domingo E, Parrish CR, & Holland JJ (Academic Press, London), Vol 2, pp 351-391.
 30. Kawaoka S, Hayashi N, Suzuki Y, Abe H, Sugano S, Tomari Y, Shimada T, & Katsuma S (2009) The Bombyx ovary-derived cell line endogenously expresses PIWI/PIWI-interacting RNA complexes. *RNA*. 15:1258-1264.
 31. Saleh MC, Tassetto M, Van Rij RP, Goic B, Gausson V, Berry B, Jacquier C, Antoniewski C, & Andino R (2009) Antiviral immunity in *Drosophila* requires systemic RNA interference spread. *Nature* 458:346-350.
 32. van Cleef KW, van Mierlo JT, van den Beek M, & Van Rij RP (2011) Identification of viral suppressors of RNAi by a reporter assay in *Drosophila* S2 cell culture. *Methods Mol. Biol.* 721:201-213.
 33. Haley B, Tang G, & Zamore PD (2003) In vitro analysis of RNA interference in *Drosophila melanogaster*. *Methods* 30:330-336.
 34. Gausson V & Saleh MC (2011) Viral small RNA cloning and sequencing. *Methods Mol. Biol.* 721:107-122.
 35. Vodovar N, Goic B, Blanc H, & Saleh MC (2011) In silico reconstruction of viral genomes from small RNAs improves virus-derived small interfering RNA profiling. *J Virol* 85:11016-11021.
 36. Crooks GE, Hon G, Chandonia JM, & Brenner SE (2004) WebLogo: A sequence logo generator. *Genome Res* 14:1188-1190.

Chapter 7

General discussion

The RNA interference (RNAi) pathway is considered to be the primary antiviral pathway in insects, including the fruit fly *Drosophila melanogaster* and the major vector mosquitoes *Aedes aegypti* and *Aedes albopictus* (reviewed in **chapter 1**) (1, 2). Recent studies suggested that another small RNA silencing mechanism, the piRNA pathway, is also implicated in antiviral defense. The studies in this thesis focused on the role of small RNA-based antiviral defense mechanisms in insects. In the following sections I will discuss our findings in relation to recent literature. First I address the antiviral RNAi pathway in insects and then I will describe other dsRNA-induced responses as well as alternative nucleic acid sensing pathways. I will also discuss the mammalian and nuclear antiviral RNAi responses and finally speculate on the role of virus-derived piRNAs in antiviral defense.

The antiviral RNAi pathway in insects

Viral dsRNA substrates

The production of dsRNA is a hallmark of viral infection, as dsRNA is normally not detected in uninfected, healthy cells (3). Single-stranded (ss) RNA viruses produce large amounts of essential dsRNA replication intermediates during their viral life cycle, which feeds into the RNAi pathway. In insects, the detection of viral dsRNA induces an antiviral RNAi response, which is characterized by the production of Dicer-2 (Dcr-2)-dependent viral small interfering RNAs (vsiRNAs). In **chapter 2** we revealed that vsiRNAs are generated in flies that are persistently infected with the positive-strand (+) RNA virus Nora virus. Indeed, vsiRNAs of positive and negative polarity were recovered in equal ratios and were uniformly distributed across the viral genome, indicating that viral replication intermediates are the major source for vsiRNA biogenesis. Other putative Dcr-2 substrates from RNA viruses include highly structured ssRNA molecules or viral dsRNA genomes (reviewed in **chapter 1**). In **chapter 3** we demonstrated that DNA viruses also produce viral dsRNA that is recognized and processed by Dcr-2. This was somewhat surprising, as DNA viruses do not rely on dsRNA intermediates for efficient virus replication. Nevertheless, we revealed that the DNA virus Invertebrate iridescent virus 6 (IIV-6) produces convergent overlapping transcripts that have the potential to base pair and form dsRNA substrates for Dcr-2-dependent vsiRNA biogenesis (**chapter 3**). In addition, structured ssRNA substrates may also be processed during DNA virus infections (discussed in **chapter 4**) (4). Together, these studies demonstrate that all major classes of viruses produce dsRNA substrates, which are processed into vsiRNAs to elicit an antiviral RNAi response.

vsiRNA biogenesis

Whilst all classes of insect viruses seem to produce dsRNA during their life cycle, it remains unclear when and where viral dsRNA is accessible to Dcr-2. RNA viruses shield their genomic material to avoid recognition by the host defense system: negative-strand (-) RNA viruses replicate in ribonucleoprotein (RNP) complexes (5, 6), double-stranded RNA viruses replicate within the viral capsid or, in some instances, in RNPs (7-9), whereas (+) RNA virus replication occurs in virus-induced intracellular membranous vesicles (10, 11).

A dsRNA-specific immunostaining revealed that following infection with many (+) RNA and DNA viruses, but not (-) RNA viruses, viral dsRNA is readily detected in the cytoplasm of mammalian cells (3). Likewise, in *Drosophila* cells infected with the (+) RNA virus Flock House virus (FHV), *Drosophila* C virus (DCV) or Cricket paralysis virus, dsRNA is successfully precipitated using a dsRNA-specific antibody (12). However, dsRNA immunoprecipitation from cells infected with the (-) RNA virus vesicular stomatitis virus (VSV) was not successful. Nevertheless, Dcr-2-dependent vsiRNAs could be recovered from VSV-challenged flies by cloning and deep sequencing of small RNAs, indicating that dsRNA is produced during (-) RNA virus infection. Using a similar approach, we demonstrated that vsiRNAs could be recovered from adult *Drosophila* infected with the (+) RNA virus Nora virus or the dsDNA virus IIV-6 (**chapter 2** and **chapter 3**, respectively) as well as from Sindbis-infected mosquito cells (**chapter 6**). Several small RNA-profiling studies independently revealed vsiRNA production by all classes of viruses that infect insects, including mosquitoes and *Drosophila* (reviewed in **chapter 1**). Thus, even though virus replication occurs in enclosed viral factories and some viruses additionally encode suppressor proteins to protect their genome (see below), vsiRNAs are readily detectable during virus infection. Clearly, the production of vsiRNAs is a key feature of an antiviral RNAi response and suggests that viral dsRNA is somehow accessible for Dcr-2-dependent processing.

Dcr-2-independent processing of viral dsRNA

Dcr-2 requires its dsRNA-binding cofactors R2D2 and Loquacious (Loqs)-PD for processing of endogenous and experimentally introduced exogenous dsRNA (13-16), while Dcr-2 alone seems sufficient to process viral dsRNA during RNA virus infection (17, 18). However, at present it remains unclear whether Dcr-2 requires other, yet unidentified, dsRNA-binding proteins for the detection and processing of viral dsRNA. Remarkably however, low levels of viral small RNAs were still observed from virus-infected *Dcr-2* knockout flies or from *Dcr-2* depleted cells (**chapter 3**) (4, 12), which suggests that in the absence of Dcr-2 other nucleases might be involved in vsiRNA biogenesis. The miRNA-producing enzyme Dcr-1 is an obvious candidate, as it cleaves

dsRNA substrates *in vitro* (19-21) and produces small RNAs from an inverted repeat transgene in *Dcr-2* mutant flies (22). Therefore, it remains to be established whether the *Drosophila* encoded Dicer proteins have redundant roles in vsiRNA biogenesis, as was observed for the plant-specific Dicer-like (DCL) enzymes (23-26). However, the lethal phenotype of *Dcr-1* mutant flies thus far restricted such *in vivo* studies. Interestingly, several studies revealed that the biogenesis of a vertebrate conserved miRNA (miR-451) was independent of *Dcr-1*, but required the miRNA-processing enzyme Drosha as well as AGO2 catalytic activity (27-29). It will be interesting to study whether viral small RNAs can also be generated from highly structured regions in a similar manner, by comparing viral small RNA profiles from *AGO2* and *Dcr-2* double knockout flies to those of *Dcr-2* knockout flies.

Functionality of vsiRNAs

The production of *Dcr-2*-dependent vsiRNAs is a hallmark of the antiviral RNAi response, but it remains unknown whether the total pool of generated vsiRNAs contributes to RNA silencing. We, for example, showed that in infected flies, IIV-6-derived vsiRNAs were highly unevenly distributed across the genome, with strong clustering to small, defined regions (hotspot). However, the abundance of vsiRNAs within these hotspot regions did not seem to correlate with the efficiency of silencing of sensor constructs carrying fragments of the IIV-6 genome (**chapter 3**). Likewise, hotspot vsiRNAs derived from mosquito cells infected with the (+) RNA virus Semliki Forest virus were inefficient at mediating antiviral RNAi when compared to coldspot vsiRNAs (30). Nevertheless, the vsiRNA-mediated gene silencing indicates that at least some vsiRNAs are incorporated into a functional RISC. Notably, vsiRNA-mediated silencing of a reporter plasmid that harbored a VSV-specific sequence required AGO2 activity (12).

AGO2 immunoprecipitation studies followed by deep sequencing of small RNAs are required to analyze the fraction of IIV-6-derived vsiRNAs that are loaded into RISC. In addition, it will be interesting to perform AGO1 immunoprecipitation studies, as crosstalk seems to occur between the miRNA and siRNA pathways (31). Indeed, endogenous miRNAs could be recovered from AGO2 immunoprecipitates (32-34), whereas endogenous (endo-) siRNAs are sometimes (e.g. in *R2D2* mutants) misloaded into AGO1 (13, 35). Interestingly, AGO1 also seems to exhibit Slicer activity when the incorporated miRNA exhibits full complementarity to the target RNA (36, 37). However, thus far it remains unknown whether cross loading of vsiRNAs into AGO1 occurs and, if so, whether AGO1-mediated slicing of viral target RNA contributes to the antiviral potential of the RNAi machinery. Of note, vsiRNAs are rarely recovered from AGO1 precipitates of *Drosophila* cells that are persistently infected with FHV (32). Remarkably

however, in some cases vsiRNA levels are slightly increased upon AGO1 depletion of virus-infected *Drosophila* cells (4, 38). These observations could hint at a direct or indirect antiviral function of the miRNA pathway. For example, the miRNA pathway can normally silence cellular genes (or perhaps viral transcripts) that support efficient virus replication. Consequently, disruption of the miRNA pathway would lead to increased virus replication, providing more viral RNA substrates for Dcr-2, which results in increased vsiRNA levels.

Alternative source of vsiRNA production

In cultured *Drosophila* cells that are persistently infected with FHV or American Noda virus (ANV), viral replication intermediates as well as defective viral RNAs, appear to be the major dsRNA substrates for vsiRNA biogenesis (38-42). Defective interfering (DI) RNAs arise during aberrant replication of the parental virus and contain large deletions of genes that are required for efficient replication and encapsidation. Nevertheless, DI RNAs are replicated by the parental virus-encoded RNA-dependent RNA polymerase, and even replicate more efficiently due to their smaller genome size. Indeed, DI RNAs derived from ANV (RNA2) account for half the amount of total vsiRNA production in *Drosophila* ovarian somatic sheet cells (39). Reporter-based assays revealed that FHV-derived vsiRNAs failed to silence complementary target sequences, suggesting that the majority of FHV-derived vsiRNAs are not incorporated into AGO2 (38). This study suggested that the dicing of viral replication intermediates by itself might limit virus infection, while the generated vsiRNAs could provide a decoy strategy for RISC saturation in order to maintain a persistent infection. Alternatively, defective RNAs can mediate persistence by interfering with replication of full-length genomic RNA directly. However, *in vitro* and *in vivo* studies both revealed that a fraction of FHV-derived vsiRNAs is 3' end modified and associated with AGO2 (32, 43). Moreover, FHV viral RNA levels were increased following AGO2 depletion of persistently infected cells, indicating that AGO2 contributes to control persistent infections (32, 38, 43). In contrast to persistently infected cell lines, DI RNAs are thus far not recovered from persistently infected flies, which argues against a physiological function for DI RNAs during authentic virus infections *in vivo*.

Different infection models

The RNA viruses Sigma virus, DCV and Nora virus are natural fly pathogens that can cause persistent infections, whereas several other viruses efficiently replicate in *Drosophila* upon experimental infection (44). Remarkably, *Drosophila* is often used as a model organism to study arthropod-borne (arbo) virus infection via intra-thoracic injection, while arboviruses orally enter mosquitoes during an infectious blood meal and

start to replicate in midgut epithelial cells. Following oral ingestion, a virus first needs to cross the epithelial barriers of the digestive tract in order to establish a productive infection. It is believed that active immune responses within intestinal epithelial cells, including Jak-Stat, ERK, and Toll-signaling pathways, provide antiviral defense (45-47). However, most studies on antiviral RNAi were performed by intra-thoracic or intra-abdominal virus injection of adult flies, thus bypassing the various immunity pathways that comprise the antiviral midgut barrier. It will, however, be interesting to study the relative contribution of the antiviral RNAi pathway after natural infection routes. This is for example already being studied in *Caenorhabditis elegans* larvae, in which Orsay virus (a positive-strand RNA virus) infection is potently suppressed by the RNAi pathway (48). Interestingly, flies can also be orally infected (47, 49) (and our unpublished observations), which provides useful avenues to study (arbo)virus-host interactions under more physiological conditions. Nevertheless, experimental injection of insects may also resemble a natural route of virus infection. For example, the hemolymph of RNAi-competent honeybees can be infected with deformed wing virus (DWV) during feeding activities of the parasitic mite *Varroa destructor* (50). Interestingly, *Varroa*-mediated virus transmission is suggested to be a major cause of honeybee colony collapse, with DWV being one of the key players. In addition, it has been suggested that parasitic mites or wasps are potential vectors for the transmission of viruses (e.g. Sigma virus) to *Drosophila* (51). Taken together, both experimental injection and oral infection methods provide useful models to study the molecular mechanisms that are involved in RNAi-mediated immunity in insects.

Viral counter-defense

The dicing of viral RNA substrates could in theory be sufficient to control virus infections. Nevertheless, several lines of evidence illustrate that both the initiation and effector steps of the RNAi pathway are required to induce a potent antiviral response. First, *in vivo* studies revealed that flies or mosquitoes that are mutant or depleted for the core RNAi components *Dcr-2*, *R2D2*, or *AGO2* are hypersensitive to virus infection. Second, several viruses encode suppressor proteins that inhibit the RNAi pathway at distinct steps. For example, *Drosophila* or mosquito-restricted RNA viruses can bind RNA duplexes and thereby prevent *Dcr-2* processing of viral dsRNA and inhibit siRNA loading into RISC (reviewed in **chapter 1**) (52-55). Our observation that the DNA virus IIV-6 encodes a suppressor protein that interferes with *Dcr-2* processing activity (**chapter 5**), supports the notion that dicing contributes to antiviral defense. In addition, two unrelated (+) RNA viruses, Nora virus and Cricket paralysis virus, encode

a suppressor protein (VP1 and 1A, respectively) that interferes with RISC enzymatic activity (**chapter 2**) (56). The observation that *AGO2* slicing mutants, that still contain a functional Dcr-2 protein, are more sensitive to VSV infection further underscores that *AGO2*-dependent slicing activity is essential for antiviral defense (17). Finally, *Dcr-2*, *R2D2* and *AGO2* are amongst the fastest evolving genes within the *Drosophila* genome, which suggests that genes involved in the initiation or effector phase of the RNAi pathway are involved in the ongoing arms race between viruses and their hosts (57, 58).

Host counter-counter-defense

In plants, virus infections can induce host counter-counter-defense or secondary defense responses, which resembles effector-triggered immunity (ETI) to non-viral pathogens (59). The plant immune system is composed of two layers for microbe detection. In the first layer, pattern-recognition receptors detect pathogen-associated molecular patterns (PAMPs) to induce PAMP-triggered immunity (PTI). As a countermeasure, plant pathogens evolved effector molecules that are secreted into host cells to antagonize the PTI response and to induce virulence. The second layer of plant immunity is composed of resistance proteins, which recognize the effector molecules and provide a protein-based guard mechanism to inactivate these PTI suppressors. This process of effector-triggered immunity (ETI) results in disease resistance and leads to a hypersensitive response (59). Likewise, virus infection also seems to trigger a secondary response in plants. However, this second layer of antiviral defense seems primarily small RNA-based and refers to the induction of resistance genes, which are normally silenced by endogenous small RNAs. When viral effector molecules (VSRs) attenuate the first layer of viral defense (RNAi), the resistance genes will be derepressed leading to the induction of a hypersensitive, secondary response (60). Several recent studies described different examples of counter-counter defense against plant viruses. For example, the plant-encoded miR-482 targets a primary disease resistant gene, resulting in the secondary amplification of RDR6 and DCL4-dependent trans-acting siRNAs (tasiRNAs) that simultaneously repress multiple resistance gene family members (61-63). Infection of plants with turnip crinkle virus (TCV) and cucumber mosaic virus (CMV), which both encode proteins that antagonize *AGO1* function, resulted in mRNA expression of this specific class of resistance genes (63). Likewise, *AGO2* itself is repressed by endogenous miR-403 in uninfected *Arabidopsis* (64), but suppression of *AGO1* function during infection results in increased *AGO2* protein levels that contribute to antiviral defense (65, 66). The antiviral effector DCL2 seems to be controlled by small tasiRNAs in a similar fashion (61). Alternatively, virus-induced expression of the tobacco encoded calmodulin-like protein rgs-CaM

provides a protein-based secondary defense in plants. Indeed, this host protein targets VSRs, together with *rgs*-CaM itself, for autophagy-mediated degradation to enhance the antiviral RNAi response (67). Thus far, counter-counter-defense mechanisms have not been observed for insects, which can partially be explained by the fact that insects lack secondary siRNA biogenesis pathways. However, resistance genes could directly be repressed by endo-siRNAs. As such, the presence of a viral protein that antagonizes the RNAi pathway could result in the expression of genes that are normally repressed by endo-siRNAs. Notably, abundant endo-siRNAs that mapped to the 3'UTR of AGO2 were identified by analyzing small RNA profiles that were recovered from *Drosophila* cells. These endo-siRNAs were generated from bidirectional overlapping transcripts in an AGO2 and Dcr-2-dependent manner (15). Therefore, it is tempting to speculate that AGO2 transcript levels would increase when the RNAi pathway is antagonized. It will be interesting to monitor whether AGO2 levels are increased during virus infection of adult flies. We could for example compare AGO2 transcript and protein levels in uninfected flies to that of flies that are persistently infected with DCV or Nora virus. Taken together, it will be interesting to study the induction of immune genes in virus-infected *Drosophila* or mosquitoes, especially because it remains unknown whether secondary defense mechanisms contribute to antiviral immunity in insects.

Mammalian RNAi

The detection of viral dsRNA in mammalian cells by the intracellular pattern-recognition receptors RIG-I and MDA5 triggers an interferon (IFN)-mediated innate immune response, which induces the production of antiviral defense genes (68). An important downstream effector molecule of the IFN pathway is the dsRNA-dependent protein kinase R (PKR). In addition, intracellular viral dsRNA can activate PKR directly, leading to translational shutdown via eIF-2 α phosphorylation, which results in the inhibition of virus replication. Recently, it was shown that RNAi also possesses antiviral activity in specific stages and lineages of mammalian cells infected with encephalomyocarditis virus (EMCV) or Nodamura virus (NoV), two unrelated positive-strand RNA viruses (69, 70). Because cytoplasmic RIG-I, MDA5, PKR and Dicer all bind intracellular viral dsRNA, it will be interesting to determine whether these proteins compete for the same dsRNA substrate, whether they operate together or explore specific and non-redundant roles within an infected cell. From the virus perspective, the binding of dsRNA by viral immune antagonists provides a very efficient strategy to evade both IFN-regulated and small RNA-guided innate immune responses. Indeed, it has been demonstrated that several proteins from mammalian RNA and DNA viruses sequester dsRNA to

support efficient virus replication by antagonizing IFN-induced responses (68, 71-73). An intriguing example is the dsRBD protein E3L from vaccinia virus, a dsDNA virus. E3L inhibits the dsRNA-activated PKR and 2' 5'-oligoadenylate synthetase (OAS)/RNaseL-mediated antiviral responses in mammalian cells and antagonizes the dsRNA-induced RNAi response in cultured *Drosophila* cells (68, 74). It will be interesting to analyze whether viral dsRNA-binding proteins contribute to antagonize an RNAi response during natural infection of the vertebrate host. For DNA viruses, the recovery of vsRNAs in infected mammalian cells has not been reported to date, despite the observation that dsRNA is produced during DNA virus infection (3). By contrast, virus-derived miRNAs are readily detected in herpesvirus-infected cells (75, 76). Therefore, it remains to be tested whether DNA viruses induce an antiviral RNAi response in mammals, as was observed for plants and insects that lack adaptive immune responses (**chapters 3 and 4**) (77).

The existence of a natural antiviral RNAi response in mammals, especially in somatic cells, is still being debated (78). For example, a recent study reported an alternative role for AGO2 in antiviral defense (79). Specifically, it was demonstrated that RISC activity was reduced through post-translational modification of AGO2 following virus infection of somatic cells. The authors proposed that RISC inactivation results in the release of miRNA-mediated suppression of antiviral defense genes (ISGs, interferon stimulated genes) in order to enhance the antiviral response. Notably, the induction of ISGs in mammals shows a striking similarity to secondary defense in plants (see above). Another recent report implicated a role for cytoplasmic Drosha, but not Dicer, in antiviral defense against Sindbis virus in IFN-sensitive somatic cells (80). Despite these controversial reports, the discovery of mammalian antiviral RNAi under specific experimental conditions provides new insights into innate antiviral immunity.

Other dsRNA-induced responses

It is believed that, in addition to viral dsRNA, other viral components are required to induce a potent immune response in *Drosophila* and mosquitoes, because injection of exogenous dsRNA does not induce a sequence non-specific antiviral response (81-83). However, in penaeid shrimp and in the non-Dipteran insect *Apis mellifera* (honeybee), dsRNA induces both sequence-specific and sequence-independent antiviral responses (84-91). For example, in the shrimp *Litopenaeus vannamei* injection of long dsRNA, regardless of sequence specificity, induces protection against the dsDNA virus white spot syndrome virus and the (+) RNA virus Taura syndrome virus (85). Similar results

were obtained in honeybees, in which dsRNA injection protected against infection with the (+) RNA virus Sindbis virus (91), indicating that dsRNA induces sequence-independent immune responses. At the same time, it remains unclear how well conserved this sequence-independent response is across invertebrate animals. Nevertheless, shrimp and honeybees provide useful model organisms to study the molecular mechanisms of dsRNA-induced antiviral responses. Moreover, it will be interesting to analyze whether the RNAi pathway and the sequence non-specific immune responses are interconnected in these invertebrate species.

Other nucleic acid sensing pathways

It is generally believed that the production of viral dsRNA is a central trigger of an innate immune response, as dsRNA is not detected in uninfected, healthy cells (3, 12). However, endo-siRNAs are detectable by small RNA sequencing studies, indicating that dsRNA is produced in uninfected cells (14, 15, 92-95), albeit that endo-siRNA production seems to depend on Dcr-2 along with its cofactor Loqs-PD, whereas vsRNAs are produced in a Loqs-PD-independent manner (17). Therefore, a key question to the initiation of the RNAi pathway is whether and how Dcr-2 acquires substrate specificity for viral RNA (non-self) versus host-derived (self) RNA substrates.

Insights from several studies led to the hypothesis that host-mediated modifications of cellular RNAs may be involved in the evasion of the RNAi machinery. For example, adenosine deaminase proteins that act on RNA (ADARs) could play a role in editing cellular dsRNA substrates to antagonize an RNAi response. Specifically, ADARs can convert adenosine into inosine within dsRNA, such as secondary structured mRNA or convergent overlapping transcripts, which alters the codon sequence and disrupts dsRNA structures. It was proposed that the latter could destroy complementarity between the siRNA guide-strand and the target mRNA or might affect Dicer dsRNA-binding and processing (96-98). In addition, ADARs might compete with Dicer itself for dsRNA substrate binding.

On the other hand, host-mediated modification of viral nucleic acids may also be an effector mechanism of an antiviral immune response. A recent study, for example, showed that in DCV-infected flies the RNA methyltransferase Dnmt2 associates with viral RNA. In addition, it was observed that *Dnmt2* mutant flies displayed increased susceptibility to DCV infection, which correlated with increased viral RNA and proteins levels. The authors therefore suggested that Dnmt2 not only methylates cytosine within tRNA substrates but also might modify viral RNA substrates (49). However, the molecular mechanisms by which Dnmt2 and ADAR proteins obtain substrate specificity, if any,

remain unknown.

Nuclear RNAi

While RNAi is a post-transcriptional gene silencing (PTGS) mechanism that operates in the cytoplasm to control mRNA expression, it also plays a crucial role in the defense against viruses (40, 99). However, there is growing evidence that small RNAs and RNAi pathway components additionally play important roles in transcriptional gene silencing (TGS) in the nucleus. An initial study demonstrated that sequestration of endo-siRNAs by nuclear expression of the viral suppressors of RNAi, FHV B2 and Tombusvirus P19, resulted in the loss of heterochromatin marks in somatic tissues of adult flies and larvae (100). Likewise, *Dcr-2*, *R2D2* and *AGO2* mutant flies, showed aberrant repressive chromatin marks and a concomitant release of silencing of reporter genes that were integrated in heterochromatin-rich pericentromeric regions. Together, these findings provide indirect evidence for the involvement of the endo-siRNA pathway in heterochromatin formation. Because several insect viruses encode proteins that bind siRNAs to antagonize RNAi (reviewed in **chapter 1**), it will be interesting to analyze whether these VSRs induce epigenetic changes during an authentic infection. Recent studies provided direct evidence for a role of nuclear RNAi in *Drosophila*. One study revealed that small RNA-loaded AGO2 as well as Dcr-2 associate with transcriptionally active, euchromatic loci and seem to control RNA Pol II activity (101). By contrast, another study revealed that AGO2-mediated transcriptional repression relies on chromatin binding and repressive chromatin formation (102). The exact mechanism of RNAi-mediated TGS thus remains controversial and is still poorly understood. Nevertheless, these studies suggest that in analogy to *Schizosaccharomyces pombe*, *C.elegans* and higher plants (103), the RNAi pathway functions in TGS in *Drosophila* and perhaps in other insects.

Are nuclear RNAi components also involved in the silencing of insect viruses, such as IIV-6, which replicate in the nucleus? For plants it was proposed that both PTGS and TGS contribute to antiviral defense against DNA viruses. Geminiviral dsDNA intermediates, which are produced by rolling-circle amplification of the ssDNA genome, associate with cellular histone proteins to form viral minichromosomes. The cytoplasmic RNAi machinery likely processes convergent overlapping transcripts that are produced from these minichromosomes (104, 105). On the other hand it was proposed that epigenetic silencing of geminiviruses relies on small RNA-directed DNA methylation of the viral genome, which involves nuclear DCL3 and AGO4 (106, 107). Geminiviruses encode proteins to counteract PTGS as well as TGS responses, which underscores that plant

DNA viruses are targeted by two distinct small RNA-based pathways (60). Whether TGS has an antiviral role in insects remains thus far elusive.

Virus-derived piRNAs

While seminal studies revealed that the RNAi pathway contributes to antiviral defense in *Drosophila* and mosquitoes (reviewed in **chapter 1**), not much was known about other small RNA-based defense mechanisms in insects. The recovery of virus-derived PIWI-interacting RNA (piRNA) sized small RNAs from persistently infected *Drosophila* ovarian sheet cells for the first time hinted at a possible antiviral function for the piRNA pathway (39). Endogenous, single-stranded small RNAs of 25-30 nt that associate with proteins of the PIWI family are at the core of the piRNA pathway. In *Drosophila*, the piRNA pathway operates in germline tissues to maintain genome integrity by repressing transposon levels (103, 108). We performed small RNA profiling studies of arbovirus-infected mosquito cells (**chapter 6**). Intriguingly, we noted that besides vsiRNAs, virus-derived small RNAs of ~25-30 nt that exhibit characteristic piRNA signatures were generated. Several other studies additionally reported the production of viral piRNAs (vpiRNA) in cells and somatic tissues of mosquitoes (109-112). This suggests that, in addition to the antiviral RNAi pathway, the piRNA pathway is involved in antiviral defense in mosquitoes. The mechanism by which vpiRNAs might contribute to the control of arbovirus infection in somatic cells is an exciting field for further study. Thus far, it remains unknown whether different small RNA-based pathways operate together, or whether the piRNA pathway serves as a back-up mechanism upon inhibition of the RNAi pathway. Alternatively, the piRNA pathway could function independently to induce an antiviral immune response.

For a long time it was assumed that arboviruses do not antagonize the RNAi pathway, as VSR activity could lead to pathogenesis and death of the arthropod vector, thereby preventing efficient virus transmission. Indeed, the introduction of FHV B2 in recombinant Sindbis virus induced pathogenicity and death of infected mosquitoes, suggesting that expression of B2 in RNAi-competent mosquitoes would not allow successful transmission and thus is disadvantageous for virus spread (113, 114). However, recent reports suggested that some arboviruses suppress the RNAi pathway in mosquitoes (reviewed in **chapter 1**). In this perspective, it will be interesting to test whether the piRNA-pathway displays increased antiviral activity when antiviral RNAi is antagonized. If the piRNA pathway indeed has antiviral potential, one could speculate that arboviruses suppress the piRNA pathway in order to establish a productive infection, which is required for successful virus transmission. A recent study suggested that FHV

B2 suppressed the production of viral piRNAs (112). Specifically, *Dcr-2* deficient cells showed increased cell death when B2 was expressed in a recombinant Chikungunya virus (CHIKV-B2) as compared to the parental virus. In addition, a mild reduction in viral piRNA levels was observed upon CHIKV-B2 infection. Therefore, the authors suggested that FHV B2 inhibits piRNA biogenesis in mosquitoes.

Alternatively, in case the piRNA-pathway is not directly involved in antiviral defense, piRNAs could serve as a memory factor to prime an efficient immune response following successive virus challenge. In line with this hypothesis, it has been shown that piRNAs mediate transgenerational epigenetic inheritance in nematodes and flies (115-119).

Future directions

Over the last few years, it has become increasingly clear that the RNAi pathway is an important determinant for insect antiviral immunity. This small RNA-based antiviral response is, however, not the sole line of host defense, as protein-based innate immune responses, including the Toll, Imd and Jak-Stat signaling pathways, also seem to contribute to control of virus infection (44). The studies in this thesis deepened our understanding of small RNA-based antiviral defense mechanisms in *Drosophila* and mosquitoes. Nevertheless, many questions remain unanswered. For example, how do viruses for which no VSR has been identified, such as VSV and Sindbis virus, establish a productive infection? Do these viruses antagonize other antiviral signaling pathways? And, how do the VSR-competent viruses Nora virus and DCV maintain a persistent infection in flies? It also remains largely unknown when and how viral RNA substrates are detected for vsRNAs or vpiRNA biogenesis. Another key question that remains unanswered is how arboviruses establish a persistent, non-pathogenic infection in RNAi-competent mosquitoes. Is persistence in mosquitoes mediated by antiviral siRNAs and piRNAs that are present in the soma? Experimental techniques to study antiviral immunity in mosquitoes are limited, which is in contrast to the extensive genetic toolbox in *Drosophila*. However, it will be important to study the course of arbovirus infection in its natural host. As such, experimental infection models and genetic tools in mosquitoes will significantly contribute to our understanding of virus-vector interactions, which might lead to improved strategies to control the transmission of pathogenic arboviruses. The recently described Crispr/Cas9 mutagenesis system could provide a perfect tool for targeted genome editing in mosquitoes (120, 121).

References

1. Sanchez-Vargas I, Travanty EA, Keene KM, Franz AW, Beaty BJ, Blair CD, & Olson KE (2004) RNA interference, arthropod-borne viruses, and mosquitoes. *Virus Res* 102:65-74.
2. Blair CD (2011) Mosquito RNAi is the major innate immune pathway controlling arbovirus infection and transmission. *Future Microbiol* 6:265-277.
3. Weber F, Wagner V, Rasmussen SB, Hartmann R, & Paludan SR (2006) Double-stranded RNA is produced by positive-strand RNA viruses and DNA viruses but not in detectable amounts by negative-strand RNA viruses. *J Virol* 80:5059-5064.
4. Sabin LR, Zheng Q, Thekkat P, Yang J, Hannon GJ, Gregory BD, Tudor M, & Cherry S (2013) Dicer-2 processes diverse viral RNA species. *PLoS One* 8:e55458.
5. Banerjee AK (1987) Transcription and replication of rhabdoviruses. *Microbiological reviews* 51:66-87.
6. Conzelmann KK (1998) Nonsegmented negative-strand RNA viruses: genetics and manipulation of viral genomes. *Annu Rev Genet* 32:123-162.
7. Ahlquist P (2006) Parallels among positive-strand RNA viruses, reverse-transcribing viruses and double-stranded RNA viruses. *Nat.Rev.Microbiol.* 4:371-382.
8. Hjalmarsson A, Carlemalm E, & Everitt E (1999) Infectious pancreatic necrosis virus: identification of a VP3-containing ribonucleoprotein core structure and evidence for O-linked glycosylation of the capsid protein VP2. *J Virol* 73:3484-3490.
9. Luque D, Saugar I, Rejas MT, Carrascosa JL, Rodriguez JF, & Caston JR (2009) Infectious Bursal disease virus: ribonucleoprotein complexes of a double-stranded RNA virus. *J Mol Biol* 386:891-901.
10. den Boon JA & Ahlquist P (2010) Organelle-like membrane compartmentalization of positive-strand RNA virus replication factories. *Annu Rev Microbiol* 64:241-256.
11. Diaz A, Gallei A, & Ahlquist P (2012) Bromovirus RNA replication compartment formation requires concerted action of 1a's self-interacting RNA capping and helicase domains. *J Virol* 86:821-834.
12. Mueller S, Gausson V, Vodovar N, Deddouche S, Troxler L, Perot J, Pfeffer S, Hoffmann JA, Saleh MC, & Imler JL (2010) RNAi-mediated immunity provides strong protection against the negative-strand RNA vesicular stomatitis virus in *Drosophila*. *Proc.Natl.Acad.Sci.U.S.A* 107:19390-19395.

13. Marques JT, Kim K, Wu PH, Alleyne TM, Jafari N, & Carthew RW (2010) Loqs and R2D2 act sequentially in the siRNA pathway in *Drosophila*. *Nat. Struct.Mol.Biol.* 17:24-30.
14. Czech B, Malone CD, Zhou R, Stark A, Schlingeheyde C, Dus M, Perrimon N, Kellis M, Wohlschlegel JA, Sachidanandam R, *et al.* (2008) An endogenous small interfering RNA pathway in *Drosophila*. *Nature* 453:798-802.
15. Okamura K, Balla S, Martin R, Liu N, & Lai EC (2008) Two distinct mechanisms generate endogenous siRNAs from bidirectional transcription in *Drosophila melanogaster*. *Nat Struct Mol Biol* 15:581-590.
16. Miyoshi K, Miyoshi T, Hartig JV, Siomi H, & Siomi MC (2010) Molecular mechanisms that funnel RNA precursors into endogenous small-interfering RNA and microRNA biogenesis pathways in *Drosophila*. *RNA* 16:506-515.
17. Marques JT, Wang JP, Wang X, de Oliveira KP, Gao C, Aguiar ER, Jafari N, & Carthew RW (2013) Functional specialization of the small interfering RNA pathway in response to virus infection. *PLoS Pathog* 9:e1003579.
18. Han YH, Luo YJ, Wu Q, Jovel J, Wang XH, Aliyari R, Han C, Li WX, & Ding SW (2011) RNA-based immunity terminates viral infection in adult *Drosophila* in the absence of viral suppression of RNA interference: characterization of viral small interfering RNA populations in wild-type and mutant flies. *J Virol* 85:13153-13163.
19. Jiang F, Ye X, Liu X, Fincher L, McKearin D, & Liu Q (2005) Dicer-1 and R3D1-L catalyze microRNA maturation in *Drosophila*. *Genes Dev* 19:1674-1679.
20. Saito K, Ishizuka A, Siomi H, & Siomi MC (2005) Processing of pre-microRNAs by the Dicer-1-Loquacious complex in *Drosophila* cells. *PLoS Biol* 3:e235.
21. Cenik ES, Fukunaga R, Lu G, Dutcher R, Wang Y, Tanaka Hall TM, & Zamore PD (2011) Phosphate and R2D2 restrict the substrate specificity of Dicer-2, an ATP-driven ribonuclease. *Mol Cell* 42:172-184.
22. Lee YS, Nakahara K, Pham JW, Kim K, He Z, Sontheimer EJ, & Carthew RW (2004) Distinct roles for *Drosophila* Dicer-1 and Dicer-2 in the siRNA/miRNA silencing pathways. *Cell* 117:69-81.
23. Deleris A, Gallego-Bartolome J, Bao J, Kasschau KD, Carrington JC, & Voinnet O (2006) Hierarchical action and inhibition of plant Dicer-like proteins in antiviral defense. *Science* 313:68-71.
24. Blevins T, Rajeswaran R, Aregger M, Borah BK, Schepetilnikov M, Baerlocher L, Farinelli L, Meins F, Jr., Hohn T, & Pooggin MM (2011) Massive production of small RNAs from a non-coding region of Cauliflower mosaic virus in plant

- defense and viral counter-defense. *Nucleic Acids Res* 39:5003-5014.
25. Blevins T, Rajeswaran R, Shivaprasad PV, Beknazariants D, Si-Ammour A, Park HS, Vazquez F, Robertson D, Meins F, Jr., Hohn T, *et al.* (2006) Four plant Dicers mediate viral small RNA biogenesis and DNA virus induced silencing. *Nucleic Acids Res* 34:6233-6246.
 26. Moissiard G & Voinnet O (2006) RNA silencing of host transcripts by cauliflower mosaic virus requires coordinated action of the four Arabidopsis Dicer-like proteins. *Proc Natl Acad Sci U S A* 103:19593-19598.
 27. Cheloufi S, Dos Santos CO, Chong MM, & Hannon GJ (2010) A dicer-independent miRNA biogenesis pathway that requires Ago catalysis. *Nature* 465:584-589.
 28. Cifuentes D, Xue H, Taylor DW, Patnode H, Mishima Y, Cheloufi S, Ma E, Mane S, Hannon GJ, Lawson ND, *et al.* (2010) A novel miRNA processing pathway independent of Dicer requires Argonaute2 catalytic activity. *Science* 328:1694-1698.
 29. Yang JS, Maurin T, Robine N, Rasmussen KD, Jeffrey KL, Chandwani R, Papapetrou EP, Sadelain M, O'Carroll D, & Lai EC (2010) Conserved vertebrate mir-451 provides a platform for Dicer-independent, Ago2-mediated microRNA biogenesis. *Proc Natl Acad Sci U S A* 107:15163-15168.
 30. Siu RW, Fragkoudis R, Simmonds P, Donald CL, Chase-Topping ME, Barry G, Attarzadeh-Yazdi G, Rodriguez-Andres J, Nash AA, Merits A, *et al.* (2011) Antiviral RNA interference responses induced by Semliki Forest virus infection of mosquito cells: characterization, origin, and frequency-dependent functions of virus-derived small interfering RNAs. *J Virol* 85:2907-2917.
 31. Forstemann K, Horwich MD, Wee L, Tomari Y, & Zamore PD (2007) Drosophila microRNAs are sorted into functionally distinct argonaute complexes after production by dicer-1. *Cell* 130:287-297.
 32. Czech B, Zhou R, Erlich Y, Brennecke J, Binari R, Villalta C, Gordon A, Perrimon N, & Hannon GJ (2009) Hierarchical rules for Argonaute loading in Drosophila. *Mol. Cell* 36:445-456.
 33. Ghildiyal M, Xu J, Seitz H, Weng Z, & Zamore PD (2010) Sorting of Drosophila small silencing RNAs partitions microRNA* strands into the RNA interference pathway. *RNA*. 16:43-56.
 34. Okamura K, Liu N, & Lai EC (2009) Distinct mechanisms for microRNA strand selection by Drosophila Argonautes. *Mol. Cell* 36:431-444.
 35. Okamura K, Robine N, Liu Y, Liu Q, & Lai EC (2011) R2D2 organizes small regulatory RNA pathways in Drosophila. *Mol Cell Biol* 31:884-896.
 36. Miyoshi K, Tsukumo H, Nagami T, Siomi H, & Siomi MC (2005) Slicer

- function of *Drosophila* Argonautes and its involvement in RISC formation. *Genes Dev.* 19:2837-2848.
37. Okamura K, Ishizuka A, Siomi H, & Siomi MC (2004) Distinct roles for Argonaute proteins in small RNA-directed RNA cleavage pathways. *Genes Dev* 18:1655-1666.
 38. Flynt A, Liu N, Martin R, & Lai EC (2009) Dicing of viral replication intermediates during silencing of latent *Drosophila* viruses. *Proc.Natl.Acad.Sci.U.S.A* 106:5270-5275.
 39. Wu Q, Luo Y, Lu R, Lau N, Lai EC, Li WX, & Ding SW (2010) Virus discovery by deep sequencing and assembly of virus-derived small silencing RNAs. *Proc. Natl.Acad.Sci.U.S.A* 107:1606-1611.
 40. Van Rij RP & Berezikov E (2009) Small RNAs and the control of transposons and viruses in *Drosophila*. *Trends Microbiol* 17:139-178.
 41. Vodovar N, Goic B, Blanc H, & Saleh MC (2011) In silico reconstruction of viral genomes from small RNAs improves virus-derived small interfering RNA profiling. *J Virol* 85:11016-11021.
 42. Jovel J & Schneemann A (2011) Molecular characterization of *Drosophila* cells persistently infected with Flock House virus. *Virology* 419:43-53.
 43. Aliyari R, Wu Q, Li HW, Wang XH, Li F, Green LD, Han CS, Li WX, & Ding SW (2008) Mechanism of induction and suppression of antiviral immunity directed by virus-derived small RNAs in *Drosophila*. *Cell Host Microbe* 4:387-397.
 44. Merklings SH & van Rij RP (2013) Beyond RNAi: antiviral defense strategies in *Drosophila* and mosquito. *Journal of insect physiology* 59:159-170.
 45. Souza-Neto JA, Sim S, & Dimopoulos G (2009) An evolutionary conserved function of the JAK-STAT pathway in anti-dengue defense. *Proc Natl Acad Sci U S A* 106:17841-17846.
 46. Xi Z, Ramirez JL, & Dimopoulos G (2008) The *Aedes aegypti* toll pathway controls dengue virus infection. *PLoS Pathog* 4:e1000098.
 47. Xu J, Hopkins K, Sabin L, Yasunaga A, Subramanian H, Lamborn I, Gordesky-Gold B, & Cherry S (2013) ERK signaling couples nutrient status to antiviral defense in the insect gut. *Proc Natl Acad Sci U S A* 110:15025-15030.
 48. Sterken MG, Snoek LB, Bosman KJ, Daamen J, Riksen JA, Bakker J, Pijlman GP, & Kammenga JE (2014) A heritable antiviral RNAi response limits Orsay virus infection in *Caenorhabditis elegans* N2. *PLoS One* 9:e89760.
 49. Durdevic Z, Hanna K, Gold B, Pollex T, Cherry S, Lyko F, & Schaefer M (2013) Efficient RNA virus control in *Drosophila* requires the RNA methyltransferase Dnmt2. *EMBO Rep* 14:269-275.

50. Martin SJ, Highfield AC, Brettell L, Villalobos EM, Budge GE, Powell M, Nikaido S, & Schroeder DC (2012) Global honey bee viral landscape altered by a parasitic mite. *Science* 336:1304-1306.
51. Carpenter JA, Obbard DJ, Maside X, & Jiggins FM (2007) The recent spread of a vertically transmitted virus through populations of *Drosophila melanogaster*. *Molecular ecology* 16:3947-3954.
52. Van Rij RP, Saleh MC, Berry B, Foo C, Houk A, Antoniewski C, & Andino R (2006) The RNA silencing endonuclease Argonaute 2 mediates specific antiviral immunity in *Drosophila melanogaster*. *Genes Dev* 20:2985-2995.
53. Lu R, Maduro M, Li F, Li HW, Broitman-Maduro G, Li WX, & Ding SW (2005) Animal virus replication and RNAi-mediated antiviral silencing in *Caenorhabditis elegans*. *Nature* 436:1040-1043.
54. Chao JA, Lee JH, Chapados BR, Debler EW, Schneemann A, & Williamson JR (2005) Dual modes of RNA-silencing suppression by Flock House virus protein B2. *Nat Struct Mol Biol* 12:952-957.
55. Van Cleef KW, Van Mierlo JT, Miesen P, Overheul GJ, Fros JJ, Schuster S, Marklewitz M, Pijlman GP, Junglen S, & Van Rij RP (2014) Mosquito and *Drosophila* entomobirnaviruses suppress dsRNA- and siRNA-induced RNAi. *Nucleic Acids Res*, **42**, 8732-8744.
56. Nayak A, Berry B, Tassetto M, Kunitomi M, Acevedo A, Deng C, Krutchinsky A, Gross J, Antoniewski C, & Andino R (2010) Cricket paralysis virus antagonizes Argonaute 2 to modulate antiviral defense in *Drosophila*. *Nat. Struct. Mol. Biol.* 17:547-554.
57. Obbard DJ, Gordon KH, Buck AH, & Jiggins FM (2009) The evolution of RNAi as a defence against viruses and transposable elements. *Philos. Trans. R. Soc. Lond B Biol. Sci.* 364:99-115.
58. Obbard DJ, Jiggins FM, Halligan DL, & Little TJ (2006) Natural selection drives extremely rapid evolution in antiviral RNAi genes. *Curr Biol* 16:580-585.
59. Jones JD & Dangl JL (2006) The plant immune system. *Nature* 444:323-329.
60. Pumphin N & Voinnet O (2013) RNA silencing suppression by plant pathogens: defence, counter-defence and counter-counter-defence. *Nat Rev Microbiol* 11:745-760.
61. Zhai J, Jeong DH, De Paoli E, Park S, Rosen BD, Li Y, Gonzalez AJ, Yan Z, Kitto SL, Grusak MA, *et al.* (2011) MicroRNAs as master regulators of the plant NB-LRR defense gene family via the production of phased, trans-acting siRNAs. *Genes Dev* 25:2540-2553.
62. Li F, Pignatta D, Bendix C, Brunkard JO, Cohn MM, Tung J, Sun H, Kumar

- P, & Baker B (2012) MicroRNA regulation of plant innate immune receptors. *Proc Natl Acad Sci U S A* 109:1790-1795.
63. Shivaprasad PV, Chen HM, Patel K, Bond DM, Santos BA, & Baulcombe DC (2012) A microRNA superfamily regulates nucleotide binding site-leucine-rich repeats and other mRNAs. *Plant Cell* 24:859-874.
64. Allen E, Xie Z, Gustafson AM, & Carrington JC (2005) microRNA-directed phasing during trans-acting siRNA biogenesis in plants. *Cell* 121:207-221.
65. Wang XB, Jovel J, Udomborn P, Wang Y, Wu Q, Li WX, Gascioli V, Vaucheret H, & Ding SW (2011) The 21-nucleotide, but not 22-nucleotide, viral secondary small interfering RNAs direct potent antiviral defense by two cooperative argonautes in *Arabidopsis thaliana*. *Plant Cell* 23:1625-1638.
66. Harvey JJ, Lewsey MG, Patel K, Westwood J, Heimstadt S, Carr JP, & Baulcombe DC (2011) An antiviral defense role of AGO2 in plants. *PLoS One* 6:e14639.
67. Nakahara KS, Masuta C, Yamada S, Shimura H, Kashihara Y, Wada TS, Meguro A, Goto K, Tadamura K, Sueda K, *et al.* (2012) Tobacco calmodulin-like protein provides secondary defense by binding to and directing degradation of virus RNA silencing suppressors. *Proc Natl Acad Sci U S A* 109:10113-10118.
68. Katze MG, He Y, & Gale M, Jr. (2002) Viruses and interferon: a fight for supremacy. *Nat Rev Immunol* 2:675-687.
69. Maillard PV, Ciaudo C, Marchais A, Li Y, Jay F, Ding SW, & Voinnet O (2013) Antiviral RNA interference in mammalian cells. *Science* 342:235-238.
70. Li Y, Lu J, Han Y, Fan X, & Ding SW (2013) RNA interference functions as an antiviral immunity mechanism in mammals. *Science* 342:231-234.
71. Haasnoot J, de Vries W, Geutjes EJ, Prins M, de Haan P, & Berkhout B (2007) The Ebola virus VP35 protein is a suppressor of RNA silencing. *PLoS Pathog* 3:e86.
72. Langland JO, Cameron JM, Heck MC, Jancovich JK, & Jacobs BL (2006) Inhibition of PKR by RNA and DNA viruses. *Virus Res* 119:100-110.
73. Randall RE & Goodbourn S (2008) Interferons and viruses: an interplay between induction, signalling, antiviral responses and virus countermeasures. *J Gen Virol* 89:1-47.
74. Li WX, Li H, Lu R, Li F, Dus M, Atkinson P, Brydon EW, Johnson KL, Garcia-Sastre A, Ball LA, *et al.* (2004) Interferon antagonist proteins of influenza and vaccinia viruses are suppressors of RNA silencing. *Proc Natl Acad Sci U S A* 101:1350-1355.
75. Pfeffer S, Zavolan M, Grasser FA, Chien M, Russo JJ, Ju J, John B, Enright AJ, Marks D, Sander C, *et al.* (2004) Identification of virus-encoded microRNAs.

- Science* 304:734-736.
76. Stark TJ, Arnold JD, Spector DH, & Yeo GW (2012) High-resolution profiling and analysis of viral and host small RNAs during human cytomegalovirus infection. *J Virol* 86:226-235.
 77. Ding SW & Voinnet O (2007) Antiviral immunity directed by small RNAs. *Cell* 130:413-426.
 78. Cullen BR, Cherry S, & tenOever BR (2013) Is RNA interference a physiologically relevant innate antiviral immune response in mammals? *Cell Host Microbe* 14:374-378.
 79. Seo GJ, Kincaid RP, Phanaksri T, Burke JM, Pare JM, Cox JE, Hsiang TY, Krug RM, & Sullivan CS (2013) Reciprocal inhibition between intracellular antiviral signaling and the RNAi machinery in mammalian cells. *Cell Host Microbe* 14:435-445.
 80. Shapiro JS, Schmid S, Aguado LC, Sabin LR, Yasunaga A, Shim JV, Sachs D, Cherry S, & tenOever BR (2014) Droscha as an interferon-independent antiviral factor. *Proc Natl Acad Sci U S A* 111:7108-7113.
 81. Keene KM, Foy BD, Sanchez-Vargas I, Beaty BJ, Blair CD, & Olson KE (2004) From the Cover: RNA interference acts as a natural antiviral response to O'nyong-nyong virus (Alphavirus; Togaviridae) infection of *Anopheles gambiae*. *Proc Natl Acad Sci U S A* 101:17240-17245.
 82. Sanchez-Vargas I, Scott JC, Poole-Smith BK, Franz AW, Barbosa-Solomieu V, Wilusz J, Olson KE, & Blair CD (2009) Dengue virus type 2 infections of *Aedes aegypti* are modulated by the mosquito's RNA interference pathway. *PLoS Pathog* 5:e1000299.
 83. Saleh MC, Tassetto M, Van Rij RP, Goic B, Gausson V, Berry B, Jacquier C, Antoniewski C, & Andino R (2009) Antiviral immunity in *Drosophila* requires systemic RNA interference spread. *Nature* 458:346-350.
 84. Robalino J, Bartlett T, Shepard E, Prior S, Jaramillo G, Scura E, Chapman RW, Gross PS, Browdy CL, & Warr GW (2005) Double-stranded RNA induces sequence-specific antiviral silencing in addition to nonspecific immunity in a marine shrimp: convergence of RNA interference and innate immunity in the invertebrate antiviral response? *J Virol* 79:13561-13571.
 85. Robalino J, Browdy CL, Prior S, Metz A, Parnell P, Gross P, & Warr G (2004) Induction of antiviral immunity by double-stranded RNA in a marine invertebrate. *J Virol* 78:10442-10448.
 86. Yodmuang S, Tirasophon W, Roshorm Y, Chinnirunvong W, & Panyim S (2006) YHV-protease dsRNA inhibits YHV replication in *Penaeus monodon* and prevents mortality. *Biochem Biophys Res Commun* 341:351-356.

87. Attasart P, Kaewkhaw R, Chimwai C, Kongphom U, Namramoon O, & Panyim S (2010) Inhibition of *Penaeus monodon* densovirus replication in shrimp by double-stranded RNA. *Arch Virol* 155:825-832.
88. Labreuche Y, Veloso A, de la Vega E, Gross PS, Chapman RW, Browdy CL, & Warr GW (2010) Non-specific activation of antiviral immunity and induction of RNA interference may engage the same pathway in the Pacific white leg shrimp *Litopenaeus vannamei*. *Developmental and comparative immunology* 34:1209-1218.
89. Maori E, Paldi N, Shafir S, Kalev H, Tsur E, Glick E, & Sela I (2009) IAPV, a bee-affecting virus associated with Colony Collapse Disorder can be silenced by dsRNA ingestion. *Insect Mol Biol* 18:55-60.
90. Desai SD, Eu YJ, Whyard S, & Currie RW (2012) Reduction in deformed wing virus infection in larval and adult honey bees (*Apis mellifera* L.) by double-stranded RNA ingestion. *Insect Mol Biol* 21:446-455.
91. Flenniken ML & Andino R (2013) Non-specific dsRNA-mediated antiviral response in the honey bee. *PLoS One* 8:e77263.
92. Ghildiyal M, Seitz H, Horwich MD, Li C, Du T, Lee S, Xu J, Kittler EL, Zapp ML, Weng Z, *et al.* (2008) Endogenous siRNAs Derived from Transposons and mRNAs in *Drosophila* Somatic Cells. *Science* 320:1077-1081.
93. Kawamura Y, Saito K, Kin T, Ono Y, Asai K, Sunohara T, Okada TN, Siomi MC, & Siomi H (2008) *Drosophila* endogenous small RNAs bind to Argonaute 2 in somatic cells. *Nature* 453:793-797.
94. Chung WJ, Okamura K, Martin R, & Lai EC (2008) Endogenous RNA Interference Provides a Somatic Defense against *Drosophila* Transposons. *Curr Biol* 18:795-802.
95. Okamura K, Chung WJ, Ruby JG, Guo H, Bartel DP, & Lai EC (2008) The *Drosophila* hairpin RNA pathway generates endogenous short interfering RNAs. *Nature* 453:803-806.
96. Tonkin LA, Saccomanno L, Morse DP, Brodigan T, Krause M, & Bass BL (2002) RNA editing by ADARs is important for normal behavior in *Caenorhabditis elegans*. *EMBO J* 21:6025-6035.
97. Tonkin LA & Bass BL (2003) Mutations in RNAi rescue aberrant chemotaxis of ADAR mutants. *Science* 302:1725.
98. Scadden AD & Smith CW (2001) RNAi is antagonized by A->I hyper-editing. *EMBO Rep* 2:1107-1111.
99. Ghildiyal M & Zamore PD (2009) Small silencing RNAs: an expanding universe. *Nat.Rev.Genet.* 10:94-108.
100. Fagegaltier D, Bouge AL, Berry B, Poisot E, Sismeiro O, Coppee JY, Theodore

- L, Voinnet O, & Antoniewski C (2009) The endogenous siRNA pathway is involved in heterochromatin formation in *Drosophila*. *Proc Natl Acad Sci U S A* 106:21258-21263.
101. Cernilogar FM, Onorati MC, Kothe GO, Burroughs AM, Parsi KM, Breiling A, Lo Sardo F, Saxena A, Miyoshi K, Siomi H, *et al.* (2011) Chromatin-associated RNA interference components contribute to transcriptional regulation in *Drosophila*. *Nature* 480:391-395.
 102. Taliaferro JM, Aspden JL, Bradley T, Marwha D, Blanchette M, & Rio DC (2013) Two new and distinct roles for *Drosophila* Argonaute-2 in the nucleus: alternative pre-mRNA splicing and transcriptional repression. *Genes Dev* 27:378-389.
 103. Castel SE & Martienssen RA (2013) RNA interference in the nucleus: roles for small RNAs in transcription, epigenetics and beyond. *Nat Rev Genet* 14:100-112.
 104. Akbergenov R, Si-Ammour A, Blevins T, Amin I, Kutter C, Vanderschuren H, Zhang P, Gruissem W, Meins F, Jr., Hohn T, *et al.* (2006) Molecular characterization of geminivirus-derived small RNAs in different plant species. *Nucleic Acids Res* 34:462-471.
 105. Chellappan P, Vanitharani R, Pita J, & Fauquet CM (2004) Short interfering RNA accumulation correlates with host recovery in DNA virus-infected hosts, and gene silencing targets specific viral sequences. *J Virol* 78:7465-7477.
 106. Raja P, Sanville BC, Buchmann RC, & Bisaro DM (2008) Viral genome methylation as an epigenetic defense against geminiviruses. *J Virol* 82:8997-9007.
 107. Raja P, Jackel JN, Li S, Heard IM, & Bisaro DM (2014) Arabidopsis double-stranded RNA binding protein DRB3 participates in methylation-mediated defense against geminiviruses. *J Virol* 88:2611-2622.
 108. Luteijn MJ & Ketting RF (2013) PIWI-interacting RNAs: from generation to transgenerational epigenetics. *Nat Rev Genet* 14:523-534.
 109. Leger P, Lara E, Jagla B, Sismeiro O, Mansuroglu Z, Coppee JY, Bonnefoy E, & Bouloy M (2013) Dicer-2- and piwi-mediated RNA interference in rift valley Fever virus-infected mosquito cells. *J Virol* 87:1631-1648.
 110. Schnettler E, Donald CL, Human S, Watson M, Siu RW, McFarlane M, Fazakerley JK, Kohl A, & Fragkoudis R (2013) Knockdown of piRNA pathway proteins results in enhanced Semliki Forest virus production in mosquito cells. *J Gen Virol* 94:1680-1689.
 111. Schnettler E, Ratnien M, Watson M, Shaw AE, McFarlane M, Varela M, Elliott RM, Palmarini M, & Kohl A (2013) RNA interference targets arbovirus

- replication in *Culicoides* cells. *J Virol* 87:2441-2454.
112. Morazzani EM, Wiley MR, Murreddu MG, Adelman ZN, & Myles KM (2012) Production of virus-derived ping-pong-dependent piRNA-like small RNAs in the mosquito soma. *PLoS Pathog* 8:e1002470.
 113. Myles KM, Wiley MR, Morazzani EM, & Adelman ZN (2008) Alphavirus-derived small RNAs modulate pathogenesis in disease vector mosquitoes. *Proc. Natl.Acad.Sci.U.S.A* 105:19938-19943.
 114. Cirimotich CM, Scott JC, Phillips AT, Geiss BJ, & Olson KE (2009) Suppression of RNA interference increases alphavirus replication and virus-associated mortality in *Aedes aegypti* mosquitoes. *BMC Microbiol* 9:49.
 115. Ashe A, Sapetschnig A, Weick EM, Mitchell J, Bagijn MP, Cording AC, Doebley AL, Goldstein LD, Lehrbach NJ, Le Pen J, *et al.* (2012) piRNAs can trigger a multigenerational epigenetic memory in the germline of *C. elegans*. *Cell* 150:88-99.
 116. Bagijn MP, Goldstein LD, Sapetschnig A, Weick EM, Bouasker S, Lehrbach NJ, Simard MJ, & Miska EA (2012) Function, targets, and evolution of *Caenorhabditis elegans* piRNAs. *Science* 337:574-578.
 117. Shirayama M, Seth M, Lee HC, Gu W, Ishidate T, Conte D, Jr., & Mello CC (2012) piRNAs initiate an epigenetic memory of nonself RNA in the *C. elegans* germline. *Cell* 150:65-77.
 118. Lee HC, Gu W, Shirayama M, Youngman E, Conte D, Jr., & Mello CC (2012) *C. elegans* piRNAs mediate the genome-wide surveillance of germline transcripts. *Cell* 150:78-87.
 119. de Vanssay A, Bouge AL, Boivin A, Hermant C, Teyssset L, Delmarre V, Antoniewski C, & Ronsseray S (2012) Paramutation in *Drosophila* linked to emergence of a piRNA-producing locus. *Nature* 490:112-115.
 120. Jinek M, Chylinski K, Fonfara I, Hauer M, Doudna JA, & Charpentier E (2012) A programmable dual-RNA-guided DNA endonuclease in adaptive bacterial immunity. *Science* 337:816-821.
 121. Deltcheva E, Chylinski K, Sharma CM, Gonzales K, Chao Y, Pirzada ZA, Eckert MR, Vogel J, & Charpentier E (2011) CRISPR RNA maturation by trans-encoded small RNA and host factor RNase III. *Nature* 471:602-607.

Chapter 8

**Summary
&
Samenvatting**

Summary

Viruses are small infectious agents that can only replicate inside the cells of organisms, including bacteria, plants and animals. The viral genome consists of ribonucleic acid (RNA) or deoxyribonucleic acid (DNA), which can be single-stranded (ss) or double-stranded (ds). A protein shell, called the capsid, protects the viral genome, while in some cases viral nucleic acids are shielded by both a capsid and a lipid membrane. Following entry, a virus releases its genomic material and uses the host cell metabolic machinery for replication to produce new infectious virus particles. Progeny viruses are subsequently released from the infected host cell to infect naive, neighboring cells.

An infected cell senses the invading viral pathogen and triggers an antiviral immune response to inhibit virus replication and spread. A major antiviral response in insects is the RNA interference (RNAi) pathway (Figure). RNAi is triggered by the detection of dsRNA, which is produced during virus infection but is absent in non-infected, healthy cells. The cellular enzyme Dicer-2 recognizes viral dsRNA and cleaves it into viral small interfering RNAs (vsiRNAs), thereby degrading these viral dsRNA substrates. The produced vsiRNAs are loaded into the Argonaute-2 protein, which is the central component of the RNA-induced silencing complex (RISC). Within RISC, the siRNA-loaded Argonaute-2 recognizes and cleaves complementary viral ssRNA. Thus, the RNAi pathway interferes with virus replication by the degradation of viral dsRNA by Dicer-2 and by the sequence-specific cleavage of viral ssRNA by Argonaute-2 (**Chapter 1**).

Insect viruses have evolved diverse counter-defense strategies to evade or suppress this small RNA-based immune response. For example, the RNA virus *Drosophila* C virus (DCV), which is a natural *Drosophila* (fruit fly) pathogen, encodes the 1A protein that inhibits the antiviral RNAi response by binding viral dsRNA, thereby preventing its cleavage by Dicer-2. In contrast, the 1A protein of the RNA virus Cricket Paralysis virus (CrPV), a family member of DCV, inhibits the RNAi response by antagonizing Argonaute-2 cleavage activity. Thus, both DCV and CrPV have evolved suppressors of RNAi (VSRs) to antagonize this small RNA-based antiviral immune response.

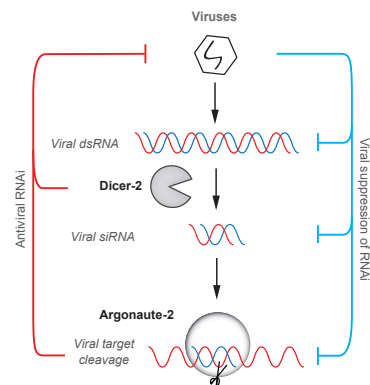


Figure. Antiviral defense and viral counter-defense in insects.

Insects are vectors for the transmission and spread of many important human and animal viruses. Mosquitoes and other blood-feeding insects (e.g. ticks) transmit arthropod-borne (arbo) viruses, some of which are associated with debilitating disease and worldwide epidemics (e.g. Dengue virus). Arbovirus-mediated disease is likely to increase due to the ongoing global spread of arboviruses, the emergence of new virus strains (which may adapt to new vectors), and the adaptation of vector species to new habitats. It is thus important to study the mechanisms of antiviral immunity in insects to uncover novel components and regulators of immune pathways and to define new strategies to restrict transmission and spread of pathogenic viruses. The fruit fly is host to a number of RNA viruses and its versatile toolkit provides a powerful model to study antiviral immunity in insects.

In this thesis we describe small RNA-based antiviral defense mechanisms in insects. In **Chapter 2**, we used Nora virus, a natural *Drosophila* pathogen, to study virus-host interactions. We detected Nora virus-derived vsRNAs in persistently infected adult flies, which suggests that Nora virus is a target of the *Drosophila* antiviral RNAi machinery. Nevertheless, the observation that Nora virus establishes a persistent, non-lethal infection in flies suggests that this RNA virus is able to evade or to potently suppress the RNAi machinery. Therefore, we studied whether Nora virus encodes a protein that inhibits the RNAi response. We found that Nora virus VP1 suppresses RNAi in cultured cells as well as in adult flies. Moreover, we generated recombinant Sindbis virus and revealed that VP1 increases pathogenicity in infected flies in an RNAi-dependent manner. Using a series of biochemical assays (electrophoretic mobility shift assay, Dicer assays, and Slicer assays) that monitor individual steps of the RNAi pathway, we subsequently showed that Nora virus VP1 specifically prevents the sequence-specific cleavage (slicing) of an ssRNA substrate. Together, these results demonstrate that Nora virus is both a target and suppressor of RNAi. In addition, this study provides support that the Argonaute-2-mediated Slicer activity of RISC contributes to the antiviral potential of the RNAi machinery.

In **Chapter 3**, we investigated whether a dsDNA virus, Invertebrate iridescent virus 6 (IIV-6), induces an antiviral RNAi response in *Drosophila*. We first showed that flies that lack the core RNAi components Dicer-2 and Argonaute-2 are more susceptible to IIV-6 infection, suggesting that the antiviral RNAi pathway controls DNA virus infection. Indeed, using small RNA cloning and next-generation sequencing technology, we identified Dicer-2-dependent vsRNAs in IIV-6-infected flies. This observation was particularly interesting because DNA viruses do not rely on a dsRNA replication intermediate for the production of new viral genomes. Therefore, other dsRNA sources must be processed by Dicer-2. We performed small RNA profiling studies, strand-specific RT-PCR assays and Northern blot analyses to identify the dsRNA substrates for

vsiRNA biogenesis. Using these techniques, we demonstrated that sense and antisense transcripts are generated *in vivo* and *in vitro* during IIV-6 replication. These results support a model in which base pairing between convergent overlapping transcripts generate the viral dsRNA substrate for vsiRNA production by Dicer-2. With this study, we were the first to show that RNAi provides antiviral defense against DNA viruses in *Drosophila*. A number of recent publications have now analyzed vsiRNA profiles in DNA virus infections in *Drosophila* and other invertebrate model systems, which we reviewed in **Chapter 4**. These studies further underscore that convergent transcripts are the main source of vsiRNAs. In addition, some DNA viruses may produce ssRNAs with strong secondary structures that could also serve as dsRNA substrates for vsiRNA production by Dicer-2. Together, these studies demonstrate that an antiviral RNAi response is mounted against distinct DNA viruses in different invertebrates.

Having found that DNA viruses induce an antiviral RNAi response in *Drosophila* (**Chapter 3**), we next wondered whether DNA viruses, like RNA viruses, evade this small RNA-based response. In **Chapter 5**, we investigated whether IIV-6 encodes a suppressor of RNAi. Using reporter-based assays, we demonstrated that the RNAi pathway is suppressed in IIV-6-infected cells and we mapped the RNAi suppressive activity to the dsRNA-binding protein 340R. Site-directed mutagenesis studies subsequently indicated that the dsRNA-binding activity of 340R is required for suppression of RNA silencing. Using biochemical assays, we revealed that 340R indeed binds dsRNA and thereby prevents its cleavage into siRNAs by Dicer-2. Moreover, we showed that 340R also binds siRNAs and thereby blocks the incorporation of siRNAs into RISC. Thus, 340R interferes with RISC assembly and, as a consequence, inhibits target RNA cleavage by Argonaute-2. Finally, we showed that 340R is able to rescue replication of an RNA virus (Flock House virus) replicon that lacks its viral suppressor of RNAi. The results from **Chapter 3** and **Chapter 5** reveal that, in analogy to RNA viruses (**Chapter 2**), DNA viruses are targets and suppressors of an antiviral RNAi response.

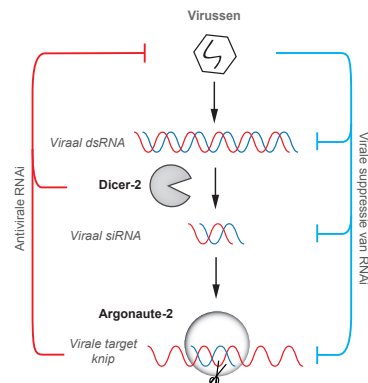
In **Chapter 6**, we analyzed the small RNA profiles of mosquito cells infected with different classes of RNA viruses. Interestingly, we observed that, besides vsiRNAs, another class of small RNAs was produced in these cells. These virus-derived small RNAs were ~25-30 nucleotides in size, exhibited typical signatures of piwi-interacting RNAs (piRNAs), and were produced in a Dicer-independent manner. Furthermore, we showed that the siRNA and piRNA pathways also target endogenous transposons. Taken together, this study revealed that parasitic nucleic acids initiate the *de novo* production of piRNAs and siRNAs in mosquito cells.

In **Chapter 7**, I discussed our findings in relation to recent literature and in a broader context. Finally, I speculated on the role of virus-derived piRNAs in antiviral defense in mosquitoes.

Samenvatting

Virussen zijn microscopisch kleine ziekteverwekkers die zich alleen kunnen vermenigvuldigen in de cel van gastheerorganismen, zoals bacteriën, planten en dieren. De genetische informatie van virussen (het virale genoom) bestaat uit ribonucleïnezuren (RNA) of deoxyribonucleïnezuren (DNA), die enkelstrengs (es) of dubbelstrengs (ds) kunnen zijn. Een eiwitmantel, genaamd het capsid, beschermt het virale genoom. In sommige gevallen worden de virale nucleïnezuren afgeschermd door zowel een capsid als een lipide membraan. Nadat een virus een gastheer cel is binnengedrongen komen de virale nucleïnezuren vrij in de cel. Voor de vermenigvuldiging van het virale genoom wordt gebruik gemaakt van de biochemische processen van de gastheer cel. Dit leidt uiteindelijk tot de productie van nieuwe infectieuze virusdeeltjes die de geïnfecteerde cel verlaten om vervolgens gezonde, aangrenzende cellen te infecteren. Echter, een geïnfecteerde cel kan een viraal pathogeen detecteren en een antivirale immunoreactie aanzetten om vermenigvuldiging en verspreiding van het virus tegen te gaan. Een belangrijke antivirale respons in insecten is het RNA interferentie (RNAi)-mechanisme (Figuur). RNAi wordt geïnduceerd door de detectie van dsRNA dat wordt geproduceerd tijdens een virusinfectie, maar dat normaal gesproken niet aanwezig is in gezonde, niet-geïnfecteerde cellen. Het cellulair enzym Dicer-2 herkent het virale dsRNA en knipt dit in kleinere dsRNA moleculen, die virale kleine interfererende RNA's (viral small interfering RNA's, vsiRNA's) worden genoemd. Door deze Dicer-2-gemedieerde knip worden de virale dsRNA moleculen afgebroken. De geproduceerde vsiRNA's worden vervolgens ingebouwd in een groter eiwitcomplex: het "RNA-induced silencing complex" (RISC), waarin het Argonaute-2 eiwit een belangrijke rol speelt. De vsiRNA die ingebouwd is in RISC herkent complementaire virale esRNA target sequenties die vervolgens worden geknipt door Argonaute-2. Het RNAi-mechanisme kan de vermenigvuldiging van het virus dus remmen via het knippen van viraal dsRNA door Dicer-2 en middels het knippen van viraal target RNA door Argonaute-2 (**Hoofdstuk 1**).

Insectenvirussen hebben echter diverse strategieën ontwikkeld om het RNAi-mechanisme te ontwijken. Zo produceert het RNA virus *Drosophila C virus* (DCV), een natuurlijke ziekteverwekker in



Figuur. Het antivirale RNAi-mechanisme in insecten en virale strategieën om RNAi te onderdrukken.

Drosophila (de fruitvlieg), het 1A eiwit dat een antivirale RNAi respons remt door viraal dsRNA te binden. Hierdoor wordt voorkomen dat viraal dsRNA wordt geknipt door Dicer-2. Het 1A eiwit van het RNA virus Cricket Paralysis virus (CrPV), een familielid van DCV, remt daarentegen de RNAi respons door de sequentie-specifieke knip van Argonaute-2 te blokkeren. Dus DCV en CrPV produceren verschillende 1A eiwitten die de antivirale RNAi respons onderdrukken (virale “suppressor” van RNAi, VSR). Insecten verspreiden belangrijke humane en dierlijke virussen. Muggen en andere bloedzuigende insecten (bijv. teken) dragen arbovirussen (virussen die worden overgedragen door geleedpotigen, arthropoda) over. Sommige van deze virussen veroorzaken slopende chronische ziektes en wereldwijde epidemieën (zoals bijv. Dengue virus, ook wel knokkelkoorts genoemd). Door de continue globale verspreiding van arbovirussen, het ontstaan van nieuwe virusstammen (die zich zouden kunnen aanpassen aan nieuwe overdragers) en de aanpassing van insecten aan een nieuwe leefomgeving is het waarschijnlijk dat het aantal ziektes dat wordt veroorzaakt door arbovirussen toeneemt. Het is daarom belangrijk om de mechanismen van antivirale immuniteit in insecten te bestuderen om zo de belangrijke componenten en besturingsmechanismen van immuunreacties te ontdekken én om nieuwe strategieën te bedenken om het overbrengen en verspreiden van pathogene virussen te beperken. *Drosophila melanogaster* is een veelzijdig modelorganisme waarvoor veel genetische tools beschikbaar zijn. Daarnaast is de fruitvlieg gastheer van een aantal natuurlijke RNA virussen. Dit maakt de fruitvlieg een krachtig model om antivirale immuniteit in insecten te bestuderen.

In dit proefschrift beschrijven we de op kleine RNA's gebaseerde antivirale afweer in insecten (“Small RNA-based antiviral defense in insects”). In **Hoofdstuk 2** hebben we het natuurlijke fruitvlieg pathogeen Nora virus gebruikt om virus-gastheer interacties te bestuderen. In persistent geïnfekteerde volwassen fruitvliegen konden we vsiRNA's afkomstig van het Nora virus detecteren. Dit impliceert dat Nora virus het antivirale RNAi-mechanisme in *Drosophila* induceert. Echter, de observatie dat Nora virus een persistente, niet-lethale infectie in vliegen veroorzaakt doet vermoeden dat dit RNA virus het antivirale RNAi-mechanisme omzeilt of krachtig remt. We hebben daarom bestudeerd of Nora virus een eiwit produceert dat de RNAi respons blokkeert. We hebben Nora virus VP1 geïdentificeerd als het eiwit dat de RNAi respons onderdrukt, zowel in gekweekte cellen als in volwassen vliegen. Daarnaast hebben we recombinant virus gemaakt en vonden we dat VP1 de pathogeniteit (ziekteverwekkend vermogen) in vliegen verhoogt; dit bleek volledig afhankelijk van RNAi. Door gebruik te maken van een aantal biochemische assays die individuele stappen van het RNAi-mechanisme monitoren, hebben we vervolgens laten zien dat het VP1 eiwit het sequentie-specifiek knippen van een esRNA target molecuul door Argonaute-2 blokkeert. Deze resultaten

tezamen tonen aan dat een antivirale RNAi respons wordt geïnduceerd, maar ook wordt onderdrukt door Nora virus.

In **Hoofdstuk 3** hebben we onderzocht of een dsDNA virus, “Invertebrate iridescent virus 6” (IIV-6) een antivirale RNAi respons in *Drosophila* induceert. Allereerst hebben we laten zien dat fruitvliegen die het Dicer-2 of Argonaute-2 gen missen (de kern componenten van het RNAi- mechanisme) gevoeliger zijn voor IIV-6 infectie. Dit suggereert dat het antivirale RNAi-mechanisme DNA virusinfecties controleert. Inderdaad, door gebruik te maken van kleine RNA-klonerings- en “next-generation” sequentie-technologieën konden we Dicer-2 afhankelijke vsiRNA's identificeren in IIV-6 geïnfecteerde vliegen. Deze observatie was met name interessant omdat DNA virussen voor de productie van nieuwe virale genomen niet afhankelijk zijn van een dsRNA replicatie intermediair. Er moeten dus andere dsRNA moleculen geknipt worden door Dicer-2 voor de productie van vsiRNA's. We hebben verschillende studies (kleine RNA profielstudies, streng-specifieke RT-PCR assays en Northern blot analyses) uitgevoerd om het dsRNA substraat voor vsiRNA productie te identificeren. Met behulp van deze technieken hebben we laten zien dat transcripten met een positieve (sense) en negatieve (antisense) polariteit worden gemaakt tijdens IIV-6 replicatie. Deze resultaten ondersteunen een model waarin basenparing tussen overlappende sense en antisense transcripten het virale dsRNA genereren dat als substraat dient voor de productie van vsiRNA's. Dit was de eerste studie die liet zien dat RNAi zorgt voor antivirale afweer tegen DNA virussen in *Drosophila*.

In een aantal recente publicaties zijn de vsiRNA profielen in DNA virus infecties in *Drosophila* en andere ongewervelde model systemen geanalyseerd. Deze studies, die we hebben besproken in **Hoofdstuk 4**, onderstrepen dat overlappende sense en antisense transcripten de voornaamste bron zijn voor vsiRNA productie. Bovendien produceren sommige DNA virussen esRNA's met een sterke secundaire structuur. Dergelijke structuren kunnen ook dsRNA substraten vormen voor vsiRNA productie door Dicer-2. Deze studies tezamen demonstreren dat een antivirale RNAi respons wordt geïnitieerd tegen verschillende DNA virussen in verschillende invertebraten.

Nadat we vastgesteld hadden dat DNA virussen een antivirale RNAi respons in *Drosophila* induceren (**Hoofdstuk 3**), vroegen we ons af of DNA virussen deze kleine RNA-gemedieerde respons onderdrukken. In **Hoofdstuk 5** hebben we daarom onderzocht of IIV-6 een suppressor van RNAi (VSR) produceert. Door gebruik te maken van een RNAi-sensor experiment hebben we laten zien dat het RNAi-mechanisme wordt onderdrukt in IIV-6 geïnfecteerde cellen. Daarnaast hebben we het door IIV-6 gecodeerde dsRNA-bindend eiwit 340R geïdentificeerd als de suppressor van de RNAi respons. Door het 340R eiwit op specifieke plekken te muteren konden we aantonen dat de dsRNA bindingsactiviteit van 340R noodzakelijk is voor het remmen van RNAi.

Met biochemische assays hebben we vervolgens laten zien dat 340R inderdaad dsRNA bindt en dat hierdoor het knippen van dsRNA door Dicer-2 geremd wordt. Bovendien hebben we laten zien dat 340R ook siRNA's bindt en daardoor het inbouwen van siRNA's in RISC waarschijnlijk blokkeert. 340R remt dus het laden van RISC, waardoor ook het knippen van een RNA target door Argonaute-2 wordt geremd. Tot slot hebben we aangetoond dat 340R de replicatie van een RNA virus replicon (Flock House virus), dat zijn virale suppressor van RNAi mist, kan herstellen. De resultaten van **Hoofdstuk 3** en **Hoofdstuk 5** laten zien dat DNA virussen, net als RNA virussen (**Hoofdstuk 2**), de antivirale RNAi respons zowel induceren als onderdrukken.

In **Hoofdstuk 6** hebben we kleine RNA profielen geanalyseerd van muggencellen die geïnfecteerd waren met RNA virussen van verschillende klassen. Tot onze verbazing vonden we dat er behalve vsiRNA's ook nog andere kleine RNA's werden geproduceerd. Deze virus-specifieke RNA's waren ~25-30 nucleotiden lang, vertoonden typische signaturen van piwi-geassocieerde RNA's (piRNA's: kleine RNA's die binden aan zogenaamde PIWI eiwitten), en werden onafhankelijk van Dicer geproduceerd. Daarnaast hebben we laten zien dat siRNA's en piRNA's ook van endogene transposons afkomen. Deze studie laat zien dat in muggencellen de herkenning van 'vreemde' nucleïnezuren de productie van nieuwe siRNA's en piRNA's induceert. In **Hoofdstuk 7** bespreek ik onze bevindingen in relatie tot de recente literatuur en in een bredere context. Tot slot speculeer ik over de rol van virus-specifieke piRNA's in de antivirale afweer in muggen.

Dankwoord

Na vier jaar promotieonderzoek ligt het boekje er dan eindelijk. Dit is een mooie mijlpaal om eens terug te kijken op mijn promotietijd en om een aantal mensen in het bijzonder te bedanken.

Allereerst wil ik mijn copromotor Ronald van Rij bedanken voor de plezierige tijd op het lab. Je bent een toegankelijk en enthousiast persoon die altijd tijd vrij maakt voor de wetenschap. Ik heb onze samenwerking als zeer prettig ervaren en ontzettend veel van je geleerd de afgelopen jaren! Tijdens onze wekelijkse bespreking bedachten we nieuwe experimenten en hebben we vele leuke en interessante discussies gevoerd over nieuwe projecten of spannende hypotheses. Je stimuleerde me om mijn eigen ideeën te volgen, maar je bleef sturend en meedenkend. Daarnaast stond je kantoordeur altijd wagenwijd open en kon ik altijd langskomen met kleine vragen of om over het vervolg van mijn wetenschappelijke carrière te praten. Ook heb je me ontzettend geholpen bij de verschillende beursaanvragen; gelukkig is dit niet voor niets geweest. Nogmaals dank voor alles: dankzij jou ben ik een betere en kritischere wetenschapper geworden!

Op deze plaats wil ik ook Joep Galama bedanken. Dank voor je tijd en belangstelling gedurende dit promotietraject en leuk dat je mijn promotor wil zijn.

Dank aan al mijn collega's op het lab, die er voor hebben gezorgd dat ik een ontzettend leuke tijd heb gehad. Koen, de afgelopen 4,5 jaar zijn we U-genootjes geweest en hebben we intensief samengewerkt. Dit is ook wel te zien aan het aantal papers in dit boekje waar je coauteur op bent. Je bent een fijne collega om mee samen te werken en je bent heel precies in je werk, zowel experimenteel als met het schrijven van papers. Je was een belangrijke raadgever wanneer ik tegen technische problemen aanliep en we hebben geregeld leuke, inhoudelijke discussies gehad. Ik wens je het allerbeste toe in je verdere carrière! Leuk dat je mijn paranimf wil zijn.

Joël, je bent al bijna een jaar niet meer werkzaam op het lab, maar je bent toch degene die veel experimenten heeft opgezet waar wij nu allemaal nog profijt van hebben. Kijk alleen maar naar de Dicer en Slicer assays in dit boekje! Ook hebben we prettig samen gewerkt bij hoofdstuk 2 van dit proefschrift en was je altijd bereikbaar voor discussies over resultaten. Ik was altijd onder de indruk van je kennis van de vakliteratuur. Dank voor alles en veel succes en plezier bij je werkzaamheden in Wageningen.

Gijs, ik sta er altijd van te kijken hoeveel werk jij op een dag verzet en hoe makkelijk alles jou afgaat. Je staat voor iedereen klaar en niets is je te veel gevraagd. Daarnaast ben je als analist ook meedenkend met anderen en ben je een goede troubleshooter. Bedankt voor

al die keren dat je vliegen voor me hebt geteld in de weekenden.

Sarah, you started your PhD one year after I started and especially in your first year we nicely collaborated on the EHMT project. I also learned a lot from you about *Drosophila* genetics and I enjoyed our many conversations in the flyroom. You are a very social person and a real science geek, in a positive way! Thanks for all the interest you always showed and I wish you all the best with the last bits and pieces of your thesis!

Pascal, jij bent als AIO verder gegaan aan het piRNA project. Het zal je waarschijnlijk niet verbazen dat ik jouw werk met bovengemiddelde interesse volg. Je bent een prettige collega die bijdraagt aan een gezellige sfeer in het lab en iemand die in is voor verschillende activiteiten, die je vaak ook nog eens (samen met Sarah) organiseert. Ik wil je ook bedanken voor je expertise en hulp bij de Northern blots en voor je analyses van kleine RNAs.

Susan, you are still at the very beginning of your PhD and I am looking forward to your work on the mammalian RNAi pathway. It was nice to chat with you in the early mornings, even though for you it wasn't early morning anymore, as you already had spent a few ours in the lab. I wish you all the best with your future PhD and regret that I cannot enjoy your baking skills anymore.

Erika and Bas, we only spent a short time together in the lab, but I think that both of you are nice colleagues and contribute to the pleasant atmosphere in the lab. I wish both of you all the best.

Rob, sinds kort ben je als PhD-student het RNAi-team komen versterken. Het is fijn om te weten dat iemand het IIV-6 werk vervolgt. Heel veel succes en ik zal je nog wel wat IIV-6 spam mail bezorgen.

Over the last years I had a lot of fun with the RNAi-team during all the coffee and lunch breaks. I also enjoyed the activities that we had after work as well as the 'celebration' activities at café Jos. I hope to catch up with you at any possible occasion.

Op deze plaats wil ik ook mijn oud-collega's van de onderzoeksgroep van Frank van Kuppeveld bedanken. Ik heb de helft van mijn promotietijd met jullie doorgebracht, voordat jullie hele lab van Nijmegen naar Utrecht verhuisde. Hierdoor werd het wel wat minder druk op onze afdeling, maar was het helaas ook meteen een stuk rustiger aan de koffietafel...

Beste Frank, ik mis de maandagochtenden dat ik binnenkwam en dat we eerst de voetbaluitslagen van het afgelopen weekend bespraken. Hoogtepunt was de foto die je me liet zien waar Sjaak Swart naast jou mocht poseren. Je was altijd oprecht geïnteresseerd in het werk van de RNAi-groep en je hebt vanuit een andere invalshoek altijd veel input gehad tijdens de algemene werkbesprekingen! Ook dank voor je tijd en moeite voor het schrijven van de referentiebrieven voor de verschillende beursaanvragen, ondanks dat je

nu een nog drukker baan hebt als professor.

Hilde, Lonneke, Kjerstin, Qian, Martijn, Jeroen, en Rachel, het was fijn om jullie als collega's te hebben en ik wens iedereen veel succes met ieders carrière. Via deze weg wil ik jullie nogmaals bedanken voor het spekken van de pot voor Hilde's baby pool en de EK pool. Lucian and Cristina, it was nice to have you as colleagues and good luck to both of you with the last steps of your PhD program.

I would also like to thank our collaborators from Paris, France. Nicolas, Hervé and Carla, thanks for the nice collaboration that resulted in two nice publications: chapters 3 and 6 of this thesis. Carla, it was nice to meet you in person several times. You are an enthusiastic scientist and a funny person with an interesting Argentinean temperament.

Linette, tijdens mijn promotie heb ik jou als HLO-student uit Deventer mogen begeleiden. Ik vond dit erg leuk om te doen, ook omdat ik hier zelf heb gestudeerd. Tijdens jouw stage heb je persoonlijk een heel moeilijke tijd doorgemaakt. Ondanks alle zorgen was je altijd opgewekt en positief ingesteld, dit bewonder ik ten zeerste. Daarnaast toonde je altijd een goede werklust en werkte je netjes. Dank je wel voor alles!

Ik wil ook de collega's van de Parasieten bedanken voor de leuke tijd op de afdeling. Het jaarlijkse gezamenlijke uitje en de gesprekken aan de koffietafel waren vaak erg gezellig.

Patrick van QM, het spijt me dat ik je de afgelopen 4 jaar lastig heb moeten vallen met eenzijdige gesprekken over voetbal. Het zal wel toeval zijn dat Ajax gedurende mijn promotietraject 4 maal achter elkaar kampioen is geworden! Het was leuk om met je over voetbal en andere belangrijke of onbelangrijke zaken te discussiëren.

Naast alle collega's wil ik ook een aantal andere mensen bedanken voor hun interesse en voor de gezelligheid buiten het werk.

Anneke, Carla, en José, wij vormden samen het kwartet dat in 2006 vanuit Deventer de Waal overstak richting Nijmegen om hier verder te gaan studeren aan de universiteit. Tijdens de introductiedagen leerden we meer HBO-instromers kennen en zo is er een leuke vriendengroep ontstaan. Omdat we allemaal min of meer dezelfde studieachtergrond hebben is het altijd leuk en interessant om bij te praten over elkaars werk. Daarnaast zijn de weekendjes weg altijd erg gezellig; ik hoop dat dit een jaarlijks terugkerend evenement blijft. Helaas moeten jullie wel op zoek naar een nieuwe locatie voor de barbecue tijdens de 4-daagse feesten. Trouwens, wie adopteert mini-Wally tijdens dit festijn? Anneke, Ronald, Maurijn, en Remy veel succes met het afronden van

jullie PhD. Carla, Rebecca, José en Karlijn, veel succes met jullie jobs.

Martijn, jij bent tijdens mijn studietijd een goede vriend geworden en het is altijd erg gezellig als we elkaar weer eens spreken. Veel succes in het onderwijs en ik ben benieuwd of je ook nog gaat promoveren.

Marieke, Marloes en Hub, ik heb jullie leren kennen via Sanne en we zijn inmiddels goede vrienden geworden, dus dat klikte wel! Dank voor jullie interesse tijdens mijn promotie en de gezellige etentjes en andere leuke activiteiten.

John, Eric, en Wilco (en aanhang), hoewel ik jullie niet zo heel vaak meer zie is het toch altijd lachen om samen een pilsje te drinken en te ouwehoeren. Ik zou het leuk vinden als jullie op het feest zijn om er een paar op mijn kosten te nemen.

Beste schoonfamilie, jullie zijn een hechte en gezellige familie die wel van een feestje houdt. Misschien voel ik me daarom altijd prima op mijn gemak in Venlo en omstreken! Jullie zijn van harte welkom op het feest, dus laat die bus maar weer komen!

Ron, Luuk en Inge, het is altijd erg gezellig met z'n allen en ik voel me altijd thuis bij jullie. Dank voor jullie interesse en voor de gezellige momenten met z'n allen. Ome Walter vindt het ook altijd erg leuk om met Lieke en Joris te spelen! Lieve Nel, we kunnen het goed met elkaar vinden en zoals ik al eens eerder heb gezegd ben je mijn allerliefste schoonmoeder. Ik waardeer het altijd hoe je voor ons en voor andere mensen klaar staat en hoe zorgzaam je voor iedereen bent!

Ik wil de familie uit Uddel ook heel erg bedanken voor de interesse die jullie altijd hebben. Het was erg gezellig toen de gehele familie in Nijmegen was en we door de Ooijpolder hebben gefietst. Zo'n 'familiedag' moeten we eigenlijk vaker doen, maar eerst is het tijd voor een feestje!

Oma Pul, bedankt voor de belangstelling die je (voor iedereen) hebt! Ik hoop zeer binnenkort dan eindelijk te promoveren.

En dan de familie thuis, waar het altijd gezellig is en er veel (maar niet alleen) over voetbal wordt gepraat. Annelies, Sander & Coby, en Richard bedankt voor jullie interesse en bezoeken aan Nijmegen. Annelies, je bent een lieve en zorgzame tweelingzus en ik wens je veel geluk en succes met alles! Sander, ondanks dat we dezelfde HBO-studie hebben gedaan heb jij voor de diagnostiek gekozen, maar als ik dat zo hoor ben je hier wel op je plek. Veel plezier en succes met je nieuwe huis. Richard, op naar 'das Oktoberfest' in

Duitsland, vraag maar vast vrij bij Landal Rabbit Hill! Pa & Ma, ik wil jullie ontzettend bedanken voor alles wat jullie voor mij hebben gedaan en hoe jullie me steeds hebben gesteund. Ik geloof dat ik zonder jullie nooit zover was gekomen. Jullie stimuleren ons om altijd ons uiterste best te doen en om met beide benen op de grond te blijven staan. Jullie zijn telkens geïnteresseerd in onze carrièreontwikkelingen en proberen ons te helpen als dat nodig is! Bedankt voor alles!

De laatste alinea heb ik gereserveerd voor de belangrijkste persoon in mijn leven: SANNE! Lieve Sanne, we kenden elkaar nog maar een paar maanden voordat ik op stage ging naar Australië. We hebben elkaar misschien in deze periode wel het beste leren kennen en ik ben blij dat ik de afgelopen 6,5 jaar alles met jou heb mogen delen. Het is altijd een feest om samen met jou dingen te ondernemen, zoals lekker uit eten, vakanties of weekendjes weg. Gelukkig houden we allebei heel erg van dezelfde dingen! Ik wil je bedanken voor al je steun, begrip en geduld voor als ik weer eens een avondje of weekend achter mijn computer zat om aan mijn boekje te werken. Ik weet dat dit voor jou misschien niet altijd even gezellig was. Daarnaast geef je veel op om nu samen met mij naar Mainz te verhuizen, waar we samen aan een nieuwe uitdaging beginnen. Ik heb er zin in! Dank je voor alles en ik hou van je!

Curriculum Vitae

Alfred Willem (Walter) Bronkhorst werd geboren op 8 februari 1985 te Apeldoorn. In 2002 behaalde hij zijn HAVO diploma aan de Jacobus Fruytier Scholengemeenschap te Apeldoorn. In datzelfde jaar startte hij de studie Biologie en Medisch Laboratoriumonderzoek aan de Saxion Hogeschool te Deventer. Tijdens deze studie liep hij stage bij de afdeling Medische Fysiologie van het UMC Utrecht onder begeleiding van Dr. Marti Bierhuizen. Hier bestudeerde hij de rol van verschillende transcriptiefactoren in de genregulatie van connexines. Zijn afstudeerstage voltooide hij op de afdeling Moleculaire Biologie van de Radboud Universiteit Nijmegen onder supervisie van Prof. dr. Gert Jan Veenstra, waar hij onderzoek deed naar het TBP2 complex dat betrokken is bij de transcriptie van bepaalde genen tijdens de *Xenopus* embryogenese.

In 2006 begon hij de studie Medische Biologie aan de Radboud Universiteit Nijmegen. Aan deze universiteit volgde hij zijn eerste masterstage op de afdeling Biomoleculaire Chemie. Onder leiding van Prof. dr. Ger Pruijn en Raymond Staals, MSc, identificeerde hij de eiwitten die associëren met het humane exosoom; een eiwitcomplex dat betrokken is bij het afbreken van RNA in de cel. Voor zijn tweede masterstage ging hij naar de La Trobe University in Melbourne, Australië. Onder supervisie van Dr. John Silke bestudeerde hij het Fn14-Receptor Signalerings Complex dat apoptose, ofwel geprogrammeerde celdood, induceert na binding van het Tweak ligand. In februari 2010 behaalde Walter zijn masterdiploma.

Van december 2009 tot en met oktober 2014 werkte Walter als promovendus op de afdeling Medische Microbiologie aan de Radboud Universiteit in Nijmegen in het lab van Dr. Ronald van Rij. Hier heeft hij onderzoek gedaan naar kleine RNA moleculen die een antivirale functie hebben in insecten, zoals in dit proefschrift staat beschreven.

In juni 2014 kreeg Walter een EMBO Long-Term Fellowship toegewezen om te onderzoeken hoe het genoom intact wordt gehouden tijdens de embryonale ontwikkeling van zebrafissen. Met deze beurs zal hij in januari 2015 als postdoc gaan werken in de groep van Prof. dr. René Ketting aan het Institute for Molecular Biology in Mainz, Duitsland.

List of publications

Bronkhorst AW, van Cleef KW, Venselaar H, & van Rij RP (2014) A dsRNA-binding protein of a complex invertebrate DNA virus suppresses the *Drosophila* RNAi response. *Nucleic Acids Res*, *in press*.

Bronkhorst AW & van Rij RP (2014) The long and short of antiviral defense: small RNA-based immunity in insects. *Current opinion in virology* 7C:19-28.

Bronkhorst AW, Miesen P, & van Rij RP (2013) Small RNAs tackle large viruses: RNA interference-based antiviral defense against DNA viruses in insects. *Fly* 7:216-223.

Bronkhorst AW, van Cleef KW, Vodovar N, Ince IA, Blanc H, Vlak JM, Saleh MC, & van Rij RP (2012) The DNA virus Invertebrate iridescent virus 6 is a target of the *Drosophila* RNAi machinery. *Proc Natl Acad Sci U S A* 109:E3604-3613.

van Mierlo JT, **Bronkhorst AW**, Overheul GJ, Sadanandan SA, Ekstrom JO, Heestermans M, Hultmark D, Antoniewski C, & van Rij RP (2012) Convergent evolution of Argonaute-2 slicer antagonism in two distinct insect RNA viruses. *PLoS Pathog* 8:e1002872.

Vodovar N, **Bronkhorst AW**, van Cleef KW, Miesen P, Blanc H, van Rij RP, & Saleh MC (2012) Arbovirus-derived piRNAs exhibit a ping-pong signature in mosquito cells. *PLoS One* 7:e30861.

Staals RH, **Bronkhorst AW**, Schilders G, Slomovic S, Schuster G, Heck AJ, Raijmakers R, & Pruijn GJ (2010) Dis3-like 1: a novel exoribonuclease associated with the human exosome. *EMBO J* 29:2358-2367.

